Cellular changes during cold-pressed ‘Hass’ avocado oil extraction

Shuo Yang

A thesis submitted in fulfilment of the requirements for the degree of
Doctor of Philosophy in Food Technology,
at Massey University, Auckland campus,
New Zealand

2019

Abstract

Cellular changes during cold-pressed extraction of 'Hass' avocado (*Persia americana* Mill.) and 'J5' olive (*Olea europaea* L.) were investigated to understand how each step in the process affects oil release from the tissue and to ascertain if and how cold-pressed oil yields were influenced by cellular changes. Electrical impedance spectroscopy (EIS), electrical conductivity, light microscopy and rheological measurements were used to examine avocado and olive flesh and pulp structure at defined processing steps during both commercial and laboratory-based cold-pressed oil extraction. Light microscopy revealed most parenchyma cells in the fruit flesh were ruptured after the destoning and grinding steps. Concomitantly, a significant reduction in electrical resistance and a concurrent increase in conductivity of pulp tissue occurred when cells were ruptured during the destoning and grinding process. Malaxing assisted aggregation of oil into larger droplets, observed by microscopy. Increasing malaxing time resulted in a decrease in the solid-like behaviour (*G'*) of fruit pulp and an increase in cold-pressed oil yield, which correlated with the oil droplets in the fruit paste coalescing together and becoming larger. Idioblast cells in avocado flesh appeared to remain unruptured and intact during the extraction process. In comparison to the cold-pressed oil extraction of 'Hass' avocado, olive oil was easier to recover from 'J5' olive during cold-pressed extraction (at lower temperatures and for shorter times) as the olive paste was less viscous allowing the oil droplets to aggregate more easily.

Processing of avocado fruit at three different stages of ripening (minimally-, fully- and over-ripe) produced higher oil yields and decreased oil quality (based on % free fatty acids and peroxide value) with riper fruit. Intact fruit and fruit pulp from the over-ripe fruit had higher conductivity and lower electrical resistance values, which indicated more

cell rupture occurred when softer, riper avocado fruit are processed.

For avocado fruit at six different stages of maturity (harvested between September and April during the 2016/17 season), light microscopy results showed there were more unbroken parenchyma cells in early season, less mature fruit. Polysaccharides in the cell walls were more strongly bound to cellulose in early-season avocado fruit. Late season fruit had more cell disruption during extraction corresponding to higher conductivity and lower electrical resistance values; hence higher extraction yields with increasing maturity. No significant compositional changes of the polysaccharides in the cell walls occurred during malaxing, which indicated that the malaxing step only promoted aggregation of the oil droplets.

The malaxing temperature and ultrasound treatment at 20–25 kHz did not assist with cellular disruption during extraction. Higher malaxing temperature reduced the viscosity and increased the mobility of oil droplets and oil droplets were more likely to collide and aggregate to form larger droplets, reducing the *G'* of the pulp tissue. The oil yield significantly increased from 1.05% to 13.43% with malaxing temperature increasing from 30 to 50 °C, for early season fruit. Ultrasound treatment at 20–25 kHz decreased the *G'* of the avocado pulp and helped the oil to aggregate.

In conclusion, the avocado flesh cellular structure ruptured more easily in softer and late maturity fruit contributing to increased oil yields. Malaxing time, temperature and ultrasound treatment at 20–25 kHz influenced the degree of oil aggregation in fruit pulp and therefore improved the cold-pressed oil yield. Olive pulp was less viscous or less solid like during malaxing, resulted in faster oil agglomeration.

Publications

Journal and peer reviewed proceedings

Yang, S., Hallett, I., Oh, H. E., Woolf, A. B., Wong, M. (2019). The impact of fruit softening on avocado cell microstructure changes monitored by electrical impedance and conductivity for cold-pressed oil extraction. *Journal of Food Process Engineering*, DOI: 10.1111/jfpe.13068.

Yang, S., Hallett, I., Oh, H. E., Woolf, A. B., Wong, M. (2019). Application of electrical impedance spectroscopy and rheology to monitor changes in olive (*Olea europaea L.*) pulp during cold-pressed oil extraction. *Journal of Food Engineering*, 245, 96-103.

Yang, S., Hallett, I., Rebstock, R., Oh, H. E., Kam, R., Woolf, A. B., Wong, M. (2018). Cellular changes in "Hass" avocado mesocarp during cold-pressed oil extraction. *Journal of the American Oil Chemists' Society*, 95(2), 229-238.

Oral presentation

Wong, M., Yang, S., Hallett, I., Oh, H. E., Woolf, A. B. (2017). New methods to monitor cell integrity during cold-pressed avocado oil extraction. Presented at the meeting of *Food Industry Forum by the University Consortium of Food Science and Nutrition*. Zhejiang Gongshang University, Hangzhou, China.

Yang, S., Hallet, I., Oh, H. E., Woolf, A. B., Wong, M. (2017). Cell structure changes during cold-pressed "Hass" avocado (*Persea americana*) oil extraction. Presented at the meeting of *AAOCS Biennial Conference*. Barossa, Australia.

Poster presentation

Yang, S., Hallet, I., Oh, H.E., Woolf, A.B., Wong, M. (2017). Changes in olive (*Olea europaea*) cell structure during oil extraction. Poster session presented at the meeting of *AAOCS Biennial Conference*. Barossa, Australia. (Best poster award).

Yang, S., Hallett, I., Oh, H, E., Woolf, A, B., Wong, M. (2017). Impact of fruit ripening on cellular structure during avocado oil extraction. Poster session presented at the meeting of *NZIFST Annual Conference*. Nelson, New Zealand.

Yang, S., Woolf, A., Hallett, I., Oh, H.E, Wong, M. (2016). Effect of fruit ripeness on microstructural changes and oil yield during cold-pressed oil extraction of 'Hass' avocado (Persea Americana 'Hass'). Poster session presented at the meeting of *Lipids, Nutraceuticals and Healthy Diets throughout the Life Cycle*. Nelson, New Zealand. (Best poster award).

Yang, S., Hallett, I., Rebstock, R., Kam, R., Woolf, A. B., Wong, M. (2016). Microstructural changes during cold-pressed oil extraction of “Hass” avocado. Poster session presented at the meeting of *NZIFST Annual Conference*. Rotorua, New Zealand.

MASSEY UNIVERSITY
GRADUATE RESEARCH SCHOOL

STATEMENT OF CONTRIBUTION
DOCTORATE WITH PUBLICATIONS/MANUSCRIPTS

We, the candidate and the candidate's Primary Supervisor, certify that all co-authors have consented to their work being included in the thesis and they have accepted the candidate's contribution as indicated below in the *Statement of Originality*.

Name of candidate:	Shuo Yang
Name/title of Primary Supervisor:	A/Prof. Marie Wong
Name of Research Output and full reference:	
Yang, S., Hallett, I., Rebstock, R., Oh, H. E., Kam, R. Woolf, A. B., & Wong, M. (2018). Cellular changes in "Hass" avocado mesocarp during cold-pressed oil extraction. Journal of the American Oil Chemists' Society, 95(2), 229-238.	
In which Chapter is the Manuscript /Published work:	Chapter 4
Please indicate:	
• The percentage of the manuscript/Published Work that was contributed by the candidate:	80%
and	
• Describe the contribution that the candidate has made to the Manuscript/Published Work:	
Experimental work and manuscript writing	
For manuscripts intended for publication please indicate target journal:	
Journal of the American Oil Chemists' Society	
Candidate's Signature:	Shuo Yang Digitally signed by Shuo Yang Date: 2019.12.05 10:45:40 +13'00'
Date:	05/12/2019
Primary Supervisor's Signature:	Marie Wong Digitally signed by Marie Wong Date: 2019.12.05 11:09:10 +13'00'
Date:	5/12/2019

(This form should appear at the end of each thesis chapter/section/appendix submitted as a manuscript/ publication or collected as an appendix at the end of the thesis)

MASSEY UNIVERSITY
GRADUATE RESEARCH SCHOOL

STATEMENT OF CONTRIBUTION
DOCTORATE WITH PUBLICATIONS/MANUSCRIPTS

We, the candidate and the candidate's Primary Supervisor, certify that all co-authors have consented to their work being included in the thesis and they have accepted the candidate's contribution as indicated below in the *Statement of Originality*.

Name of candidate:	Shuo Yang
Name/title of Primary Supervisor:	A/Prof. Marie Wong
Name of Research Output and full reference:	
Yang, S., Hallett, I., Oh, H. E., Woolf, A. B., & Wong, M. (2019). The impact of fruit softening on avocado cell microstructure changes monitored by electrical impedance and conductivity for cold-pressed oil extraction. Journal of Food Process Engineering	
In which Chapter is the Manuscript /Published work:	Chapter 5
Please indicate:	
• The percentage of the manuscript/Published Work that was contributed by the candidate:	80%
and	
• Describe the contribution that the candidate has made to the Manuscript/Published Work:	
Experimental work and manuscript writing	
For manuscripts intended for publication please indicate target journal:	
Journal of Food Process Engineering	
Candidate's Signature:	Shuo Yang Digitally signed by Shuo Yang Date: 2019.12.05 10:47:30 +13'00'
Date:	05/12/2019
Primary Supervisor's Signature:	Marie Wong Digitally signed by Marie Wong Date: 2019.12.05 11:10:09 +13'00'
Date:	5/12/2019

(This form should appear at the end of each thesis chapter/section/appendix submitted as a manuscript/ publication or collected as an appendix at the end of the thesis)

MASSEY UNIVERSITY
GRADUATE RESEARCH SCHOOL

STATEMENT OF CONTRIBUTION
DOCTORATE WITH PUBLICATIONS/MANUSCRIPTS

We, the candidate and the candidate's Primary Supervisor, certify that all co-authors have consented to their work being included in the thesis and they have accepted the candidate's contribution as indicated below in the *Statement of Originality*.

Name of candidate:	Shuo Yang
Name/title of Primary Supervisor:	A/Prof. Marie Wong
Name of Research Output and full reference:	
Yang, S., Hallett, I., Oh, H. E., Woolf, A. B., & Wong, M. (2019). Application of electrical impedance spectroscopy and rheology to monitor changes in olive (Olea europaea L.) pulp during cold-pressed oil extraction. Journal of Food Engineering, 245, 96-	
In which Chapter is the Manuscript /Published work:	Chapter 7
Please indicate:	
• The percentage of the manuscript/Published Work that was contributed by the candidate:	80%
and	
• Describe the contribution that the candidate has made to the Manuscript/Published Work:	
Experimental work and manuscript writing	
For manuscripts intended for publication please indicate target journal:	
Journal of Food Engineering	
Candidate's Signature:	Shuo Yang Digitally signed by Shuo Yang Date: 2019.12.05 10:49:27 +13'00'
Date:	05/12/2019
Primary Supervisor's Signature:	Marie Wong Digitally signed by Marie Wong Date: 2019.12.05 11:10:40 +13'00'
Date:	5/12/2019

(This form should appear at the end of each thesis chapter/section/appendix submitted as a manuscript/ publication or collected as an appendix at the end of the thesis)

Acknowledgements

I would like to express my sincere gratitude to my supervisors A/Prof. Marie Wong (Massey University), Dr. Allan Woolf, Dr. Ian Hallett (Plant and Food Research Ltd), and Dr. Eustina Fraser (Synlait Milk Ltd) for their exemplary guidance, monitoring and constant encouragement throughout the duration of this study. The help and guidance given by them will carry me a long way in the journey of life on which I am about to embark. Also, many thanks are due to Olivado NZ Ltd for providing funding for this research project, and Mr. Gary Hannam and Ms. Sarah Nicholls (Olivado NZ Ltd) for their input into this project and support.

I would like to express a deep sense of gratitude to Dr. Christina Fullerton, Ms. Ria Rebstock (Plant and Food Research Ltd), and Dr. Rothman Kam (Auckland University of Technology) for their invaluable assistance and guidance, which helped me in completing this project through various stages. Thanks are also due to Ms. Kerry Cardoso and Mr. Allan Penney (Olivado NZ Ltd) who assisted with factory trials.

My appreciation and thanks also go to Dr. Liangjue Lin, Dr. Kenneth Teh, Ms. Rachel Liu, Mr. Jarod Young (Massey University), Mr. Shane Olsson, Dr. Rosie Schroeder, Dr. Roger Harker, Dr. Paul Sutherland, Ms. Ruiling Wang, Dr. Ringo Feng, Mr. David Billing, Mr. Paul Pidakala, Ms. Anne White, Ms. Yongyan Peng, and Mr. Roneel Prakash (Plant and Food Research Ltd) for their valuable suggestion and technical assistance in various aspects of my experimental work, and Ms. Sue Pearce and Ms. Sarah Journeaux (Massey University) for their assistance in administrative matters.

Lastly, I would like to thank my families and friends who inspired, encouraged and fully supported me in every trial that came my way.

Table of Contents

Abstract i

Publications iii

Acknowledgements v

Table of Contents vi

List of Figures xi

List of Tables xvii

List of Abbreviations xviii

Chapter 1: Introduction 1

Chapter 2: Literature review 6

2.1 Overview of avocado fruit 7

2.1.1 Avocado fruit production 7

2.1.2 Avocado fruit growth and maturation 9

2.1.3 Postharvest ripening of avocado fruit 11

2.2 Cellular changes during avocado growth and ripening 13

2.2.1 Oil localization in avocado fruit 13

2.2.2 Cell development during fruit growth 16

2.2.3 Enzyme activity changes and cell degradation during fruit ripening 18

2.3 Development of avocado oil commercial extraction 22

2.3.1 History of avocado oil and the avocado fruit for oil production 22

2.3.2 Applications and uses for avocado oil 23

2.4 Avocado oil extraction 24

2.4.1 Commercial extraction systems 24

2.4.2 Laboratory based extraction systems 30

2.4.3 Processing extraction aids 34

2.5 Factors affecting cold-pressed oil yield and quality 39

2.5.1 Maturity (Time of harvest in season) of avocado fruit 39

2.5.2 Ripening of avocado fruit 40

2.5.3 Fruit quality after storage 41

2.5.4 Processing conditions for avocado oil extraction 43

2.6 Methods for monitoring cell rupture and oil aggregation 44

2.6.1 Microscopy 44

2.6.2 Electrical impedance spectroscopy 46

2.6.3 Electrical conductivity 51

2.6.4 Rheological properties 52
2.7 Avocado oil composition 54
2.7.1 Fatty acid composition 54
2.7.2 Tocopherols 55
2.7.3 Sterols 56
2.7.4 Pigments 56
2.8 Virgin olive oil extraction 57
2.8.1 Overview of olive fruit 57
2.8.2 Virgin olive oil 58
2.8.3 Commercial extraction systems 59
2.9 Literature review conclusions 61
Chapter 3: Materials and methods 63
3.1 Raw materials 64
3.1.1 Avocado fruit for commercial factory trial 64
3.1.2 Avocado fruit for laboratory trial 64
3.1.3 Olive fruit for commercial factory trial 65
3.2 Postharvest assessments 65
3.2.1 Dry matter determination for avocado fruit 65
3.2.2 Dry matter determination for avocado/olive pulp 65
3.2.3 Firmness measurement for avocado fruit 66
3.2.4 Firmness measurement for olive fruit 66
3.3 Cold-pressed oil extraction 66
3.3.1 Commercial cold-pressed extraction of avocado oil 66
3.3.2 Laboratory based cold-pressed extraction of avocado oil 68
3.3.3 Commercial cold-pressed extraction of olive oil 70
3.3.4 Determination of the cold-pressed oil yield at each stage of malaxing in the commercial trial 71
3.4 Ultrasound treatment 72
3.4.1 Ultrasound treatment without malaxing 72
3.4.2 Ultrasound treatment with malaxing 73
3.5 Total oil content measurement 73
3.6 Electrical impedance measurements 75
3.6.1 Electrical impedance measurements for commercial factory trial 75
3.6.2 Electrical impedance measurements for laboratory trial 76

3.6.3 Effect of sample storage time on impedance measurements 76
3.7 Electrical conductivity measurements 77
3.7.1 Electrical conductivity measurements for commercial factory trial 77
3.7.2 Electrical conductivity measurements for laboratory trial 77
3.7.3 Effect of sample storage time on electrical conductivity measurements 78
3.8 Light microscopy 78
3.8.1 Samples embedded in London Resin (LR) White resin 78
3.8.2 Samples embedded in Spurr's resin 79
3.9 Rheological properties measurements 80
3.9.1 Rheological profiling of avocado pulp during laboratory based malaxing 80
3.9.2 Rheological profiling of avocado pulp during malaxing in rheometer 81
3.9.3 Rheological profiling of olive pulp during malaxing in commercial factory 82
3.9.4 Effect of olive pulp sample storage time on rheological measurements 82
3.10 Cell wall isolation and sequential extraction 83
3.10.1 Water-soluble fraction 83
3.10.2 Cell wall material 86
3.10.3 CDTA-soluble fraction 86
3.11 Oil quality analysis 87
3.11.1 Peroxide value 87
3.11.2 Free fatty acids 87
3.12 Statistical Analysis 88
Chapter 4: Cellular changes in 'Hass' avocado mesocarp during commercial cold-pressed oil extraction 90
4.1 Introduction 91
4.2 Experimental design 92
4.2.1 Effect of sample storage time on electrical impedance and conductivity measurements from laboratory based experiments 92
4.2.2 Cellular changes in 'Hass' avocado mesocarp during commercial cold-pressed oil extraction 94
4.3 Results and discussion 96
4.3.1 Effect of sample storage time on electrical impedance and conductivity measurements from laboratory based experiments 96
4.3.2 Cellular changes in 'Hass' avocado mesocarp during commercial cold-pressed oil extraction 99
4.4 Conclusions 113

Chapter 5: Effect of fruit ripeness and maturity on microstructural changes and oil yield during cold-pressed oil extraction of 'Hass' avocado 114

5.1 Introduction 115

5.2 Experimental design 117

5.2.1 Effect of fruit ripeness on microstructural changes and oil yield during laboratory based cold-pressed extraction 117

5.2.2 Effect of fruit maturity on microstructural changes and oil yield during commercial cold-pressed extraction 119

5.3 Results and discussion 122

5.3.1 Effect of fruit ripeness on laboratory cold-pressed avocado oil extraction 122

5.3.2 Effect of fruit maturity on commercial cold-pressed avocado oil extraction 134

5.4 Conclusions 147

Chapter 6: Effect of malaxing conditions and ultrasound treatment on microstructural changes, rheological characterization and cold-pressed oil yield 148

6.1 Introduction 149

6.2 Experimental design 150

6.2.1 Effect of malaxing temperature on microstructural changes and oil yield during laboratory based (1L malaxer) cold-pressed extraction 150

6.2.2 Effect of malaxing temperature on rheological properties and oil yield during malaxing in rheometer (50mL malaxer) 152

6.2.3 Effect of ultrasound treatments on microstructural changes and oil yield during laboratory based cold-pressed extraction 154

6.3 Results and discussion 157

6.3.1 Effect of malaxing temperature on cold-pressed avocado oil extraction 157

6.3.2 Effect of ultrasound treatment on cold-pressed avocado oil extraction 171

6.4 Conclusions 179

Chapter 7: Cellular changes in 'J5' olive mesocarp during commercial cold-pressed oil extraction 180

7.1 Introduction 181

7.2 Experimental design 182

7.2.1 Effect of sample storage time on electrical impedance, conductivity and rheology measurements from laboratory based experiments 182

7.2.2 Cellular changes in 'J5' olive mesocarp during commercial cold-pressed oil extraction 184

7.3 Results and discussion 186

7.3.1 Effect of sample storage time on electrical impedance, conductivity and rheological measurements 186

7.3.2 Cellular changes in 'J5' olive mesocarp during commercial cold-pressed oil extraction 189
7.4 Conclusions 203
Chapter 8: Overall discussion 204
8.1 Factors affecting 'Hass' avocado cold-pressed oil yield and quality 205
8.2 Techniques for monitoring microstructural changes and oil aggregation 210
8.3 Improvements of cold-pressed avocado oil extraction process for the factory 215
Chapter 9: Overall conclusions and recommendations for future work 219
9.1 Overall conclusions 220
9.2 Recommendations for future work 221
References 223
Appendices 244

List of Figures

Figure 2.1: Lipid content and dry matter content of 'Hass' avocado fruit harvested in 1998/1999 season from a New Zealand orchard (Woolf et al., 2007). 11
Figure 2.2: Low-magnification electron micrograph of a thin section of avocado mesocarp, original magnification×640 (Platt-Aloia & Thomson, 1992). 13
Figure 2.3: Electron micrograph of a thin section through a portion of the cell wall of parenchyma cells from avocado mesocarp, original magnification ×10000 (Platt-Aloia et al., 1980). 14
Figure 2.4: Electron micrograph of a thin section through a portion of the cell wall of an idioblast oil cell from avocado mesocarp, original magnification ×12100 (Platt-Aloia & Thomson, 1992). 15
Figure 2.5: Changes in fruit mass of 'Hass' avocado in 2004/2005 season from a New Zealand orchard (Dixon et al., 2006). 16
Figure 2.6: Postharvest trends in PME (□) and PG (▲) activity in 'Fuerte' avocado fruit (Awad & Young, 1979). 18
Figure 2.7: Postharvest trends in cellulase (△) activity in 'Fuerte' avocado fruit (Awad & Young, 1979). 19
Figure 2.8: Postharvest trends in CO2 (○) and C2H4 (●) production in 'Fuerte' avocado fruit (Awad & Young, 1979). 19
Figure 2.9: Process flow diagram for cold-pressed extraction of avocado oil (Wong et al., 2012). 25
Figure 2.10: Equipment and process of cold-pressed avocado oil extraction system; A) Avocado washer and destoner; B) Grinder; C) Line flash thermal conditioning system; D) Atmosphera malaxers; E) Decanter centrifuge; F) Polishing disk centrifuge; G) Example of a complete cold-pressed extraction process solution from grinder to centrifuge (Costagli & Betti, 2015). 26
Figure 2.11: Schematic diagram of typical Soxhlet apparatus (Dean, 2010). 31
Figure 2.12: Schematic of accelerated solvent extraction system (ThermoScientific, 2012). 33
Figure 2.13: Effect of various process additives on oil yield of early-season 'Hass' avocados (Wong et al., 2012). 35
Figure 2.14: Effect of various enzymes on oil yield of late season 'Hass' avocados (Wong et al., 2012). 36
Figure 2.15: Schematic diagram of various types of ultrasonic systems: a) ultrasonic bath; b) batch type probe system and c) continuous probe system used for liquid food processing (Zinoviadou et al., 2015). 37
Figure 2.16: Typical changes in dry matter content, total oil content and commercial cold-pressed yield over a commercial harvest and oil extraction season in New Zealand 'Hass' avocados (Woolf et al., 2009). 40
Figure 2.17: Mean incidence of sound 'Hass' avocado fruit as a percentage of total ripe fruit processed in the oil factory following up to 7 weeks in storage at 6 °C (Woolf et al., 2009). 43
Figure 2.18: The complex impedance plotted as a planar vector using rectangular and polar coordinates (Lvovich, 2012). 47
Figure 2.19: Pattern diagram of plant cells and flow of the electric current (Ando et al., 2014). 49
Figure 2.20: Impedance of fruit sample before (●) and after (○) cell disruption over a

frequency range between 50 Hz and 1MHz (Ohnishi et al., 2004). 50
Figure 2.21: Nyquist plot of fruit sample before (●) and after (○) cell disruption over a frequency range between 50 Hz and 1MHz (Ohnishi et al., 2004). 50
Figure 2.22: Process flow diagram for cold-pressed extraction of virgin olive oil (Wong et al., 2012). 60
Figure 3.1: Process flow diagram for commercial cold-pressed extraction of avocado oil. .....**Error! Bookmark not defined.**
Figure 3.2: Process flow diagram for laboratory based cold-pressed extraction of avocado oil. 69
Figure 3.3: Process flow diagram for commercial cold-pressed extraction of olive oil.71
Figure 3.4: Sonic-650WT ultrasonic processor (MRC Ltd, 2018). 72
Figure 3.5: ASE 300 Accelerated Solvent Extractor (ThermoScientific, 2018)..... 74
Figure 3.6: The system for electrical impedance measurement (Ando et al., 2014). 75
Figure 3.7: Discovery HR-3 hybrid rheometer with a starch pasting cell (TA Instruments, 2018). 81
Figure 3.8: Flow diagram for the experimental procedure to extract water-soluble fraction and cell wall materials from avocado pulp sample..... 85
Figure 4.1: Process flow diagram for the laboratory based experiment looking at the effect of sample storage time on electrical impedance and conductivity measurements for cold-pressed 'Hass' avocado oil extraction. Electrical impedance and electrical conductivity measurement were carried out on samples collected at each sampling point during the extraction process. 93
Figure 4.2: Flow diagram for the experimental procedure to investigate cellular changes during commercial cold-pressed oil extraction for 'Hass' avocado. Light microscopy observation, electrical impedance measurement, electrical conductivity measurement and cold-pressed oil yield determination were carried out for samples collected at each sampling point during the extraction process. 95
Figure 4.3: Comparison of electrical resistance of 'Hass' avocado pulp tissue at 50 Hz, 10 kHz and 1 MHz before and after 4 h storage at 4 ± 1 °C (mean ± SE, n = 3)..... 97
Figure 4.4: Comparison of electrical conductivity of 'Hass' avocado pulp tissue before and after 4 h storage at 4 ± 1 °C (mean ± SE, n = 3)..... 98
Figure 4.5: Resistance (Ω) of 'Hass' avocado flesh during commercial cold-pressed oil extraction at various stages of the oil extraction process (a) Resistance range 0–1500 Ω with 'Intact flesh' sample (mean ± SE, n = 10); (b) data is replotted for the resistance range 150–550 Ω without 'Intact flesh' (mean ± SE, n = 3). 101
Figure 4.6: Nyquist plot of avocado flesh during cold-pressed oil extraction (mean ± SE, n = 3)..... 104
Figure 4.7: Reactance (Ω) of 'Hass' avocado flesh during commercial cold-pressed oil extraction at various stages of the oil extraction process (mean ± SE, n = 3)..... 106
Figure 4.8: Electrical conductivity (µS/cm) of 'Hass' avocado flesh during cold-pressed oil extraction at various stages in the oil extraction process (mean ± SE, n = 3)..... 107
Figure 4.9: Light microscopy images of the microstructure of (a) intact avocado flesh embedded in LR White resin, (b) intact avocado flesh embedded in Spurr's resin, (c) pulp after destoning embedded in LR White resin, (d) pulp after destoning embedded in Spurr's resin, (e) pulp after grinding embedded in LR White resin, (f) pulp after grinding embedded in Spurr's resin. Cell walls stain blue in the LR White embedded tissue, lipid from parenchyma cells shows a grey colouration in the Spurr's embedded material. . 110
Figure 4.10: Light microscopy images of the microstructure of (a) pulp at 0 min malaxing embedded in LR White resin, (b) pulp at 0 min malaxing embedded in Spurr's resin, (c)

pulp after 60 min malaxing embedded in LR White resin, (d) pulp after 60 min malaxing embedded in Spurr's resin, (e) pulp after 120 min malaxing embedded in LR White resin, (f) pulp after 120 min malaxing embedded in Spurr's resin. 111
Figure 4.11: Light microscopy images of the microstructure of (a) pomace from decanter embedded in LR White resin, (b) pomace from decanter embedded in Spurr's resin, (c) waste water from decanter embedded in LR White resin, (d) waste water from decanter embedded in Spurr's resin. 112
Figure 5.1: 'Hass' avocado fruits at the three different stages of ripening; 55, 80 and 105 Fv. 117
Figure 5.2: Flow diagram for the experimental procedure to investigate the effect of fruit ripeness on microstructural changes and oil yield during laboratory based cold-pressed extraction. Electrical impedance measurement, electrical conductivity measurement and light microscopy observation were carried out at each sampling point during the extraction process. 118
Figure 5.3: Flow diagram for the experimental procedure to investigate the effect of fruit maturity on microstructural changes and oil yield during commercial cold-pressed extraction. Electrical impedance measurement, electrical conductivity measurement and light microscopy observation were carried out at each sampling point during the extraction process. 120
Figure 5.4: Free fatty acid content (FFA%) and peroxide value (PV) for oil extracted from 'Hass' avocado fruits ripened to different firmness; 55, 80 and 105 Fv after laboratory based cold-pressed oil extraction (mean ± SE, n = 3)..... 124
Figure 5.5: Resistance (Ω) of 'Hass' avocado flesh from fruit at three fruit firmness stages (55, 80, 105 Fv) (a) Resistance range 200–2000 Ω with intact 'Hass' avocado sample (mean ± SE, n = 10). Graphs (b), (c), and (d) show the resistance range 180–380 Ω with avocado pulp; (b) 0 min malaxing (after grinding); (c) after 60 min malaxing; (d) after 120 min malaxing' (mean ± SE, n = 3)..... 127
Figure 5.6: Electrical conductivity (µS/cm) of 'Hass' avocado flesh and pulp samples from fruit at three fruit firmness stages (55, 80, 105 Fv; mean ± SE, n = 3). Pulp samples collected during laboratory based cold-pressed oil extraction 129
Figure 5.7: Laboratory based cold-pressed oil yield of malaxed 'Hass' avocado pulp samples at 55, 80 and 105 Fv as a function of (a) electrical resistance (Ω; at 50 Hz) and electrical conductivity (µS/cm) of avocado pulp collected at 0 min malaxing. 130
Figure 5.8: Light microscopy images of the microstructure of parenchyma and idioblast cells in intact 'Hass' avocado mesocarp at different firmness, (a) parenchyma cells at 55 Fv, (b) parenchyma cells at 80 Fv, (c) parenchyma cells at 105 Fv, (d) idioblast cell at 55 Fv, (e) idioblast cell at 85 Fv, (f) idioblast cell at 105 Fv. 132
Figure 5.9: Light microscopy images of the microstructure of 'Hass' avocado flesh at different firmness, (a) 0 min malaxing, 55 Fv, (b) 0 min malaxing, 80 Fv, (c) 0 min malaxing, 105 Fv, (d) 60 min malaxing, 55 Fv, (e) 60 min malaxing, 80 Fv, (f) 60 min malaxing, 105 Fv, (g) 120 min malaxing, 55 Fv, (h) 120 min malaxing, 80 Fv, (i) 120 min malaxing, 105 Fv. 133
Figure 5.10: Changes in 'Hass' avocado fruit flesh dry matter content % (g dry flesh/100 g fresh flesh), total oil % present in flesh (g oil/100 g fresh flesh; determined by ASE solvent extraction) and commercial cold-pressed extraction oil yield% (g oil/100 g fresh flesh) over the 2016-2017 commercial harvest and oil processing season in New Zealand (mean ± SE, n = 3)..... 135
Figure 5.11: Resistance (Ω) of 'Hass' avocado flesh from fruit at six different stages of maturity (harvested between September to April 2016/17 season) (a) Resistance range

200–2000 Ω with intact 'Hass' avocado flesh sample (mean ± SE, n = 10); Resistance range 180–550 Ω with avocado pulp (b) At 0 min malaxing (after grinding); (c) At 60 min malaxing; (d) At 120 min malaxing (mean ± SE, n = 3). 138
Figure 5.12: Electrical conductivity (µS/cm) of 'Hass' avocado flesh and pulp samples from fruit at six different stages of maturity (mean ± SE, n = 3). Pulp samples collected during commercial cold-pressed oil extraction 139
Figure 5.13: Commercial cold-pressed oil yield of malaxed 'Hass' avocado pulp samples at six different stages of maturity as a function of (a) electrical resistance (Ω; at 50 Hz) and electrical conductivity (µS/cm) of avocado pulp collected at 0 min malaxing. 140
Figure 5.14: Representative light microscopy images of the microstructure of 'Hass' avocado pulped flesh at three different stage of maturity (a) early-season (September), 0 min malaxing; (b) mid-season (December), 0 min malaxing; (c) late-season (March), 0 min malaxing; (d) early-season, 120 min malaxing; (e) mid-season, 120 min malaxing; (c) late-season, 120 min malaxing. Cell walls were stained with toluidine blue staining. 142
Figure 5.15: Representative light microscopy images of the microstructure of pomace from decanting centrifuge at three different stage of maturity (a) early-season (September), (b) mid-season (December), (c) late-season (March). Cell walls were stained with toluidine blue staining. 143
Figure 5.16: Polysaccharide yields of (a) water- and (b) CDTA-soluble fractions of 'Hass' avocado pulp samples at three different stages of maturity (mean ± SE, n = 3). Pulp samples collected during commercial cold-pressed oil extraction 146
Figure 6.1: Flow diagram for the experimental procedure to investigate the effect of malaxing temperature on microstructural changes and oil yield during laboratory based cold-pressed extraction. Electrical impedance measurement, electrical conductivity measurement, light microscopy observation and viscosity measurement were carried out at each sampling point during the extraction process. 151
Figure 6.2: Flow diagram for the experimental design to investigate the effect of malaxing conditions on rheological properties and oil yield during malaxing on rheometer. 153
Figure 6.3: Flow diagram for the experimental design to investigate the effect of ultrasound treatments on microstructural changes and oil yield during laboratory based cold-pressed extraction. 155
Figure 6.4: Percentage of free fatty acids (FFA%) and peroxide value (PV) for oil extracted from 'Hass' avocado fruit (harvested in October 2016) at 30, 40 and 50 ℃ malaxing temperature during laboratory based cold-pressed oil extraction (mean ± SE, n = 3)..... 159
Figure 6.5: Resistance (Ω) of 'Hass' avocado pulp tissue at various stage during malaxing at three different temperatures (30, 40 and 50 ℃), (a) At 0 min malaxing (after grinding); (b) At 60 min malaxing; (c) At 120 min malaxing' (mean ± SE, n = 3)..... 161
Figure 6.6: Electrical conductivity (µS/cm) of 'Hass' avocado pulp tissue at the various stages during malaxing at three different temperatures (30, 40 and 50 ℃) (mean ± SE, n = 3)..... 162
Figure 6.7: Light microscopy images of the microstructure of 'Hass' avocado pulp tissue at 0 min malaxing (after grinding)..... 163
Figure 6.8: Light microscopy images of the microstructure of 'Hass' avocado pulp tissue at three different temperatures (a) 30 ℃, 60 min malaxing, (b) 30 ℃, 120 min malaxing, (c) 40 ℃, 60 min malaxing, (d) 40 ℃, 120 min malaxing, (e) 50 ℃, 60 min malaxing, (f) 50 ℃, 120 min malaxing. 164

Figure 6.9: Change of apparent viscosity at a shear rate of 40 s^{-1} for 'Hass' avocado pulp during laboratory based cold-pressed oil extraction at 30, 40 and 50 ℃ (mean ± SE, n = 3). 166
Figure 6.10: Changes of the apparent viscosity (Pa·s) of 'Hass' avocado pulp during malaxing at 20 rpm for 120 min in a rheometer with concentric cylinder geometry at different malaxing temperatures (mean, n = 3). 167
Figure 6.11: Changes of the G', G'' (Pa) of 'Hass' avocado pulp over a range of frequencies from 0.01 to 10 Hz and at a constant strain of 0.5% after malaxing in rheometer for (a) 30 min; (b) 60 min and (c) 120 min at 30, 40 and 50 °C (mean ± SE, n = 3)..... 169
Figure 6.12: 'Hass' avocado extraction oil yield after ultrasound treatment at 20–25 kHz for 0 to 25 min at 45 °C, without a malaxing step (mean ± SE, n = 3). 172
Figure 6.13: Resistance (Ω) of 'Hass' avocado pulp before and after ultrasound treatment at 20–25 kHz for 5 to 25 min without malaxing step (mean ± SE, n = 3)..... 173
Figure 6.14: Electrical conductivity (µS/cm) of 'Hass' avocado pulp tissue before and after ultrasound treatment at 20–25 kHz for 5 to 25 min without malaxing step (mean ± SE, n = 3). 174
Figure 6.15: Changes of the G', G'' (Pa) of 'Hass' avocado pulp after ultrasound treatment at 20–25 kHz for 5 to 25 min without malaxing step (mean ± SE, n = 3). .. 175
Figure 6.16: 'Hass' avocado extraction oil yield effect without and with (20–25 kHz) ultrasound treatment (20 min) at various malaxing times for 20, 40 and 60 min (mean ± SE, n = 3). 176
Figure 6.17: Changes of the G', G'' (Pa) of 'Hass' avocado pulp after malaxing for a) 20 min; b) 40 min and c) 60 min at 45 °C, with and without 20 min ultrasound treatment at 20–25 kHz (mean ± SE, n = 3). 178
Figure 7.1: Flow diagram for the experimental procedure to investigate the effect of sample storage time on electrical impedance, conductivity and rheological measurements for virgin olive oil extraction. Electrical impedance measurement, electrical conductivity measurement and rheological measurement were carried out at each sampling point during the extraction process. 183
Figure 7.2: Flow diagram for the experimental procedure to investigate cellular changes during commercial cold-pressed oil extraction for 'J5' olive fruit. Electrical impedance measurements, electrical conductivity measurements, light microscopy observations, cold-pressed oil yield determination and rheological measurements were carried out at each sampling point during the extraction process. 185
Figure 7.3: Comparison of resistance of 'J5' olive pulp tissue at 50 Hz, 10 kHz and 1 MHz before and after 4 h storage at 4 ± 1 °C (mean ± SE, n = 3). 188
Figure 7.4: Comparison of electrical conductivity of 'J5' olive pulp tissue before and after 4 h storage at 4 ± 1 °C (mean ± SE, n = 3). 188
Figure 7.5: Comparison of viscoelastic properties (G', G'') of 'J5' olive pulp tissue at 0.1 Hz, 1 Hz and 10 Hz before and after 4 h storage at 4 ± 1 °C (mean ± SE, n = 3)..... 189
Figure 7.6: Resistance (Ω) determined by electrical impedance spectroscopy of 'J5' olive flesh (mean ± SE, n = 10) and pulp (mean ± SE, n = 3) before grinding and at various times during the oil extraction process. 192
Figure 7.7: Nyquist plot of 'J5' olive flesh and pulp during cold-pressed oil extraction at various stages of the oil extraction process (mean ± SE, n = 3). 193
Figure 7.8: Electrical conductivity (µS/cm) of 'J5' olive flesh during cold-pressed oil extraction at various stages of oil extraction process (mean ± SE, n = 3). 194

Figure 7.9: Microstructure of intact 'J5' olive flesh under light microscopy. (a) Image from samples embedded in LR white resin, cell walls stain blue by toluidine blue staining in the LR White embedded tissue. (b) Image from samples embedded in Spurr's resin, oil from parenchyma cells shows a grey colouration by osmium tetroxide fixation/staining of the Spurr's embedded material. 195
Figure 7.10: Microstructure of 'J5' olive paste (a) at 0 min malaxing, embedded in LR White resin, (b) at 0 min malaxing, embedded in Spurr's resin, (c) after 30 min malaxing, embedded in LR White resin, (d) after 30 min malaxing, embedded in Spurr's resin, (e) after 60 min malaxing, embedded in LR White resin, (f) after 60 min malaxing, embedded in Spurr's resin. 197
Figure 7.11: Microstructure of 'J5' olive pulp after 60 min malaxing at 26 °C (a) and 'Hass' avocado pulp after 60 min malaxing at 45 °C (b) under light microscopy. Images were from samples embedded in Spurr's resin. 198
Figure 7.12: Microstructure of pomace and wastewater under light microscopy, (a) pomace, embedded in LR White resin, (b) pomace, embedded in Spurr's resin, (c) wastewater, embedded in LR White resin, (d) wastewater, embedded in Spurr's resin. 199
Figure 7.13: Rheological properties (G', G'') of 'J5' olive pulp during factory based malaxing (mean ± SE, n = 3). 200
Figure 7.14: Viscoelastic properties of 'J5' olive paste during commercial oil extraction evaluated at a constant frequency (1 Hz) as a function of average oil droplet size (D) in malaxed olive paste samples (mean ± SE, n = 3). 201
Figure 7.15: Comparison of viscoelastic properties (G', G'') of 'J5' olive pulp tissue and 'Hass' avocado pulp tissue during malaxing (mean ± SE, n = 3) in commercial extraction. 202

List of Tables

Table 2.1: Production of avocados in the main avocado-growing countries in 2006, 2011 and 2016 (FAOSTAT, 2018). 8
Table 2.2: Effect of 'Hass' avocado fruit ripeness on oil yield (% of flesh tissue) and quality (FFA%) (Woolf et al., 2009). 41
Table 2.3: 'Hass' avocado oil quality as measured by FFA% (FFA% w/w; as oleic acid) immediately following extraction from fruit with a range of fruit disorders including body rots, bruising, and greying (Woolf et al., 2009). 42
Table 2.4: Fatty acids composition of 'Hass' avocado oil from five countries (Woolf et al., 2009). 55
Table 2.5: Changes in oil droplet size during malaxing for 90 min (Di Giovacchino et al., 2002a; Di Giovacchino et al., 2002b). 61
Table 4.1: Total available oil and extraction yield from commercial cold-pressed 'Hass' avocado oil extraction and from samples collected during the extraction process (mean ± SE, n = 3). 100
Table 5.1: 'Hass' avocado fruit flesh dry matter, total oil present in flesh (determined by ASE solvent extraction) and laboratory based cold-pressed extraction oil yield for fruit ripened at different firmness; 55, 80 and 105 Fv (mean ± SE, n = 3). 123
Table 6.1: 'Hass' avocado laboratory based cold-pressed extraction oil yield at 30, 40 and 50 ℃ during malaxing, total oil present in flesh (determined by ASE solvent extraction) and fruit flesh dry matter (mean ± SE, n = 3) for fruit harvested at different maturity in the season; early-season (October 2016, August 2017), mid-season (December 2016) and late-season (March 2017) 158
Table 7.1: Total available oil and extraction yield from commercial cold-pressed 'J5' olive extraction and from samples collected during the extraction process (mean ± SE, n = 3)..... 191

List of Abbreviations

ASE	accelerated solvent extraction
C16:0	palmitic acid
C16:1	palmitoleic acid
C18:0	stearic acid
C18:1	oleic acid
C18:2	linoleic acid
C18:3	linolenic acid
CDTA	trans-1,2-diaminocyclohexane-N,N,N',N'-tetraacetic acid
DAG	diacylglycerols
EC	European Commission
EIS	electrical impedance spectroscopy
FFA	free fatty acids
FFA%	free fatty acids levels/content (as oleic acid)
Fv	firmometer value
g	gravitational acceleration (m/s^2)
G'	storage/elastic modulus
G"	loss/viscous modulus
IOC	International Olive Council
LR White resin	London Resin White resin
K_{232}	the oil absorbance at 232 nm
K_{270}	the oil absorbance at 270 nm
PG	polygalacturonase
PME	pectin methyl esterase
PV	peroxide values

SPC	starch pasting cell
TAG	triacylglycerols

Chapter 1:

Introduction

Cold-pressed avocado oil has valuable nutritional properties, including a high level of unsaturated fatty acids, pigments (chlorophylls and carotenoids), sterols and tocopherols (Eyres, Sherpa, & Hendriks, 2001). In 2000, New Zealand companies began the commercial production of cold-pressed avocado oil for the culinary market, extracting the oil from the flesh of 'Hass' (*Persia americana* Mill.) avocados using an aqueous extraction process (Woolf et al., 2009). The commercial aqueous extraction process for avocado oil is based on the continuous virgin olive oil extraction process, which primarily uses only mechanical means of extraction, including washing, grinding, malaxing (slow mixing) and centrifugation (Wong, Eyres, & Ravetti, 2012). The temperature of the avocado pulp during malaxing is controlled between 45 and 50 °C, the malaxing time can vary from 60 to 120 min depending on the time in the season (Wong et al., 2012).

While there is some oil in the avocado skin and seed (Wong, Requejo-Jackman, & Woolf, 2010), the oil extracted in the cold-pressed process is located in the mesocarp of avocado fruit, which consists primarily of parenchyma cells (≈ 98%) with minor quantities of idioblast cells and a few vascular strands (Platt-Aloia & Thomson, 1981; Platt-Aloia, Thomson, & Young, 1980). The ultrastructural changes of avocado mesocarp during the aqueous cold-pressed extraction process have not been studied. Cold-pressed oil extraction from olive fruit is very similar process to that of avocado oil (Woolf et al., 2009). It has been hypothesized that the fruit cells in olive fruit are disrupted to release the droplets of oil from the vacuoles by grinding and the oil/water emulsions are then broken up during malaxing so that the oil droplets merge to form larger droplets (Petrakis, 2006). In olive oil extraction, the oil extraction yield also increased significantly when malaxing time increased from 15 to 90 min (Di Giovacchino, Costantini, Ferrante, & Serraiocco, 2002a; Di Giovacchino, Sestili, & Di Vincenzo, 2002b).

Extraction of oil from early season avocado fruit flesh by mechanical means currently used in commercial oil extraction results in a relatively low oil extraction efficiency relative to the total oil present in the flesh (Wong et al., 2012; Woolf et al., 2009). The cold-pressed avocado oil yield can be affected by various factors including fruit ripening, fruit maturity and malaxing conditions (Woolf et al., 2009). Various techniques have been tried to alleviate the low oil yields early in the season including the use of exogenous enzymes in the malaxing step to assist with cellular breakdown. Unlike olives, avocado oil processors use product rejected from the fresh fruit industry, and thus harvest timing cannot be prescribed by the processor leading to poor (or even uneconomic) returns for processing early season fruit for cold-pressed oil. Hence it is important for the oil industry to identify strategies to increase oil yields by understanding how postharvest factors of fruit and processing conditions affect microstructural changes and oil aggregation during cold-pressed oil extraction of 'Hass' avocado. New techniques such as ultrasound treatment have potential as a novel technique in cold-pressed avocado oil extraction process to improve the cold-pressed oil yield.

Various techniques can be applied to monitor the changes in microstructure of avocado flesh and oil aggregation during cold-pressed oil extraction process. Analysis of microscope images is commonly used to determine the intactness and size of the cells as well as the degree of oil aggregation in the fruit pulp (Platt-Aloia, Oross, & Thomson, 1983; Platt-Aloia & Thomson, 1981). Electrical conductivity is a measure of the concentration of ions in a solution; after incubating fruit tissue for a given period, conductivity can give an estimate of the degree of electrolyte leakage from cells in a fruit tissue and thus can indicate the degree of cell wall and membrane integrity in a fruit tissue sample (Palta, Levitt, & Stadelmann, 1977). Electrical impedance spectroscopy (EIS) and

rheological properties measurement are new alternative methods to the traditional microscopy and conductivity analysis methods and are relatively simple, providing rapid results. Thus, these alternative techniques will be investigated to be used for monitoring oil extraction and aggregation in avocado pulp, something that has not been carried out in avocado oil extraction.

Cold-pressed olive oil extraction is a very similar process to the process used for 'Hass' avocado oil extraction. The main differences between the oil extraction process for olive and avocado are the malaxing temperature and time. Cold-pressed olive oil extraction must be carried out at no higher than 27 °C (to be classified as extra virgin) and the malaxing time is normally less than 90 min (Codex Alimentarius, 2017; European Commission, 2002; International Olive Council, 2006; Petrakis, 2006; Wong et al., 2012). The microstructural changes in olive mesocarp can also be investigated to understand the impact of each step in the extraction process on cellular disruption and oil aggregation using the measurement techniques used to study the avocado oil process.

The overall aim of this project was to understand cellular changes during cold-pressed 'Hass' avocado oil extraction with respect to improving oil yield. The specific objectives of this project were to:

1. Monitor the cellular changes and oil aggregation in fruit tissue during processing of 'Hass' avocado and, as a comparison, 'J5' olive fruit for cold-pressed oil extraction, looking at how each step in the process affects oil release from the tissue.

2. Investigate the effect of ‘Hass’ avocado fruit ripeness, fruit maturity and malaxing temperature on microstructural changes and oil aggregation in fruit tissue during cold-pressed oil extraction.
3. Develop rapid techniques, including EIS and rheological properties measurements, for monitoring the degree of cellular disruption and oil aggregation in fruit pulp tissue during the cold-pressed oil extraction of ‘Hass’ avocado and ‘J5’ olive fruit in a commercial oil factory.
4. Investigate the potential application of ultrasound treatments for oil separation during cold-pressed oil extraction of ‘Hass’ avocado.

Chapter 2:

Literature review

2.1 Overview of avocado fruit

2.1.1 Avocado fruit production

The avocado (*Persea americana* Mill.) is a high oil content fruit originating in Mexico and Central America and classified as a member of the flowering plant family Lauraceae (Schaffer, Wolstenholme, & Whiley, 2013). Avocados are generally grown in frost-free subtropical regions. Historically, the avocado is also known as alligator pear, vegetable butter, butter pear and midshipman's butter (Yahia & Woolf, 2011). The major cultivars produced worldwide in approximate order of priority are 'Hass', 'Fuerte', 'Ryan', 'Pinkerton' and 'Edranol' (Avocadosource, 2006).

Avocado fruit are comprised of the skin (exocarp), the flesh (mesocarp), and the seed (stone or pit). The flesh comprises 50–80% of the total fruit weight depending on the cultivar, while the seed makes up 10–25% of the total fruit weight (Lewis, 1978). On average, a ripe 'Hass' avocado consists of 68% flesh, 18% seed and 14% skin on a fresh weight basis (Wong et al., 2008).

From 2006 to 2016, world production of avocado increased 1.5 fold from 3.62 million tons to 5.57 million tons (FAOSTAT, 2018). Worldwide avocado production in 2006, 2011 and 2016 is summarised in Table 2.1. The main avocado producers are Mexico, Dominican Republic, Peru, Colombia, Indonesia, Brazil, Kenya and United States. The majority of the avocado-growing countries are primarily producers for domestic consumption while exporting less than 10% of their total production. However, Mexico, Peru and Chile are exceptions to this rule and have industries geared towards export (Paz-Vega, 2015). In New Zealand, export of fresh avocado fruit in 2015 accounted for 79% of total production (Plant & Food Research Ltd., 2015). Overall, approximately 13% of

the global production of avocado is traded internationally (Bost, Smith, & Crane, 2013; Paz-Vega, 2015).

Table 2.1: Production of avocados in the main avocado-growing countries in 2006, 2011 and 2016 (FAOSTAT, 2018).

Country	2006 Production (metric tonnes)	2011 Production (metric tonnes)	2016 Production (metric tonnes)
Mexico	1,134,250	1,264,141	1,889,354
Dominican Republic	216,378	295,081	601,349
Peru	113,259	213,662	455,394
Colombia	191,710	215,089	309,431
Indonesia	239,463	275,953	304,938
Brazil	164,441	160,376	195,492
Kenya	103,935	149,241	176,045
United States	247,000	205,432	172,630
Chile	205,000	156,247	137,365
China	90,000	105,000	122,942
Australia	34,452	36,352	67,600
New Zealand	15,000	21,500	27,003
Worldwide Total	3,619,147	4,173,951	5,567,044

The cultivar 'Hass' constitutes more than 90% of total production in many large avocado-growing countries including Mexico, Chile and the United States, and other smaller avocado-producing countries such as New Zealand, Spain, and Australia (Avocadosource, 2006). For this reason, the 'Hass' cultivar is most likely to be used for avocado oil extraction or other processing (Woolf et al., 2009). The popularity of the 'Hass' cultivar is mostly attributed to its postharvest features (Crane et al., 2013; Schaffer et al., 2013; Whiley, Schaffer, & Wolstenholme, 2002). Its relatively thicker skin and high calcium concentrations in the fruit provide some tolerance to pest and diseases, and excellent storage and shipping ability (Crane et al., 2013; Whiley et al., 2002). Moreover, the

changes in skin colour from green to black can provide an easy index for fruit ripeness, and masks minor rind imperfections (Crane et al., 2013).

2.1.2 Avocado fruit growth and maturation

On average, avocado flesh contains 74.0% moisture, 13.5% lipids, 7.6% total carbohydrate, 2.5% fiber and 1.6% proteins (Dorantes-Alvarez, Ortiz-Moreno, & Garcia-Ochoa, 2012). Lipids and water are thus the two major components of an avocado fruit. Once a fruit has formed on the tree, it slowly matures over approximately ten months and increases in size; the dry matter content and lipid content also increase in the flesh tissue while the moisture content decreases (Kikuta & Erickson, 1968; Lawes, 1980; Pearson, 1975; Wong et al., 2008). In some countries, avocados can be held on tree for a long period due to the climate. For example in New Zealand, fruit hang on the tree for up to 14 months, as avocado trees flower in October, and the fruit forms in November, to be harvested from August to February the following year (Scoular, 2019).

Maturity has two definitions, the first being horticultural maturity where the fruit is harvested at a stage of development that will allow the fruit to meet consumer requirements (ripen to an acceptable taste and overall quality), and the second being physiological maturity where the fruit will continue to physiologically develop (ripen for seed dispersal) after harvest (Watada, Herner, Kader, Romani, & Staby, 1984). Avocados are unique in that they can be horticulturally mature but they do not ripen while attached to the tree, which means the fruit can be "tree-stored" to meet supply chain requirements over an extended period of time.

The dry matter content and the total lipid content in the fruit flesh are highly correlated

(Figure 2.1), thus either can be used as measures of horticultural maturity of avocados (Brown, 1984; Lee, Young, Schiffman, & Coggins, 1983). Measurement of dry matter content is the most common method used by the avocado industry because it is simple, cheap and rapid (Lee & Young, 1983; Lewis, 1978; Morris & O'Brien, 1980; Ranney et al., 1992). Most avocado-producing countries have guidelines for fruit harvest based on horticultural maturity as measured by dry matter. Depending on cultivar and the country of production, the recommended minimum dry matter values range between 20–25% by fresh weight. For example in 2006, the minimum dry matter values for 'Hass' cultivar were 20.8% in Mexico and the United States, 21% in Chile and Australia, 25% in South Africa and 24% in New Zealand (Avocadosource, 2006). Avocado fruit harvested at a low dry matter content is likely to give an undesirable flavour and texture profile. Moreover, the fruit may fail to ripen if it is harvested at very low dry matter values (< 20%) (Brown, 1984; Pak, Dixon, & Cutting, 2003; Ranney et al., 1992).

Depending on the cultivar and the time of harvest, oil content in physiologically mature avocado flesh can range between 10–32% by fresh weight. For 'Hass' avocados, the oil content of the flesh can be as high as 30% by fresh weight, depending on the growing region (Kaiser, Smith, & Wolstenholme, 1992; Requejo-Tapia, 1999). Experiments performed by Requejo-Tapia (1999) in New Zealand showed that the oil content of 'Hass' avocado was 16–17% in September at early season and then increased to 29–31% in April at the end of the season (Figure 2.1).

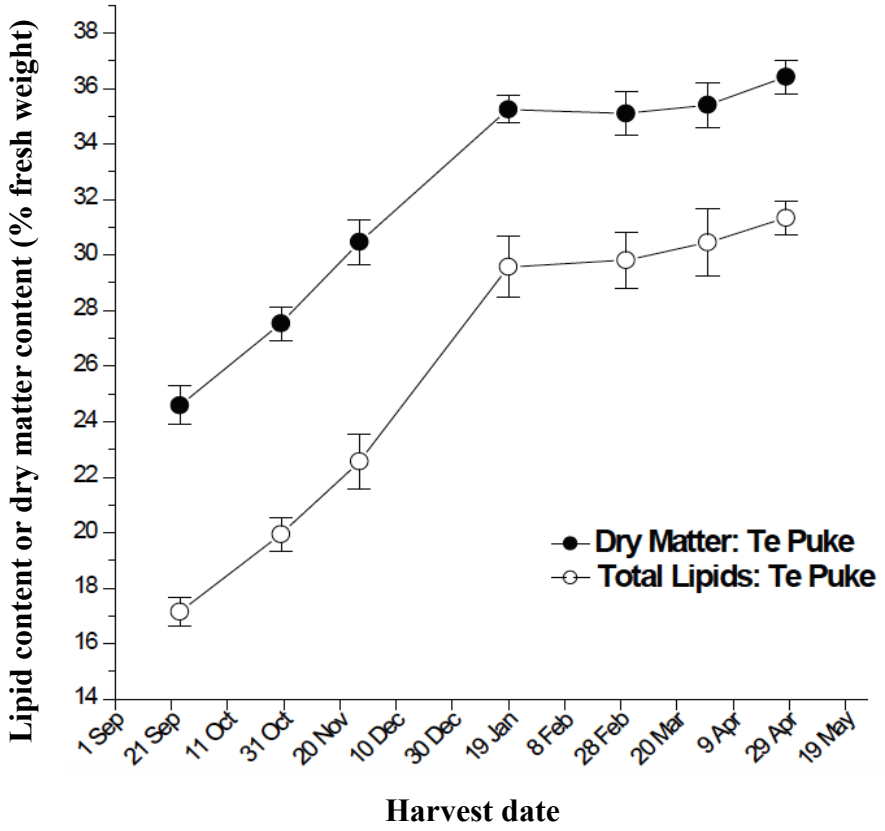

Figure 2.1: Lipid content and dry matter content of 'Hass' avocado fruit harvested in 1998/1999 season from a New Zealand orchard (Woolf et al., 2007).

2.1.3 Postharvest ripening of avocado fruit

As mentioned earlier, avocados have a noteworthy characteristic that they do not ripen while attached on the tree even though they are physiologically mature, and thus can be held on the tree for as long as two years from flowering (Schaffer et al., 2013). As a commercial crop, once avocados have reached the desired horticultural maturity, the fruit are harvested from the tree and then commence ripening, which generally takes around 6–10 days at room temperature. The timing and variability of ripening is influenced by various factors including cultivar, the stage of maturity, storage time, ripening temperature and ethylene exposure. The fruit ripening period can be as short as 3–4 days or as long as 18–21 days (Woolf et al., 2009).

During ripening, the key change observed is fruit softening due to the cell wall degradation of the parenchyma cells (Platt-Aloia et al., 1980; Redgwell et al., 1997). The softening can be measured by compression by hand or by a mechanical device such as a Firmometer and the result reported as fruit firmness (White, Woolf, Hofman, & Arpaia, 2005). To ensure maximum oil yields in avocado oil production, the ripeness of the fruit is required to be equivalent to "firm ripe" which is equal to a hand firmness score of 4 or a Firmometer reading between 65–95 Firmometer value (Fv) (Woolf et al., 2009). To achieve uniform, controlled and faster ripening, ethylene treatment is commonly used by the fresh fruit and oil extraction industries to ripen avocados. Avocado fruit treated with 100 μL^{-1} ethylene at 20–22 °C for 24 h will ripen in approximately four to six days at 20–22 °C (Hofman et al., 2002). During ripening of the main commercial cultivar 'Hass', a distinct change in skin colour from green to black accompanies fruit softening (Cox, McGhie, White, & Woolf, 2004; Williams, 1977). The skin colour changes are more subtle for the majority of other cultivars such as 'Fuerte', 'Ryan' and 'Pinkerton', with a darkening of the green colour from more emerald to darker green (Crane et al., 2013; Woolf et al., 2009).

Low-temperature storage is a common method for fruit storage and transport in the fresh-avocado industry. Cool storage of avocados at 4–8 °C for up to four weeks can reduce the ripening rate and fruit-to-fruit variability (Bower, 1988). However, longer storage periods can cause an internal-chilling injury (vascular browning and diffuse flesh discoloration) and general reduction of ripe-fruit quality. Lower storage temperatures (< 4 °C) can cause external chilling injury (skin scalding) of avocado fruits (Bower, 1988; Cutting & Wolstenholme, 1992; Van Rooyen & Bower, 2006).

2.2 Cellular changes during avocado growth and ripening

2.2.1 Oil localization in avocado fruit

There is a fairly uniform cellular composition in the mesocarp of the avocado fruit, which consists primarily of parenchyma cells, specialized oil cells or idioblasts and a few vascular strands (Figure 2.2; vascular strands are not shown on the figure) (Platt-Aloia & Thomson, 1981). The majority of cells in avocado flesh are parenchyma cells with a diameter of 40–60 µm (Platt-Aloia & Thomson, 1981). The cell walls of parenchyma cells are approximately 2.5 µm thick, composed of a primary cell wall and shared middle lamella (Figure 2.3) (Platt-Aloia et al., 1980). The cell walls are mainly composed of cellulose, pectin and hemicellulose (Gupta, 2007). Approximately 85% of the total lipids present in avocado flesh are triacylglycerols (TAG), which occur as numerous droplets or oil bodies scattered in the cytoplasm of the parenchyma cells (Platt-Aloia & Thomson, 1981).

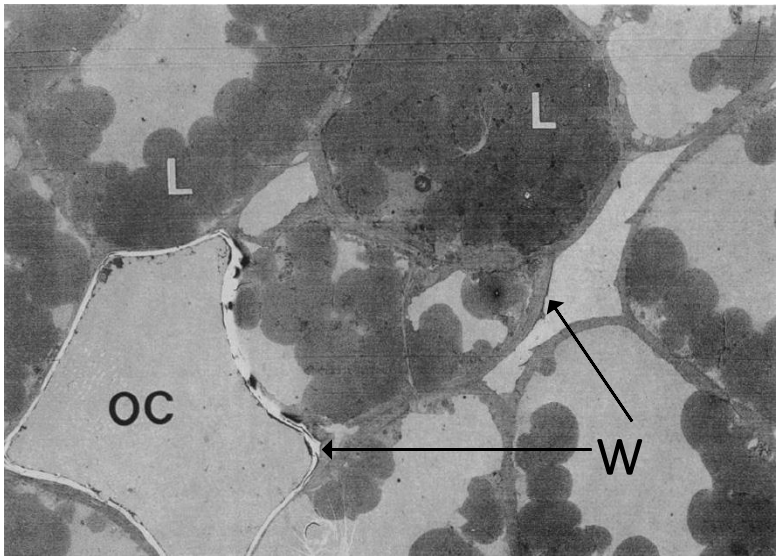

Figure 2.2: Low-magnification electron micrograph of a thin section of avocado mesocarp, original magnification×640 (Platt-Aloia & Thomson, 1992).
L: Oil in parenchyma cells;
OC: Oil in an idioblast oil cell;
W: Cell walls.

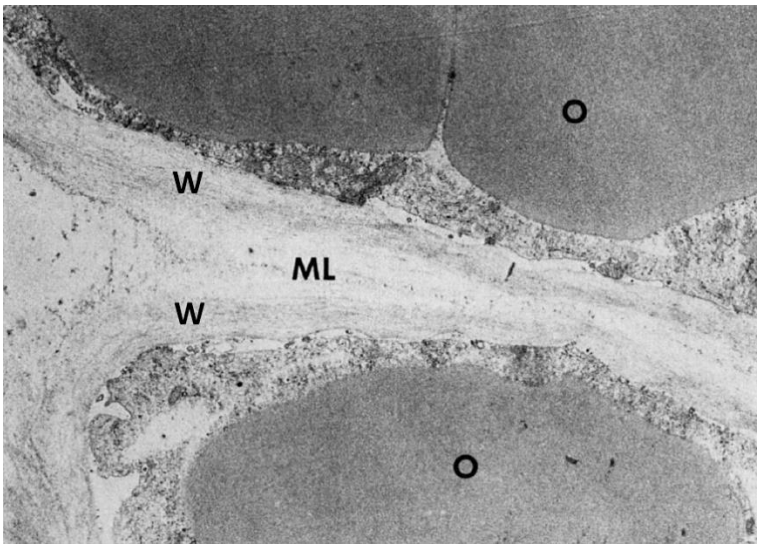

Figure 2.3: Electron micrograph of a thin section through a portion of the cell wall of parenchyma cells from avocado mesocarp, original magnification ×10000 (Platt-Aloia et al., 1980).
ML: The middle lamella in the parenchyma cell;
W: The primary cell wall of the parenchyma cell;
O: Oil in the parenchyma cell.

Idioblast oil cells are scattered throughout the mesocarp of avocado and make up approximately 2% of the tissue volume (Cummings & Schroeder, 1942). Ultrastructural studies showed that the idioblast oil cells are larger than the parenchyma cells with a diameter of approximate 80 µm (Platt-Aloia et al., 1980). In addition, the walls of these specialized oil cells are 4 µm in thickness, consisting of a primary cellulosic wall, a secondary suberin layer and a tertiary cellulosic wall (Figure 2.4) (Platt-Aloia et al., 1983). Rather than the smaller individual oil droplets in the parenchyma cells, the oil in idioblast cells occur as a single large oil body filling the entire cell (Cummings & Schroeder, 1942). The oil in the idioblast cells has a different composition to the oil in the parenchyma cells, which stains with a different density than the TAG of the parenchyma cells when using osmium tetroxide dye, and has a different appearance in freeze-fracture replicas compared with the TAG (Platt-Aloia et al., 1983; Platt-Aloia & Thomson, 1989). The idioblast oil has a polarity less than phospholipids but greater than TAG or diacylglycerols (DAG),

and contains alkaloids, sesquiterpene hydroperoxides and possibly other terpenes (Platt-Aloia & Thomson, 1992). Several of these constituents found in the idioblast cells have the ability to inhibit the in-vitro vegetative growth of the avocado fungal pathogen *Colletotrichum gloeosporioides* (Sivanathan & Adikaram, 1989).

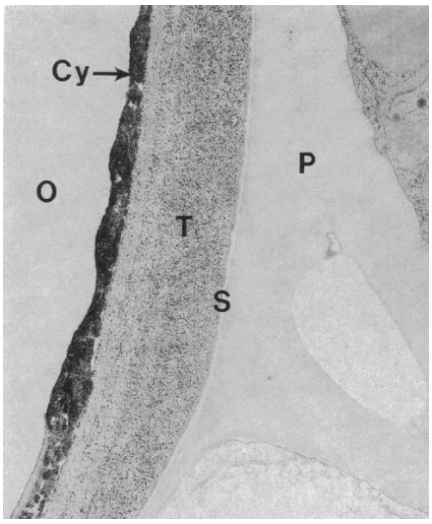

Figure 2.4: Electron micrograph of a thin section through a portion of the cell wall of an idioblast oil cell from avocado mesocarp, original magnification ×12100 (Platt-Aloia & Thomson, 1992).
P: The primary wall of the idioblast oil cell;
S: The secondary suberin layer of the idioblast oil cell;
T: The tertiary wall of the idioblast oil cell;
Cy: Cytoplasm of the idioblast oil cell;
O: Oil in the idioblast oil cell.

In the cold-pressed aqueous extraction process for avocado oil, the parenchyma cells are mostly disrupted during the grinding and malaxing step, however, the fate of the idioblast oil cells has not been determined. The idioblast cells may be broken down during the extraction process, remaining in the solid phase (pomace) or liquid stream (Woolf et al., 2009).

2.2.2 Cell development during fruit growth

A number of researchers have published information on avocado maturity and cell development (Barmore, 1977; Lee & Young, 1983; Moore-Gordon, Cutting, & Wolstenholme, 1994; Schroeder, 1953; Yahia & Woolf, 2011). Avocados are unique in that cell division of the mesocarp parenchyma and idioblast cells continues during fruit development, whereas most other fruit development patterns involve cell replication in the initial stages of fruit growth and then increase in size by taking up water approaching harvest (Woolf et al., 2009).

Seasonal growth of the avocado from full bloom to fruit maturity follows a single sigmoidal growth pattern and can be divided into three major stages (Figure 2.5) (Dixon, Lamond, Smith, & Elmlsy, 2006; Moore-Gordon et al., 1994).

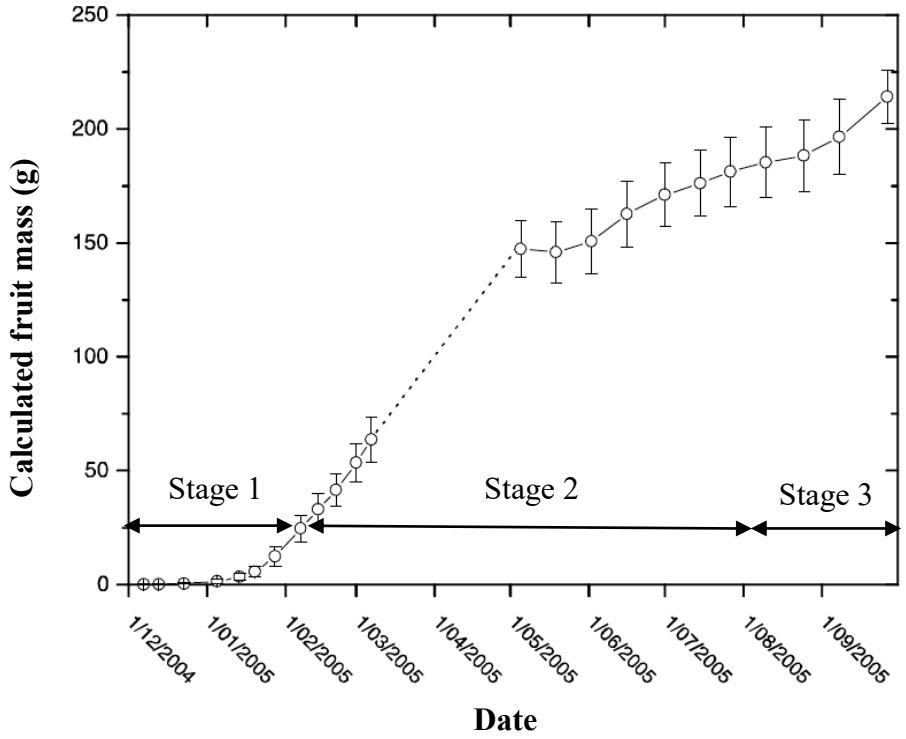

Figure 2.5: Changes in fruit mass of 'Hass' avocado in 2004/2005 season from a New Zealand orchard (Dixon et al., 2006).

During the first stage (0–2 months for ‘Hass’ cultivar), both cell division and cell enlargement occurs though the rate is slow and can involve the "decision" to abort or proceed with further cell replication and fruit development, which is known as fruit set. Approximately 90% of fruit abscission takes place during this initial stage (Dixon et al., 2006; Lee & Young, 1983; Moore-Gordon et al., 1994).

The second stage (3–8 months for ‘Hass’ cultivar) is characterized by rapid cell expansion and cell division, during which 80% of the growth of the fruit takes place (Dixon et al., 2006; Moore-Gordon et al., 1994). Cell enlargement ceases when avocado fruit reaches 50% of its size at full maturity, and from thereafter cell size remains constant while cell division accounts for continued growth (Barmore, 1977; Moore-Gordon et al., 1994; Yahia & Woolf, 2011). Rapid lipid synthesis occurs during this stage, where oleic acid (C18:1) is predominantly synthesized and deposited as TAG in the flesh of avocado fruit (Kikuta & Erickson, 1968).

During the third stage (9–10 months for ‘Hass’ cultivar) physiological maturation of the fruit proceeds during which the rate of cell division and fruit growth slows down (Dixon et al., 2006; Lee & Young, 1983; Moore-Gordon et al., 1994). However, the lipid accumulation in parenchyma and idioblast cells continues until the fruit has been attached on the tree for approximately 15 months (Kaiser, 1993; Requejo-Tapia, 1999). Schroeder (1953) observed that mature fruits with different sizes all have the same mean cell size. It was therefore concluded that size variation of fruit at maturity is mostly due to variation in number of cells, where relatively smaller fruits have limited cell division (Schroeder, 1953). Differences in fruit size of avocados maturing at approximately the same time results primarily from differences in the rate of cell division during the initial six months

of development (Barmore, 1977). This pattern was the same for many cultivars, but the length of each stage varies for different cultivars (Lee & Young, 1983; Moore-Gordon et al., 1994).

2.2.3 Enzyme activity changes and cell degradation during fruit ripening

Avocado is a climacteric fruit which exhibits the increase in respiration and ethylene production during fruit ripening (Wills, Lee, Graham, McGlasson, & Hall, 1981). During ripening of avocado fruit, the activities of cellulase and polygalacturonase (PG) increased dramatically (Figure 2.6; Figure 2.7, respectively). Therefore these two enzymes were believed to be cell wall-degrading enzymes in the avocado mesocarp (Awad & Young, 1979). On the other hand, pectin methylesterase (PME) is not involved in the cell wall hydrolysis. PME activity was found to decline from its maximum value at the time of harvest to a low level early in the climacteric (Figure 2.6).

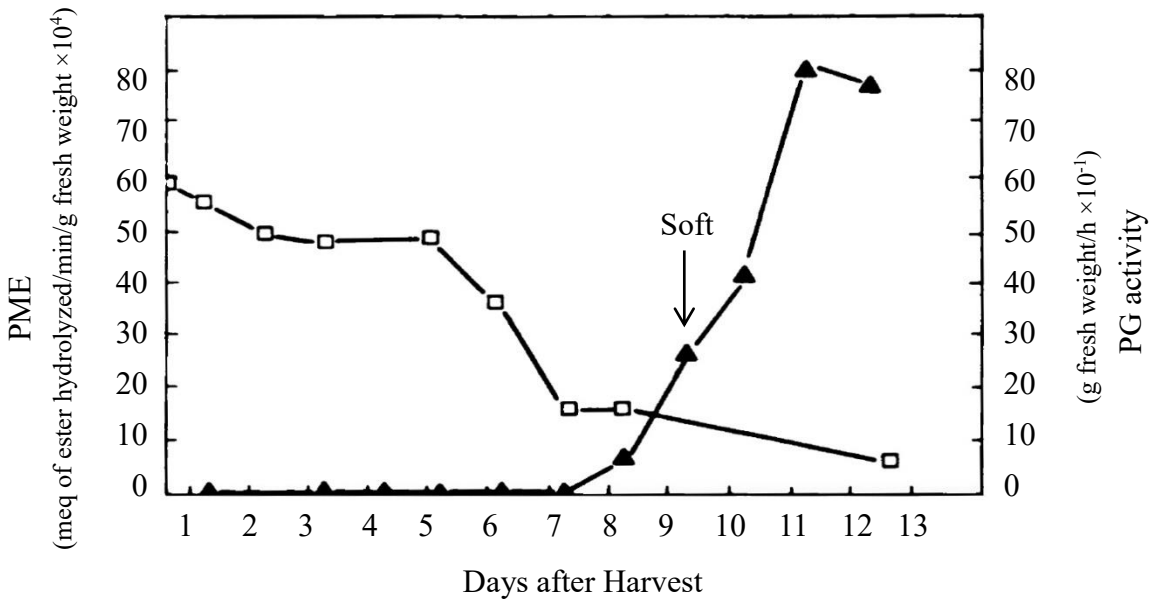

Figure 2.6: Postharvest trends in PME (□) and PG (▲) activity in 'Fuerte' avocado fruit (Awad & Young, 1979).

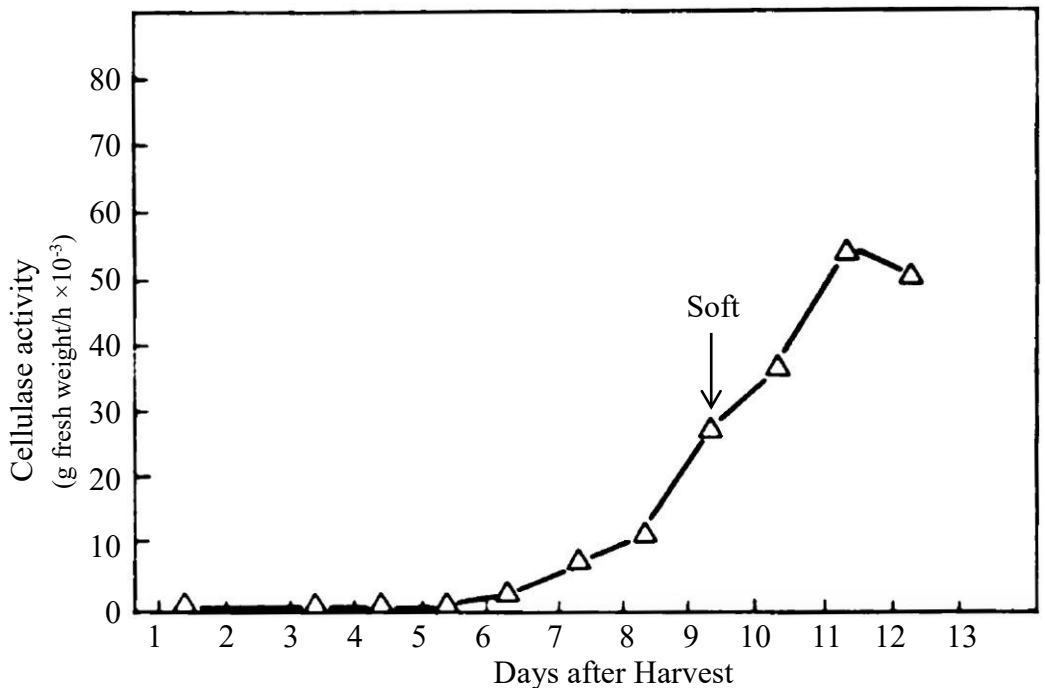

Figure 2.7: Postharvest trends in cellulase (△) activity in 'Fuerte' avocado fruit (Awad & Young, 1979).

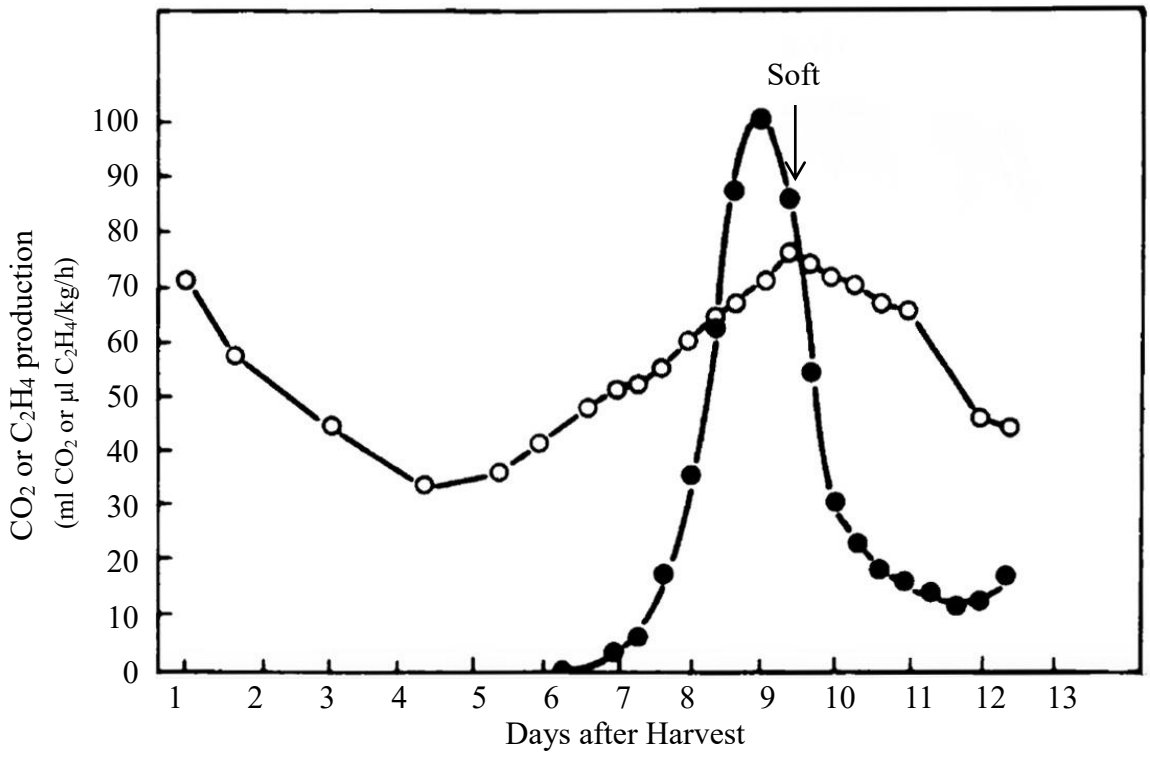

Figure 2.8: Postharvest trends in CO_2 (○) and C_2H_4 (●) production in 'Fuerte' avocado fruit (Awad & Young, 1979).

In the pre-climacteric stage of avocado ripening, PG activity was not detectable. However, it increased during the climacteric stage (6-9 days after harvest) and continued to increase during the post-climacteric stage to a level approximately three times higher than when the avocado reached the edible soft stage (9 days after harvest) (Awad & Young, 1979). Cellulase activity was low in the pre-climacteric stage of ripening but started to increase just as respiration increased (6 days after harvest; as shown is Figure 2.8) and reached a level two times higher than when the fruit reached the edible soft stage. Cellulase activity started to increase three days before PG activity could be detected. Increased ethylene production from the fruit occurred after the increase in respiration and cellulase activity by approximately 1.5 days (Figure 2.8) (Awad & Young, 1979). These findings indicate that a close correlation exists between the rapid increase in the activities of cell wall-degrading enzymes and the increase in respiration and ethylene production (Awad & Young, 1979).

Hatfield and Nevins (1986) have purified and characterised cellulase in avocado mesocarp. The enzyme is classified as endo-(1-4)-β-D-glucanase, and that its hydrolytic activity is limited to (1-4)-β-D-glucans of four or more glucosyl residues. This enzyme is incapable of effectively hydrolysing crystalline cellulose or cellulosic polymers contained within native fruit cell walls (Hatfield & Nevins, 1986). Hatfield and Nevins (1986) considered that the role of the cellulase during cell wall degradation may be to solubilize specific regions of xyloglucans or cellulose fibrils that could lead to changes in cellulose fibrillar orientation. This may also alter hydrogen bonding to other matrix polysaccharides, thus disrupting the cell wall matrix, which could allow greater accessibility to polygalacturonase in the wall matrix (Hatfield & Nevins, 1986). This process could explain the reason for an increase in cellulase activity preceding PG activity

in the avocado mesocarp (Awad & Young, 1979; Hatfield & Nevins, 1986).

During fruit ripening, a coordinated series of modifications to the polysaccharide components of the primary cell wall and middle lamella occurs. Degradation of cell wall polysaccharides and alterations in the bonding between polymers result in an increase in cell separation, a softening and swelling of the wall, and a weakening of the cell structure; this causes fruit softening and textural changes (Brummell, 2006a, 2006b). Early in ripening, cell wall pectic galactan side chains are rapidly degraded and a depolymerisation of matrix glycans begins, followed by a loss of pectic arabinan side chains and pectin solubilisation. A depolymerisation of polyuronides can begin during early or mid-ripening, but it is usually more pronounced later in ripening (Brummell, 2006a, 2006b). Cell wall swelling may be related to a loosening of the xyloglucan–cellulose network and to pectin solubilisation, and these processes combined with the loss of pectic side chains increase wall porosity. An increase in wall porosity later in ripening may allow increased access of degradative enzymes to their substrates (Brummell, 2006a, 2006b).

Detailed ultrastructural studies of the parenchyma cells have been carried out, investigating the cell wall organisation during ripening of avocado fruit (Platt-Aloia & Thomson, 1981; Platt-Aloia et al., 1980). During ripening, the middle lamella of the parenchyma cells begins to disappear, with pectin removal from the cell wall's matrix, which corresponded to the reported increase in PG activity in the mesocarp tissue (Awad & Young, 1979; Platt-Aloia et al., 1980). Later, a loss of organization and density in the cell walls occurs, accompanied by an increase in fruit softening. Finally, the walls of the parenchyma cells almost completely disappear during the post-climacteric phase (Platt-Aloia & Thomson, 1981). The ultrastructural changes of the idioblast oil cells during

ripening have not been studied extensively. Platt-Aloia and Thomson (1992) reported that the suberised wall of the idioblast oil cells is immune to the activity of cellulase and PG thus remains intact during ripening.

2.3 Development of avocado oil commercial extraction

2.3.1 History of avocado oil and the avocado fruit for oil production

Throughout history, avocado oil has been well-known for its properties of healing and regenerating. As early as the 16th century, the applications of avocado oil to treat rashes and scars was reported (Sinha, Hui, Evranuz, Siddiq, & Ahmed, 2011). The bulk of avocado oil is produced by relatively harsh extraction methods which involve high temperature and/or solvents, followed by refining, bleaching and deodorizing. In the 21st century, a cold-pressed extraction process for avocado oil was successfully commercialised to produce oil for culinary uses. The technologies, which are similar to those used to extract extra-virgin olive oil, were commercialised in 2000 when two commercial producers in New Zealand started cold-pressing avocado oil (Woolf et al., 2007; Woolf et al., 2009).

Because avocados are generally grown for fresh fruit consumption, avocado oil is primarily extracted from the avocados rejected from the fresh-fruit trade. This is different to other oils, such as palm oil and olive oil (grown solely for oil production) or rice-bran oil (produced from processing by-products) (Wong et al., 2008; Woolf et al., 2009). The avocado fruit quality required is usually dictated by the ultimate market of the oil. For the high-quality cold-pressed culinary oil production, the avocado fruit used must be good-quality rejected fruit not suitable for fresh fruit export, generally due to cosmetic issues, or being too small for sale. When poor-quality rejected avocado fruit (often with rots) are

used, the subsequent oil may need refining steps after extraction (Woolf et al., 2009).

2.3.2 Applications and uses for avocado oil

Avocado oil is used in the cosmetic industry as it has beneficial effects on the skin (Swisher, 1988). In skin care, the avocado oil has four major advantages including its notable softening and soothing nature, its high stability, its marked absorption, and its high concentration of vitamin E (α-tocopherol). Compared with other cosmetic oils such as almond oil, corn oil, olive oil, and soybean oil, avocado oil provides the highest skin-penetration rate (Human, 1987; Swisher, 1988). For its application in the cosmetic industry, crude avocado oil requires further refining steps. The resulting oil has a pale yellow colour and little remaining avocado flavour or odour (Eyres et al., 2001). Because avocado oil is one of the most penetrating oils suitable for cosmetics and soaps, the oil is available for making muscle oils, massage creams, and other cosmetics or skin care products where lubrication and penetration are essential. In addition, avocado oil can form finer emulsions as it reduces surface tension, which can be used in soaps to form smoother creams as well as to provide improved lathering (Human, 1987; Poucher, 1974).

Cold-pressed avocado oil is a relatively new arrival in culinary circles and has chemical properties similar to olive oil. Cold-pressed avocado oil is composed of at least 60% monounsaturated fatty acids, and approximately 10% polyunsaturated fatty acids. In addition, high contents of pigments including chlorophylls and carotenoids are found in cold-pressed avocado oil, which act as antioxidants. Because of the pigments, cold-pressed avocado oil has a brilliant emerald green colour (Wong et al., 2010). Cold-pressed ‘Hass’ avocado oil has been reported to have an avocado flavour, with delicate grassy and butter/mushroom-like flavours. Different varieties of avocado may produce oils with

slightly different flavour profiles. For example, cold-pressed ‘Fuerte’ avocado oil has been described to give less avocado but more mushroom-like flavour (Wong et al., 2010). Cold-pressed avocado oil has a smoke point over 250 °C. The high smoke point makes it suitable for pan frying (Woolf et al., 2009).

Currently, cold-pressed avocado oil retails at about US$7 per bottle (250 mL) on the Australia and New Zealand market (Grove, 2018; Olivado, 2018). Bulk avocado oil sales are at approximately US$10 per litre. Sales are increasing with an average annual growth rate of 2.73% since 2014 as more and more people are becoming aware of the health benefits of avocado oil (Trent, 2019).

2.4 Avocado oil extraction

2.4.1 Commercial extraction systems

2.4.1.1 Cold-pressed extraction of avocado oil

Cold-pressed avocado oil recovered by aqueous extraction is free of solvent impurities and suitable for food use; it has been reported to have a superior nutritional quality (Eyres et al., 2001). Cold-pressed extraction of avocado oil was first attempted in the late 1980s when centrifugal force was used in the laboratory to extract oil from unripe avocado flesh (Buenrostro & López-Munguia, 1986; Swisher, 1988; Werman & Neeman, 1987). The oil yields of this method were significantly lower than with solvent extraction, ranging from 30–80% of the total oil available (Buenrostro & López-Munguia, 1986; Werman & Neeman, 1987).

In the late 1990s, a novel avocado oil extraction technique was developed in New Zealand based on the continuous virgin olive oil extraction. This extraction technique produces

high quality cold-pressed avocado oil that is comparable in quality with the extra virgin olive oils and contains high concentrations of pigments (Requejo-Jackman et al., 2005; Wong et al., 2012). The current cold-pressed avocado oil extraction procedures conducted in commercial plants in New Zealand have been reported by Wong et al. (2012) and Costagli and Betti (2015), and are shown in Figures 2.9 and 2.10.

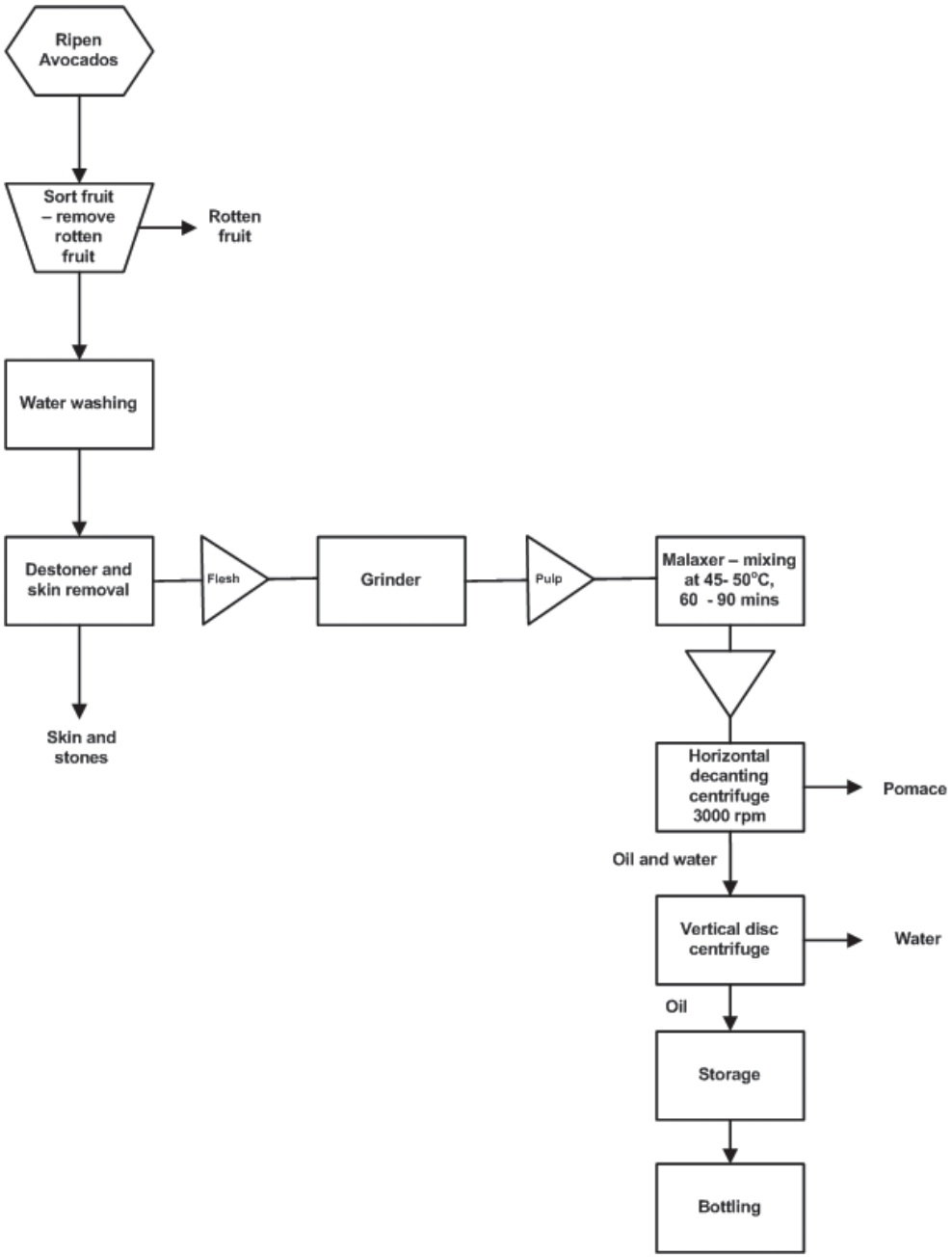

Figure 2.9: Process flow diagram for cold-pressed extraction of avocado oil (Wong et al., 2012).

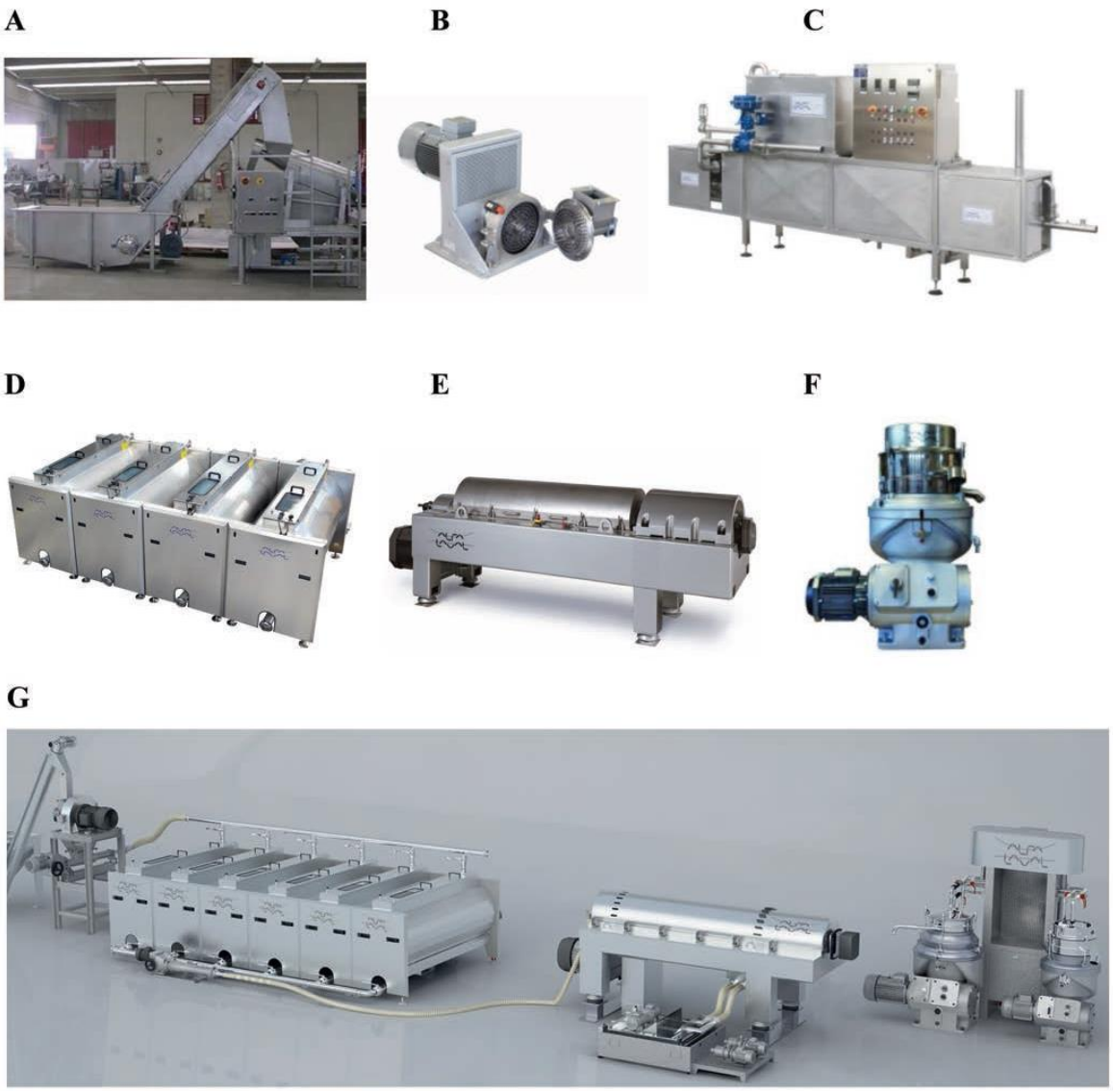

Figure 2.10: Equipment and process of cold-pressed avocado oil extraction system; A) Avocado washer and destoner; B) Grinder; C) Line flash thermal conditioning system; D) Atmosphera malaxers; E) Decanter centrifuge; F) Polishing disk centrifuge; G) Example of a complete cold-pressed extraction process solution from grinder to centrifuge (Costagli & Betti, 2015).

Wong et al. (2012) describes the process for cold-pressed aqueous extraction of avocado oil. During the extraction, firstly, the ripe whole avocados are washed by a fruit washing machine (Figure 2.10A) to remove dirt, spray residues, and other undesirable matter. Next, the washed fruit enters the destoner (Figure 2.10A) to separate the skin and stone from

the flesh. In the destoner, the avocados are smashed against the chamber wall that consists of a stainless steel screen. The skin and stone, as well as the unripe or hard fruit, are expelled from the chamber and discarded as waste. The smashed avocado flesh is then ground to a pulp by using an attrition mill or grinder (Figure 2.10B) to aid in disrupting the cells in the flesh. The exact mechanism of oil extraction from cells is still unclear, however, adequate grinding of the flesh plays an important role to liberate the oil as it breaks down the cellular structure (Woolf et al., 2009).

After grinding, the pulpy avocado flesh is transferred into D-shaped semi-cylindrical tanks (Figure 2.10D) called malaxers. The malaxers, which can vary in size from 250 to 1000 kg, are made of stainless steel inside and equipped with a shaft with rotating arms and stainless steel blades of varying shapes and sizes (Petrakis, 2006; Wong et al., 2012). Depending on the rotation axis location, the malaxers can be classified into horizontal and vertical tanks. Based on technical and economic reasons, horizontal malaxers are more popular in the oil industry (Clodoveo, 2012). The walls of the malaxer are hollow to allow hot water to flow through these jackets to heat the pulpy avocado flesh contained in the malaxer. During malaxing, the avocado pulp is continuously stirred by the blades at 15–25 rpm and at a controlled temperature (between 45–50 °C; Figure 2.10C) (Woolf et al., 2009). The ultrastructural changes of the cells and oil from the avocado flesh during malaxing has not been studied. Based on the previous study from Di Giovacchino (1989) and Di Giovacchino (1996) on olive oil, it is hypothesized the aim of the malaxing step in avocado oil extraction is to assist the small oil droplets join together to form larger drops that can be easily separated through the following centrifugal extraction systems.

After malaxing, the horizontal decanter centrifuge (Figure 2.10E) is used to separate the

oil phase from the solids (pomace) and water phase (wastewater). The centrifugal extraction method is based fundamentally on the principle that any combination of immiscible liquids with varying densities tends to separate spontaneously into its individual constituents (Petrakis, 2006). Therefore, the lighter oil will split up to a layer above the heavier aqueous solution and remaining pomace when avocado pulp is exposed to the high *g* forces of a centrifuge for long periods of time (Bizimana, Breene, & Csallany, 1993). The horizontal decanter centrifuge is comprised of a cylindrical-conical rotating bowl and a helical hollow-axis screw rotating coaxially inside it and at a slightly different speed to the bowl (Wong et al., 2012). During centrifugal extraction, the avocado pulp is pumped into the decanter centrifuge through an opening in the screw axis, water is usually added during pumping as the pulp can be very viscous (Wong et al., 2012; Woolf et al., 2009). The decanter operates at 3,000–4,000 rpm and with the applied centrifugal force, the pomace is displaced towards the wall of the bowl and is slowly dragged toward the end of the decanter by the differential speed between the auger and the bowl (Wong et al., 2012; Woolf et al., 2009). The lighter oil phase forms an internal ring around the axis and is drained through outlets placed at the opposite end of the pomace outlet. Also, the water ring formed between the oil ring and the pomace ring is drained separately (Wong et al., 2012). The oil phase from the decanter is then passed through vertical polishing disc centrifuges to remove the residual water from the oil (Figure 2.10F) (Wong et al., 2012).

After polishing, the oil is flushed with nitrogen gas to remove dissolved oxygen and to cool the oil. Lastly, the oil is passed through 100 μm filter bags or cartridges to filter out protein and solid residues, then stored in a stainless steel tank (Wong et al., 2012).

The yield and quality of cold-pressed avocado oil depends on the maturity at harvest,

degree of ripeness, fruit quality, fruit storage, and processing condition (Woolf et al., 2009). The oil yield achieved from ripe 'Hass' cultivar varies between 10–18% of the fresh weight of avocado fruit (Eyres et al., 2001). Good quality oil obtained by cold-pressed extraction is 'extra virgin' quality with a free fatty acids level (FFA%) and peroxide value (PV) of < 0.5% w/w (as oleic acid) and < 4 meq/kg of oil, respectively (Wong et al., 2010; Woolf et al., 2009). Although no standards have been set internationally for 'extra virgin' avocado oil, in contrast the international standard values for 'extra virgin' olive oil are, FFA% < 0.8% w/w and a PV < 20 meq/kg oil (International Olive Council, 2006).

2.4.1.2 Solvent extraction

In the past, avocado oil has been produced using only solvent extraction methods (petroleum ether, ethyl ether, or benzene), which results in recoveries of 60–90% of the total oil available (Wong et al., 2008; Woolf et al., 2009). In solvent extraction of avocado oil, hexane has become the most common solvent choice due to its high stability, low evaporation loss, low corrosiveness, little greasy residue, as well as the better odour and flavour of the extracted oil products (Johnson, 1997). The extracted oil from these methods is dark green in colour and requires further refining, bleaching and deodorizing before it is used (Woolf et al., 2007). The resulting oil is yellow to colourless since the pigments have been removed during the bleaching step (De Greyt & Kellens, 2000). Historically, the avocado oil from solvent extraction was predominantly used for cosmetics purposes.

In contrast to the cold-pressed oil extraction method, the solvent extraction method gives a higher oil yield. However, this method requires considerable capital investment

including high capital equipment cost and operational expenditures. The recovery of the used solvents can also become costly. In addition, solvents are dangerous to work with because they are hazardous and can cause fire and explosion. It is also difficult to separate all the solvent from the oil and traces left may reduce the quality of the oil (Owusu-Ansah, 1997; Petrovic, Eljarrat, De Alda, & Barceló, 2004).

2.4.2 Laboratory-based extraction systems

For determining the amount of lipid available in commercial extraction and for research purposes, a reliable and reproducible technique is required to determine the total lipid content in avocado fruit. A range of methods, including Soxhlet method (using petroleum ether or other solvent), Bligh and Dyer method (using chloroform and methanol), and the refractometric method (using monochloronaphthalene), have been employed to determine the total lipid content of avocado (Lewis, 1978). However, they are relatively slow, time-consuming and expensive (Requejo-Tapia, 1999; Woolf et al., 2009). These solvent extraction methods also lead to the breakdown of other compounds of interest such as sterols and pigments (Woolf et al., 2009). This section will now describe the laboratory based solvent extraction systems for determining the total lipid content in avocado flesh, including the traditional Soxhlet extraction system and the relatively new accelerated solvent extraction system.

2.4.2.1 Soxhlet extraction

Soxhlet extraction is well-established and the most widely used organic solvent extraction method in a laboratory. It is considered to be a standard technique, used as the main reference method to evaluate other novel extraction methods (Montoro, Masullo, Piacente, & Pizza, 2015; Skalicka-Wozniak, Widelski, & Glowniak, 2008). Soxhlet extraction is a

hot continuous extraction process, in which, lipids are concentrated by repeated washings with an organic solvent, typically hexane or petroleum ether. During the extraction, fresh solvent comes in contact with the dried material several times, until the lipid is completely extracted (Montoro et al., 2015).

The apparatus for Soxhlet extraction is shown in Figure 2.11 (Dean, 2010). During extraction, the flask is gently heated and clean solvent vapour passes around the thimble holding the sample, travelling up to the condenser. Vapour condenses in the condenser and drips back into the thimble chamber. When the lipid-laden solvent reaches the top of the thimble chamber, it flows back into the bottom flask through the siphon device (Kou & Mitra, 2004).

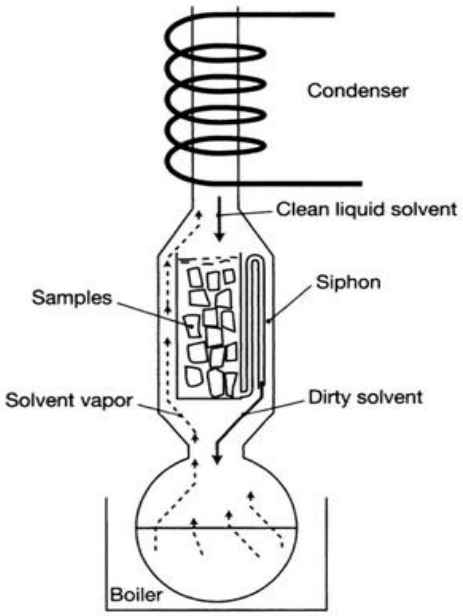

Figure 2.11: Schematic diagram of typical Soxhlet apparatus (Dean, 2010).

The major advantage of Soxhlet extraction is that it is a continuous process for the oil extraction of a sample. No further filtration is required after extraction. In addition, Soxhlet extraction is a simple and non-labour-intensive process, which is economical and scalable to compare other novel extraction methods such as supercritical fluid extraction (Guldhe, Singh, Ansari, Sharma, & Bux, 2016; Skalicka-Wozniak et al., 2008). The most noticeable disadvantages of Soxhlet extraction is that it is time consuming, there can be poor penetration by the solvent, and it also requires a significant amount of solvent, which is expensive and not environmentally friendly (Guldhe et al., 2016; Skalicka-Wozniak et al., 2008).

2.4.2.2 Accelerated solvent extraction system

The accelerated solvent extraction (ASE) system (Figure 2.12) combines elevated temperature and pressurised organic solvent, which allows the lipid extraction to be achieved within a short extraction time using a low volume of solvent (Richter et al., 1996). ASE can be used to recover the total lipid content in avocado, as it can be used to extract the majority of the available lipid, with minimal effects on the nutritional compounds such as pigments and sterols (Woolf et al., 2009). During extraction, samples are enclosed in stainless-steel extraction cells, filled with an extraction solvent, pressurized with oxygen-free nitrogen gas and heated to a designated temperature (Richter et al., 1996; ThermoScientific, 2012; Woolf et al., 2009). The high temperature leads to the extraction of lipids into the solvent. The high pressure can keep the solvent below its boiling point, which results in high penetration of the solvent into the sample (ThermoScientific, 2013). The samples are held under this pressure and temperature for a fixed period of time for a static extraction, then the lipid and solvent are released from the cells and collected in the bottle (Richter et al., 1996; ThermoScientific, 2012; Woolf

et al., 2009).

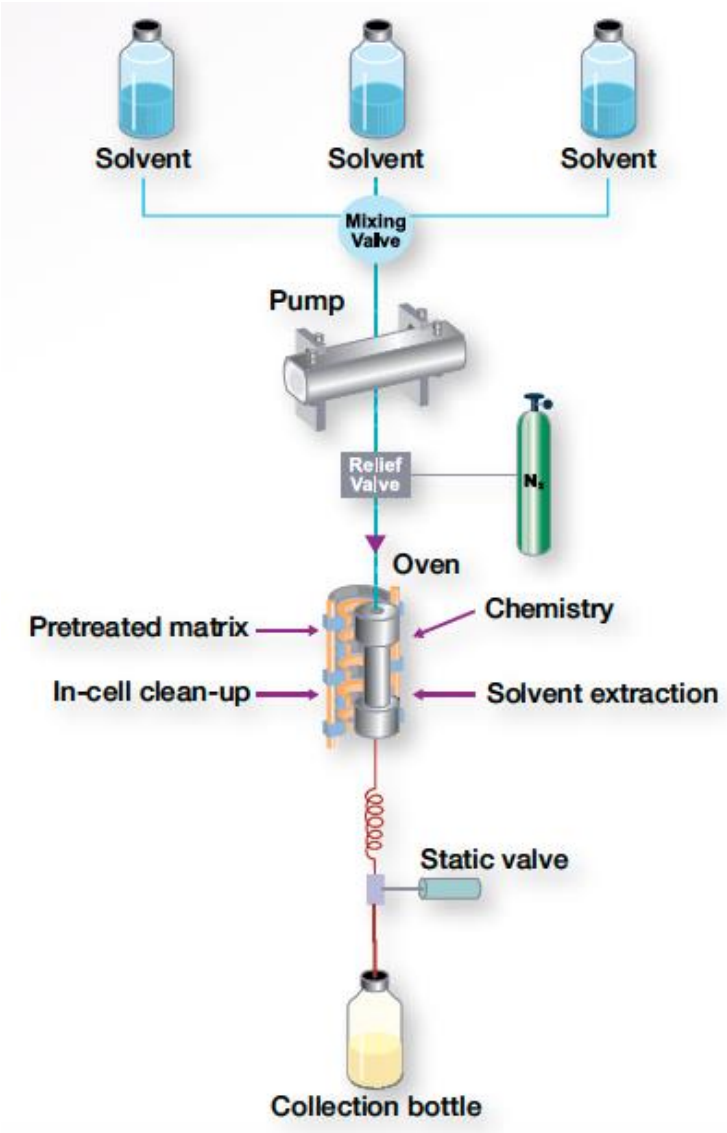

Figure 2.12: Schematic of accelerated solvent extraction system (ThermoScientific, 2012).

Woolf et al. (2009) suggested that hexane is the most suitable solvent for avocado oil extraction by using ASE due to its nonpolar properties, which can minimize the deterioration of the compounds in the oil. The processing temperature of ASE is recommended to be at 60 °C for avocado oil extraction. The oil recovery of avocado can be improved by 3.5% by increasing the extraction temperature from 60 °C to 120 °C with

a 15 min static time (Woolf et al., 2009). However, increasing the temperature can result in degradation of TAG and destruction of labile compounds such as pigments and antioxidants (e.g. chlorophyll is destroyed at 60 °C and above) (Kidmose, Edelenbos, Nørbæk, Christensen, & MacDougall, 2002; Woolf et al., 2009). Woolf et al. (2009) suggested increasing the static time from 15 min to 40 min at 60 °C, which can improve the lipid, carotenoid and chlorophyll recovery.

2.4.3 Processing extraction aids

2.4.3.1 Enzyme

In the avocado flesh, TAG are mostly found in the parenchyma cells (Platt-Aloia & Thomson, 1981). Cell wall disruption can either be conducted by mechanical methods e.g. grinding, or non-mechanical methods, such as exogenous enzymatic action (Buenrostro & López-Munguia, 1986; Werman & Neeman, 1987). In the avocado oil extraction process, commercial exogenous enzymes are added for two reasons: firstly (and primarily), to assist disruption of the cell walls and release the oil from the parenchyma cells hence to increase oil yield; secondly, to decrease the viscosity of the avocado pulp during malaxing resulting in less energy being required (Buenrostro & López-Munguia, 1986).

Laboratory-based enzyme trials were conducted by Wong et al. (2012), where a simple pectinase preparation or a mixed enzyme solution containing macerating and pectolytic activity were added into early and mid-season avocado fruit during malaxing at 45 °C and at concentrations of less than 0.1% w/w. The results indicated that there was no significant improvement in oil yields and standard pectinase formulations were not suitable for early and mid-season avocados although they improved the cellular disruption for most other

fruit extraction processes.

In another experiment, two additives including 0.3% citric acid and cellulase enzyme mix were applied during malaxing of early-season avocado fruit at 45 °C. Although the oil yields were very low for early season avocados, adding cellulase enzyme mix was found to increase the oil yield (Figure 2.13). The results also indicated that citric acid led to slightly increased oil yields. The adjustment of pH to 4.0 in rendering systems breaks the emulsion, allowing better separation (Wong et al., 2012).

Experiments with late-season avocados (Figure 2.14) showed the addition of pectinase or cellulase-based enzymes during malaxing (at 45 °C) increased oil yields (Wong et al., 2012). This was a logical result as the parenchyma cell walls are mainly composed of cellulose and pectin hence can be degraded by the enzymes (Gupta, 2007).

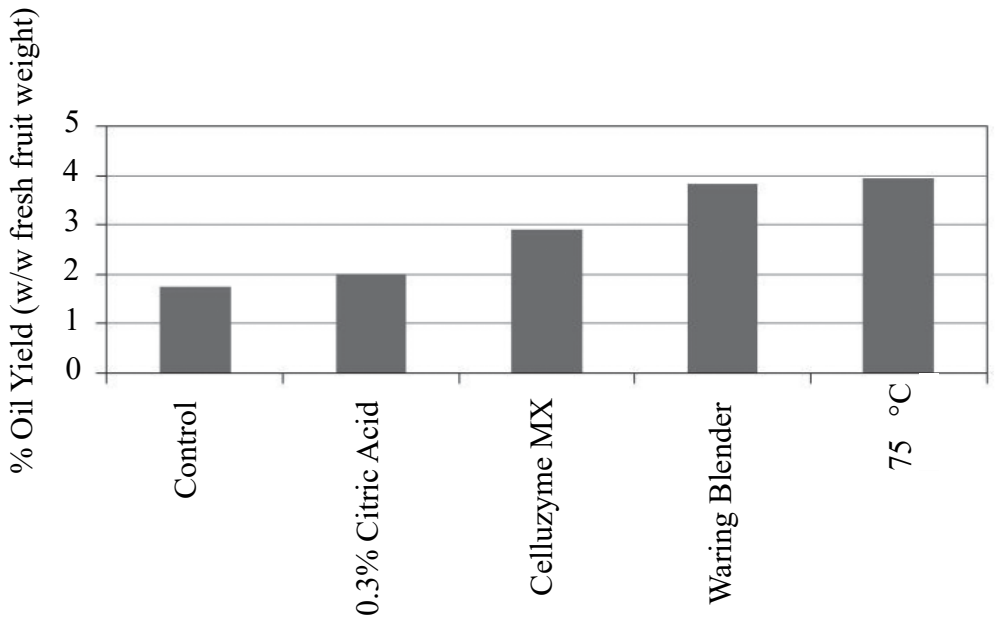

Figure 2.13: Effect of various process additives on oil yield of early-season 'Hass' avocados (Wong et al., 2012).

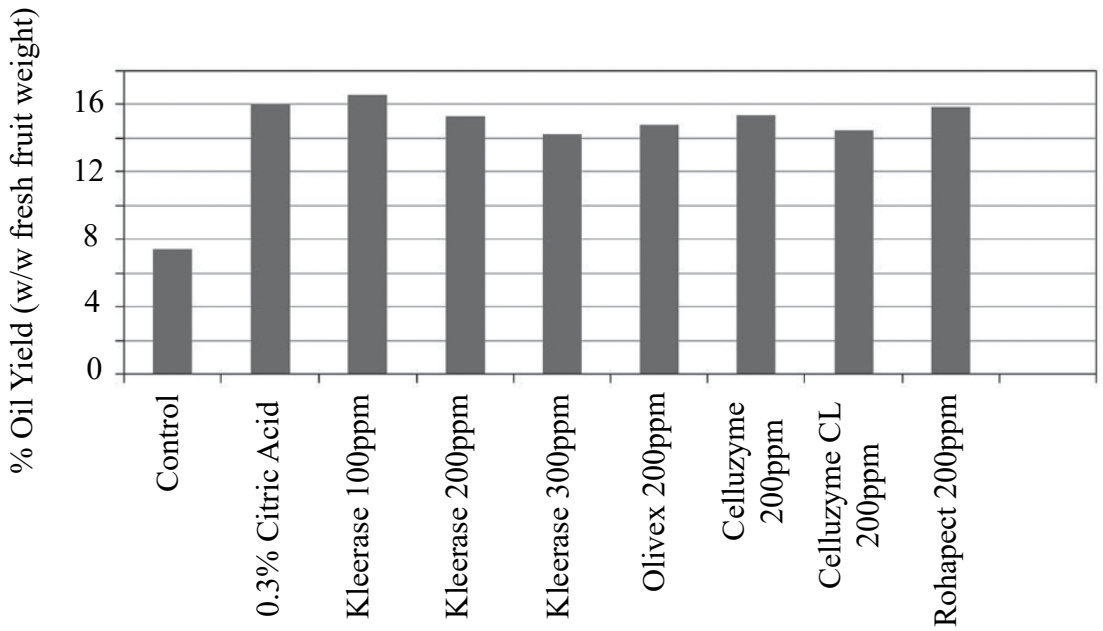

Figure 2.14: Effect of various enzymes on oil yield of late season 'Hass' avocados (Wong et al., 2012).

2.4.3.2 Ultrasonication

Ultrasonication is a potential novel technology for oil extraction processes that can improve cellular disruption and oil separation to increase the oil yield (Figure 2.15). This method applied ultrasound energy to crack cell walls and membranes through the cavitation effect (Mercer & Armenta, 2011). The cells are subjected to ultrasonic vibrations by introducing an ultrasonic vibration emitting tip into the cell suspension. Cavitation occurs when bubbles of liquid vapour are produced in an area where its vapour pressure is higher than the pressure of the liquid. The vapour bubbles that are created by ultrasonic waves collapse near the cell wall producing shock waves and damaging cell walls and membranes (Bermúdez-Aguirre, Mobbs, & Barbosa-Cánovas, 2011; Mercer & Armenta, 2011).

Ultrasound can also be applied to enhance oil separation. Acoustic separation is based on the formation of an acoustic standing pressure wave field in the material under treatment

(Juliano et al., 2011). The rate of separation is related to the relative density of the suspended matter and the viscosity of the continuous phase (Batchelor, 2000). Ultrasonic waves have the ability to alter the interaction between oil globules through acoustic pressure and cause coalescence of oil globules, which then improve the separation and recovery of oil (Juliano et al., 2011; Vilkhu, Manasseh, Mawson, & Ashokkumar, 2011).

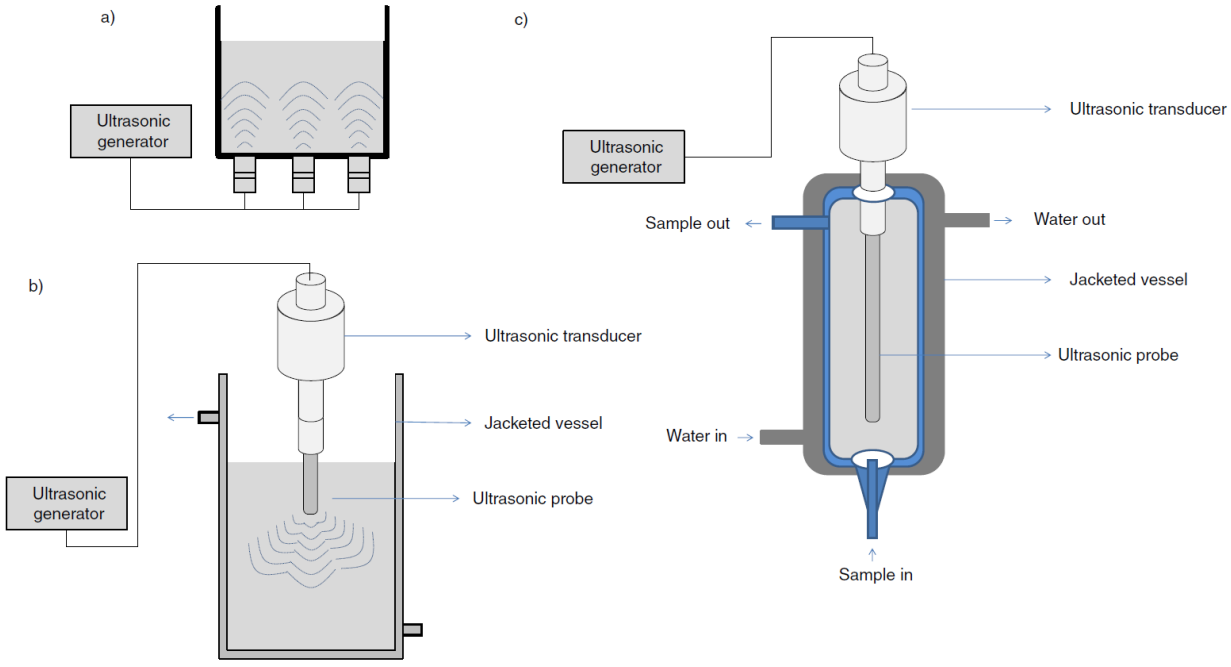

Figure 2.15: Schematic diagram of various types of ultrasonic systems: a) ultrasonic bath; b) batch type probe system and c) continuous probe system used for liquid food processing (Zinoviadou et al., 2015).

To improve extraction oil yield, ultrasound treatment has been successfully applied on aqueous extraction of olive oil (before or after malaxing) and palm oil (during gravity settling) (Bejaoui, Beltran, Aguilera, & Jimenez, 2016; Clodoveo, Durante, La Notte, Punzi, & Gambacorta, 2013; Clodoveo & Hbaieb, 2013; Jiménez, Beltrán, & Uceda, 2007; Juliano, Augustin, Xu, Mawson, & Knoerzer, 2017; Juliano et al., 2013a; Juliano, Swiergon, Mawson, Knoerzer, & Augustin, 2013b). In the cold-pressed olive oil extraction process, laboratory scale trials were carried out by Clodoveo and Hbaieb (2013)

to study the mechanical effect of ultrasound treatment on olive paste and oil yield. Ultrasound treatment (35 kHz, 10 min, at 30 °C) increased the olive oil extraction yield from 1.0% to 5.4% without a malaxing step.

In addition, low (24–40 kHz) and high frequency (400–600 kHz) ultrasound treatments have been tested during cold-pressed olive oil extraction before or after malaxing (Bejaoui et al., 2016; Clodoveo et al., 2013; Clodoveo & Hbaieb, 2013; Jiménez et al., 2007; Juliano et al., 2017). Ultrasound treatments at both frequencies improved the oil yield (g oil extract/100 g fresh flesh) by up to 2.0% and the oil extraction efficiency (g oil extract/100 g total oil in fresh flesh) by up to 5.7% when they were applied before or after malaxing step.

The effect of ultrasound treatments on oil quality parameters, fatty acid composition, and nutritional and sensory characteristics of virgin olive oil were also studied previously (Bejaoui et al., 2016; Clodoveo & Hbaieb, 2013; Jiménez et al., 2007). The oil quality parameters including FFA%, PV and specific extinction coefficients (K_{232} and K_{270}, the oil absorbance at 232 and 270 nm), and fatty acid composition of virgin olive oil were not affected by the ultrasound treatments at 24, 35 and 40 kHz. Also, off-flavour volatiles were not detected in the olive oils obtained from ultrasound treatments at 24 and 40 kHz applied before malaxing. However, oil extracted from olive pulp treated with ultrasound treatments at 24, 35 and 40 kHz showed a reduction in phenolic content and bitterness index whereas a higher concentration of tocopherols, chlorophylls and carotenoids was found.

The application of ultrasound treatment during cold-pressed extraction of avocado oil has

not been studied extensively and the ultrastructural changes in avocado flesh during ultrasound treatment have not been previously reported.

2.5 Factors affecting cold-pressed oil yield and quality

2.5.1 Maturity (Time of harvest in season) of avocado fruit

Horticultural maturity has the most affect on the oil yield for cold-pressed avocado oil manufacturers (Woolf et al., 2009). This is firstly due to the significant difference between the total oil content (available yield) of fruit at different times in the season; and secondly, due to the difference found between the available yield and the cold-pressed yield (Woolf et al., 2009). Woolf et al. (2009) reported for 'Hass' avocados the seasonal change in average dry matter content and the increase in total oil content, and the typical commercial cold-pressed oil yield (Figure 2.16). Since the avocado fruit used in commercial cold-pressed extraction are extracted at the same firmness stage, the difference in oil yield in the early season was not because of ripeness differences. The cold-pressed extraction of avocado oil from fruit harvested in the early season (October) resulted in lower yields of total oil available than when extraction was from fruit harvested in the late season (March and April). Early in the season, the commercial cold-pressed oil yield was only about 14%, but the available oil present was approximately 18%. The total oil content of the fruit increased up to 23–25% later in the season, and the oil extraction yield also increased. The reason for the low efficiency of cold-pressed oil extraction in early-season fruit compared to late-season fruit is still unclear. It is possibly because of the levels of endogenous cell-wall degrading enzyme may vary over the season for avocados at the same degree of ripeness (Woolf et al., 2009).

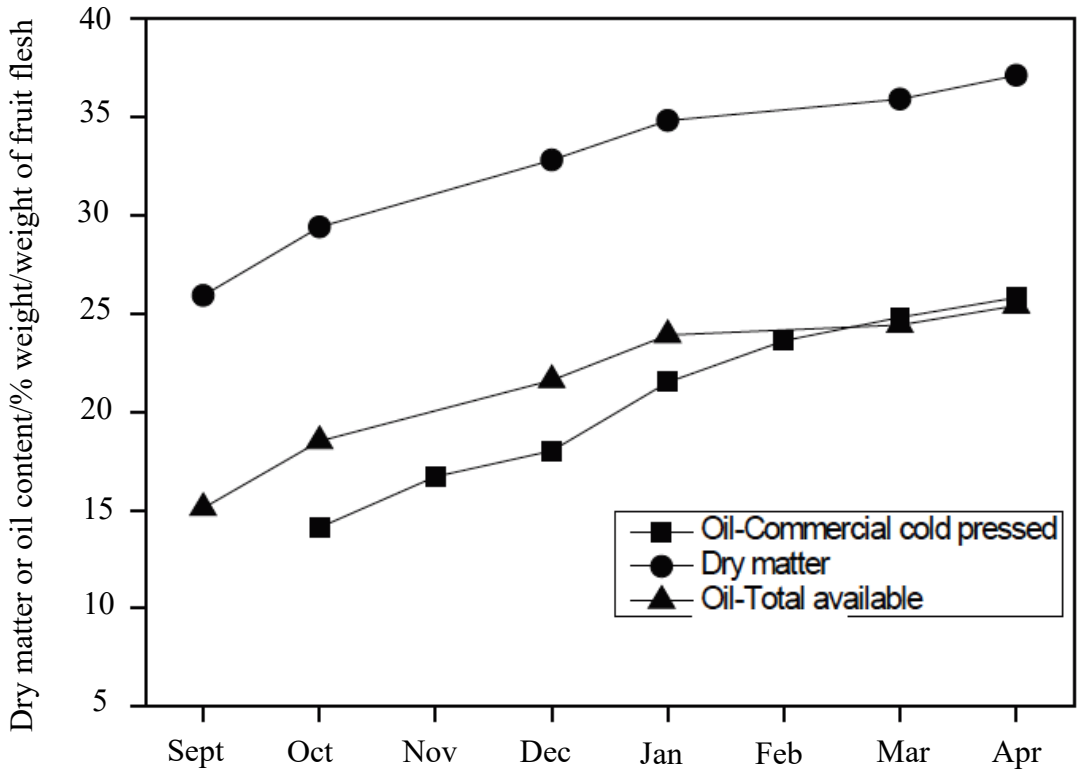

Figure 2.16: Typical changes in dry matter content, total oil content and commercial cold-pressed yield over a commercial harvest and oil extraction season in New Zealand 'Hass' avocados (Woolf et al., 2009).

2.5.2 Ripening of avocado fruit

Ripening is another factor that may affect avocado cold-pressed oil yield and quality (Woolf et al., 2009). The effect of 'Hass' avocado ripeness on oil yield and quality was studied by Woolf et al. (2009). In the experiment, 'Hass' avocado fruits with three different ripeness levels (minimal, fully ripe and overripe) were processed, where firmness hand ratings corresponded to 4, 5, and 6, respectively (White et al., 2005). The results indicated the cold-pressed oil yield increased from 7 to 9 to 11% (g of oil/100 g of fresh flesh weight) respectively, with an increase in fruit ripeness (Table 2.2). However, the oil quality decreased with increased fruit ripeness as the FFA% in the oil increased from 0.03 to 0.12% w/w (as oleic acid).

Table 2.2: Effect of 'Hass' avocado fruit ripeness on oil yield (% of flesh tissue) and quality (FFA%) (Woolf et al., 2009).

Ripeness	**4**	**5**	**6**
Oil yield % **(g oil/100 g fresh flesh weight)**	7.0 ± 0.84	8.5 ± 0.22	11.04 ± 0.33
FFA%	0.029 ± 0.017	0.093 ± 0.021	0.127 ± 0.037

2.5.3 Fruit quality after storage

In the commercial cold-pressed extraction of avocado oil, avocados are normally stored for 1–2 weeks at 5–7 °C (the commercial recommended storage temperature), before ripening and subsequent extraction (Woolf et al., 2009). However, during the peak-harvest season, the capacity of the oil extraction facilities are usually exceeded, which results in the fruits being stored for longer periods. Fruit storage for longer than 3–4 weeks generally leads to increases in physiological and pathological disorders which results in reduced fruit quality (Hopkirk, White, Beever, & Forbes, 1994).

In cold-pressed oil extraction, oil quality is affected by fruit disorders. Since avocado fruit is required to be ripened to achieve maximum oil yield, postharvest rots are one of the greatest challenges for oil extraction as they increase dramatically with fruit ripening (Hopkirk et al., 1994). Moreover, cool storage of fruit over four weeks (long-term storage) can result in internal-chilling injury (flesh discoloration/flesh greying) and general reduction of fruit quality (White et al., 2005). In addition, physical damage can also cause physiological disorders (flesh bruising) of fruit, which lower the oil quality (Woolf et al., 2009).

The effect of avocado fruit quality on quality of oil extracted was studied by Woolf et al. (2009). In laboratory based trials, varying degrees of fruit disorders including body rots,

bruising, and flesh greying of avocado fruit were included in fruit from which oil was extracted and the oil quality was determined by FFA%. The result indicated that higher levels of body rots, flesh bruising, or flesh greying all lead to a reduction in the quality of oil (Table 2.3). These trials showed that higher levels of avocado fruit ripeness increased the oil yield but the oil quality decreased with an increase in fruit disorders. Prior to extraction, good postharvest handling of fruit is required to minimize postharvest rots and disorders and thus maximize oil quality.

Table 2.3: 'Hass' avocado oil quality as measured by FFA% (FFA% w/w; as oleic acid) immediately following extraction from fruit with a range of fruit disorders including body rots, bruising, and greying (Woolf et al., 2009).

Rot level	Control	5%	10%	15%	20%	30%
Body rots (FFA%)	0.38 ± 0.02	0.36 ± 0.02	0.42 ± 0.03	0.80 ± 0.04		0.91 ± 0.14
Bruising (FFA%)	0.77 ± 0.16				1.06 ± 0.48	
Greying (FFA%)	0.77 ± 0.16				0.85 ± 0.09	

The effect of storage period on the cold-pressed oil quality was examined by Woolf et al. (2009) under commercial conditions. The study showed that the level of chilling disorders (flesh greying, vascular browning, and stringy vascular tissue) and the ripe rots (body and stem-end rots) significantly increased with storage time. However, as the storage time increased, the amount of flesh browning (i.e. bruising) did not increase significantly (Figure 2.17). The proportion of unsound fruit (fruit with any significant disorders) increased from 15% to 80% following 1–7 weeks of cool storage. As storage period increased from 1–3 weeks, the peroxide values (PV) of the extracted oils increased from 0.75 to 1.00 mEq/kg. However, the PV of the extracted oils increased sharply after 4

weeks of storage and reached 2.25 mEq/kg after 7 weeks of storage. The higher PV meant the oil had started to oxidise, which will reduce its shelf life (Frankel, 2014; Woolf et al., 2009). The decrease in extracted oil quality correlated strongly with the increase in fruit storage time, as the amount of fruit disorders increased. Based on this research, it was recommended that the storage duration of avocado fruits is less than 3–4 weeks prior to oil extraction (Woolf et al., 2009).

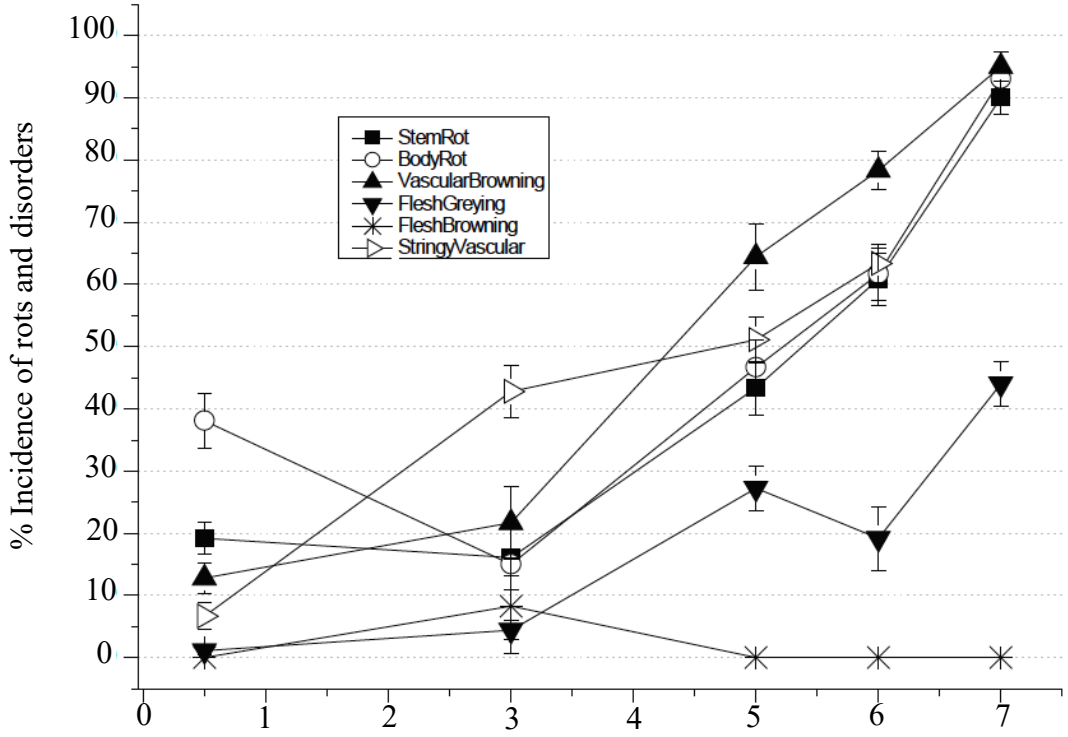

Figure 2.17: Mean incidence of sound 'Hass' avocado fruit as a percentage of total ripe fruit processed in the oil factory following up to 7 weeks in storage at 6 °C (Woolf et al., 2009).

2.5.4 Processing conditions for avocado oil extraction

During cold-pressed extraction of avocado oil, different processing conditions including malaxing temperature, malaxing time, speed of decanter or polishing centrifuge and extent of oxidation can influence oil yield and quality (Wong et al., 2012). Firstly, the cold-pressed oil yield was found to be increased with a higher malaxing temperature

during cold-pressed olive oil extraction (Di Giovacchino et al., 2002b). However, the effect of malaxing temperature on cold-pressed avocado oil yield has not been studied extensively. Woolf et al. (2009) found the quality of the cold-pressed avocado oil was affected at high malaxing temperatures. Malaxing temperatures around 45 to 50 °C are recommended for cold-pressed avocado oil extraction, which leads to high oil yields without a significant effect on oil quality (Wong et al., 2012). Secondly, adequate malaxing time was required to aggregate the oil droplets to form larger drops, and the required malaxing time is varied based on the harvest time in the season (Wong et al., 2012; Woolf et al., 2009). Thirdly, the degree of separation in the decanter and polishing centrifuges can also affect the oil yield and a minimal loss of oil in the pomace and wastewater is desired (Woolf et al., 2009). In addition, it is important to ensure that the water is separated from the oil in the polishing centrifuges so that the extracted oil contains < 0.1% of water (Brown, 2007). High water content in the oil could accelerate oil decomposition to form free fatty acids thus reducing the quality of the oil (Brown, 2007). Lastly, excessive aeration of the avocado flesh and the extracted oil should be avoided as it can result in oxidation of the oil and hence reduce the oil quality (Sherpa, 2002; Woolf et al., 2009). During malaxing, the malaxer is required to be covered to reduce exposure to air. Furthermore, once the oil is separated from the polishing centrifuge, it should be pumped into the storage tanks and flushed with nitrogen immediately to minimise oxidation (Sherpa, 2002; Woolf et al., 2009).

2.6 Methods for monitoring cell rupture and oil aggregation

2.6.1 Microscopy

The significance of microstructure has been well recognized in food technology. Many key phenomena such as transport properties, physical and rheological behaviours in food

and biological materials take place at the microstructural level (Aguilera, 2005). Analysis of microscope images has been commonly used in the scientific literature to reveal microstructural features that support data obtained by other measurements (Gonzalez, Jernstedt, Slaughter, & Barrett, 2010). In relation to plant-based products, information on the structural alteration of cellular and tissue associated with environmental changes or processing conditions is essential. It helps to obtain a better understanding of biological systems, to optimize processing procedures and final product quality (Gonzalez et al., 2010).

Light microscopes use a series of glass lenses to focus light in order to form an image, which will magnify about 1500 times more than human eyes (Wilson & Walker, 2000). The resolution limit is approximately 0.2μm (Wilson & Walker, 2000). Light microscopes produce colour images, and many specimen staining techniques make use of colour to highlight structures or localize chemical activity (Burgess, Marten, & Taylor, 1990; Russ, 2015). Light and electron microscopic examination are often combined with image analysis to study the integrity of cells and to correlate structure with function, where transmission electron microscopy gives much higher resolution and magnification of images at the expense of depth of focus, whilst scanning electron microscopy has significantly more depth of field, which gives three-dimensional images (Wilson & Walker, 2000).

Analysis of microscope images has been applied for a number of purposes such as monitoring cellular structure changes during fruit ripening, determination of degree of cell disruption from different methods, and investigation of cell integrity before and after cellular extraction (Campbell & Glatz, 2009; Crookes & Grierson, 1983; Gavahian,

Farhoosh, Farahnaky, Javidnia, & Shahidi, 2015; Gonzalez et al., 2010; Platt-Aloia et al., 1980). In the case of avocado mesocarp cells, microscopy has been utilized to monitor the parenchyma cells of avocado before and after ripening (Platt-Aloia & Thomson, 1981). The microscopic images showed small holes or pits in the cell wall of parenchyma cell in ripe avocado mesocarp, which was probably caused by the action of cell wall degrading enzymes during ripening (Mostert, Botha, Du Plessis, & Duodu, 2007; Platt-Aloia et al., 1980). Also, microscopy was used to observe the structural changes of avocado cells before and after several solvent extractions. The images gave clear indications of the degree of cell disruption caused by the extraction processes (Ortiz, Dorantes, Gallndez, & Cardenas, 2004). The idioblast cells retained their structure after using a microwave-squeezing method, but oval-shaped and rough-surfaces were observed after hexane extraction and acetone extraction (Ortiz et al., 2004). The parenchyma cells showed no major changes after the microwave-squeezing. However, the parenchyma cells became elongated after hexane extraction, and the cells appeared to be ruptured after acetone extraction (Ortiz et al., 2004).

2.6.2 Electrical impedance spectroscopy

Electrical properties of fruit tissues are believed to provide information about the microstructure of the cells (Sugiyama, 1988). Electrical impedance spectroscopy (EIS) evaluates the dielectric properties of a medium as a function of frequency. This is based on the interaction of an external electric field with the electric dipole moment of materials (Wu, Ogawa, & Tagawa, 2008). Impedance can be defined as a complex resistance encountered when current flows through a circuit composed of various resistors, capacitors, and inductors (Lvovich, 2012). Impedance (Z) is generally separated into real and imaginary components, where the real part of impedance is the resistance (R) and the

imaginary part is the reactance (X) (Lvovich, 2012; Macdonald & Johnson, 2005):

$$\mathrm{Z} = \mathrm{R} + j\mathrm{X} \tag{1}$$

Equation (1) can be plotted in the plane with either rectangular coordinates or polar coordinates, as shown in Figure 2.18 (Lvovich, 2012; Macdonald & Johnson, 2005). In rectangular coordinates:

$$\mathrm{R} = |\mathrm{Z}|\cos\theta \text{ and } \mathrm{X} = |\mathrm{Z}|\sin\theta \tag{2}$$

with the phase angle:

$$\theta = \tan^{-1}\frac{\mathrm{X}}{\mathrm{R}} \tag{3}$$

and the modulus:

$$|\mathrm{Z}| = \sqrt{\mathrm{R}^2 + \mathrm{X}^2} \tag{4}$$

When impedance is expressed in polar coordinates:

$$\mathrm{Z} = |\mathrm{Z}|e^{j\theta} \tag{5}$$

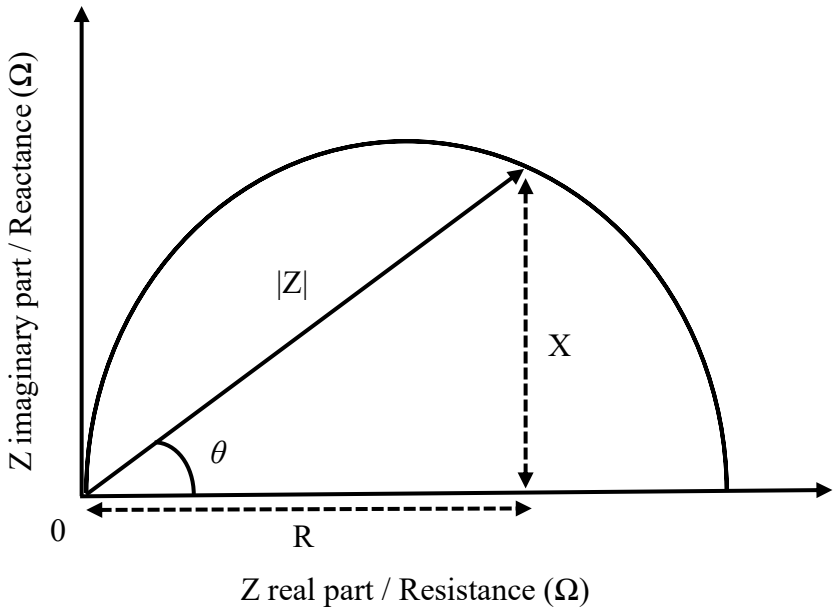

Figure 2.18: The complex impedance plotted as a planar vector using rectangular and polar coordinates (Lvovich, 2012).

Traditional EIS is based on linear response theory, where the current response is measured for small amplitude excitations of the applied harmonically oscillating voltage (i.e. < 20 ~ 30 mV), the resulting current is directly proportional to a change in the applied voltage. Modern EIS can go to higher voltages and thus into the non-linear region, and can thereby provide additional information on the conduction mechanisms at higher electrical fields. For larger excitation voltages, the resulting current is not directly proportional to the change in the applied voltage (Fasmin & Srinivasan, 2017; Lvovich, 2012).

In most fruit tissue, cells and extracellular fluid are the two main components. The electrical properties of fruit tissues are associated with the distribution and composition of these two components (Fuentes et al., 2014). Both intracellular and extracellular fluids in fruit tissue are composed of water, free ions, electrolytes, salts and other components, thus their electrical behaviour is mainly resistive (Yu, Liu, & Zhou, 2004). However, the cell membrane, which surrounds the cell, consists of a thin lipid bilayer that serves as an interface between the intracellular and the extracellular media. The cell membrane has a capacitive behaviour because of the presence of this double lipid layer (Harker & Forbes, 1997; Yu et al., 2004). Reactance of a plant tissue is related to the presence of membranes and the capacitance of the tissue (Harker & Forbes, 1997). These two behaviours affect the EIS results observed in the fruit tissues.

Figure 2.19 shows a pattern diagram of the unprocessed plant cells and the flow of the electric current. At low frequency, the electrical current can only flow through extracellular fluid due to the high electrical capacitance of cell membranes (Ando, Mizutani, & Wakatsuki, 2014). The extracellular pathway has relatively high resistance (Figure 2.19) as a result of the small cross-sectional area between membranes of two

adjacent cells and the low concentration of mobile ions (Ando et al., 2014; Harker & Maindonald, 1994). However, at high frequency, the electric current is capable of flowing through intracellular fluid that has relatively low resistance, thus the resistance decreases significantly (Ando et al., 2014). To analyze the measured dielectric functions, the resistance component is plotted on the x-axis and the reactance component on the y-axis, which is known as a complex impedance plot (Figure 2.18) or a Nyquist plot (Lvovich, 2012). In fresh fruit samples, the characteristic Nyquist arcs for a range of frequencies (Figure 2.21), which corresponds to the aggregation of closed cell structures, can be clearly observed (Dejmek & Miyawaki, 2002; Ohnishi, Fujii, & Miyawaki, 2002).

When cell membranes are disrupted, the cellular compartmentation is broken down, which allows the low frequency electrical current to flow through the entire cross-section of the tissue. This results in a reduction in resistance (Figure 2.20) (Hayden, Moyse, Calder, Crawford, & Fensom, 1969). In plant and fruit tissues, for example, in potato tissue, the Nyquist arc completely disappears when the cell membranes are disrupted (Figure 2.21). However, in some fruit such as grapes, the arc is still partly observed but the arc has become much smaller than that of the fresh samples (Ohnishi, Shimiya, Kumagai, & Miyawaki, 2004).

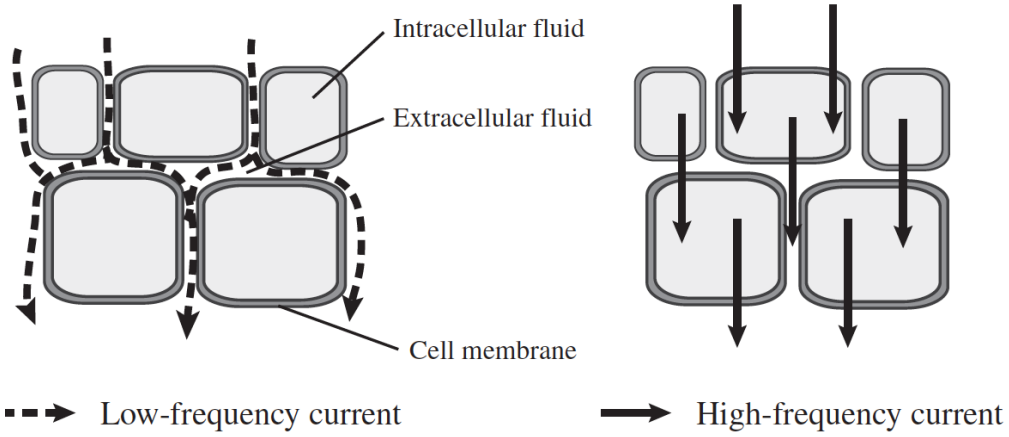

Figure 2.19: Pattern diagram of plant cells and flow of the electric current (Ando et al., 2014).

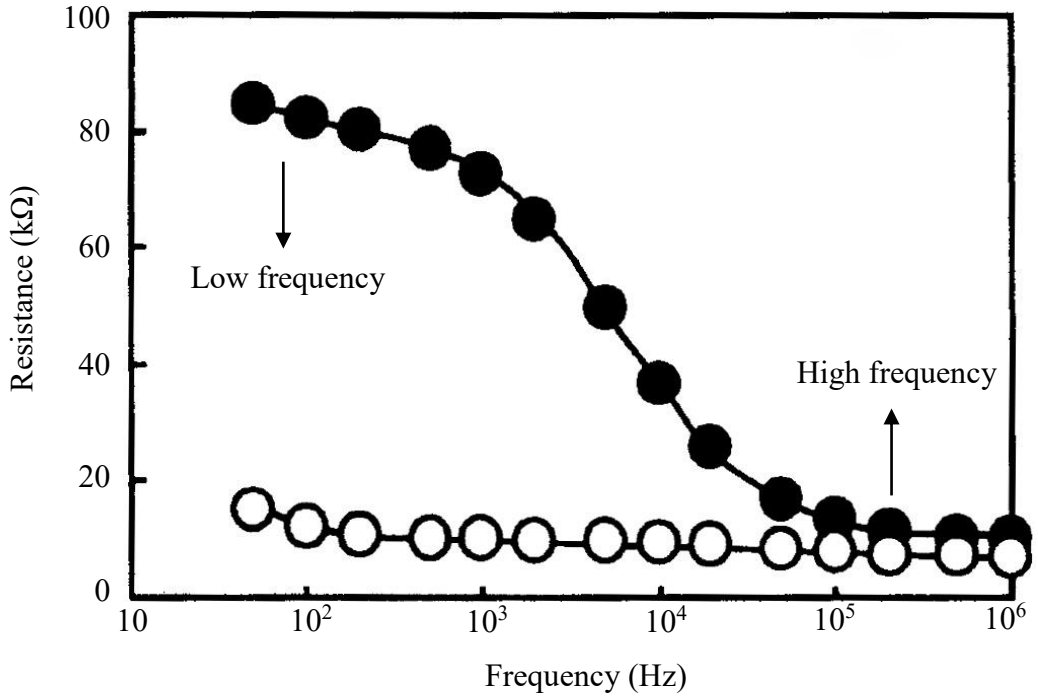

Figure 2.20: Impedance of fruit sample before (●) and after (○) cell disruption over a frequency range between 50 Hz and 1MHz (Ohnishi et al., 2004).

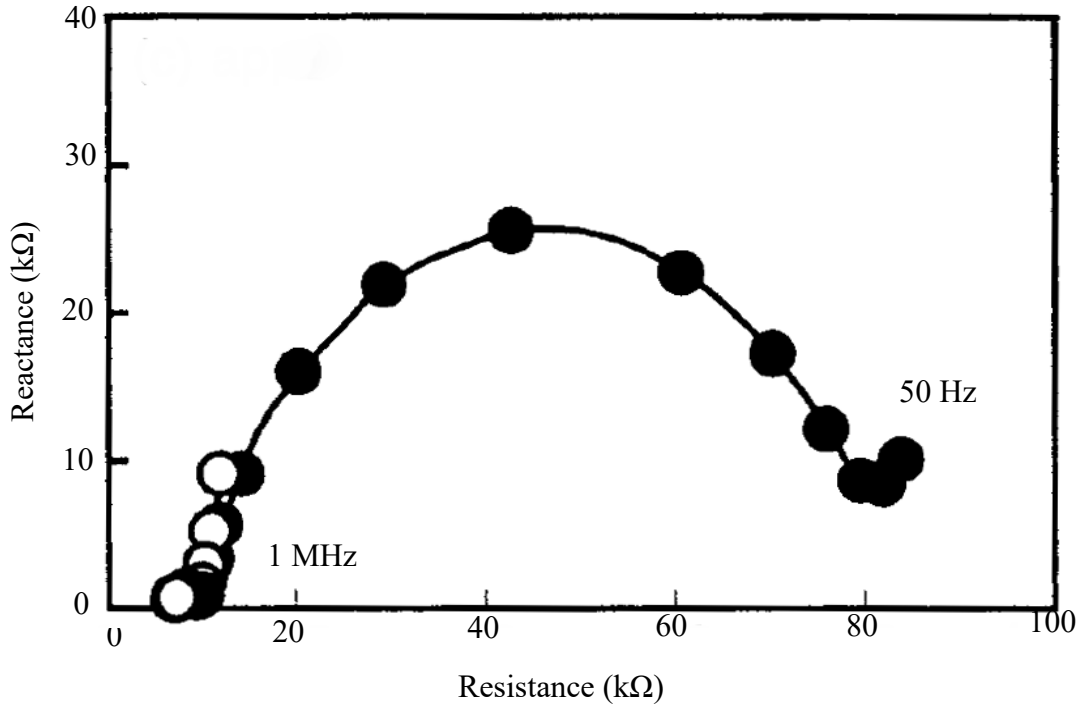

Figure 2.21: Nyquist plot of fruit sample before (●) and after (○) cell disruption over a frequency range between 50 Hz and 1MHz (Ohnishi et al., 2004).

Numerous previous investigations have shown that EIS measurements are appropriate for evaluating the ripening of fruits and fruit quality, and assessing the effect of freezing and heating injury on fruits and vegetables (Fuentes et al., 2014; Harker & Forbes, 1997; Ohnishi et al., 2004; Wu et al., 2008). Changes in electrical properties of plant tissues during freezing-thawing were studied by Ohnishi et al. (2004). After freezing-thawing, the cellular structure of plant tissues had been physically damaged by the formation of intracellular ice crystals during the freezing process, which destroyed the cell structure after thawing (Burke, Gusta, Quamme, Weiser, & Li, 1976; Ishikawa et al., 1997; Steponkus, 1984; Webb, Uemura, & Steponkus, 1994). This caused drastic changes in the electrical properties of the plant tissues. Their impedance in the low frequency range (50 Hz–10 kHz) greatly decreased, and the Nyquist arc disappeared.

For the study of fruit tissues, EIS measurement is a fast and simple method for cell structure determination compared with other techniques such as microscopy and ion leakage (%) determination (Wu et al., 2008). However, the use of EIS in the analysis of cell structure changes in avocados mesocarp during lipid extraction has not been studied.

2.6.3 Electrical conductivity

Electric conductivity values of a fruit tissue sample may indicate cell electrolyte leakage and can be used to estimate the degree of cell membrane intactness. It has been used to estimate drying, lipid extraction, fruit maturity or chilling injury of plant cells (Reilly, 2012). The leakage of electrolytes, as a result of diffusion from high concentrations inside the cell to low concentrations outside it, may be considered passive diffusion (Palta et al., 1977). When a cell wall and membrane is damaged during processing, the ions diffuse through into the extracellular liquid, which results in a change in measured solute

conductivity. By measuring the changes, it is possible to estimate the degree of rupture. Increased electrical conductivity is due to increased ion leakage which, in turn indicates a reduced membrane integrity (Pesis et al., 2003).

Measurement of ion leakage has been used to study various tissues. Electrical conductivity was used to investigate changes of avocado fruit during storage by Montoya, De La Plaza, and Lopez-Rodriguez (1994). The conductivity rise was found to be associated with long-time low-temperature storage of the fruit. This was believed to be caused by damage to cell membranes due to chilling injury. Electrical conductivity was suggested to be a suitable index of avocado quality during cold-storage (Montoya et al., 1994). Cell integrity of onion tissue was studied by using ion leakage measurement coupled with microscopic images (Ersus & Barrett, 2010). With a pulsed electric field continuous treatment, an increase in cell rupture and electrical conductivity were observed. It was suggested that ion leakage measurements combined with microscopic methods are an easy way to monitor cell rupture that requires low investment cost (Ersus & Barrett, 2010). Conductivity of apple, peach, pear, pineapple and strawberry was measured to determine the effect of ohmic heating on membrane integrity (Sarang, Sastry, & Knipe, 2008). Increases in the electrical conductivity of all five types of fruit were observed during heating of biological tissue due to the breakdown of cell walls and membranes, which increases the ionic mobility (Sarang et al., 2008).

2.6.4 Rheological properties

Food rheology is the study of flow and deformation of food and when subjected to normal and tangential stresses (Barnes, 1999; Rao, 2010). Rheological measurements have many applications in the food industry including the fields of food acceptability, food

processing and food handling (Barbosa-Cánovas, Kokini, Ma, & Ibarz, 1996). This has been considered to be an important analytical tool to provide fundamental information on the dependence of food structure on overall composition and interaction between the components (Shoemaker & Borwankar, 1992). Foods can be classified according to their rheological behaviours as liquids, suspensions of solids in liquids (semi-solids or semi-liquids) and solids (Gallegos & Franco, 1999; Van Vliet, Van Aken, De Jongh, & Hamer, 2009). Avocado fruit pulp is classified as semi-solid (semi-liquid) material due to its multiphase nature, which comprises a particle-in-water suspension as well as an oil-in-water emulsion (20–30% of solid particles and oil droplets dispersed in a liquid phase) (Martínez-Padilla, Franke, & Juliano, 2017).

Viscosity is a measure of a fluid's resistance to motion (flow) when a shearing stress is applied, which is used to characterize flow behaviour of liquid and semi-liquid foods (Tabilo-Munizaga & Barbosa-Cánovas, 2005). Foods with low viscosity flow relatively easily when subjected to shear; in contrast, high-viscosity foods can be relatively immobile when a shear stress is applied to make them move or require the need to overcome a yield stress (Hill & Carrington, 2006). Viscoelasticity is the property of semi-liquid food material that exhibits both viscous and elastic behaviours. *G'* is the storage modulus, which is a measure of the degree of elastic behaviour in a material; in contrast, *G"* is the loss modulus, which is an indicator of the degree of viscous behaviour in a material (Miri, 2011; Tabilo-Munizaga & Barbosa-Cánovas, 2005). In food materials, a larger value of *G'*, in comparison to *G"*, represents that the material has predominantly elastic behaviour. However, if *G"* is greater than *G'*, the material exhibits a more viscous behaviour (Miri, 2011; Rao, 2010).

Recent studies showed that monitoring rheological properties of fruit pulp tissues provides information about the oil aggregation during extraction of oil from oleaginous fruit (Martínez-Padilla et al., 2017; Romaniello, Leone, & Tamborrino, 2017; Tamborrino et al., 2017). The application of rheological properties measurement for this purpose is a relatively new technique. The effect of malaxing time on viscosity of olive pulp has been studied by Tamborrino et al. (2017). Increasing malaxing time resulted in a decrease in the viscosity of olive pulp, which could be explained as an increasing availability of the liquid fraction, as a result of oil droplets coalescing, depending on the malaxing process.

The effect of malaxing time on viscoelastic properties of avocado pulp has been investigated by Martínez-Padilla et al. (2017) who reported that the storage modulus (G') of the avocado pulp decreased after 60 min malaxing at 45 °C. This phenomenon indicated an increase in the liquid-like behaviour of the avocado pulp, which could also be explained as an increased degree of oil aggregation during malaxing.

Thus, the rheological properties of fruit pulp represent a fundamental means to characterise fruit pulp behaviour, which can be very useful for monitoring oil coalescence in avocado pulp as a more continuous oil phase develops during malaxing. In addition, it is very important for the design of many processes and processing equipment that apply shear forces. There are only a few studies on rheological properties of avocado pulp and none has considered the effect of temperature during malaxing.

2.7 Avocado oil composition

2.7.1 Fatty acid composition

The fatty acid composition (Table 2.4) of avocado oil is similar to olive oil, which has a

very high percentage of oleic acid (C18:1). The fatty acid composition can be significantly affected by the growing environment (Woolf et al., 2009). The main fatty acids in a typical avocado oil includes palmitic acid (C16:0) and stearic acid (C18:0) (saturated fatty acids), palmitoleic acid (C16:1) and oleic acid (C18:1) (monounsaturated fatty acids), and linoleic acid (C18:2) and linolenic acid (C18:3) (polyunsaturated fatty acids) (Eaks, 1990; Inoue & Tateishi, 1995; Ratovohery, Lozano, & Gaydou, 1988).

Table 2.4: Fatty acids composition of 'Hass' avocado oil from five countries (Woolf et al., 2009).

Fatty acids (% of total)	New Zealand		Australia	Chile	Mexico	California
	Range	Mean	Mean	Mean	Mean	Mean
Palmitic acid C16:0	9.7-15.2	12.3	21.7	13.1	14.8	14.5
Palmitoleic acid C16:1	1.7-8.2	4.1	9.3	3.6	7.9	4.1
Stearic acid C18:0	0.1-0.4	0.3	0.4	0.4	0.4	0.3
Oleic acid C18:1	61.7-77.8	71.5	51.8	68.2	66.8	65.3
Linoleic acid C18:2	7.7-18.9	11.6	16.0	13.2	9.5	15.0
Linolenic acid C18:3	0.2-0.9	0.5	0.8	0.8	0.6	0.8

Monounsaturated fatty acids contribute to a large portion (≅70%) of avocado oil. It is generally accepted that unsaturated lipids instead of saturated lipids have a positive effect on the low-density lipoprotein cholesterol level and risk of coronary heart disease in middle-aged and older women and men (Jacobsen, Let, Nielsen, & Meyer, 2008; Kris-Etherton, 1999).

2.7.2 Tocopherols

Vitamin E, which is an essential vitamin, has powerful antioxidant properties that can assist to extend the shelf life of oil (Coppen, 1994). In cold-pressed avocado oil, α-tocopherol is the major form of vitamin E; minor amounts (< 10 μg g^{-1} oil) of β-tocopherol, δ-tocopherol and γ-tocopherol are also detected in the oil. The concentration of α-

tocopherol in cold-pressed avocado oil is 70–190 μg g^{-1} oil, which is similar to olive oil (100–140 μg g^{-1} oil) (Boskou, 2006; Wong et al., 2010). Compared to solvent extraction and refining methods, cold-pressed extraction can help to retain higher concentrations of the tocopherols. These antioxidants can assist to scavenge the harmful free radicals from the normal oxidation processes of the body, thus reducing the risk of cardiovascular disease (Pryor, 2000; Tiwari, Brunton, & Brennan, 2013).

2.7.3 Sterols

Consumption of adequate amounts of plant sterols has a favourable effect on the reduction of blood-cholesterol levels, which can help reduce the incidence of heart disease (Piironen, Lindsay, Miettinen, Toivo, & Lampi, 2000; Weststrate & Meijer, 1998). Avocado contains the highest concentration of plant sterols of any fleshy fruit (Duester, 2001). β-Sitosterol is the major plant sterol found in avocado oil, with low concentration of Δ-5-avenasterol, campesterol, and stigmasterol. In avocado oil, the concentration of β-sitosterol was reported to be approximately 2.3–4.5 mg g^{-1} oil, which is significantly higher than that of olive oil (1.62–1.93 mg g^{-1} oil) (Phillips, Ruggio, Toivo, Swank, & Simpkins, 2002; Verleyen et al., 2002; Wong et al., 2010).

2.7.4 Pigments

During cold-pressed extraction, significant amounts of plant pigments including carotenoids and chlorophyll are extracted into the oil. The carotenoid detected at the highest concentration in the oil is lutein (0.5–3.3 μg g^{-1} oil), which is associated with reduction of age-related macular degeneration and is therefore beneficial for eye health (Lu et al., 2005). Avocado oil contains approximately twice the concentration of lutein in olive oil (Criado, Motilva, Goñi, & Romero, 2007).

Chlorophyll (11.1–18.5 μg g^{-1} oil) is another pigment found in cold-pressed avocado oil. Chlorophyll has been reported to be beneficial for health, although the exact mechanism is still unclear (Mínguez-Mosquera, Gandul-Rojas, Gallardo-Guerrero, Roca, & Jarén-Galán, 2008). However, chlorophyll is a strong photosensitizer, which does not contribute to oil stability but does contribute to any photo-oxidation occurring. Therefore, it is important to eliminate light and oxygen during processing and storage of the oil (Mínguez-Mosquera et al., 2008).

2.8 Virgin olive oil extraction

2.8.1 Overview of olive fruit

The olive fruit (*Olea europaea* L.) is a high oil content fruit composed of three principal tissues, the skin (exocarp), the flesh (mesocarp), and the seed (endocarp) (Rapoport, Fabbri, & Sebastiani, 2016). The mesocarp, which is composed of parenchyma cells, is the major and edible part of the olive fruit as well as the site for oil metabolism and storage in the fruit. In olive fruit, the accumulation of oil bodies takes place in the cytoplasm of parenchyma cells. Oil droplet enlargement occurs by a continuous coalescence of oil bodies throughout development and maturation of the fruit, resulting in the formation of a large single oil droplet (≅30 μm in diameter) in most parenchyma cells in mature fruit (Rangel, Platt, & Thomson, 1997).

A strong correlation was found between dry matter content and total oil content in the olive flesh (Requejo-Jackman et al., 2010). The dry matter and total oil content largely increase during the ripening period of olive then slows as full maturity approaches, and slightly declines as the fruit becomes over ripe (Beltrán, del Río, Sánchez, & Martínez,

2004; Requejo-Jackman et al., 2010; Salvador, Aranda, & Fregapane, 2001). The olive flesh at maturity contains 20–25% oil (by fresh weight) (Wong et al., 2012). The optimal harvest time of olive fruit for oil extraction is when the fruit are at optimum maturity, when the oil content is high in the fruit flesh (Petrakis, 2006). Traditionally, the harvest time can be judged by the colour of the fruit skin. Olives should be harvested at the green-yellow or black-purple stage before natural fruit drop (Petrakis, 2006).

2.8.2 Virgin olive oil

Virgin olive oil is a high-value culinary oil that is prized for its fatty acid composition, and particularly, its vitamin and antioxidant contents, which are extremely important for health and nutrition (Petrakis, 2006; Wong et al., 2012). The extraction of the oil and the standards determining the different grades of olive oil are defined by the International Olive Council (IOC), European Commission (EC) regulations and Codex Alimentarius for food (Codex Alimentarius, 2017; European Commission, 2002; International Olive Council, 2006). These standards specify that virgin and extra virgin grades of olive oil must be extracted from olives solely by mechanical means, without the use of solvents or heat. The mechanical extraction of olive oil must not alter the composition or organoleptic characteristics of the oil, so must be carried out at no higher than 27 °C and use hydraulic presses or centrifugation to recover the oil from the olive paste (Codex Alimentarius, 2017; European Commission, 2002; International Olive Council, 2006). The virgin olive oil will have exceptional chemical and organoleptic characteristics when they are produced by using appropriate extraction techniques, from high quality fresh fruit that have no disorders or damage and the fruit have been harvested at the suitable stage of maturity (Petrakis, 2006; Wong et al., 2012).

2.8.3 Commercial extraction systems

The commercial extraction system of virgin olive oil is shown in Figure 2.22 and comprises three main operations: fruit cleaning (defoliation, olive washing), preparation of the paste (grinding, malaxing) and oil separation. The first step for oil extraction is fruit cleaning, which includes leaf removal and washing. The leaves, twigs and dirt on the olive fruit are sucked by defoliators through a powerful airflow generated by an exhaust fan, then the olive fruit are passed through the washer to be washed in a current of water (Petrakis, 2006; Wong et al., 2012). Next, the whole washed fruit (with seed) are ground by using an attrition mill to disrupt the parenchyma cells and release the oil droplets (Petrakis, 2006; Wong et al., 2012). Not all the oil can be liberated from the parenchyma cells by grinding because it is virtually impossible to disrupt all the cells in the mesocarp (Petrakis, 2006). After grinding, a malaxing process is used to help form a larger continuous oil phase, coalescing the oil droplets released from the cells by grinding (Petrakis, 2006). By slowly malaxing (15–25 rpm) the ground olive paste, oil droplets aggregate to form larger drops and eventually a continuous oil phase, which improves oil yield in the subsequent separation step (Di Giovacchino et al., 2002a; Petrakis, 2006; Wong et al., 2012).

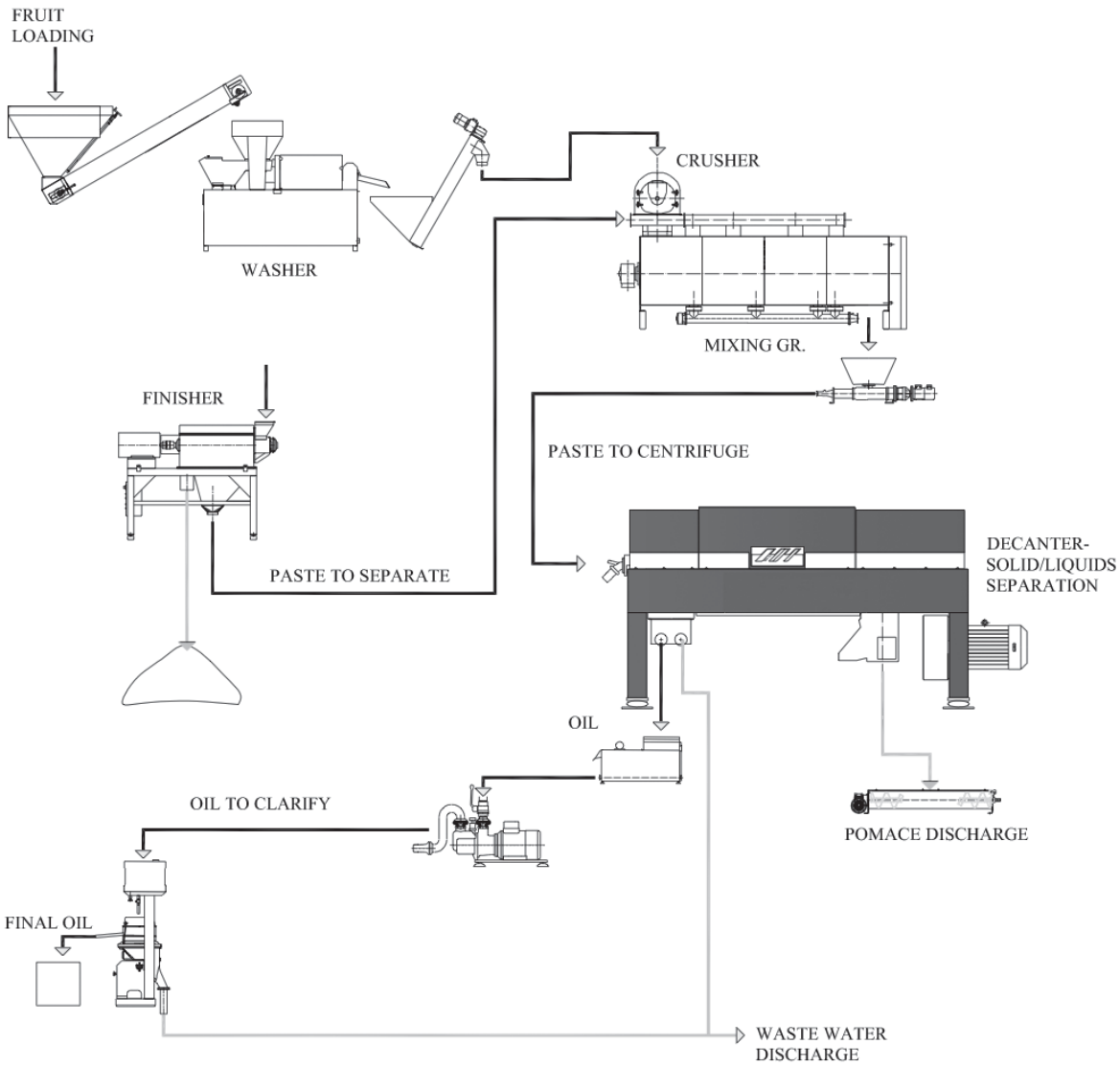

Figure 2.22: Process flow diagram for cold-pressed extraction of virgin olive oil (Wong et al., 2012).

The change in oil droplet size in olive paste during malaxing has been studied by Di Giovacchino (1989) and Di Giovacchino (1996) who reported that the minimum size of oil droplets to achieve a good oil yield during continuous-process separation (centrifugation) was more than 30 µm diameter. However, they found only 45% of the oil droplets were this size after grinding. After malaxing, this percentage increased to 80% (Table 2.5). So, oil extraction yield increased significantly with increased malaxing time to 90 min (Di Giovacchino et al., 2002a; Di Giovacchino et al., 2002b). Oil extraction

(recovery rate) was dependent on the extent of cellular disruption and oil aggregation (Petrakis, 2006). Hence methods to help monitor these two processes during malaxing could assist to identify the minimum malaxing time required to optimise oil yield.

Table 2.5: Changes in olive oil droplet size during malaxing for 90 min (Di Giovacchino et al., 2002a; Di Giovacchino et al., 2002b).

	Diameter of olive oil droplets (μm)					
	<15	15–30	30–45	45–75	75–150	>150
Before malaxing (%)	6	49	21	14	4	6
After malaxing (%)	2	18	18	18	19	25

After malaxing, the oil separation operations followed similar procedures as the commercial centrifugation system for cold-pressed avocado oil extraction in Section 2.4.1. The olive paste is transferred into the horizontal decanter to remove the solid phase (pomace) from the liquid phase (water and oil). Next, the oil and water phase is passed through disc centrifuges to separate the water from the oil (Petrakis, 2006; Wong et al., 2012).

2.9 Literature review conclusions

Cold-pressed avocado oil is a popular culinary oil, which is high in monounsaturated fatty acids and pigments (chlorophyll and carotenoids), has a characteristic flavour and a high smoke point (over 250 °C). In avocado fruit flesh, the oil is mostly found as numerous droplets or oil bodies scattered throughout the cytoplasm of the parenchyma cells. Also, a small amount oil was found in idioblast oil cells as a single large drop filling the cell. However, it is still unclear if the idioblast cells are ruptured during the cold-pressed avocado oil extraction process or remain intact during the extraction process.

Cold-pressed avocado oil extraction uses mechanical means to liberate the oil after first breaking the cellular structure, followed by malaxing (mixing) at ≤ 50 °C. The malaxing step may lead to more cellular disruption and help the oil droplets to aggregate to form larger drops that can be easily recovered through the centrifugal extraction systems. However, the microstructural changes in avocado fruit prior to and during cold-pressed oil extraction, and how these microstructural changes impact on oil yield have not been investigated in previous studies.

Cold-pressed avocado oil yield and quality might be affected by different factors including avocado fruit maturity, fruit ripening, fruit quality and oil extraction processing conditions, but the mechanism behind these effects are still unclear. Novel processing such as ultrasonication is also a potential new technology in avocado oil extraction processing that may improve the cold-pressed oil yield. Changes in cell integrity and oil aggregation in avocado pulp during cold-pressed oil extraction can be monitored using various techniques, including EIS, electrical conductivity measurement, light microscopy, and rheology to fill these research gaps in the area of avocado oil study.

Chapter 3:

Materials and methods

3.1 Raw materials

3.1.1 Avocado fruit for commercial factory trial

'Hass' avocado fruit (*Persia americana* Mill.) were harvested from commercial orchards in Northland, New Zealand, from two avocado harvesting seasons, firstly in October 2015 and secondly from September 2016 through to April 2017. Fruit were transported to Olivado Ltd NZ's, Kerikeri plant then held outside without temperature control for 6–10 days and allowed to ripen naturally (without ethylene treatment) in 1000 L wooden bins to the target fruit firmness at 80 ± 3 firmometer value (Fv).

3.1.2 Avocado fruit for laboratory trial

'Hass' avocado fruit were harvested from Plant and Food Research Ltd orchards in Bay of Plenty, New Zealand, over three avocado harvesting seasons, firstly from October through to November 2015, secondly from July 2016 through to March 2017 and thirdly from August 2017 and January 2018. Fruit were transported to the Mt. Albert Research Centre of Plant and Food Research Ltd, Auckland and stored for 2–4 days at 6.0 ± 0.5 °C prior to ripening and subsequent oil extraction. To ripen the avocados, they were treated with 100 μL L^{-1} ethylene for 24 h at 20 ± 1 °C in 360 L tubs. After removal from ethylene, the fruit were held at 20 ± 1 °C and allowed to ripen for around 12 h, 30 h and 48 h to the target fruit firmness at 55 Fv (minimally ripe), 80 Fv (fully ripe) and 105 Fv (over ripe), respectively. Ripe rots were detected in avocado fruit at 80 and 105 Fv, the rot parts of fruit were also used in the laboratory-based cold-pressed extraction (in Section 3.3.2). Assessment of the rots on the fruit body was carried out visually by determining the area of rot relative to the entire surface area of the whole fruit.

3.1.3 Olive fruit for commercial factory trial

Olive fruit from the 'J5' cultivar (*Olea europaea* L.), which is similar to the more commonly grown 'Frantoio' cultivar (Edwards, 2007), were harvested when the fruit were mature and maximum oil yield was anticipated from a commercial orchard in Northland, New Zealand, in May 2017. The fruit were transported to Olivado Ltd NZ's Kerikeri plant then held at 20 ± 3 °C and were extracted within 12 h of harvesting.

3.2 Postharvest assessments

3.2.1 Dry matter determination for avocado fruit

Twenty fruit for laboratory trials were cut into quarters, peeled and destoned by hand, then sliced. One avocado transverse slice (2–3 g) was taken from the middle of each fruit. Twenty avocado slices were weighed accurately to three decimal places in a Petri dish and dried in an oven (Ezidri Ultra FD1000; Hydraflow Industries Ltd, Upper Hutt, New Zealand) at 65 ± 1 °C for 48 h to a constant mass. The percentage of dry matter content in fruit was calculated as follows:

$$\text{Dry matter content (\%)} = \frac{\text{Weight of dry flesh,g}}{\text{Weight of fresh flesh,g}} \times 100 \quad (1)$$

3.2.2 Dry matter determination for avocado/olive pulp

Avocado/olive fruit pulp samples (≅ 50 g) were collected from a D-shaped horizontal malaxer tank (Alfa Laval, Lund, Sweden) at 0 min malaxing stage of the commercial oil extraction process. Fruit pulp samples were stored immediately in a chilly bin on ice at 4 ± 1 °C for 4 h (transport time to laboratory). Avocado fruit pulp samples were weighed accurately to three decimal places in a Petri dish then dried in an oven at 65 ± 1 °C for 48 h to a constant mass. The percentage of dry matter content of the fruit was calculated as follows:

$$\text{Dry matter content (\%)} = \frac{\text{Weight of dry pulp,g}}{\text{Weight of fresh pulp,g}} \times 100 \quad (2)$$

3.2.3 Firmness measurement for avocado fruit

The firmness expressed as a Fv of whole avocado fruit was measured using a digital firmometer (Anderson Manufacturing, Tauranga, New Zealand) (Ashton et al., 2006). The firmometer evaluates firmness of whole intact fruit (skin on) by using a compression test, which measures the resistance to compression of the whole fruit when a force is applied through a 17 mm diameter probe over a ten second period. Force is applied by using a 200 g weight. Firmness measurement was carried out for each batch of fruit collected on a sample size of n = 30 fruit (White et al., 2005).

$$\text{Fv} = \text{Firmometer reading (mm displacement)} \times 10 \text{ (dimensionless)} \quad (3)$$

3.2.4 Firmness measurement for olive fruit

Fruit firmness was recorded using a Firmtech machine (Model FT4; BioWorks Inc, Wamego, KS, USA) which evaluates firmness of fruit by using a compression test to squeeze the fruit and measures the force required to deform the fruit by 1 mm. Fruit are placed on a turntable (25 places) and automatically rotated for assessment. The data collected by the computer software (Inst300, BioWorks Inc, Wamego, KS, USA) was used to determine the slope of the force/distance curve to calculate force as g/mm (grams of force required to compress the fruit 1 mm). This was converted to kg mm^{-1}. Firmness measurement was carried out on a sample size of n = 50 fruit.

3.3 Cold-pressed oil extraction

3.3.1 Commercial cold-pressed extraction of avocado oil

The commercial cold-pressed avocado oil extraction was carried out at Olivado Ltd NZ's

Kerikeri plant following the procedure (Figure 3.1) as described in Woolf et al. (2009). Ripe avocados (650 kg/malaxer) were washed by a fruit washing machine (Alfa Laval, Lund, Sweden) then transferred to a destoner (Alfa Laval, Lund, Sweden) to separate the skin and stone from the flesh. The smashed avocado flesh was ground using a attrition mill grinder (Alfa Laval, Lund, Sweden) then collected in a pre-malaxer tank (720 mm width × 2200 mm length × 720mm height; Alfa Laval, Lund, Sweden) and mixed at 20 rpm using a ribbon mixer for 30 min until the pre-malaxer tank was full. The pulp was then transferred (within 5 min) into a D-shaped horizontal malaxer tank (720 mm width × 2200 mm length × 720mm height) and mixed at 20 rpm using a ribbon mixer for 120 min at 45 ± 3 °C. After malaxing, the pulp was pumped immediately into a horizontal decanting centrifuge (Model NX20; Alfa Laval, Lund, Sweden) which was operating at 3,574 × *g* (4,000 rpm) at 20 ± 3 °C to separate the oil phase from the solids (pomace) and water phase (wastewater). The oil phase was then passed through polishing disc centrifuges (Model UVPX; Alfa Laval, Lund, Sweden) to remove any residual water in the oil.

Ten samples were collected during the extraction process: 1. Fresh (unprocessed) whole avocado fruit (50 fruit); 2. Pulp after destoning; 3. Pulp after grinding (pulp sample existing the grinder); 4. Pulp at 0 min malaxing (the pre-malaxer took 30 min to fill and then the pulp was transferred to the malaxer, 0 min was when the malaxer was full); 5. Pulp after 30 min malaxing; 6. Pulp after 60 min malaxing; 7. Pulp after 90 min malaxing; 8. Pulp after 120 min malaxing; 9. Pomace from the decanting centrifuge; 10. Waste water from the decanting centrifuge.

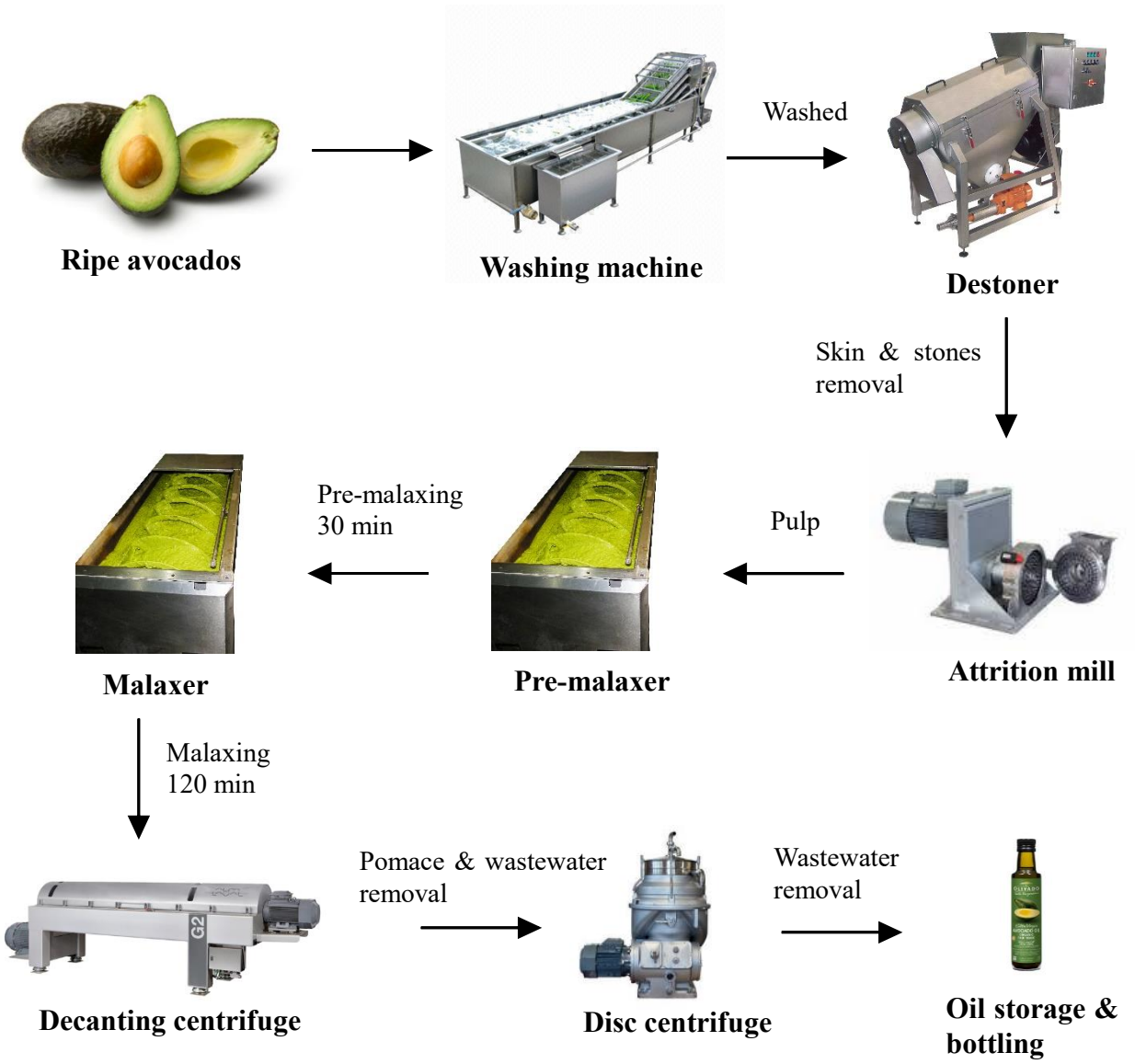

Figure 3.1: Process flow diagram for commercial cold-pressed extraction of avocado oil.

3.3.2 Laboratory-based cold-pressed extraction of avocado oil

The laboratory-based cold-pressed avocado oil extraction was carried out based on procedures (Figure 3.2) recommended by Woolf et al. (2009) and Wong et al. (2011). For each trial, twenty fruits were washed, cut into quarters, peeled and destoned by hand and ground using a bench top hammer mill (Siemens, Munich, Germany). The pulp was then transferred into a 1 L stainless steel jacketed vessel (malaxer; Massey University,

Auckland, New Zealand) and mixed with overhead mixers (Model RW20 digital; IKA-Works Inc, Wilmington, NC, USA) at 45 ± 1 °C at 20 rpm for 120 min. After malaxing, the pulp (300 g) was put in a 500 mL plastic centrifuge bottle and centrifuged at 12,278 × *g* (8,500 rpm) for 30 min at 20 ± 1 °C (Thermo Fisher Scientific Inc, Waltham, MA, USA) to separate the oil phase from the solids (pomace) and water phase. The oil phase was then collected in a 50 mL plastic centrifuge tube and re-centrifuged at 3,214 × *g* (5,000 rpm) for 10 min at 20 ± 1 °C to remove any residual water from the oil. The oil samples were stored at -80 ± 2 °C for further quality analysis.

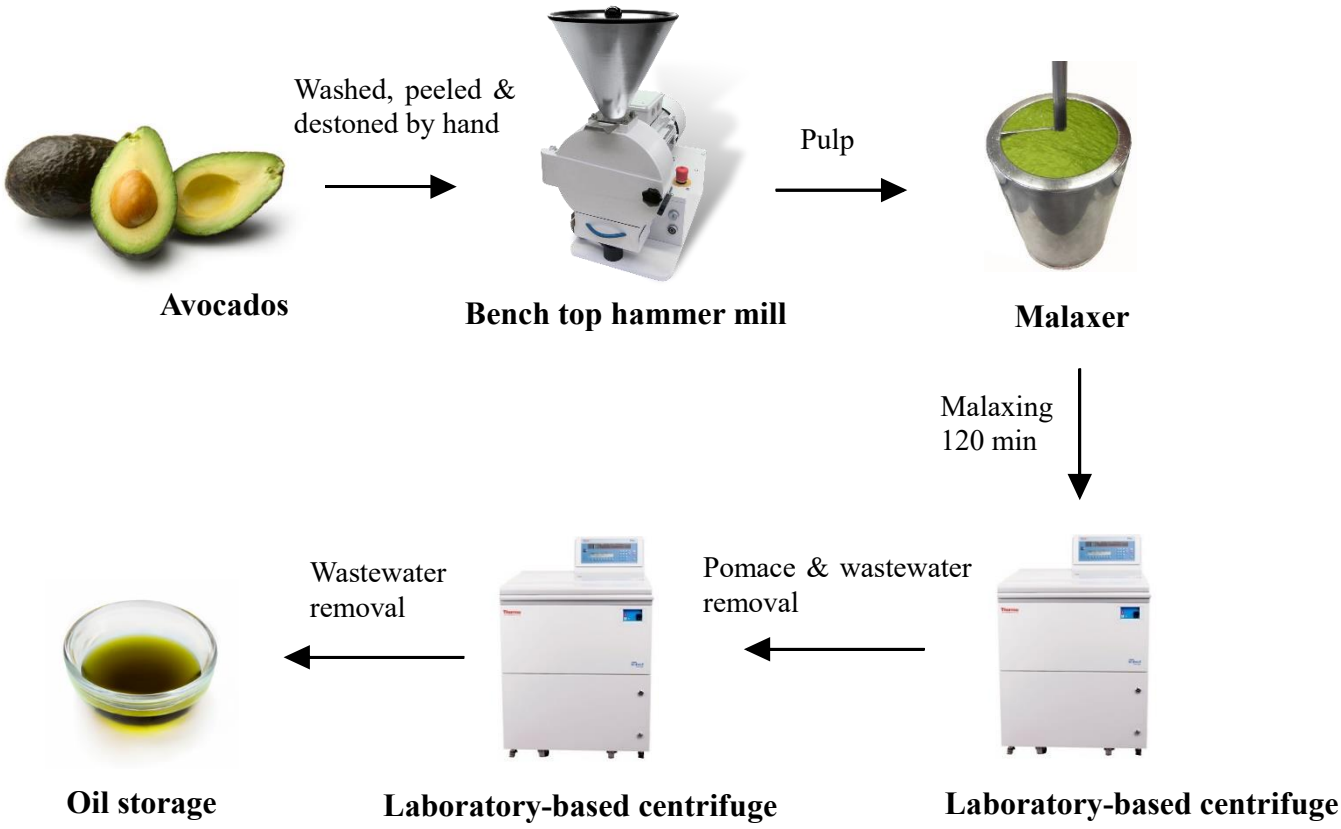

Figure 3.2: Process flow diagram for laboratory-based cold-pressed extraction of avocado oil.

Five samples were collected during the extraction process: 1. Fresh (unprocessed) whole avocado fruit (20 fruit); 2. Pulp after grinding (at 0 min malaxing); 3. Pulp after 60 min malaxing; 4. Pulp after 120 min malaxing; 5. Cold-pressed oil sample after centrifugation. Note there was no pre-malaxing step in the laboratory extraction procedure (Figure 3.2).

3.3.3 Commercial cold-pressed extraction of olive oil

The commercial cold-pressed olive oil extraction (Figure 3.3) method followed similar procedures as the commercial cold-pressed extraction of avocado oil in Section 3.3.1 except for two changes: 1) After the olive fruit were washed, they were transferred directly to the attrition mill grinder, without the destoning step; 2) After the pulp was transferred into a D-shaped horizontal malaxer tank, they were mixed at 20 rpm using a ribbon mixer for 60 min at 26 ± 1 °C, in accordance with Codex specified methods for olive oil extraction, which states it must be below 27 °C (Codex Alimentarius, 2017).

Eight samples were collected during the extraction process: 1. Fresh (unprocessed) whole olive fruit (70 fruit); 2. Pulp at 0 min malaxing; 3. Pulp after 15 min malaxing; 4. Pulp after 30 min malaxing; 5. Pulp after 45 min malaxing; 6. Pulp after 60 min malaxing; 7. Pomace from the decanting centrifuge; 8. Waste water from the decanting centrifuge.

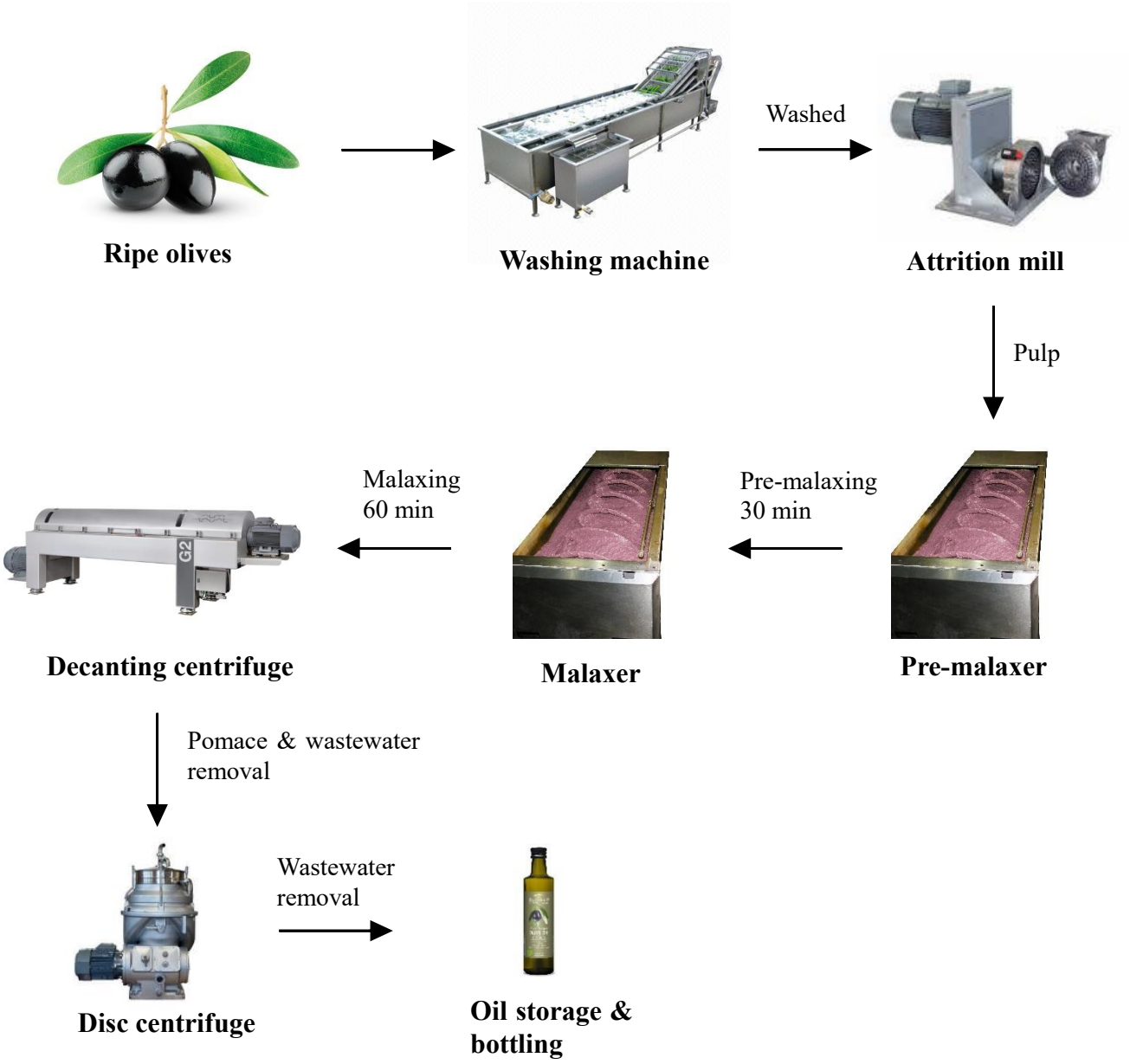

Figure 3.3: Process flow diagram for commercial cold-pressed extraction of olive oil.

3.3.4 Determination of the cold-pressed oil yield at each stage of malaxing in the commercial trial

Fruit pulp samples (300 g) at various stages during the commercial oil extraction process were collected and weighed accurately to two decimal place in 500 mL plastic centrifuge bottle and stored immediately in a chilly bin with ice to maintain a temperature of 4 ± 1 °C for 4 h (transport time to laboratory). Fruit pulp was centrifuged at 12,278 × *g* for

30 min at 20 ± 1 °C (Thermo Fisher Scientific Inc, Waltham, MA, USA) to separate the oil phase from the solids (pomace) and water phase. The oil phase was then collected in a 50 mL plastic centrifuge tube and re-centrifuged at 3,214 × *g* rpm for 10 min at 20 ± 1 °C to remove any residual water from the oil.

3.4 Ultrasound treatment

3.4.1 Ultrasound treatment without malaxing

For each trial, twenty avocado fruits were cut into quarters, peeled and destoned by hand and ground using a bench top hammer mill (Siemens, Munich, Germany). The pulp (50 g) was then weighed accurately to two decimal places in a 100 mL plastic vial and sonicated directly with a sonotrode (Figure 3.4; Model Sonic-650WT; MRC Ltd, Frankfurt, Germany) at 20–25 kHz for 5, 10, 15, 20 and 25 min, respectively, with pulsing intervals of 5 s on and 5 s off. After ultrasound treatment, the pulp (30 g) was weighed accurately to two decimal places in a 50 mL plastic centrifuge tube and centrifuged (Thermo Fisher Scientific Inc, Waltham, MA, USA) at 12,278 × *g* for 30 min at 20 ± 1 °C to separate the oil phase from the solids (pomace) and water phase. The oil phase was then collected in a 10 mL plastic centrifuge tube and re-centrifuged at 3,214 × *g* for 10 min at 20 ± 1 °C to remove any residual water from the oil.

Figure 3.4: Sonic-650WT ultrasonic processor (MRC Ltd, 2018).

3.4.2 Ultrasound treatment with malaxing

For each trial, twenty avocado fruits were cut into quarters, peeled and destoned by hand and ground using a bench top hammer mill (Siemens, Munich, Germany). The pulp was then transferred into a 1 L stainless steel jacketed vessel (malaxer) and mixed at 45 ± 1 °C at 20 rpm for 20, 40 and 60 min, respectively. The pulp (50 g) was then weighed accurately to two decimal places in a 100 mL plastic vial and sonicated directly with a sonotrode at 20–25 kHz for 20 min with pulsing intervals of 5 s on and 5 s off. After ultrasound treatment, the pulp (30 g) was weighed accurately to two decimal places in a 50 mL plastic centrifuge tube and centrifuged (Thermo Fisher Scientific Inc, Waltham, MA, USA) at 12,278 × *g* for 30 min at 20 ± 1 °C to separate the oil phase from the solids and water phase. The oil phase was then collected in a 10 mL plastic centrifuge tube and re-centrifuged at 3,214 × *g* for 10 min at 20 ± 1 °C to remove any residual water from the oil.

3.5 Total oil content measurement

Accelerated solvent extraction (ASE) was used to determine the total oil content in the avocado flesh (Ashton et al., 2006). The procedure was conducted under minimal light (0.001 μmol s^{-1} m^{-2}); the extraction solvent was hexane (Liquid chromatography grade purity, LiChrosolv, Darmstadt, Germany) and the purge gas was oxygen-free N_2 (99.99% purity; The BOC Group Ltd, Auckland, New Zealand). Oven-dried avocado/olive flesh samples (from Section 3.2.1 and 3.2.2) were ground for 2 min using a coffee grinder (Breville Group Ltd, Sydney, Australia). An accurately weighed sample of avocado/olive powder (5 g) was placed into a 20 mL stainless steel closed cell (Dionex Corp, Sunnyvale, CA, USA) fitted with a 30 mm cellulose filter (Dionex Corp, Sunnyvale, CA, USA). The extraction was conducted using the following ASE method (Figure 3.5; Model ASE 300;

Dionex Corp, Sunnyvale, CA, USA). The samples were pre-heated for 5 min to 60 ± 1 °C and then extracted for a total time of 100 min at 10 MPa. The run included five cycles of 20 min with a N_2 gas purge cycle of 90 s. The oil dissolved in the solvent was collected in dark glass bottles. Hexane was removed with a solvent evaporator (RapidVap N_2 Evaporation Systems; Labconco Corp, Kansas City, MO, USA) for 2 h at 30 ± 1 °C under flowing N_2. The percentage of total oil content in the fruit was calculated as follows:

$$\text{Total oil content (\%)} = \frac{O \times M}{D} \times 100 \quad (4)$$

Where:

O = Weight of solvent extracted oil, g

M = percentage of dry matter content in fruit, %

D = Weight of ground, oven-dried sample, g

Figure 3.5: ASE 300 Accelerated Solvent Extractor (ThermoScientific, 2018).

3.6 Electrical impedance measurements

3.6.1 Electrical impedance measurements for commercial factory trial

Fruit pulp samples (≅ 50 g) at various stages during the commercial oil extraction process were collected in 100 mL plastic vials and stored immediately in a chilly bin with ice to maintain a temperature of 4 ± 1 °C for 4 h (transport time to laboratory). Electrical impedance measurements were carried out using two Ag/AgCl electrodes (Figure 3.6; 2 mm diameter × 4 mm length, model EP2; World Precision Instruments, Sarasota, FL, USA). Once the samples had been warmed and equilibrated to 20 ± 1 °C (Appendix I), the two electrodes were placed into the samples 10 mm apart, to a depth of 4 mm (Harker & Forbes, 1997; Jackson & Harker, 2000). The electrodes were connected to a Hewlett-Packard Precision LCR Meter (Model HP4284A; Hewlett-Packard, Hyogo, Japan). The resistance (Ω) and reactance (Ω) values of electrical impedance at 500 mV were collected over the frequency range from 50 Hz and 1 MHz.

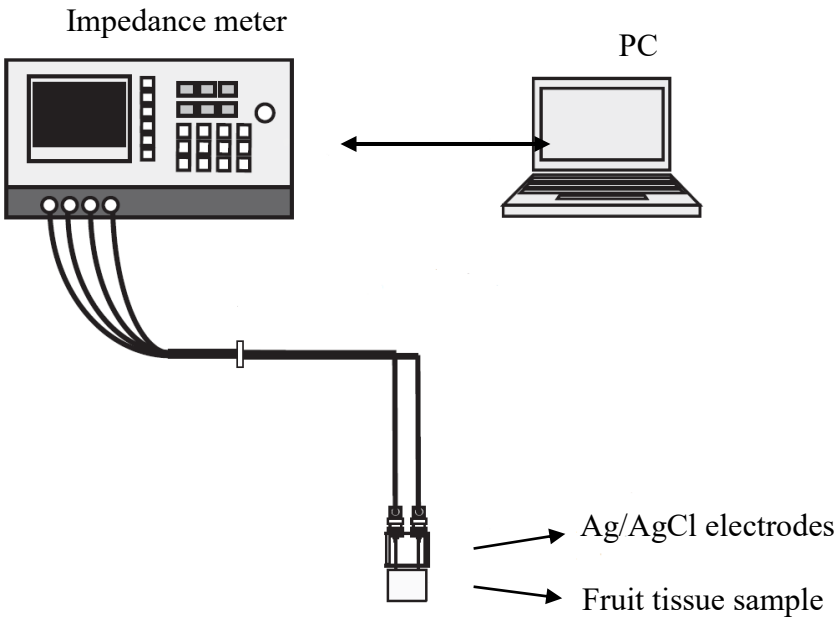

Figure 3.6: The system for electrical impedance measurement (Ando et al., 2014).

3.6.2 Electrical impedance measurements for laboratory trial

The electrical impedance measurements for laboratory trial experiments followed similar procedures as the electrical impedance measurements for commercial factory trial in Section 3.6.1 except for one change: After the fruit pulp samples were collected, the impedance of samples were measured immediately once the samples had equilibrated to 20 ± 1 °C.

3.6.3 Effect of sample storage time on impedance measurements

An experiment was carried out to determine if the impedance of samples changed within the 4 h required to transport samples back to from Olivado Ltd NZ's Kerikeri plant to the laboratory at the Mt. Albert Research Centre of Plant and Food Research Ltd, Auckland.

Twenty ripe 'Hass' avocado fruit at firmness of 85 ± 2 Fv (fully ripe) were washed, ground and malaxed using the laboratory-based cold-pressed extraction process as described in Section 3.3.2. Five samples were collected during the extraction process: 1. Pulp at 0 min malaxing (after grinding); 2. Pulp after 30 min malaxing; 3. Pulp after 60 min malaxing; 4. Pulp after 90 min malaxing; 5. Pulp after 120 min malaxing. Samples were divided into two groups: one group of samples were measured for impedance immediately after collection, another group of samples were stored in a chilly bin with ice at 4 ± 1 °C for 4 h then the impedance was measured.

Ripe 'J5' olive fruit (≅ 5 kg) at firmness of 650 ± 20 g mm^{-1} were washed, leaf removed by hand and ground using a bench top hammer mill (Siemens, Munich, Germany). The pulp was then transferred into a 1 L stainless steel jacketed vessel (malaxer; Massey University, Auckland, New Zealand) and mixed with overhead mixers at 26 ± 1 °C at 20

rpm for 60 min. Five samples were collected during the extraction process: 1. Pulp at 0 min malaxing (after grinding); 2. Pulp after 15 min malaxing; 3. Pulp after 30 min malaxing; 4. Pulp after 45 min malaxing; 5. Pulp after 60 min malaxing. Samples were divided into two groups: one group of samples were measured for impedance immediately after collection, another group of samples were stored in a chilly bin with ice at 4 ± 1 °C for 4 h then the impedance was measured.

3.7 Electrical conductivity measurements

3.7.1 Electrical conductivity measurements for commercial factory trial

The electrical conductivity of the fruit tissue and fruit pulp was measured based on a method from Woolf (1997). An accurately weighed fruit tissue sample (1 g) collected at various stages of the commercial oil extraction process was placed into 20 mL of 0.4 M mannitol solution (as mannitol is non-ionic) (Sigma-Aldrich Corp, St. Louis, MO, USA) and immediately stored in a chilly bin on ice with the temperature maintained at 4 ± 1 °C for 4 h. The sample was then shaken at 150 rpm, 30 ± 1 °C in an orbital shaker (New Brunswick Scientific Co. Inc, Hartford County, CT, USA) for 80 min (Appendix II), then the conductivity of the samples was measured at 20 ± 1 °C by using a conductivity meter (Model CG875; Schott Instruments GmbH, Hofheim, Germany).

3.7.2 Electrical conductivity measurements for laboratory trial

The electrical conductivity measurements for laboratory extraction trials followed similar procedures as the electrical conductivity measurements for commercial factory trial in Section 3.7.1 except for one change: After the fruit tissue was sampled and put into the mannitol solution, it was immediately shaken at 150 rpm, 30 ± 1 °C for 80 min in an orbital shaker (New Brunswick Scientific Co. Inc, Hartford County, CT, USA) prior to

conductivity measurement at 20 ± 1 °C.

3.7.3 Effect of sample storage time on electrical conductivity measurements

An experiment was carried out to determine if the electrical conductivity of samples changed within the 4 h required to transport samples back to laboratory from the factory (Kerikeri) following a similar procedure as that used to determine the effect of storage time on impedance measurements (Section 3.6.2).

Samples were divided into two groups after collection: one group of samples were immediately shaken in the orbital shaker for 80 min at 150 rpm, 30 ± 1 °C and then the conductivity was measured at 20 ± 1 °C; the second group of samples were stored in a chilly bin with ice at 4 ± 1 °C for 4 h, then shaken in the orbital shaker as described above and then the conductivity was measured at 20 ± 1 °C.

3.8 Light microscopy

3.8.1 Samples embedded in London Resin (LR) White resin

Collected fruit pulp samples (≅ 5 mm diameter) were covered with 5% alginate (Sigma-Aldrich Corp, St. Louis, MO, USA) then immediately placed into a 0.1 M calcium chloride solution (Sigma-Aldrich Corp, St. Louis, MO, USA) for 30 s. Fixative was prepared by combining 10 mL 25% stock glutaraldehyde (ProSciTech Pty Ltd, Townsville, Australia), 20 mL 10% fresh formaldehyde solution (Merk KGaA, Darmstadt, Germany), 50 mL 0.2 M cacodylate buffer (pH 7.2; Merk KGaA, Darmstadt, Germany) and then made up to 100 mL in a volumetric flask with distilled water. The alginate-coated granules were transferred into 15 mL fixative solution and stored at 4 ± 1 °C for 2–3 days before further embedding steps. Blocks of tissue approximately 3 × 4 × 2 mm were excised from

the fixed, alginate-coated granules, washed three times in 0.1 M cacodylate buffer (pH 7.2), then rinsed quickly in distilled water then replaced with 5 mL 10% ethanol (Merk KGaA, Darmstadt, Germany). Samples were agitated on the rotator (Model Pelco R2; Ted Pella Inc, Redding, CA, USA) at 15 rpm for 15 min. Samples were dehydrated using progressively more concentrated ethanol solutions (30%, 50%, 70%, 95%), finishing with two changes of 100% dried ethanol. Ethanol was exchanged with London Resin (LR) White resin (London Resin Co. Ltd, Reading, UK) and the samples were agitated on the rotator at 15 rpm. The resin was replaced every 16 h, three times, then the samples were placed in empty gelatin capsules with resin and polymerised at 60 ± 1 °C for 16 h. The embedded samples were stored at 20 ± 1 °C before sectioning. Sections (1 µm thick) were cut using a diamond knife in a Leica UCT ultramicrotome (Leica Microscopy Systems Ltd, Wetzlar, Germany). Sections were stained with a 0.5% toluidine blue in 0.1% sodium carbonate (pH 11.1; Sigma-Aldrich Corp, St. Louis, MO, USA) and observed using an Olympus Vanox AHT3 at 10×, 20× and 40× magnification (Olympus Optical Co. Ltd, Tokyo, Japan). The representative microscopic image was selected after examining over 100 fields of view.

3.8.2 Samples embedded in Spurr's resin

Spurr's resin (Ellis' modified formulation) was prepared by combining four liquid chemical reagents: 4.1g vinylcyclohexene dioxide (ProSciTech Pty Ltd, Townsville, Australia), 1.43g diglycidyl ether of a propylene glycol (ProSciTech Pty Ltd, Townsville, Australia), 5.9g nonenylsuccinic anhydride (ProSciTech Pty Ltd, Townsville, Australia) and 0.1g dimethylaminoethanol (ProSciTech Pty Ltd, Townsville, Australia) (Ellis, 2006; Spurr, 1969). The method using Spurr's resin followed a similar procedure as the one using LR White resin except for three changes: 1) After the sample was washed in

cacodylate buffer for 1 h, it was covered with 1% osmium tetroxide fixative in 0.1 M cacodylate buffer (Sigma-Aldrich Corp, St. Louis, MO, USA) the sample was then rotated using the rotator for 2 h. The sample was then rinsed with distilled water three times rapidly, and then placed in 10% ethanol; 2) After dehydration with 100% ethanol, instead of using LR White resin, the sample was covered with 50:50, Spurr's resin:100% ethanol. The mixture was agitated overnight and then replaced with Spurr's resin (without ethanol) every 16 h, three times; 3) After the samples were placed in empty gelatin capsules with Spurr's resin, they were placed in an embedding oven at 70 ± 1 °C instead of 60 ± 1 °C. Samples were then sectioned to 1 μm thick using a diamond knife in the ultramicrotome, stained by a 0.5% toluidine blue in 0.1% sodium carbonate (pH 11.1) and viewed under an Olympus Vanox AHT3 at 20× magnification.

3.9 Rheological properties measurements

3.9.1 Rheological profiling of avocado pulp during laboratory-based malaxing

Avocado fruit pulp samples (≅ 50 g) collected from various stages of the laboratory-based oil extraction process were collected for the rheological measurements. Rheological measurements were carried out using a starch pasting cell (SPC; TA Instruments, New Castle, DE, USA) attached to a Discovery HR-3 hybrid rheometer (Figure 3.7; TA Instruments, New Castle, DE, USA). The SPC consists of an impeller and a stainless steel cylindrical cup that is 36 cm wide and 64 mm high. The system was controlled with TRIOS software (TRIOS v4.2.1, TA Instruments, New Castle, DE, USA). The viscosity of each fruit pulp samples (50 g) was measured at a constant shear rate of 40 s^{-1} at 20 ± 0.5 °C. The viscoelastic properties (the elastic modulus, *G'*, and the viscous modulus, *G''*) of fruit pulp samples (50 g) were measured at 20 ± 0.5 °C over a range of frequencies from 0.01 to 10 Hz and at a constant strain of 0.5%.

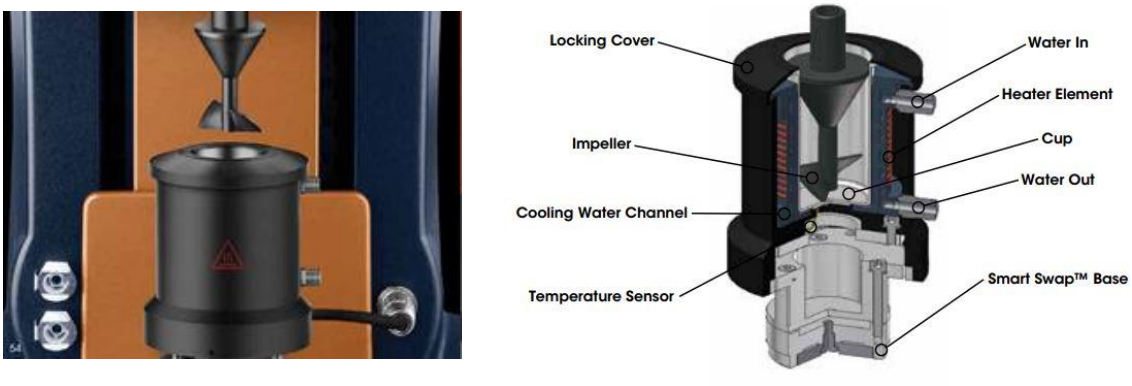

Figure 3.7: Discovery HR-3 hybrid rheometer with a starch pasting cell (TA Instruments, 2018).

3.9.2 Rheological profiling of avocado pulp during malaxing in rheometer

The malaxer in the commercial avocado oil production mixed the avocado pulp with a stirrer speed of 20 rpm. To try to simulate this mixing in the Discovery HR-3 hybrid rheometer using a starch pasting cell (SPC) geometry cup, the rheometer was set to a constant shear rate of 0.33 s^{-1}. During malaxing in the commercial malaxers, the shear rate experienced by the pulp would have varied with time as the pulp changed in viscosity.

Twenty ripe avocado fruit at 80 ± 2 Fv were washed, cut into quarters, then peeled and pitted by hand. The flesh was ground to a pulp by using a laboratory scale hammer mill (Siemens, Munich, Germany). The malaxing of avocado pulp was simulated on a Discovery HR-3 hybrid rheometer with a starch pasting cell which provided the same shear rate (20 rpm) as the malaxer in the commercial avocado oil production.

The effect of malaxing temperature was examined by comparing the rheological properties of avocado pulp while malaxing at 30 ± 1, 40 ± 1 and 50 ± 1 °C. The apparent viscosity of avocado pulp samples was measured every minute while malaxing constantly at 20 rpm. The viscoelastic properties (*G'* and *G"*) of avocado pulp samples were

measured at 20 ± 0.5 °C after 30, 60, and 120 min malaxing over a range of frequencies from 0.01 to 10 Hz and at a constant strain of 0.5%. At each stage of malaxing, separate avocado pulp samples were used for viscoelastic property measurement, as the measurement induced a shear deformation in the sample (Miri, 2011). After malaxing, the pulp was centrifuged (Thermo Fisher Scientific Inc, Waltham, MA, USA) at 12,278 × *g*, 20 ± 1 °C for 30 min to recover the oil phase from the solids and water. The oil phase was centrifuged again at 3,214 × *g*, 20 ± 1 °C for 10 min to separate any residual water from the oil.

3.9.3 Rheological profiling of olive pulp during malaxing in commercial factory

Olive fruit pulp samples (≅ 10 g) at various stages of malaxing during commercial oil extraction were collected in 50 mL plastic vials and stored immediately in a chilly bin with ice to maintain a temperature of 4 ± 1 °C for 4 h (transport time to laboratory). Rheological measurements were carried out using an AR550 rheometer (TA Instruments, New Castle, DE, USA) with attached computer software (Rheology Advantage Data Analysis Program, TA Instruments, New Castle, DE, USA). A parallel-plate geometry was used with a gap of 2000 μm. The elastic modulus, *G'*, and the viscous modulus, *G"*, of olive pulp sample (≅ 10 g) were measured at 20 ± 0.5 °C over a range of frequencies from 0.1 to 10 Hz and at a constant strain of 0.5%.

3.9.4 Effect of olive pulp sample storage time on rheological measurements

An experiment was carried out to determine if the viscoelastic properties of olive pulp samples changed within the 4 h required to transport samples back to the laboratory and followed a similar procedure used to determine the effect of storage time on impedance measurements trial in Section 3.6.2.

Olive pulp samples were divided into two groups after collection: one group of samples were analysed for viscoelastic properties immediately after collection, another group of samples were stored in a chilly bin with ice at 4 ± 1 °C for 4 h then the viscoelastic properties was measured.

3.10 Cell wall isolation and sequential extraction

The procedure for cell wall isolation and sequential extraction from avocado tissue was based on those of Huber and O'Donoghue (1993) and Jeong, Huber, and Sargent (2002). Fruit pulp samples (50 g) were collected at 0 min and 120 min malaxing during the commercial cold-pressed avocado oil extraction process throughout the 2016/2017 oil production season from September 2016 to April 2017. Samples were accurately weighed to two decimal places and immediately frozen in liquid N_2 and stored in a polystyrene box on dry ice for 4 h. The samples were then stored at -80 ± 2 °C until further extraction trials.

3.10.1 Water-soluble fraction

The main procedures in the experiment extracting water-soluble fraction and cell wall materials from avocado pulp samples are shown in Figure 3.8. Frozen avocado pulp samples were ground into a fine powder with liquid N_2 by using a bench top mill (Model A11 Basic; IKA-Works Inc, Wilmington, NC, USA). An accurately weighed fruit tissue sample (50 g) was homogenized in 200 mL of cold 95% ethanol using a dispersing homogenizer (Model T10 Basic; IKA-Works Inc, Wilmington, NC, USA) on high speed for 3 min at 20 ± 1 °C. The homogenates were then centrifuged (Thermo Fisher Scientific Inc, Waltham, MA, USA) at 12,278 × *g*, 4 ± 1 °C for 20 min. The ethanol-insoluble solids

were filtered through Miracloth (inert rayon-polyester "fabric" with an acrylic binder; Sigma-Aldrich Corp, St. Louis, MO, USA) and washed with 100 mL 95% ethanol. The ethanol-insoluble solids (solids on the top of Miracloth) were transferred to 200 mL of chloroform–methanol (1:1, v/v) and homogenized at high speed for 5 min at 20 ± 1 °C then centrifuged at 12,278 × *g*, 20 ± 1 °C for 20 min. The ethanol-insoluble solids were filtered again through Miracloth and washed with 100 mL of acetone (Merk KGaA, Darmstadt, Germany) then the ethanol-insoluble solids on the filter were re-suspended in 150 mL of Milli-Q water and homogenized at high speed for 3 min at 20 ± 1 °C, re-centrifuged at 12,278 × *g*, 20 ± 1 °C for 20 min and filtered again through Miracloth, both of the water-wash supernatant from the centrifuge tube and the residue ethanol-insoluble solids on the filter were collected. This water-wash step was repeated once more by re-suspending the ethanol-insoluble solids in 150 mL of Milli-Q water and homogenizing on high speed for 3 min at 20 ± 1 °C, re-centrifuging the mixture at 12,278 × *g*, 20 ± 1 °C for 20 min and filtering the sample again through Miracloth. Again, both of the water-wash supernatant and the residue ethanol-insoluble solids were collected. The water-wash supernatant was transferred to dialysis tubes with a molecular weight cut-off 14,000 Da (Sigma-Aldrich Corp, St. Louis, MO, USA) that had been pre-treated by placing them in warm Milli-Q water for 20 min. The dialysis tubes were filled with Milli-Q water to 1 L and dialyzed in a 10 L bucket with 10 L Milli-Q water for eight days at 4 ± 1 °C with daily water changes. After dialysis, the solutions were filtered through glass microfibre filter paper (Grade GF/C; Whatman, Maidstone, UK) to remove precipitated, denatured cell debris (including protein) and then freeze-dried (Labconco Corp, Kansas City, MO, USA) at -50 ± 2 °C for four days to obtain the water-soluble fraction. The freeze-dried water-soluble fraction was weighed to determine the yield.

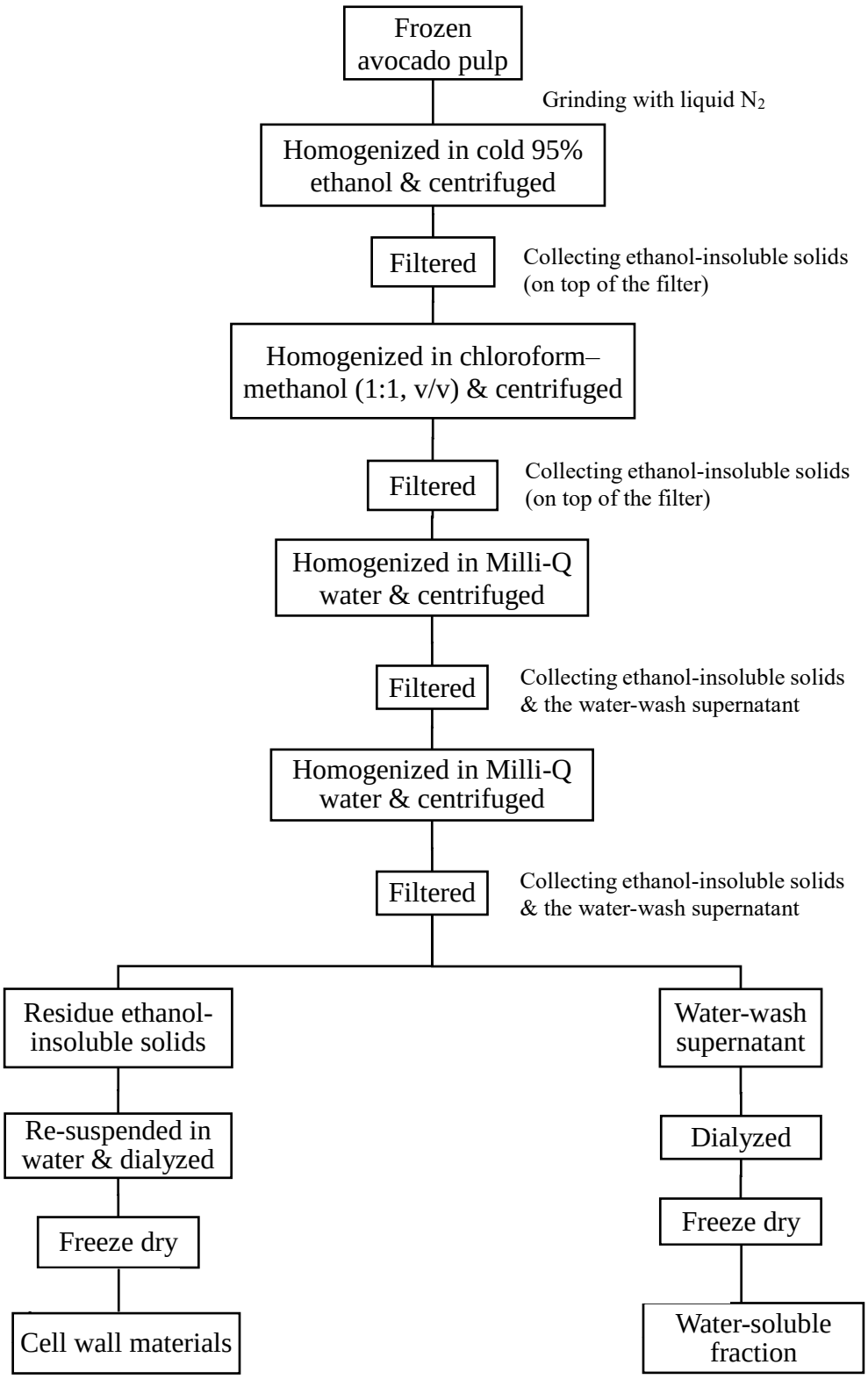

Figure 3.8: Flow diagram for the experimental procedure to extract water-soluble fraction and cell wall materials from avocado pulp sample.

3.10.2 Cell wall material

The ethanol-insoluble solids (residue solids on the filter) remaining after water extraction in Section 3.10.1 (Figure 3.8) were re-suspended in 1 L of water to form thick slurries and transferred to dialysis tubes. They were then dialyzed against Milli-Q water for eight days at 4 ± 1 °C with daily water changes, removed from the dialysis membranes, and then freeze-dried at -50 ± 2 °C for four days to produce the cell wall material. The freeze-dried cell wall material was weighed to determine yield.

3.10.3 CDTA-soluble fraction

Cell wall material (200 mg), collected in Section 3.10.2, was stirred in 100 mL of 0.05 M trans-1,2-diaminocyclohexane-N,N,N',N'-tetraacetic acid (CDTA; Sigma-Aldrich Corp, St. Louis, MO, USA) for 6 h at 20 ± 1 °C. The mixture was then centrifuged at 12,278 × *g*, 20 ± 1 °C for 20 min and filtered through Miracloth, both of the CDTA-wash supernatant from the centrifuge tube and the residue solids on the top of Miracloth were collected. The residues were re-suspended in 75 mL of Milli-Q water and homogenized on high speed for 3 min at 20 ± 1 °C, re-centrifuged at 12,278 × *g*, 20 °C ± 1 for 20 min and filtered again through Miracloth; both of the water-wash supernatant from the centrifuge tube and the residue solids on the top of Miracloth were collected. This water-wash step was repeated once more. The CDTA and water-wash supernatants were combined and transferred to dialysis tubes. The dialysis tubes were filled with Milli-Q water to 1 L and dialyzed against 5 L of 0.1 M ammonium acetate buffer (pH 5.2) for three days (to aid removal of CDTA) with a daily change of buffer, followed by dialysis with Milli-Q water for eight days with daily water changes. The CDTA and water-wash supernatants were then freeze-dried at -50 ± 2 °C for four days to produce the CDTA-soluble fraction.

3.11 Oil quality analysis

3.11.1 Peroxide value

Analysis of peroxide value (PV) of the samples was carried out according to a modified AOCS (2009) Official Method CD 8-53. The oil sample (5 g) was accurately weighed to three decimal places in a 250 mL Erlenmeyer flask with glass stopper. Glacial acetic acid (18 mL; Merk KGaA, Darmstadt, Germany) and chloroform (12 mL; Merk KGaA, Darmstadt, Germany) were mixed and added to the sample. The flask was swirled to dissolve the sample. Saturated potassium iodide (0.5 mL; BDH Chemicals, London, UK) solution was added to the mixture and the flask was shaken for one minute before 30 mL of Milli-Q water was added. The mixture was titrated with 0.01N sodium thiosulfate (BDH Chemicals, London, UK) gradually with constant agitation until the yellow iodine colour had almost disappeared. Starch indicator solution (2 mL; Hopkin & William Ltd., Birmingham, UK) was added and the titration was continued with constant agitation until the blue colour totally disappeared. A blank determination of the reagent was carried out using the same procedure. The PV was calculated as follows:

$$\text{PV (milliequivalents peroxide/1000g sample)} = \frac{(S-B)\times N\times 1000}{\text{Weight of sample,g}} \qquad (5)$$

Where:

B = volume of titrant for blank titration, mL

S = volume of titrant for sample titration, mL

N = normality of sodium thiosulfate solution

3.11.2 Free fatty acids

Determination of free fatty acids (FFA) in the oils was carried out according to AOCS (2009) Official Method Ca5a-40. To standardize the sodium hydroxide (NaOH; BDH Chemicals, London, UK) titre used in this test, dried potassium acid phthalate (0.2 g)

(KHP; Sigma-Aldrich Corp, St. Louis, MO, USA) was dissolved with 25 mL distilled water in a 100 mL Erlenmeyer flask by heating on a hot plate. The solution was cooled before three drops of phenolphthalein indicator (1%; Sigma-Aldrich Corp, St. Louis, MO, USA) was added and titrated with NaOH solution until the first faint pink colour remained for 30 s. The volume titrated was recorded and used to calculate the normality of the NaOH.

$$\mathrm{N} = \frac{\text{g of KHP}}{\text{mL of NaOH} \times 0.204} \quad (6)$$

To determine the FFA in the oils, the oil sample (1 g) was accurately weighed to three decimal places in a 100 mL Erlenmeyer flask. Ethanol (95%; 20 mL) was neutralized to the end point by adding a few drops of phenolphthalein into it, and then it was titrated with 0.1N NaOH until a permanent faint pink colour appeared. The neutralized 95% ethanol was heated to 50 ± 1 °C and then added into the flask to dissolve the sample. The sample was titrated with 0.1N ethanolic NaOH and gently shaken until the appearance of the first permanent pink colour of the same intensity as that of the neutralized solvent before the latter was added to the sample. The percentage of %FFA was calculated as oleic acid based on follows:

$$\%\text{FFA as oleic acid} = \frac{\text{mL of NaOH} \times \mathrm{N} \times 28.2}{\text{Weight of sample,g}} \quad (7)$$

Where N = normality of NaOH, mol/L

3.12 Statistical Analysis

For commercial based avocado and olive oil extraction, a single oil extraction trial was performed at each fruit harvest time. Due to the shortage of avocados during the 2015/2016 in New Zealand, Olivado Ltd NZ's Kerikeri plant had reduced production for the whole season (from November 2015 to 2016/2017 season). For 'Hass' avocado oil production in early and late season for 2015/2016 and 2016/2017, the commercial based

oil extraction could only be performed once per month due to the fruit shortage. In commercial avocado and olive oil extraction, electrical impedance measurement for intact whole avocado/olive fruit was carried out on ten replicates. Three batches of fruit pulp samples were collected from one malaxer (≅ 650 kg fruit pulp per malaxer) at each stage of malaxing. For various analyses, including the dry matter and total oil content, electrical impedance, conductivity, rheological properties and the cold-pressed oil yield measurements (at each stage of malaxing) for avocado pulp, these were carried out in triplicate.

For laboratory-based oil extraction experiments, the cold-pressed oil extraction were performed in triplicate. Postharvest assessments of avocado fruit were performed in triplicate. Electrical impedance measurement for intact avocado fruit was carried out on ten replicates. Electrical impedance, conductivity, rheological properties and cold-pressed oil yield measurements for avocado pulp were carried out in triplicate. FFA% and PV determination for cold-pressed avocado oil were performed in triplicate.

Statistical analysis was performed by using Minitab 17 Statistical Software for Windows (Minitab Inc, State College, PA, USA). One way ANOVA and Tukey test were used to determine significant differences between samples ($p < 0.05$). Sample uncertainty was determined by calculating standard errors of the mean, and presented as mean ± standard error (SE), sample size n.

Chapter 4:

Cellular changes in ‘Hass’ avocado mesocarp during commercial cold-pressed oil extraction

4.1 Introduction

In the mesocarp of avocado flesh, the oils are stored in parenchyma and idioblast cells (Platt-Aloia & Thomson, 1981; Platt-Aloia et al., 1980). During cold-pressed oil extraction, the cell walls and membranes must be broken to release oil droplets so that the oil can be separated from the cellular material (Wong et al., 2012; Woolf et al., 2009). However, there is no information as to whether the avocado oil extracted by cold-pressed extraction is mostly from the parenchyma cells or from both parenchyma and idioblast cells. Also, the microstructural changes of avocado mesocarp during the aqueous extraction process have not been studied. Work in olive oil extraction has hypothesized that fruit cells are disrupted during grinding to release the droplets of oil from the vacuole, then the oil droplets merge to form larger droplets during malaxing (Petrakis, 2006). No research has been carried out in this area for the cold pressed avocado oil extraction process.

It is important for the oil industry to identify strategies to increase oil yields. One approach to understanding the factors that influence the oil yields is to investigate the microstructural changes in the avocado fruit flesh during various stages of the oil extraction process. Various techniques are available to determine the cellular changes in avocado mesocarp during cold-pressed oil extraction. Microscopy examination allows observation of oil aggregation as well as the integrity and size of the cells (Platt-Aloia et al., 1983; Platt-Aloia & Thomson, 1981). Electrical conductivity measurement of a fruit tissue sample indicates cell electrolyte leakage and can be used to estimate the degree of cell membrane intactness (Palta et al., 1977). The application of electronic sensors based on electrical impedance spectroscopy (EIS) is an alternative to these methods for cellular changes in food materials, they can provide a fast response and high sensitivity (Masot et

al., 2010).

The objective of the research presented in this chapter was to monitor cellular changes during processing of 'Hass' avocado for extraction of cold-pressed avocado oil, using EIS, electrical conductivity measurement and light microscopy to understand how each step in the process affects oil release from the tissue. The work presented in this chapter was carried out in the first season of work to determine the best sampling and evaluation methods, and it was carried out using early-season fruit (mature but relatively low dry matter). This chapter will present results on the cellular changes in 'Hass' avocado mesocarp during commercial cold-pressed oil extraction and of a laboratory trial investigate the effect of sample storage time on EIS and conductivity measurements. The results in this chapter have been published in Yang et al. (2018).

4.2 Experimental design

4.2.1 Effect of sample storage time on electrical impedance and conductivity measurements from laboratory-based experiments

Laboratory-based experiments were carried out to determine if the electrical impedance and conductivity of avocado pulp samples changed within the 4 h required to transport samples back from Olivado Ltd NZ's Kerikeri plant to the laboratory at the Mt. Albert Research Centre of Plant and Food Research Ltd, Auckland.

The main steps in the laboratory-based experiment looking at the effect of storage time on electrical impedance and conductivity measurements for cold-pressed avocado oil extraction are shown in Figure 4.1.

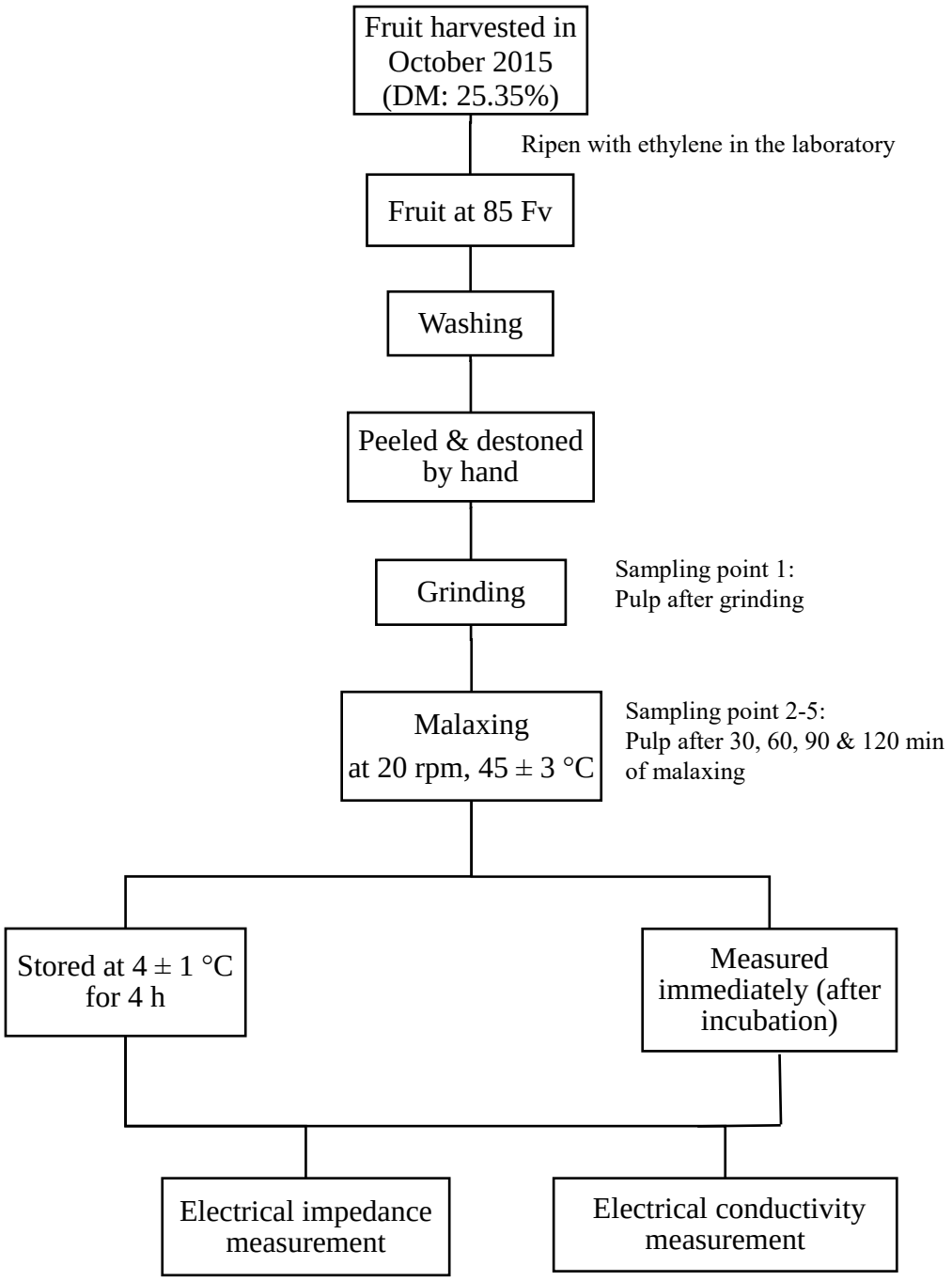

Figure 4.1: Process flow diagram for the laboratory-based experiment looking at the effect of sample storage time on electrical impedance and conductivity measurements for cold-pressed 'Hass' avocado oil extraction. Electrical impedance and electrical conductivity measurement were carried out on samples collected at each sampling point during the extraction process.

DM: Dry matter content (g dry flesh/100 g fresh flesh weight).

‘Hass’ avocado fruit (*Persia americana* Mill, ≅ 10 kg) were harvested in October 2015 and ripened to 85 ± 2 Fv in the laboratory following the procedures described in Section 3.1.2. Firmness measurements of fresh fruit were carried out on twenty avocado fruit following the method described in Sections 3.2.3. Effect of sample storage time on electrical impedance and conductivity measurements was studied following the methods described in Sections 3.6.3 and 3.7.3. Statistical analysis of data was carried out following the methods as described in Section 3.12. Firmness measurement and the laboratory-based avocado oil extraction experiments were performed in triplicate. Electrical impedance and conductivity measurements were carried out in triplicate.

4.2.2 Cellular changes in ‘Hass’ avocado mesocarp during commercial cold-pressed oil extraction

The main steps in the experiment looking at cellular changes during commercial based cold-pressed oil extraction for avocado in October 2015 (early season) are shown in Figure 4.2.

‘Hass’ avocado fruit (≅ 650 kg) were harvested and processed at Olivado Ltd, Kerikeri, New Zealand in October 2015 following the procedures described in Sections 3.1.1 and 3.3.1. The cold-pressed oil yield at each stage of malaxing in the commercial trial was determined following the method described in Section 3.3.4. Postharvest assessments of avocado fruit, including dry matter determination, firmness measurement, and total oil content determination of fruit were carried out following the methods described in Sections 3.2.2, 3.2.3 and 3.5. Firmness measurement of fresh fruit were performed on 30 avocado fruit.

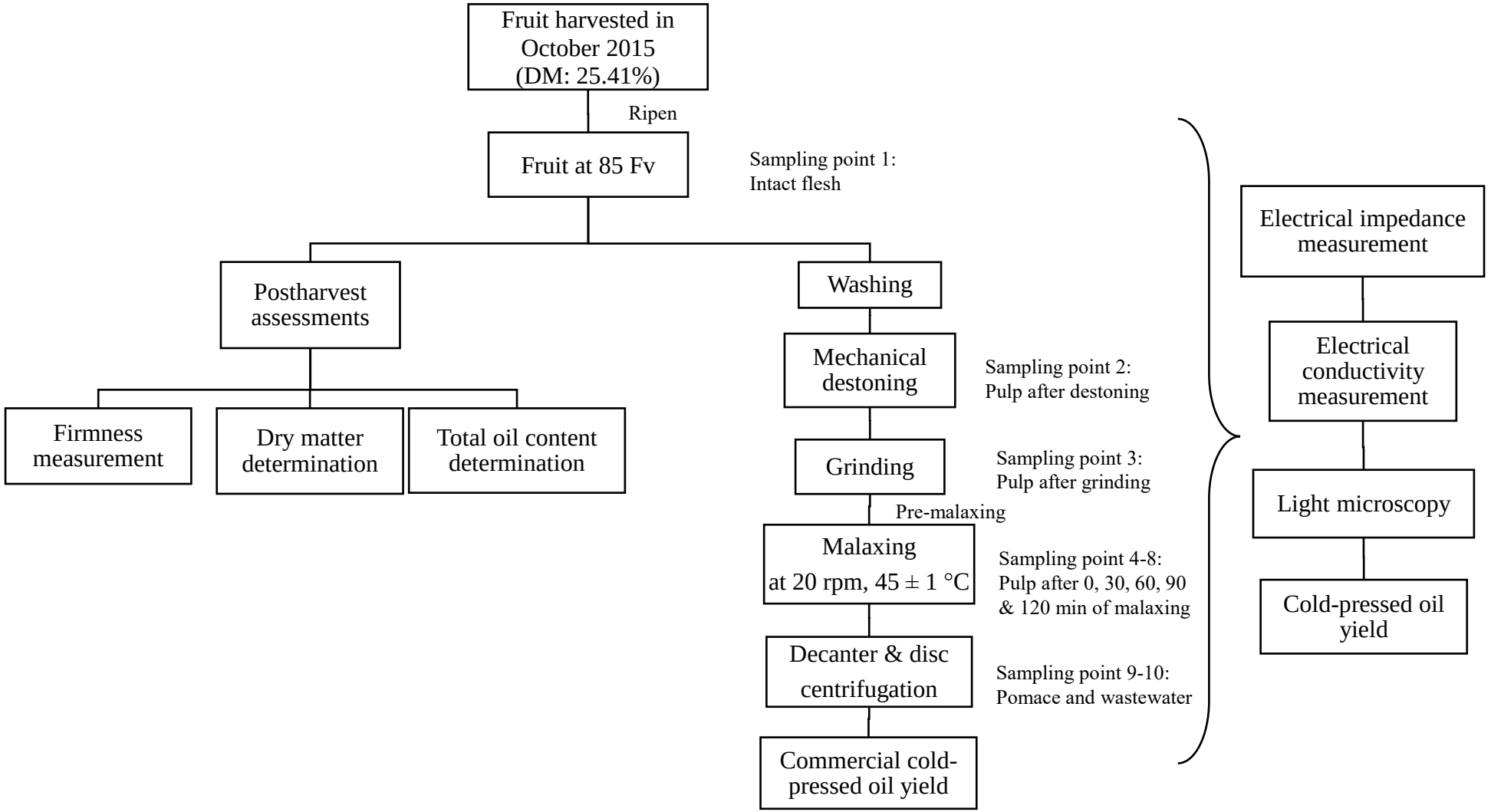

Figure 4.2: Flow diagram for the experimental procedure to investigate cellular changes during commercial cold-pressed oil extraction for 'Hass' avocado. Light microscopy observation, electrical impedance measurement, electrical conductivity measurement and cold-pressed oil yield determination were carried out for samples collected at each sampling point during the extraction process.

DM: Dry matter content (g dry flesh/100 g fresh flesh weight).

Sampling point 3 was the pulp sample existing the grinder; the pre-malaxer took 30 min to fill and then the pulp was transferred to the main malaxer, Sampling point 4 was when the main malaxer was full (0 min malaxing); Sampling point 5-8 were 30, 60, 90 and 120 min after the malaxer was full.

EIS, electrical conductivity and light microscopy were used to examine avocado flesh structure at defined steps during the extraction process (destoning, grinding, malaxing and decanting) following the procedures described in Sections 3.6.1, 3.7.1 and 3.8. Avocado pulp samples were stored at 4 ± 1 °C immediately after collection. EIS, electrical conductivity and cold-pressed oil yield (at each stage of malaxing) measurements were carried out within 4 h of collection. Microscopy experiments were carried out within 72 h of collection.

Statistical analysis of data was carried out following the methods as described in Section 3.12. A single commercial based avocado oil extraction trial and firmness measurement was performed. Dry matter and total oil content determinations for avocado pulp were carried out in triplicate. Electrical impedance measurements for intact avocado fruit were carried out on ten replicates. Electrical impedance, conductivity and cold-pressed oil yield measurements for avocado pulp were carried out in triplicate.

4.3 Results and discussion

4.3.1 Effect of sample storage time on electrical impedance and conductivity measurements from laboratory-based experiments

Avocado fruit pulp samples collected at Olivado Ltd NZ's Kerikeri plant during the factory extraction trials had to be held for four hours during transport before electrical impedance and conductivity measurements were carried out at the Mt. Albert Research Centre of Plant and Food Research Ltd, Auckland (the impedance instrument could not be transported back and forth to the factory). The samples were rapidly cooled at the factory with ice and stored in a chilly bin to keep the samples at 4 ± 1 °C. During the oil extraction process, the ruptured cells may release more endogenous enzymes which assist

with further cell wall disruption during transport and storage. The experiment was carried out to determine if the electrical impedance and conductivity of samples changed over the 4 h required to transport samples back to the laboratory.

In October 2015, a separate 10 kg batch of 'Hass' avocado fruit were treated with ethylene then held at 20 °C to ripen to a firmness of 85 ± 2 Fv. The avocado fruit flesh was ground and malaxed using the laboratory-based cold-pressed extraction process and samples were collected at 0 (after grinding), 30, 60, 90 and 120 min during malaxing. Samples were divided into two groups: one group of samples were measured for electrical impedance and conductivity immediately after collection, another group of samples were stored at 4 ± 1 °C for four hours then the electrical impedance and conductivity were measured.

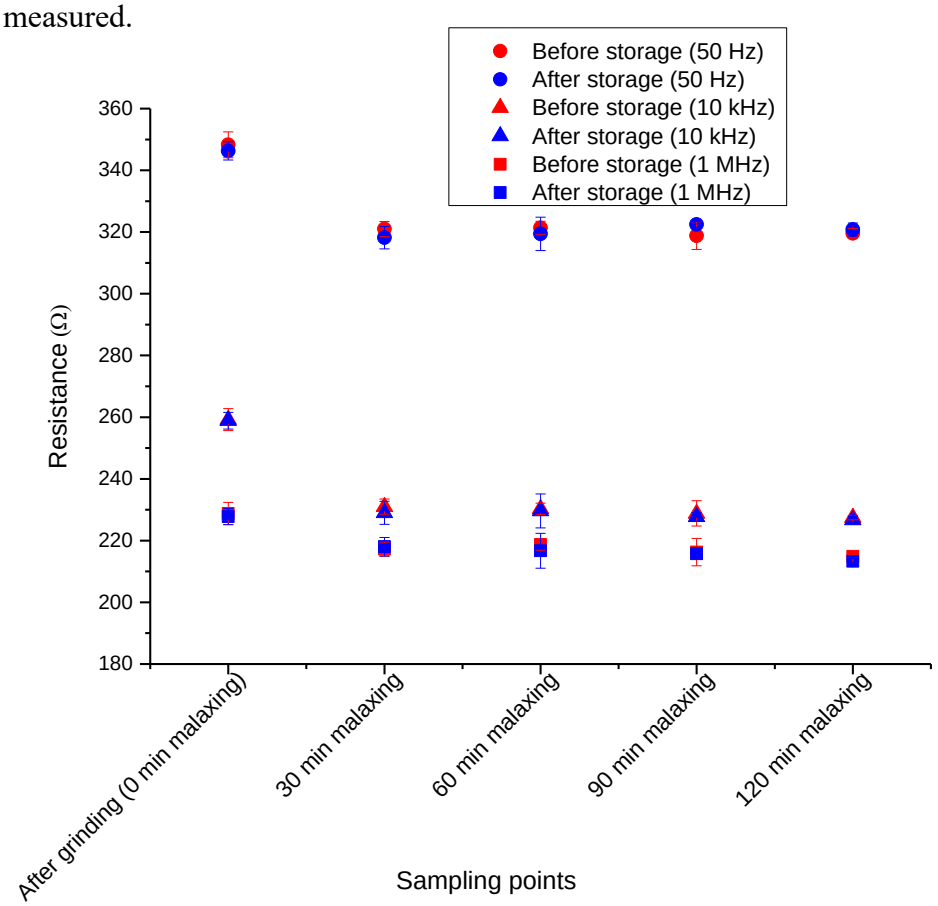

Figure 4.3: Comparison of electrical resistance of 'Hass' avocado pulp tissue at 50 Hz, 10 kHz and 1 MHz before and after 4 h storage at 4 ± 1 °C (mean ± SE, n = 3).

The results in Figure 4.3 show that at low frequency (50 Hz), medium frequency (10 kHz), and high frequency area (1 MHz), there were no significant differences ($p < 0.05$) between the electrical resistance of avocado pulp tissue, collected from various sampling points during cold-pressed oil extraction, before and after 4 h of sample storage at 4 ± 1 °C. The 4 h storage at 4 ± 1 °C was also found to not affect the electrical conductivity of the avocado pulp tissue which had been placed into the mannitol solution immediately after collection (Figure 4.4). Hence, it can be concluded that transporting the samples for 4 h at 4 ± 1 °C from Olivado Ltd NZ's Kerikeri plant to the Mt. Albert Research Centre of Plant and Food Research Ltd, Auckland did not affect the EIS and electrical conductivity results for the avocado pulp tissue samples collected during the extraction process. Endogenous enzyme activity is inhibited during chilled storage (Bettelheim, Brown, Campbell, Farrell, & Torres, 2010; Saini, 2010).

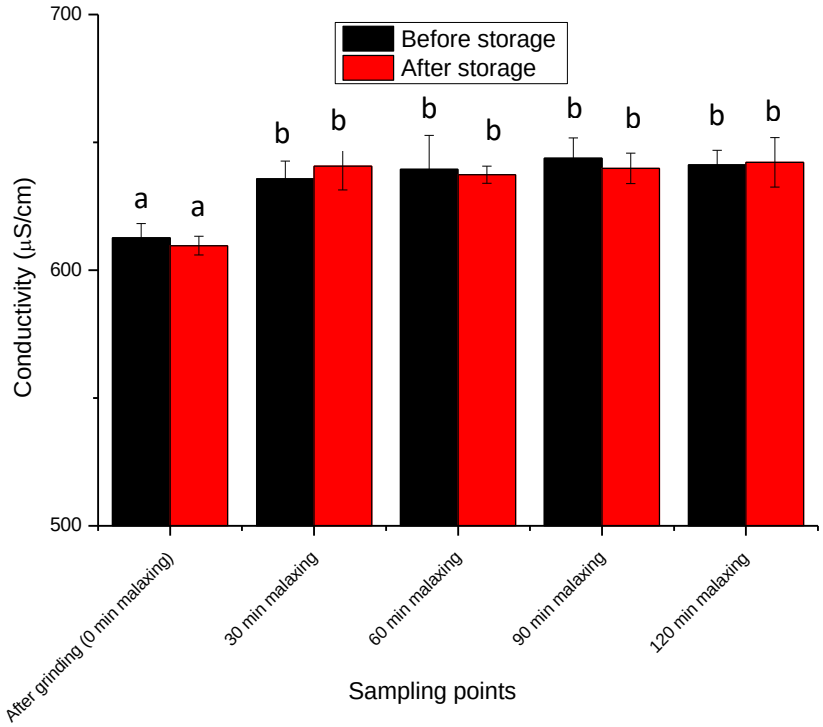

Figure 4.4: Comparison of electrical conductivity of 'Hass' avocado pulp tissue before and after 4 h storage at 4 ± 1 °C (mean ± SE, n = 3).

[a,b] Different letters denote significantly different conductivity values ($p < 0.05$).

4.3.2 Cellular changes in 'Hass' avocado mesocarp during commercial cold-pressed oil extraction

4.3.2.1 Avocado fruit for commercial trial

In avocado oil production, the ripeness of the fruit is required to be the equivalent to "firm ripe", which is equal to a firmometer reading between 65 and 95 firmometer value (Fv) (Woolf et al., 2009). This firmness has been reported to result in a balance of maximising oil yield while minimizing the incidence of fruit rots (Woolf et al., 2009). The firmometer reading of the avocado fruit selected for oil production in October 2015 was 85.05 ± 2.48 Fv, which is within the required target firmness range.

Before harvest, the avocado fruit increases in dry matter content and oil content in the flesh tissue, while the moisture content of flesh tissue decreases (Lawes, 1980; Pearson, 1975; Wong et al., 2008). The dry matter content and the total oil content in the fruit flesh are highly correlated, this is generally used as a horticultural measure of commercial maturity of avocados (Brown, 1984; Lee et al., 1983). The average dry matter content of the fruit flesh extracted in the commercial trial in October 2015 (early season) was 25.41 ± 0.03% (g of dry flesh/100 g of fresh flesh) which is above the minimum dry matter level (24%) recommended in New Zealand.

4.3.2.2 Total oil content and commercial oil yield

The total oil content in the avocados, the cold-pressed oil yield at different stages during malaxing and the final commercial oil yield from the commercial trial in October 2015 are presented in Table 4.1. The total oil content of the fruit flesh was determined by accelerated solvent extraction (ASE) method. For determining the cold-pressed oil yield at each stage of malaxing in the commercial trial (Table 4.1), avocado pulp samples were

collected at 30, 60, 90 and 120 min of malaxing and centrifuged by using a laboratory centrifuge to mimic the commercial centrifugation system to determine oil yield. The cold-pressed oil yield increased with an increasing malaxing time, which agrees with the previous studies on olive oil extraction (Di Giovacchino et al., 2002a; Di Giovacchino et al., 2002b). The commercial oil yield obtained for the batch of fruit sampled was 11.47% (g of oil/100 g of fresh flesh), which is less than the 15.4% (g of oil/100 g of fresh flesh) total oil content by ASE. The incomplete extraction corresponds to the findings of Woolf et al. (2009) that cold-pressed oil extraction efficiency in early-season fruit is low. The reason why all the oil was not recovered from the fruit in early season was unclear and this is part of the purpose of this research study. It is hypothesized that the cells in the early season avocado flesh are more resistant to rupture during the extraction process and hence the oil is more difficult to separate from the pomace and wastewater. This is examined in more detail in Chapter 5.

Table 4.1: Total available oil and extraction yield from commercial cold-pressed 'Hass' avocado oil extraction and from samples collected during the extraction process (mean ± SE, n = 3).

	Malaxing time (min)				
	0	30	60	90	120
Total oil content measured by ASE (g of oil/100 g of fresh flesh)	15.4 ± 0.3^{e}				
Extraction yield at different malaxing times (g of oil/100 g of fresh flesh)	-	0.8 ± 0.1^{a}	5.7 ± 0.3^{b}	10.1 ± 0.2^{c}	12.0 ± 0.4^{d}
Commercial cold-pressed oil yield (g of oil/100 g of fresh flesh)	-	-	-	-	11.5

[a-e] Different letters denote significantly different oil yield values, across rows and columns ($p < 0.05$).

4.3.2.3 Change in electrical impedance during commercial oil extraction

Electrical impedance spectroscopy (EIS) was used to determine the degree of cell rupture during the commercial extraction process. EIS is a measure of the ability of an electrical AC current to flow through a material (Section 2.6.2). Fully ruptured cells provide a low resistance to the current flow, and the different frequencies provide additional information.

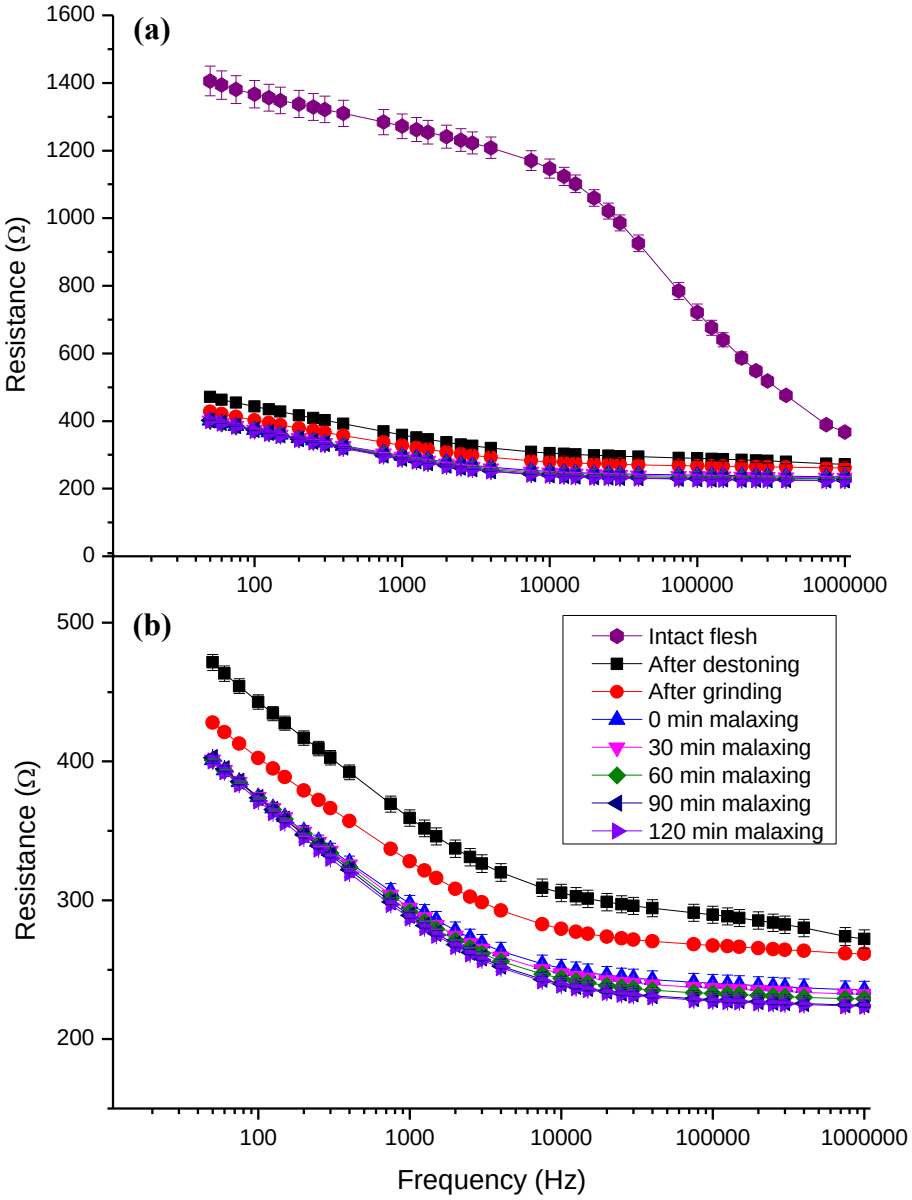

Figure 4.5: Resistance (Ω) of 'Hass' avocado flesh during commercial cold-pressed oil extraction at various stages of the oil extraction process (a) Resistance range 0–1500 Ω with 'Intact flesh' sample (mean ± SE, n = 10); (b) data is replotted for the resistance range 150–550 Ω without 'Intact flesh' (mean ± SE, n = 3).

The impedance spectra of avocado samples collected during the commercial cold-pressed oil extraction trial are shown in Figure 4.5. In all the samples, the electrical resistance decreased as frequency increased ($p < 0.05$). This pattern has also been reported for other fruits (Fuentes et al., 2014; Harker & Dunlop, 1994; Ohnishi et al., 2004; Wu et al., 2008; Zhang & Willison, 1991). The cell membrane has a high electrical capacitance, which insulates against low frequency current passing through the tissue (Zhang, Shen, & Luo, 2010). Thus, at low frequency, the electrical current can only flow through extracellular fluid (Ando et al., 2014). The extracellular pathway has relatively high resistance as a result of the small cross-sectional area through which the current can flow between the membranes of two adjacent cells and also due to the low concentration of mobile ions (Ando et al., 2014; Harker & Dunlop, 1994). However, at higher frequencies, the electrical current is capable of flowing through intracellular fluid with relatively low resistance (Ando et al., 2014). Therefore, the reduction in electrical resistance at high frequency was due to the current flow through the cell membranes and intracellular fluid.

When cell membranes are disrupted, the cellular compartmentation is broken and this allows the low frequency electrical current to flow through the entire cross-section of the tissue. Because of the low resistance to the current flow, this resulted in a reduction in the low frequency electrical resistance value (Hayden et al., 1969). At low frequencies (50 Hz; Figures 4.5(a) and 4.5(b), there was a significant decrease ($p < 0.05$) in the electrical resistance from intact flesh (1405 ± 44 Ω) to flesh after destoning (471.2 ± 5.7 Ω), after grinding (428.0 ± 2.9 Ω) and after sitting in the pre-malaxer tank for 30 min prior to malaxing (0 min malaxing; 401.1 ± 2.6 Ω). This confirms that in the extraction process, cells in the avocado flesh are broken during destoning, grinding and while sitting in the pre-malaxer tank for 30 min (corresponds to time 0 min malaxing). During the destoning

step, avocado fruit was smashed against the destoner drum and cylinder wall, which can lead to damage and rupture of cell walls and membranes. Grinding also breaks cell walls and membranes of fruit samples, and in addition, endogenous enzymes are released that may assist with cell walls and membranes disruption enabling oil release (Woolf et al., 2009). However, malaxing did not result in any changes to EIS ($p > 0.05$). There were no significant changes ($p > 0.05$) in the low frequency electrical resistance from pulp at 0 min malaxing (401.1 ± 2.6 Ω) to pulp after 30 min malaxing (401.2 ± 3.7 Ω), 60 min malaxing (401.1 ± 0.7 Ω), 90 min malaxing (402.6 ± 2.3 Ω) and 120 min malaxing (400.3 ± 3.0 Ω).

Impedance is generally separated into resistance and reactance components. To analyze the measured dielectric functions, the resistance component is plotted on the x-axis and the reactance component on the y-axis, which is known as the Nyquist plot or a complex plane impedance plot (Lasia, 2014). Nyquist plots generally produce semi-circular patterns that disappear or contract as the cell membranes are disrupted. Previous studies on fresh fruit and vegetable samples report that the characteristic Nyquist arc corresponds to the aggregation of closed cell structures (Dejmek & Miyawaki, 2002; Ohnishi et al., 2002). During processing (e.g. drying or freezing) of fruit and vegetable samples, the semi-circular arcs of the Nyquist plots of the samples gradually shrink with increasing processing time or due to the damage to the cell membranes (Halder, Datta, & Spanswick, 2011; Repo, Zhang, Ryyppö, Vapaavuori, & Sutinen, 1994; Wu et al., 2008; Zhang & Willison, 1992b; Zhang, Willison, Cox, & Hall, 1993). In most plant and fruit tissues, the Nyquist arc disappeared when the cells in the tissue are mostly or fully disrupted. However, in some fruit such as grape, the arc can still be formed when the fruit is crushed but the arc was much smaller than that of the fresh samples (Ando et al., 2014; Ohnishi

et al., 2004). The Nyquist plot of avocado samples collected during the cold-pressed oil extraction showed the typical characteristic arc shape expected of whole intact fruit tissue in that as the resistance increased the corresponding reactance produced a smooth arcing curve ('Intact flesh' - Figure 4.6). The clear Nyquist arc in the 'Intact flesh' avocado samples agrees with the findings in previous studies indicating intact cells in the unprocessed avocado mesocarp. However, in the present study the Nyquist arc relationship did not exist in the pulp samples ('After destoning', 'After grinding', and '0 min malaxing' to '120 min malaxing'), which indicated that the cell membranes were disrupted.

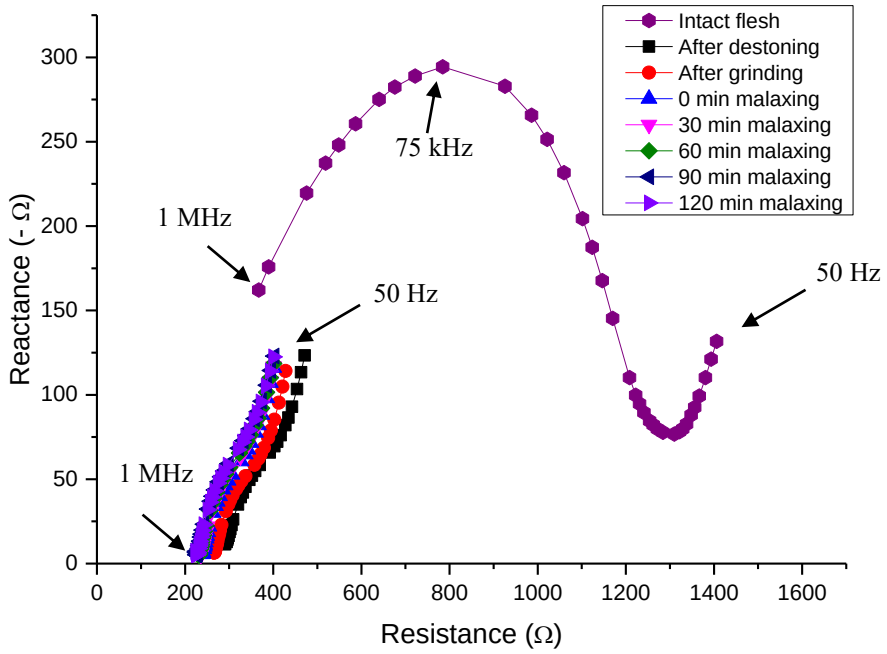

Figure 4.6: Nyquist plot of avocado flesh during cold-pressed oil extraction (mean ± SE, n = 3).

Electrical reactance of a plant tissue is related to the presence of membranes and the capacitance of the tissue (Harker & Forbes, 1997). However, in previous studies of fruit processing and storage, the electrical reactance was not found to be as useful a tool as electrical resistance, which can be singly used to estimate the degree of cellular changes

during fruit processing and fruit storage (Harker & Dunlop, 1994; Harker, White, Freeth, Gunson, & Triggs, 2003; Jackson & Harker, 2000). The electrical behaviour of avocado fruit is mainly resistive as both intracellular and extracellular fluids in tissue are composed of water, free ions, electrolytes, salts and other components (Yu et al., 2004). In this study, the electrical reactance of intact flesh tissue increased from -131.7 ± 7.8 Ω at a frequency of 50 Hz, to -76.8 ± 7.3 Ω as the frequency of the current increased to 400 Hz, then decreased to -294.4 ± 11.4 Ω as the frequency increased to 75 kHz, and lastly increased to -162.1 ± 5.0 Ω as the frequency of the current increased to 1 MHz (Figure 4.7). A similar pattern of reactance change also occurred in other plant tissue including nectarine, eggplant and potato, although the magnitude of the changes were different (Ando et al., 2014; Harker & Dunlop, 1994; Wu et al., 2008). However, the relationship between the reactance of the plant tissue and the frequency of the current has not been studied extensively and is still unclear. The reactance of the avocado fruit pulp samples ('After destoning', 'After grinding', and '0 min malaxing' to '120 min malaxing') increased from ≅ -115.0 Ω at a frequency of 50 Hz, to ≅ -7.5 Ω as the frequency of the current increased to 1 MHz, which gave a different pattern of reactance change compared to the intact avocado flesh. This is likely because the greatest cellular disruption occurred in fruit tissue after the destoning step. There were no significant changes ($p > 0.05$) in the electrical reactance (at 50 Hz, 10 kHz and 1 MHz) from pulp after destoning to pulp after grinding, pulp at 0 min malaxing, pulp after 30, 60 , 90 and 120 min malaxing.

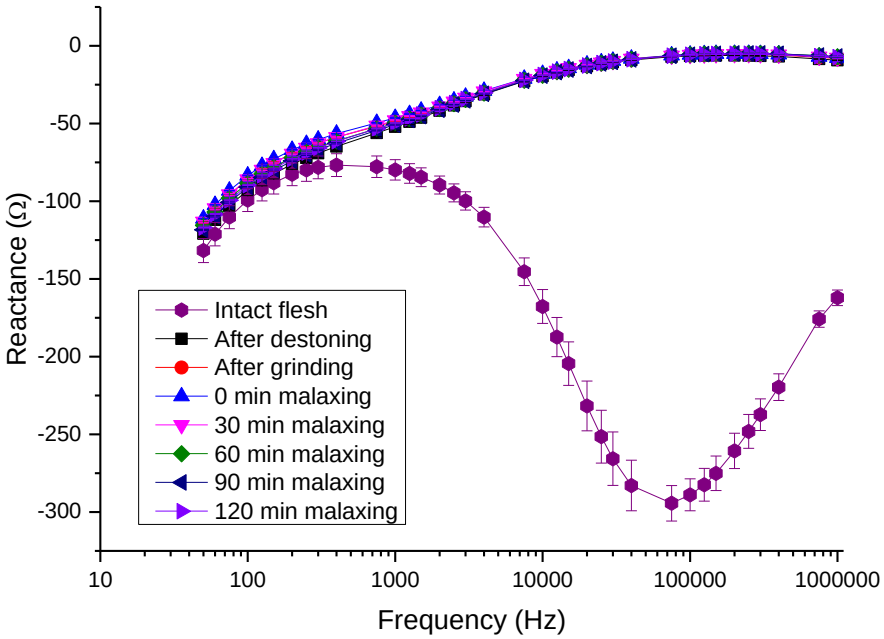

Figure 4.7: Reactance (Ω) of 'Hass' avocado flesh during commercial cold-pressed oil extraction at various stages of the oil extraction process (mean ± SE, n = 3).

4.3.2.4 Change in electrical conductivity during commercial oil extraction

Electrical conductivity measurements were used in this study to support EIS results for determining the degree of cell rupture during the extraction process. By measuring changes in electrical conductivity, it is possible to estimate the degree of cellular disruption. Increased electrical conductivity is due to increased ion leakage which, in turn, indicates a loss of membrane integrity (Pesis et al., 2003).

The electrical conductivity of fruit pulp tissue increased significantly ($p < 0.05$) from intact flesh to flesh after destoning, after grinding, and after accumulating in the pre-malaxer tank for 30 min prior to malaxing (corresponds to time 0 min malaxing; Figure 4.8), which indicated cellular disruption occurred at these three steps during the cold-pressed oil extraction process. However, the electrical conductivity of the fruit pulp did not change ($p > 0.05$) during the 120 min malaxing period. These results are in agreement

with the impedance results (Figure 4.5).

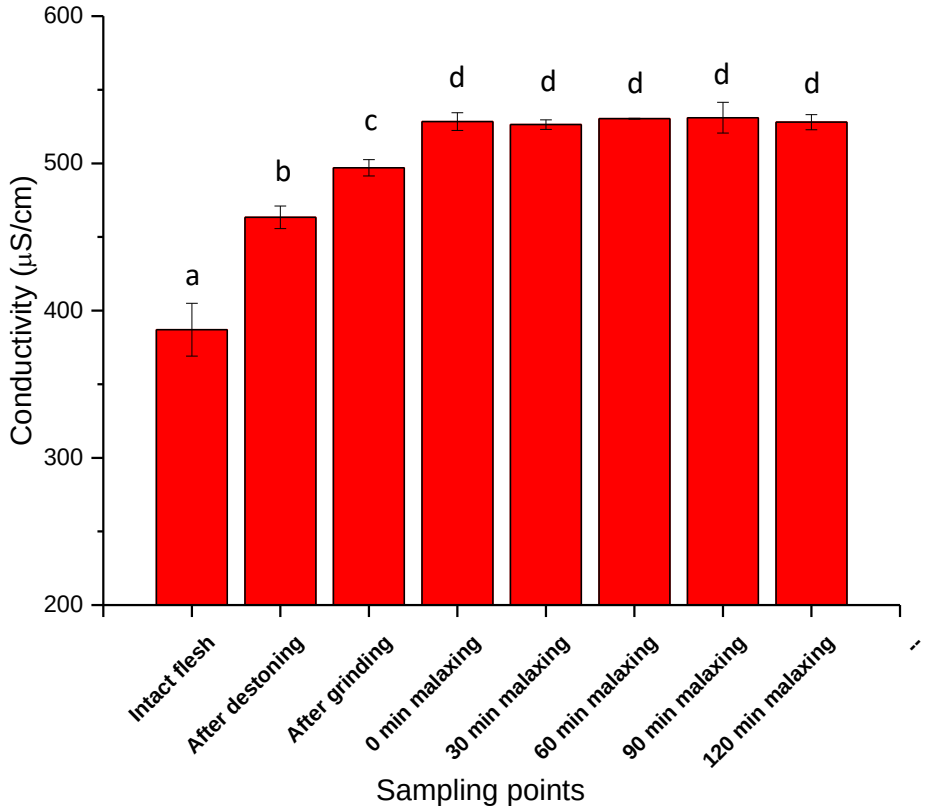

Figure 4.8: Electrical conductivity (µS/cm) of 'Hass' avocado flesh during cold-pressed oil extraction at various stages in the oil extraction process (mean ± SE, n = 3).
[a-d] Different letters denote significantly different conductivity values ($p < 0.05$).

4.3.2.5 Change in avocado cellular microstructure during commercial oil extraction monitored with light microscopy

The cellular microstructure changes in tissue during the cold-pressed avocado oil extraction process were examined with light microscopy using two contrasting methods: toluidine blue staining, which stained the cell walls, and osmium tetroxide fixative, which stained the lipids due to the dye's interaction with the lipids. After examining 100 fields of view on each sample, Figures 4.9, 4.10 and 4.11 were selected as being truly representative of the tissue. After staining, the cell walls of both the parenchyma and idioblast cells could be clearly observed under the light microscope when the pulp tissue

was embedded in LR White resin. For samples embedded in Spurr's resin, the oil droplets inside the parenchyma cells and the cell walls of idioblasts are highlighted with the osmium tetroxide fixative.

The microstructure of unprocessed intact flesh exhibited a uniform cellular structure (Figures 4.9(a) and (b)), which consisted primarily of parenchyma cells and a smaller number of idioblast cells, as was found in previous studies (Platt-Aloia & Thomson, 1981). In Figure 4.9(a) (intact flesh), all cells were intact, and the idioblast cells were distinct from the parenchyma cells due to their intense cell wall staining. The difference in staining was likely to be due to the distinct difference in the cell wall composition between the two different types of cells (Platt-Aloia et al., 1983; Platt-Aloia et al., 1980). The number of idioblast cells per field of view was counted to estimate the number of idioblasts as a percentage of total cells in the fresh tissue. The idioblast cells were approximately 2% of the total cells per view, which agrees with previous studies (Platt-Aloia & Thomson, 1981; Platt-Aloia et al., 1980). Small circular oil droplets (grey areas) were scattered throughout the cytoplasm of the parenchyma cells (Figure 4.9(b)). In the idioblast cells, a large single oil droplet filled the cells, staining a different colour (white colour) than the oil in the parenchyma cells, as also found by Platt-Aloia and Thomson (1981). This different staining may be due to the oil in the idioblast cells having a different composition to the oil in the parenchyma cells (Platt-Aloia et al., 1983; Platt-Aloia & Thomson, 1989). Platt-Aloia & Thomson (1992) reported the idioblast oil has a polarity less than phospholipids but greater than TAG or diacylglycerols (DAG), and contains alkaloids, sesquiterpene hydroperoxides and possibly other terpenes.

There were a series of cellular changes throughout the extraction process. Although some

parenchyma cells were broken by the destoning step of the extraction process (Figures 4.9(c) and (d)), after grinding, almost all the parenchyma cells in Figure 4.9(e) were broken and oil droplets were released (Figure 4.9(f)) in agreement with the impedance results (Figure 4.5). Di Giovacchino et al. (2002b) suggested that adequate grinding of the flesh plays an important role in the extraction process to liberate the oil from the oil bearing cells. In contrast to the parenchyma cells, in this study the idioblast cells were not broken by grinding (Figure 4.9(f)). The idioblast cell wall is reported to contain a primary and tertiary cellulosic wall, as well as a specialized secondary suberin layer rather than the single cellulosic wall of parenchyma cells (Platt-Aloia et al., 1983; Platt-Aloia et al., 1980). It appears that this stronger cell wall is more resistant to grinding. Platt-Aloia et al. (1983) suggested that the function of the specialized suberin layer may be to isolate the contents of the idioblast cell from neighboring parenchyma cells, hence preventing the occurrence of autotoxicity. Autotoxicity is a phenomenon where a plant species inhibits the growth of its own kind through the release of toxic chemicals into the environment (Singh et al., 1999).

The changes in avocado tissue microstructure during malaxing showed that the malaxing steps can help the oil droplets to aggregate (Figures 4.10(a) to (f)). At 0 min malaxing, the free oil droplets were scattered in the field of vision observed (Figure 4.10(a) and (b)); however, after 60 min (Figure 4.10(d)) and 120 min (Figure 4.10(f)) malaxing, the oil droplets were much larger, increasing from ≅ 5 μm to ≅ 80 μm average diameter. This result is similar to the findings that malaxing assists olive oil droplets to accumulate more easily into larger droplets to form a continuous oil phase (Di Giovacchino, 1989, 1996). Therefore, the result of the malaxing step appeared not to break mesocarp (or idioblast) cells in the tissue, but to accumulate the oil droplets to form a larger oil phase thus making

it easier to recover the oil during the decanting (centrifuge) step.

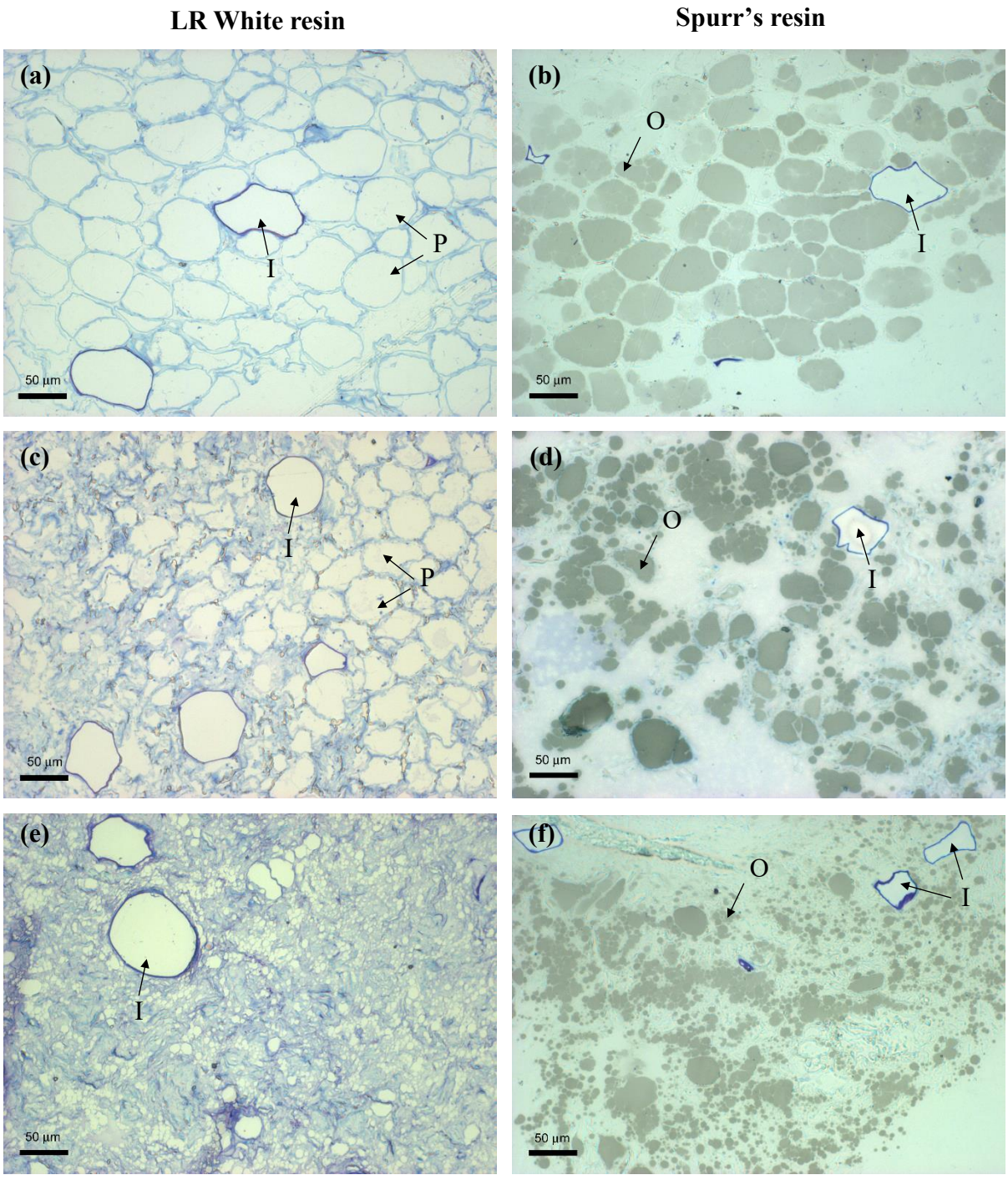

Figure 4.9: Light microscopy images of the microstructure of (a) intact avocado flesh embedded in LR White resin, (b) intact avocado flesh embedded in Spurr's resin, (c) pulp after destoning embedded in LR White resin, (d) pulp after destoning embedded in Spurr's resin, (e) pulp after grinding embedded in LR White resin, (f) pulp after grinding embedded in Spurr's resin. Cell walls stain blue in the LR White embedded tissue, lipid from parenchyma cells shows a grey colouration in the Spurr's embedded material.

P: Parenchyma cells; **I**: Idioblast cells; **O**: Oil droplet(s) from parenchyma cells.

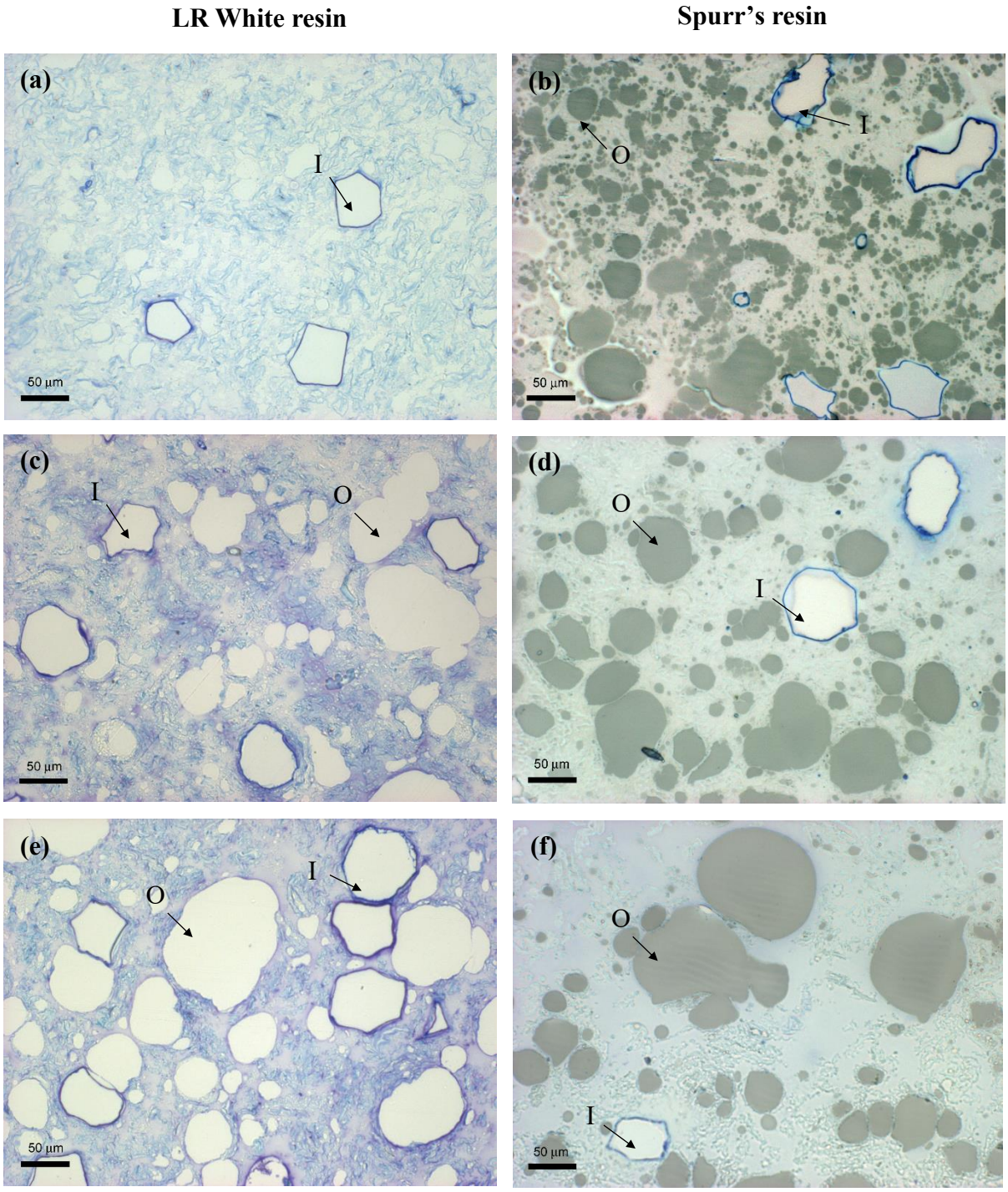

Figure 4.10: Light microscopy images of the microstructure of (a) pulp at 0 min malaxing embedded in LR White resin, (b) pulp at 0 min malaxing embedded in Spurr's resin, (c) pulp after 60 min malaxing embedded in LR White resin, (d) pulp after 60 min malaxing embedded in Spurr's resin, (e) pulp after 120 min malaxing embedded in LR White resin, (f) pulp after 120 min malaxing embedded in Spurr's resin.

I: Idioblast cells; **O**: Oil droplet(s) from parenchyma cells.

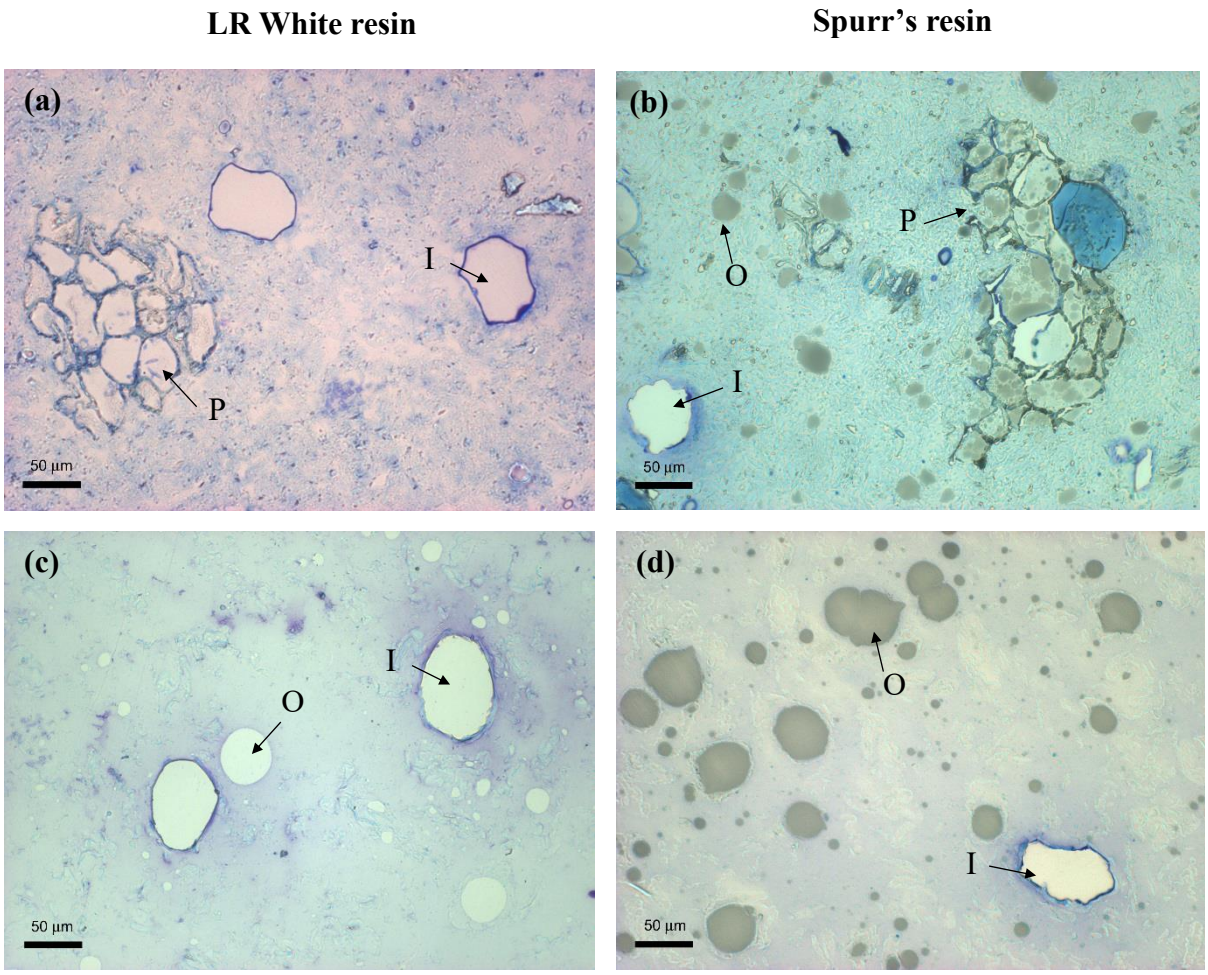

Figure 4.11: Light microscopy images of the microstructure of (a) pomace from decanter embedded in LR White resin, (b) pomace from decanter embedded in Spurr's resin, (c) waste water from decanter embedded in LR White resin, (d) waste water from decanter embedded in Spurr's resin.
P: Parenchyma cells; **I**: Idioblast cells; **O**: Oil droplet(s) from parenchyma cells.

The observations of both pomace and wastewater samples (Figures 4.11(a) to (d)) showed some free oil droplets in both streams. This indicated that not all of the oil was separated from the pomace and wastewater in the decanter. Also, some unbroken parenchyma cells remained in the pomace (Figures 4.11(a) and (b)), which indicated that not all the parenchyma cells in the flesh were completely ruptured during the grinding process. Some oil droplets were still trapped in the cytoplasm of the unbroken parenchyma cells (Figure 4.11(b)), which will have led to loss of oil and reduced oil yield. This result agreed

with the findings for ‘total oil content’ (Table 4.1) compared with ‘commercial oil yield’ in that not all the oil was recovered from the avocados processed during the commercial cold-pressed extraction process. Thus, it is suggested that there are two reasons for oil loss during extraction: firstly, oil droplets did not coalesce into large enough droplets during malaxing, therefore making separation difficult during the decanter centrifugation step. Secondly, some parenchyma cells were not ruptured during the destoning, grinding and malaxing steps to release the oil droplets from their cytoplasm, and these whole intact cells remained in the pomace after centrifugation. It should be noted that these findings were observed with early season fruit. The discrepancy in the oil yields from total oil content versus commercial cold-pressed oil yield is examined further in Chapter 5.

4.4 Conclusions

This work is the first published work showing the changes in cell structure during the cold-pressed avocado oil extraction process. During commercial cold-pressed avocado oil extraction processing, oil is only recovered from the parenchyma cells in the flesh and not the idioblast cells. The parenchyma cells were ruptured during destoning, grinding, and after sitting for 30 min in the pre-malaxer tank (time 0 min malaxing). The two hours of malaxing enabled the oil droplets to coalesce, which although it improved oil recovery, some oil was still lost in both the solid and liquid waste streams. The measures of electrical impedance and conductivity showed a correlation with microscopic cellular structure and provided useful information to understand the cold-pressed avocado oil extraction process. As these results showed the applicability of these electrical methods, further experiments will be carried out which report on the influence of fruit maturity, fruit ripeness, malaxing conditions and ultrasound treatment on microstructural changes and oil yield during cold-pressed oil extraction of ‘Hass’ avocado.

Chapter 5:

Effect of fruit ripeness and maturity on microstructural changes and oil yield during cold-pressed oil extraction of ‘Hass’ avocado

5.1 Introduction

Fruit maturity can be defined in two ways: the first is horticultural maturity, where the fruit is harvested at a stage of development that will allow the fruit to ripen to an acceptable taste and overall quality in order to meet consumer requirements, and the second is physiological maturity, where the fruit will continue to physiologically develop after harvest i.e. ripen for seed dispersal (Watada et al., 1984). Hereafter we will refer to horticultural maturity when discussing maturity since this is the most relevant term for the oil extraction process. Once an avocado fruit has formed on the tree, it slowly matures over approximately ten months, and increases in size, dry matter content and oil content in the flesh tissue, while the moisture content of flesh tissue decreases (Kikuta & Erickson, 1968; Lawes, 1980; Pearson, 1975; Wong et al., 2008). Avocados are unique in that they do not ripen while they are attached to the tree, even if they have attained both physiological maturity, and even high horticultural maturity. Healthy avocado fruits stay firm (unripe) and remain attached to the tree, continuing to grow and to accumulate oil for several months after reaching horticultural maturity but once harvested they begin to ripen (Whiley et al., 2002). During ripening, the activities of cellulase and polygalacturonase in the avocado mesocarp tissue increase dramatically leading to the disappearance of the middle lamella of the parenchyma cells and to pectin removal from the cell wall matrices (Seymour & Tucker, 2012). A loss of organisation and density in the cell walls is accompanied by an increase in fruit softening (Platt-Aloia & Thomson, 1981; Seymour & Tucker, 2012).

The degree of fruit ripening, monitored by fruit softness, affects cold-pressed avocado oil yield and quality (Woolf et al., 2009). The effect of ‘Hass’ avocado ripeness on cold-pressed oil yield and quality was studied by Woolf et al. (2009) who found the cold-

pressed oil yield increased from 7 to 11% (g of oil/100 g of fresh flesh weight) with increasing fruit ripeness. They also found there was a corresponding increase in free fatty acids content (FFA%) from 0.03 to 0.12% w/w (as oleic acid).

Horticultural maturity has also been found to have a significant impact on the oil yield for cold-pressed avocado oil manufacturers (Woolf et al., 2009). It has been observed that there is a significant increase in total oil in the fruit as they mature over the season; the total oil content of the fruit increases up to 23 – 25% (g of oil/100 g of fresh flesh) later in the season compared to 15 – 18% (g of oil/100 g of fresh flesh) early in the season. However, over the harvest season (6 months), there is a significant change in the proportion of total oil available that could be extracted by cold-pressed oil extraction, as nearly 100% of oil can be recovered from late season avocado fruit, but only ≅ 75% of oil is able to be recovered from early season fruit (Woolf et al., 2009).

Optimising oil extraction yields from avocado flesh is important for the avocado oil industry. The effect of fruit ripeness and maturity on microstructural changes during cold-pressed avocado oil extraction can be used to identify the factors that influence avocado oil extraction. The hypothesis is that the cells in riper and late maturity fruit flesh are easier to rupture during the cold-pressed oil extraction process, which results in a higher oil extraction efficiency. The objective of this study was to use electrical impedance spectroscopy (EIS) and electrical conductivity to investigate microstructural changes in avocado tissue during both laboratory-based and commercial cold-pressed extraction from fruit at different stages of ripening and maturity. The disruption of the parenchyma cell walls during commercial cold-pressed oil extraction of avocado for fruit at different stages of maturity and ripening was also observed with light microscopy examination. As

fruit are ripened to a similar ripeness value for commercial oil extraction, to evaluate the impact of fruit ripeness on cell structure and oil yield, the fruit were extracted using the laboratory-based extraction procedure.

5.2 Experimental design

5.2.1 Effect of fruit ripeness on microstructural changes and oil yield during laboratory-based cold-pressed extraction

'Hass' avocado fruit (*Persia americana* Mill, ≅ 10 kg) were harvested from Plant and Food Research Ltd orchards in the Bay of Plenty, New Zealand, in August 2016 and ripened to the target firmness values of 55, 80 and 105 Fv following the procedures as described in Section 3.1.2 (Figure 5.1).

Figure 5.1: 'Hass' avocado fruits at the three different stages of ripening; 55, 80 and 105 Fv.

The main steps in the experiment looking at the effect of fruit ripeness on microstructural changes and oil yield during laboratory-based cold-pressed extraction are shown in Figure 5.2.

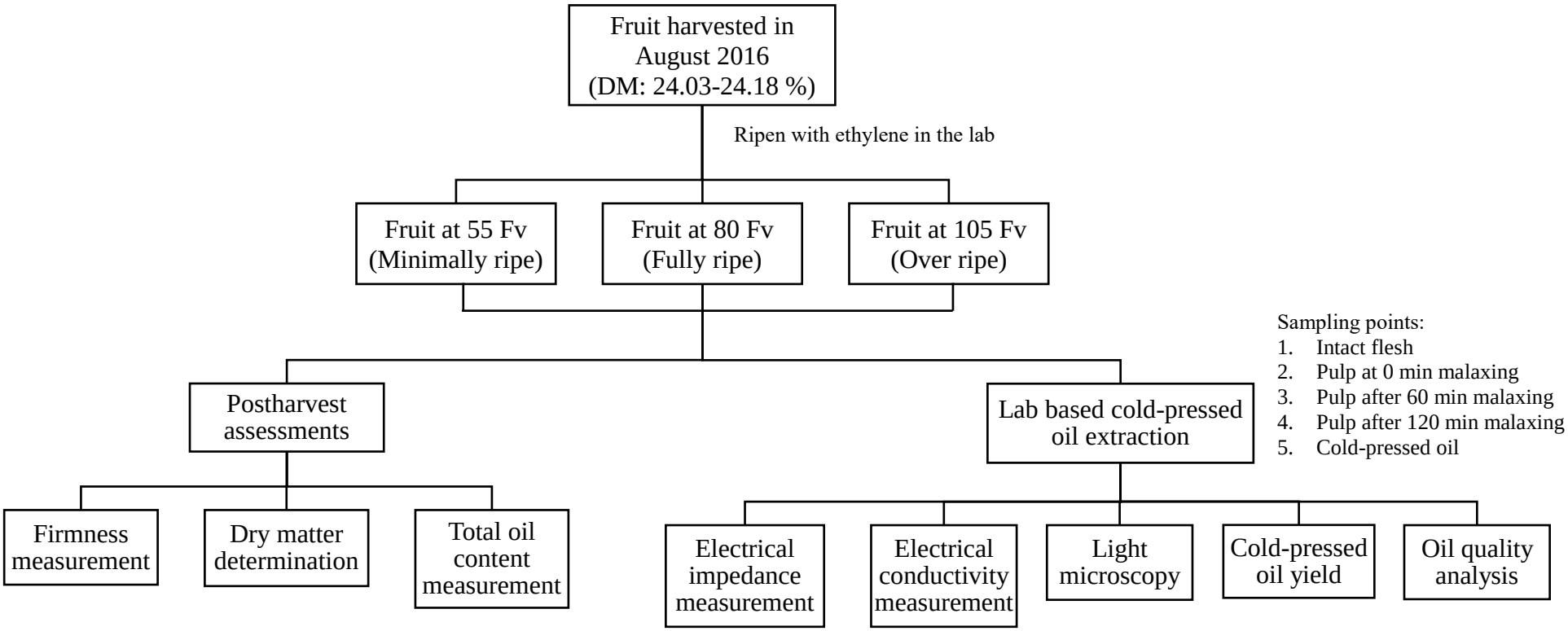

Figure 5.2: Flow diagram for the experimental procedure to investigate the effect of fruit ripeness on microstructural changes and oil yield during laboratory-based cold-pressed extraction. Electrical impedance measurement, electrical conductivity measurement and light microscopy observation were carried out at each sampling point during the extraction process.

DM: Dry matter content (g dry flesh/100 g fresh flesh weight).

Postharvest assessments of avocado fruit, including dry matter determination, firmness measurement and total oil content determination of fresh fruit were carried out on 20 avocado fruit following the methods described in Sections 3.2.1, 3.2.3 and 3.5.

Laboratory-based cold-pressed oil extraction of avocado fruit at three different stages of ripening were carried out following the procedures as described in Section 3.3.2. EIS, electrical conductivity and light microscopy were used to examine avocado flesh structure at defined steps (intact flesh before grinding, fruit pulp at 0 min malaxing, fruit pulp after 60 min malaxing and fruit pulp after 120 min malaxing) during the extraction process following the procedures as described in Sections 3.6.2, 3.7.2 and 3.8.1. Analysis of oils, including the free fatty acid content (FFA%) and the peroxide value (PV) determination, were carried out following the procedures as described in Section 3.11.

Statistical analysis of data was carried out following the methods as described in Section 3.12. Postharvest assessments of avocado fruit and the laboratory-based avocado oil extraction experiments were performed in triplicate. Electrical impedance measurement for intact avocado fruit was carried out on ten replicates. Electrical impedance, conductivity and cold-pressed oil yield measurements for avocado pulp were carried out in triplicate. FFA% and PV determination for cold-pressed avocado oil were performed in triplicate.

5.2.2 Effect of fruit maturity on microstructural changes and oil yield during commercial cold-pressed extraction

The steps in the experiment to investigate the effect of fruit maturity on microstructural changes and oil yield during commercial cold-pressed extraction are shown in Figure 5.3.

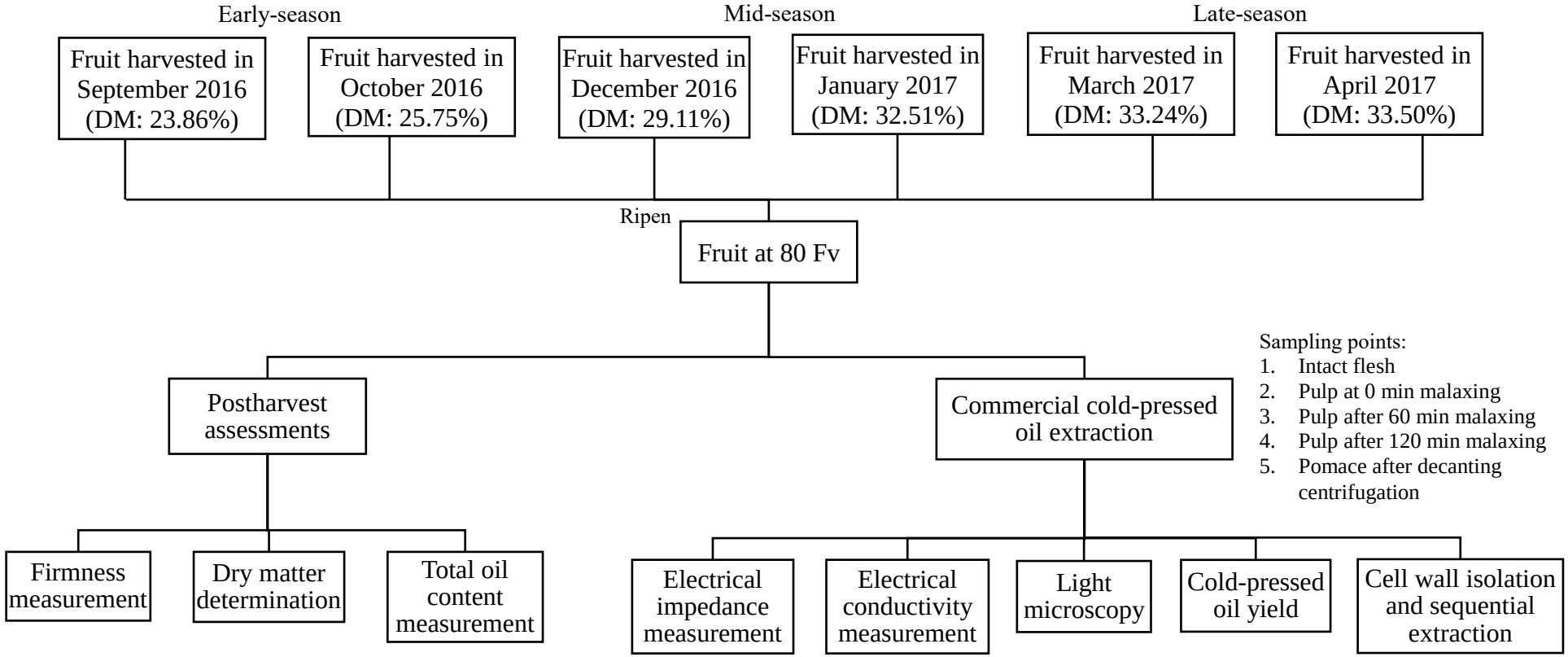

Figure 5.3: Flow diagram for the experimental procedure to investigate the effect of fruit maturity on microstructural changes and oil yield during commercial cold-pressed extraction. Electrical impedance measurement, electrical conductivity measurement and light microscopy observation were carried out at each sampling point during the extraction process.

DM: Dry matter content (g dry flesh/100 g fresh flesh weight).

‘Hass’ avocado fruit were harvested from commercial orchards in Northland, New Zealand, from September 2016 through April 2017 (Figure 5.3), and ripened to the target fruit firmness at 80 ± 2 Fv following the procedures as described in Section 3.1.1. Postharvest assessments of avocado fruit, including dry matter determination, firmness measurement, and total oil content determination of fruit were carried out following the methods described in Sections 3.2.2, 3.2.3 and 3.5. Firmness measurement of fresh fruit were performed on 30 avocado fruit.

Commercial cold-pressed oil extraction of avocado fruit (≅ 650 kg) at six different stages of maturity was carried out at the Olivado Ltd, Kerikeri, New Zealand as described in Section 3.3.1. The dry matter values of fruit ranged from 24% (which is just at the minimum level for commercial harvest in New Zealand), to 34% by the end of the harvest season (April) seven months later, thus spanning the period that fruit would be harvested for fresh fruit consumption (oil fruit in New Zealand being sourced from rejected fresh fruit). EIS, electrical conductivity and light microscopy were used to examine avocado flesh structure at defined steps during the extraction process (intact flesh before grinding, fruit pulp at 0 min malaxing, fruit pulp after 60 min malaxing, fruit pulp after 120 min malaxing and fruit pomace after decanting centrifugation), following the procedures as described in Sections 3.6.1, 3.7.1 and 3.8.1. Cell wall extraction trials for selected samples were carried out following the procedures as described in 3.10.

Statistical analysis of data was carried out following the methods as described in Section 3.12. At each fruit harvest time, triplicate samples were collected at different times during the extraction process from one malaxer. Dry matter determination and total oil content determination for avocado pulp were carried out in triplicate. Electrical impedance

measurement for intact avocado fruit was carried out on ten replicates. Electrical impedance, conductivity measurements and cell wall extraction trails for avocado pulp were carried out in triplicate.

5.3 Results and discussion

5.3.1 Effect of fruit ripeness on laboratory cold-pressed avocado oil extraction

5.3.1.1 Laboratory cold-pressed oil yield and quality

In this study to determine the effect of fruit ripeness on microstructural changes and oil yield during laboratory-based cold-pressed extraction, fruit dry matter and the total oil present in the flesh, as determined by solvent extraction (ASE), were found to be the same ($p > 0.05$) for the fruit from three different firmness values (Table 5.1). Fruit of the same dry matter would be expected to have similar quantities of oil present based on fresh fruit flesh weight. In contrast, the laboratory scale cold-pressed oil yield increased significantly ($p < 0.05$) with decreasing fruit firmness (i.e. riper fruit). These results are similar to the findings of Woolf et al. (2009) on late season 'Hass' avocado where they also found a higher cold-pressed oil yield was obtained from riper 'Hass' avocado fruit.

In terms of oil quality extracted by laboratory-based cold pressing, the FFA% and PV of the oils significantly increased with fruit ripeness from 0.24 to 0.37% (as oleic acid) and 1.18 to 2.23 (meq/kg oil), respectively (Figure 5.4). During fruit ripening, the incidence of rots (body and stem-end rots) and internal disorders (flesh browning) increased markedly from ≅ 0% (amount of rots in fruit) at 55 Fv, to ≅ 5% at 80 Fv, to ≅ 10% at 105 Fv, this results in the reduction in cold-pressed oil quality. This result agrees with Woolf et al. (2009) who found that the increased rots level in avocado fruit resulted in a significant increase in FFA% of the oils. FFA% of the cold-pressed avocado oil increased

from 0.36% to 0.42% to 0.80% when the rot level in fruit increased from 5% to 10% to 15%. Similar results were also found in the cold-pressed olive oil extraction that the FFA% and PV of olive oil significantly increased with the increased rots level in olive fruit (García et al., 1996; Kiritsakis, Nanos, Polymenopulos, Thomai, & Sfakiotakis, 1998). The increases in FFA% and PV are related to the lipid hydrolysis reactions and oxidation of oil after oil is released from the cells. The lipid hydrolysis reactions could be the result of fungal lipase activity reported for olive oil (Kiritsakis et al., 1998). In avocados, the presence of rots could lead to increased lipid hydrolysis with damaged fruit cells.

Table 5.1: 'Hass' avocado fruit flesh dry matter, total oil present in flesh (determined by ASE solvent extraction) and laboratory-based cold-pressed extraction oil yield for fruit ripened at different firmness; 55, 80 and 105 Fv (mean ± SE, n = 3).

	Fruit firmness		
	55 Fv (minimally ripe)	**80 Fv (fully ripe)**	**105 Fv (over ripe)**
Laboratory-based cold-pressed oil yield (g oil/100 g fresh flesh weight)	7.38 ± 0.22% [a]	8.92 ± 0.35% [b]	9.95 ± 0.29% [c]
Total oil present in flesh (g oil/100 g fresh flesh weight)	12.79 ± 0.27% [d]	12.90 ± 0.19% [d]	12.83 ± 0.22% [d]
Fruit flesh dry matter (g dry flesh/100 g fresh flesh weight)	24.18 ± 0.17% [A]	24.03 ± 0.15% [A]	24.18 ± 0.20% [A]

[A] Same upper case letters denote no significant difference between dry matter values ($p > 0.05$).

[a-d] Different lower case letters denote significantly different oil yield values for comparison between rows and columns ($p < 0.05$).

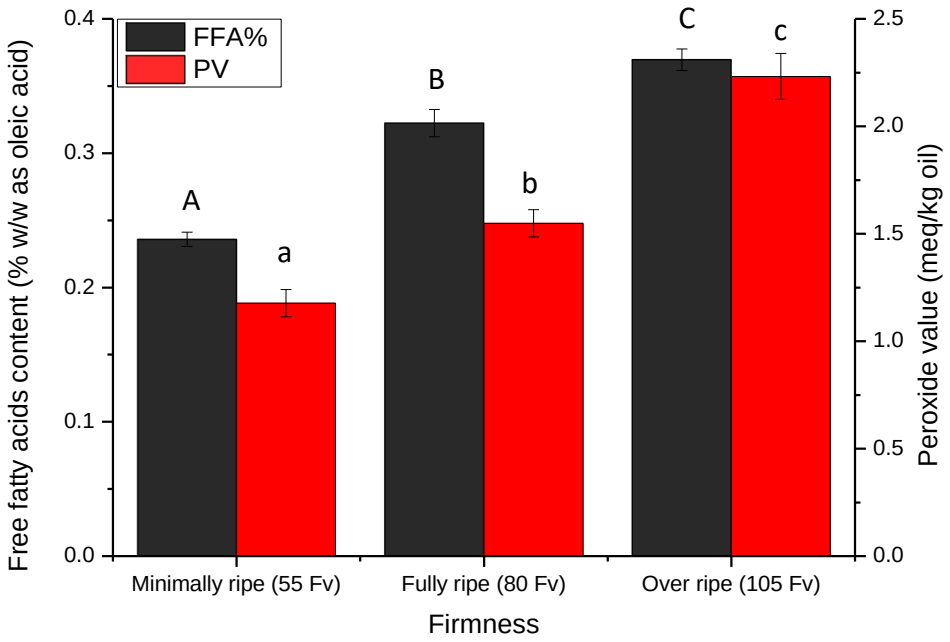

Figure 5.4: Free fatty acid content (FFA%) and peroxide value (PV) for oil extracted from 'Hass' avocado fruits ripened to different firmness; 55, 80 and 105 Fv after laboratory-based cold-pressed oil extraction (mean ± SE, n = 3)

[A,B,C] Different upper case letters denote significantly different values for free fatty acid content ($p < 0.05$).

[a,b,c] Different lower case letters denote significantly different peroxide values ($p < 0.05$).

5.3.1.2 Electrical impedance spectroscopy

Electrical impedance measurements are used to monitor rapid changes (within hours) associated with physiological dysfunction and cell membrane damage of the intact fruit flesh (e.g. chilling or heating injury) or to monitor changes that occur over a longer period and are associated with cell wall degradation of the fruit (e.g. fruit ripening) (Harker & Maindonald, 1994; Zhang & Willison, 1992a). A number of studies have demonstrated that electrical impedance measurements are able to provide a useful insight into ripening of fruit including nectarines, persimmon, tomato and kiwifruit (Bauchot, Harker, & Arnold, 2000; Harker & Dunlop, 1994; Harker & Forbes, 1997; Harker & Maindonald, 1994; Varlan & Sansen, 1996).

For fruit of different ripeness, the resistance of intact avocado fruit tissue at a low frequency (50 Hz) decreased as the fruit softened from 55–105 Fv (Figure 5.5(a)). During fruit ripening, the low frequency resistance of flesh tissue decreased by about 30% from 1856 ± 50 Ω to 1344 ± 35 Ω. In intact fruit tissue, higher resistances normally indicated there was a lower concentration of ions in the apoplast, the tissue's cell wall had a dense structure and the plasma membranes were intact (Harker & Dunlop, 1994). A decrease in resistance of fruit flesh tissue may be related to increased concentrations of mobile ions in the apoplast and/or an increase in cross-section of the cell accessible to low frequency current. A decreased resistance indicated degradation of the parenchyma cell walls in avocado flesh with the corresponding leakage of ions from intracellular compartments during avocado fruit ripening (Hershkovitz, Saguy, & Pesis, 2005; Platt-Aloia & Thomson, 1981; Platt-Aloia et al., 1980). Therefore, the reduction in resistance observed in this experiment, in the intact flesh, was highly likely to be due to enzymatic degradation of parenchyma cells in the avocado mesocarp from increased cellulase and polygalacturonase activity during avocado ripening. Such enzyme activity leads to a loss of middle lamella structure (more hydrated and open structure) in the parenchyma cells (Awad & Young, 1979; Platt-Aloia et al., 1980). The electrical reactance (the imaginary part of impedance) of a plant tissue is related to the capacitance of the tissue (Harker & Forbes, 1997). The electrical reactance of intact avocado fruit tissue did not change significantly ($p > 0.05$) as fruit softened from 55 to 105 Fv. For example at 50 Hz, for avocado fruit at 55, 80 and 105 Fv, the mean electrical reactance of the fruit tissues were -107.6 ± 6.4, -107.0 ± 2.7 and -110.2 ± 6.9 Ω, respectively. These results agree with previous studies on kiwifruit and nectarine fruit ripening, which showed that the electrical reactance of fruit tissue did not change during fruit ripening (Harker & Maindonald, 1994; Bauchot, et al., 2000). Harker & Maindonald (1994) proposed that the cell membranes in

fruit tissue remained structurally intact during fruit ripening, resulting in no observed change in reactance although membrane permeability and function may have changed.

The electrical resistance was monitored in fruit pulp during the laboratory oil extraction process for fruit at the three firmness levels. For all firmness levels, a significant reduction ($p < 0.05$) in electrical resistance was observed after the grinding step (Figure 5.5(b)). The majority of cell disruption was a result of the grinding step. This result supports the findings of Petrakis (2006) and Woolf et al. (2009) and their research into cold-pressed olive and avocado oil extraction; the grinding step in the process is designed to rupture the fruit cells to release the oil droplets from inside the cell structure/cell membrane. The electrical reactance (data not shown) of avocado fruit pulp tissue was not found to be significantly affected by the fruit ripeness in this study. As found in Chapter 4 and the previous studies from Harker and Dunlop (1994) and Jackson and Harker (2000), reactance may not be used alone to investigate the cellular changes in plant tissues during processing.

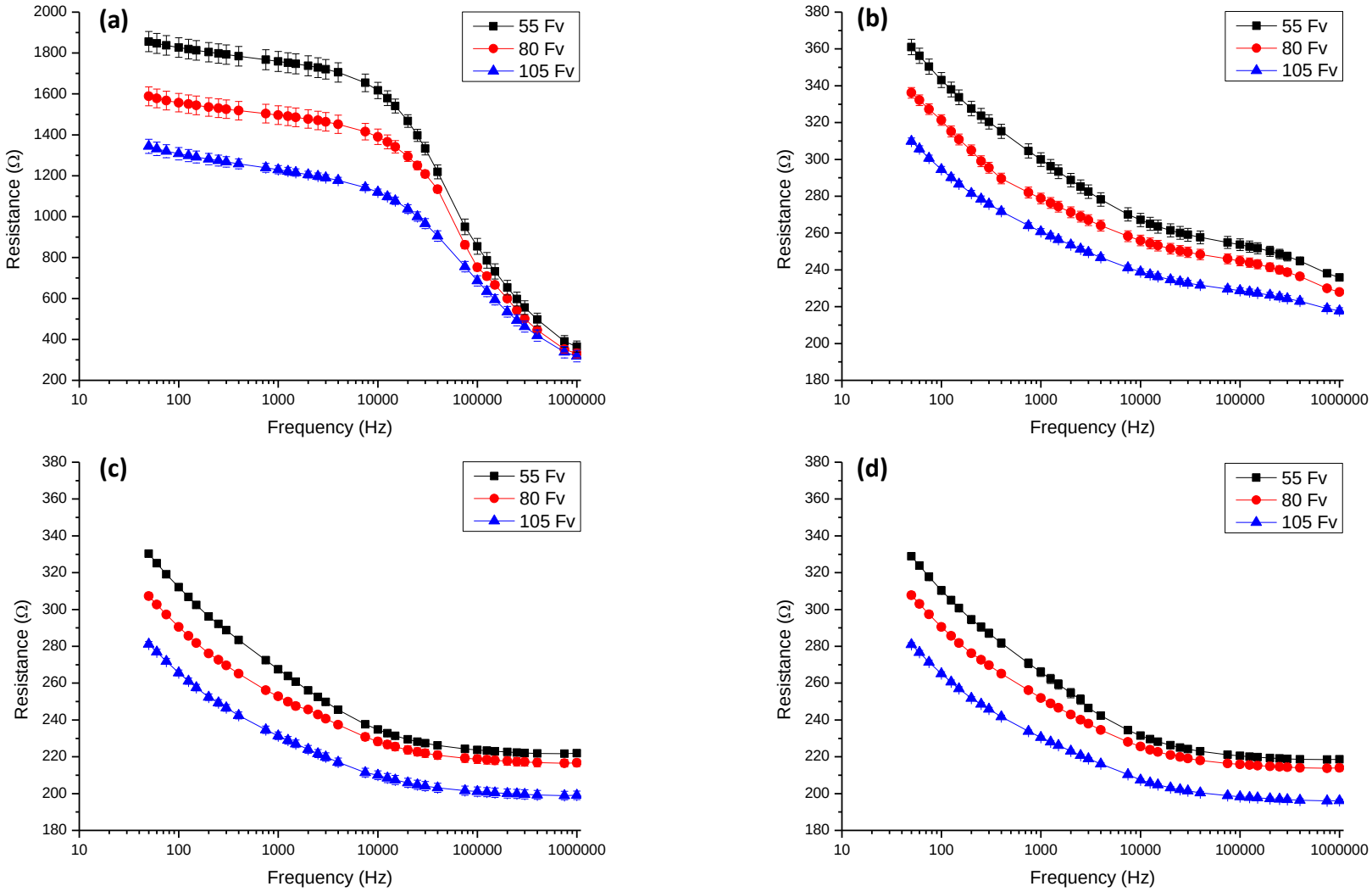

Figure 5.5: Resistance (Ω) of 'Hass' avocado flesh from fruit at three fruit firmness stages (55, 80, 105 Fv) (a) Resistance range 200–2000 Ω with intact 'Hass' avocado sample (mean ± SE, n = 10). Graphs (b), (c), and (d) show the resistance range 180–380 Ω with avocado pulp; (b) 0 min malaxing (after grinding); (c) after 60 min malaxing; (d) after 120 min malaxing' (mean ± SE, n = 3).

Figures 5.5(b) to 5.5(d) show at 50 Hz, 10 kHz and 1 MHz, the softer fruit (105 Fv) was found to have lower electrical resistance values at each sampling point during the oil extraction process, which suggested more cell rupture occurred during extraction of the softer and riper avocado fruit. The differences in resistance for avocados of different firmness observed in Figures 5.5(b) to 5.5(d) could be related to the microstructural changes in the avocado mesocarp caused by ripening. During avocado fruit ripening, most of the cell wall polysaccharides of the parenchyma cells are subjected to some degree of controlled degradation and a loosening of the polymer networks of the cell wall occurs. These changes lead to reduced intercellular adhesion, a loosening of the cell wall structure and a weakening of cell wall strength (Brummell, 2006b; Jeong et al., 2002; Platt-Aloia & Thomson, 1981; Platt-Aloia et al., 1980). This may then result in the cell walls of the parenchyma cells being softer in riper avocado fruit, which are easier to rupture during the grinding step and thus results in lower electrical resistance values. Previous studies have indicated that softer and riper avocado fruit yield more oil when extracted using cold-pressed (Woolf et al., 2009) and solvent (hexane, SC-CO_2) extraction systems (Mostert et al., 2007), which in this experiments appears to be related to changes in the avocado tissue at the microstructural level.

5.3.1.3 Electrical conductivity

Electrical conductivity measurements were used in this study to support EIS results to determine the degree of cell rupture during the extraction process. Increased electrical conductivity is due to an increase in ion leakage which, in turn, indicates a loss of membrane integrity (Pesis et al., 2003).

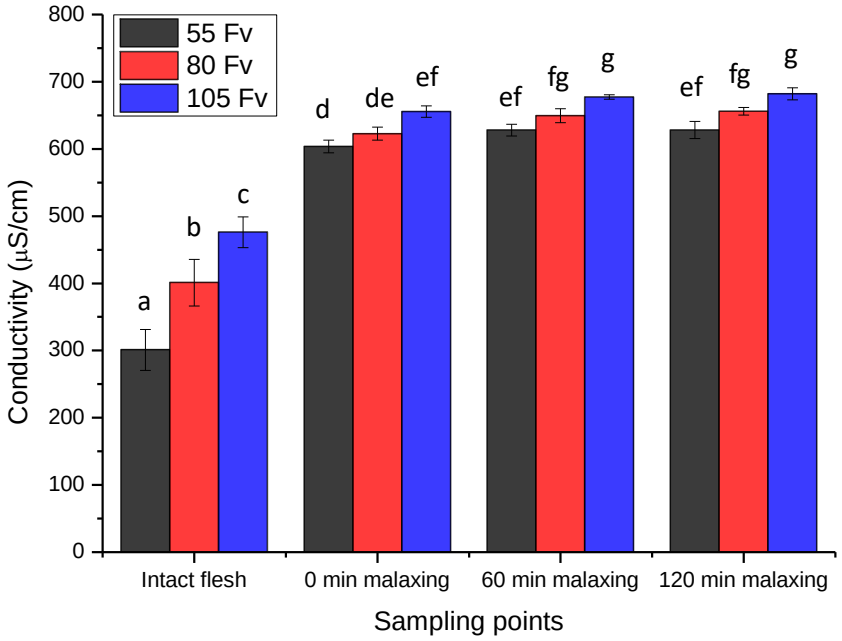

Figure 5.6: Electrical conductivity (µS/cm) of 'Hass' avocado flesh and pulp samples from fruit at three fruit firmness stages (55, 80, 105 Fv; mean ± SE, n = 3). Pulp samples collected during laboratory-based cold-pressed oil extraction

[a-g] Different letters denote significantly different conductivity values ($p < 0.05$).

In this study, the electrical conductivity of intact 'Hass' avocado flesh increased significantly ($p < 0.05$) as the fruit ripened (Figure 5.6), suggesting a loss of cell membrane integrity in the avocado mesocarp of intact flesh as the fruit ripened. These results agree with the previous study of Montoya et al. (1994) and Ahmed, Yousef, and Hassan (2010) where electrical conductivity of the 'Hass' and 'Fuerte' avocado fruit tissue increased as the fruit softened due to ripening. At each stage of malaxing (0, 60 and 120 min of malaxing), the softer and riper avocado fruit (105 Fv) showed higher conductivity values compared to the unripe fruit (55 Fv; Figure 5.6), which indicated greater cellular disruption occurred during the extraction of softer avocado fruit and more ions were released into the apoplast.

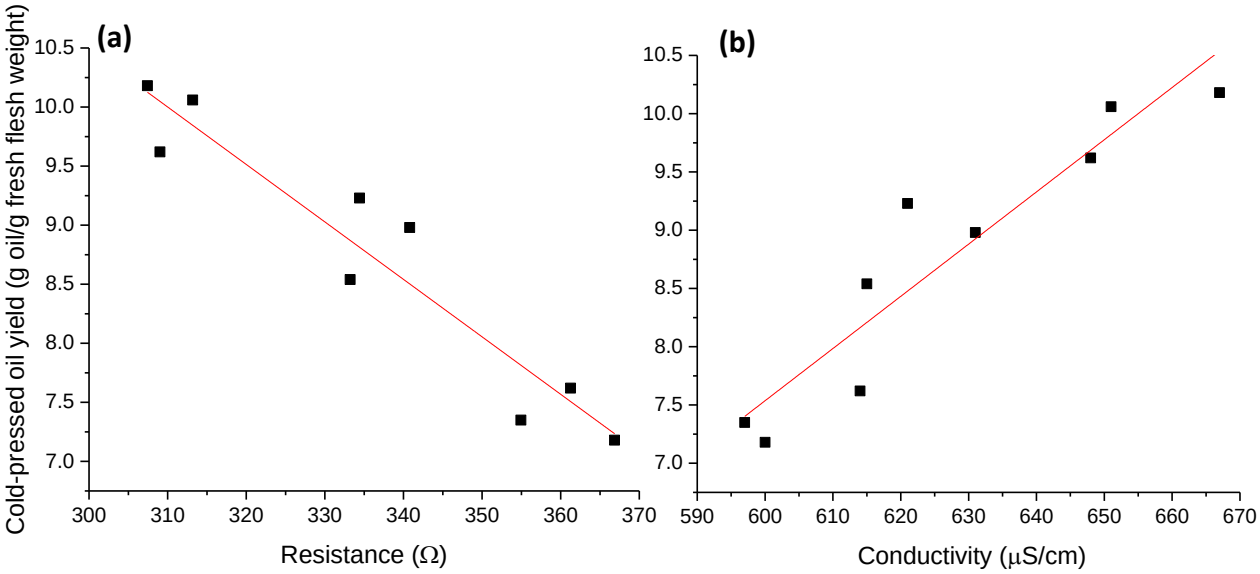

Figure 5.7: Laboratory-based cold-pressed oil yield of malaxed 'Hass' avocado pulp samples at 55, 80 and 105 Fv as a function of (a) electrical resistance (Ω; at 50 Hz) and electrical conductivity (µS/cm) of avocado pulp collected at 0 min malaxing.

The cold-pressed oil yield of malaxed avocado pulp samples at 55, 80 and 105 Fv are plotted against the respective electrical resistance (at 50 Hz) and electrical conductivity of fruit pulp samples collected at 0 min malaxing and are shown in Figure 5.7. The cold-pressed oil yield showed a linear decrease (R^2 0.91) with increasing electrical resistance (R) and a linear increase (R^2 0.88) with increasing electrical conductivity (C) (Equations 1 and 2). The following models (Equations 1 and 2) are proposed after correlating the laboratory cold-pressed oil yield after malaxing the pulp at 45 ± 1 °C at 20 rpm for 120 min to measured electrical resistance and electrical conductivity value at 0 min malaxing, equations only apply to R and C at 0 min malaxing:

Laboratory-based cold-pressed oil yield = –0.049R + 25.08 (1)

Laboratory-based cold-pressed oil yield = 0.045C – 19.34 (2)

Therefore, there is a strong correlation between the cold-pressed oil yield of the pulp and the electrical resistance and conductivity of a fruit pulp sample. The measurement of the electrical resistance and electrical conductivity of the avocado pulp sample at 0 min

malaxing can be applied in the oil industry to estimate the cold-pressed oil yield after 120 min malaxing.

5.3.1.4 Light microscopy

The microstructural changes in fruit tissue at different stages of firmness and during the laboratory cold-pressed avocado oil extraction process were examined with light microscopy. The light microscopy images of the fresh intact tissue from avocado fruit with firmness of 55, 80 and 105 Fv are shown in Figure 5.8. Intact parenchyma cell walls were visible (Figures 5.8(a) to 5.8(c)), but swelling of cell walls was observed during fruit ripening and a loss of organization in the cell walls was found in the over-ripe avocado fruit (Fv 105) (Figure 5.8(c)). In the over-ripe fruit, the cell walls were also observed to be splitting apart from adjacent cells. This loss of cell wall organization could be due to the action of the cell wall-degrading enzymes in the avocado mesocarp tissue. No swelling of the idioblast cell walls was visible as the fruit softened (Figures 5.8(d) to 5.8(f)), and these cells remained intact after grinding and malaxing (Figure 5.9), as reported in Chapter 4. The idioblast cell wall contains a specialised secondary suberin layer rather than the single cellulosic wall of parenchyma cells, which may be the reason the idioblast cell wall was more resistant to enzyme degradation and grinding (Platt-Aloia et al., 1983; Platt-Aloia et al., 1980). Most of the parenchyma cells were disrupted after grinding (Figures 5.9(a) to 5.9(c)) and less intact parenchyma cells were found in the pulp of softer and riper avocado at different stages of malaxing (0 min, 60 min and 120 min) than in the pulp of unripe avocado fruit (Figure 5.9). The light microscopy results support the findings observed with EIS and electrical conductivity (Figures 5.5 and 5.6).

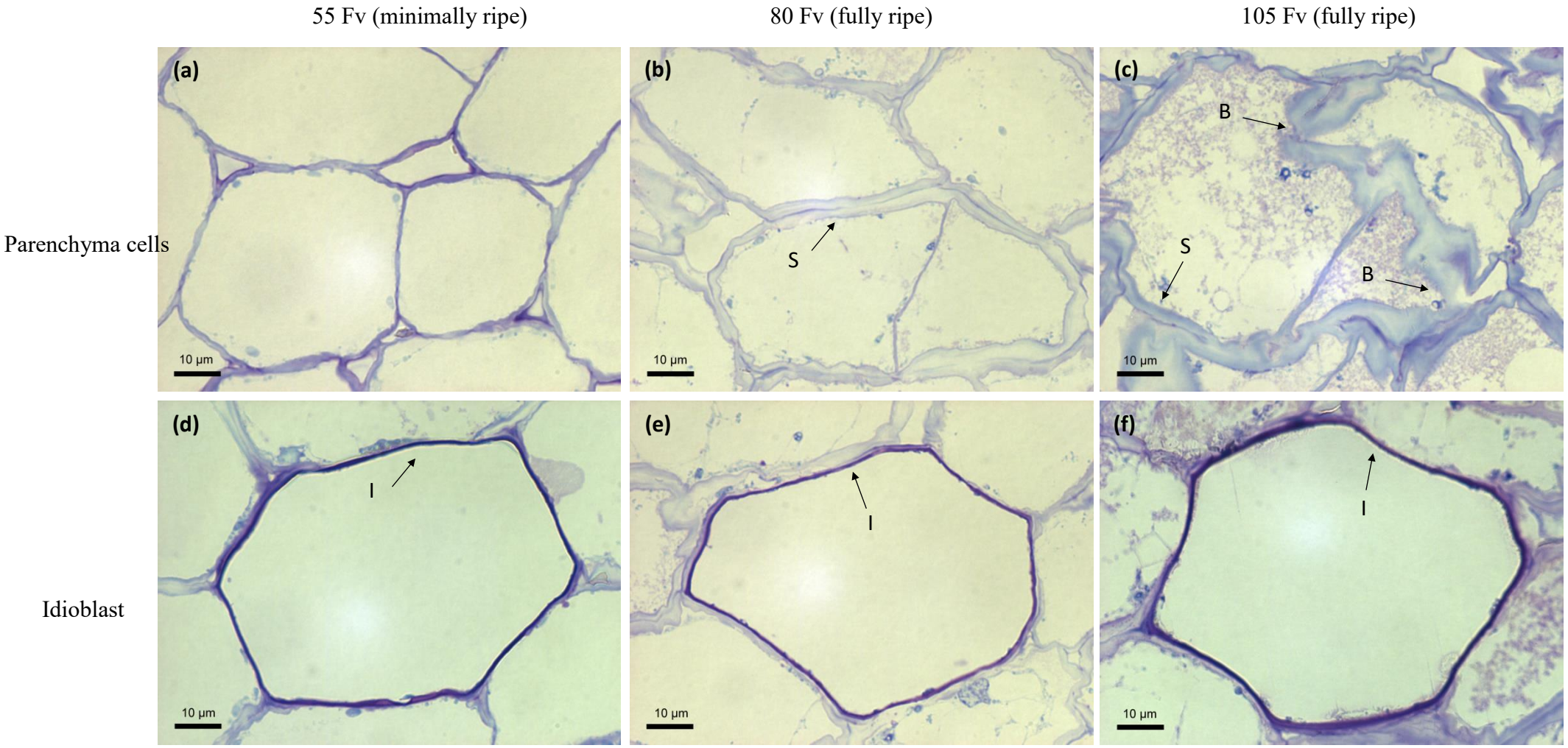

Figure 5.8: Light microscopy images of the microstructure of parenchyma and idioblast cells in intact 'Hass' avocado mesocarp at different firmness, (a) parenchyma cells at 55 Fv, (b) parenchyma cells at 80 Fv, (c) parenchyma cells at 105 Fv, (d) idioblast cell at 55 Fv, (e) idioblast cell at 85 Fv, (f) idioblast cell at 105 Fv.

S: Swelling of parenchyma cell wall; **B**: Break of parenchyma cell wall; **I**: Idioblast cell wall.

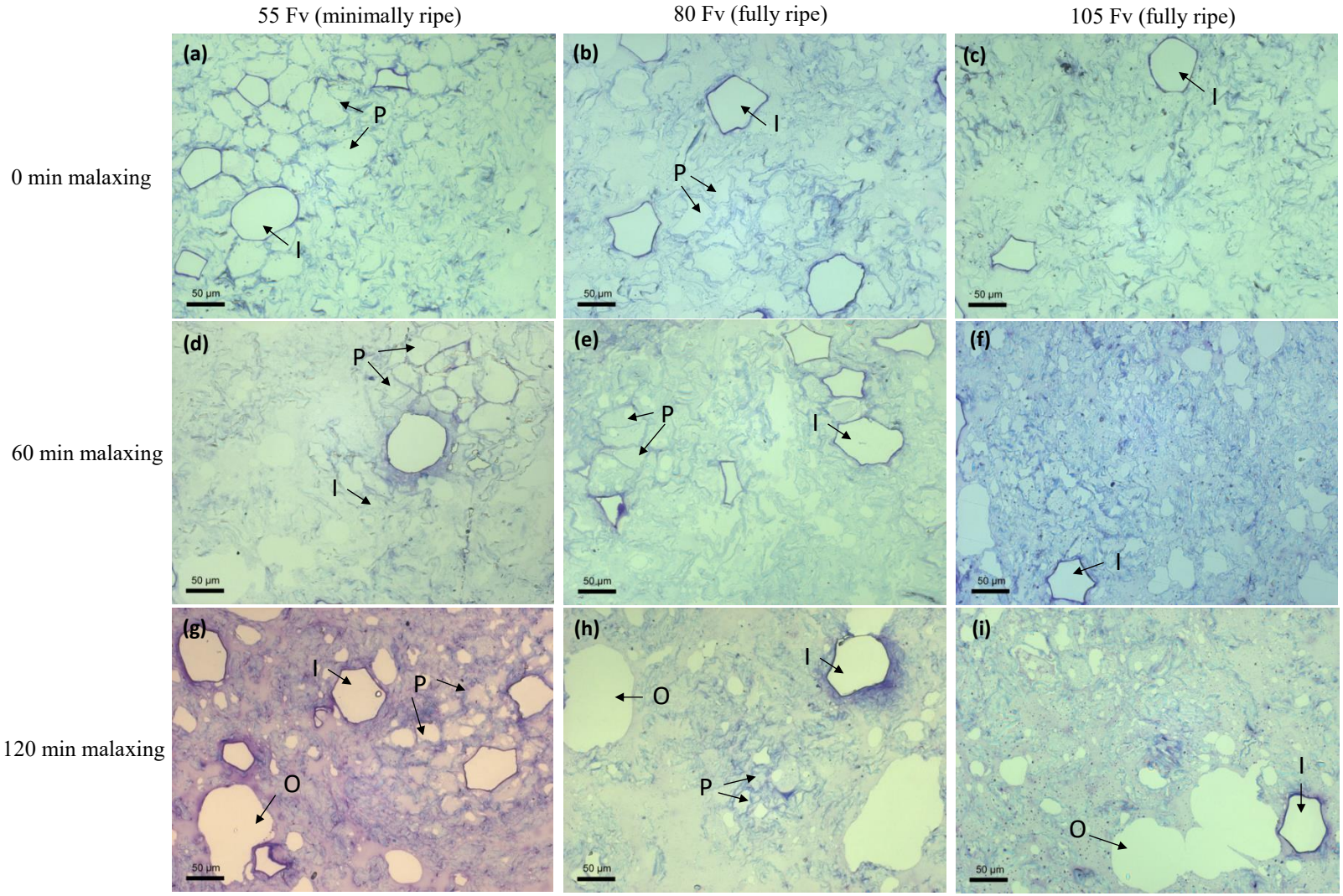

Figure 5.9: Light microscopy images of the microstructure of 'Hass' avocado flesh at different firmness, (a) 0 min malaxing, 55 Fv, (b) 0 min malaxing, 80 Fv, (c) 0 min malaxing, 105 Fv, (d) 60 min malaxing, 55 Fv, (e) 60 min malaxing, 80 Fv, (f) 60 min malaxing, 105 Fv, (g) 120 min malaxing, 55 Fv, (h) 120 min malaxing, 80 Fv, (i) 120 min malaxing, 105 Fv.

P: Unbroken parenchyma cells; **I**: Idioblast cell; **O**: Oil droplet from parenchyma cells.

Avocado fruit firmness was correlated to cell wall swelling and ion leakage which was monitored by EIS and electrical conductivity. The softer and riper fruit sample had lower electrical resistance and higher conductivity. The ripe softer fruit (Fv 105) had a more diffuse cell structure and thus were more easily disrupted by grinding, which lead to improved cold pressed oil yields. During avocado fruit ripening the polymer networks of the cell wall, primarily polysaccharides, begin to breakdown. This leads to a reduced intercellular adhesion, a loosening and weakening of the cell wall strength and structure (Brummell, 2006; Jeong et al., 2002; Platt-Aloia & Thomson, 1981; Platt-Aloia, et al., 1980). Hence, softer parenchyma cells in riper avocado fruit cells are easier to rupture during the grinding step resulting in a lower electrical resistance values.

5.3.2 Effect of fruit maturity on commercial cold-pressed avocado oil extraction

5.3.2.1 Commercial cold-pressed oil yield

In the study to determine the effect of fruit maturity on microstructural changes and oil yield during commercial cold-pressed extraction, for each commercial factory sampling date over the 2016/2017 season the firmometer readings were taken from an average of 30 fruit per sampling date. For the entire season, the firmness of the avocado fruits processed were an average firmness of 80 ± 2 Fv, which was within the recommended firmness for oil extraction (Woolf et al., 2009).

In New Zealand, the commercial harvest season for ‘Hass’ avocados starts in June (with limited fruit available), followed by a general peak between September and February-March, then there is a tail of late season fruit that goes to April or May of the following year. The harvests are dictated by the demand for local and export supply and may even change from year to year depending on the target export markets. The main export season

is November to February (New Zealand Avocado, 2019). The avocados harvested for this experiment were horticulturally mature (dry matter content > 24% (g dry flesh/100 g fresh flesh)) with harvest starting in September in New Zealand, 2016 (Figure 5.10). Before harvest, the fruit development on the tree results in an increase in dry matter content ≅ 24% (g dry flesh/100 g fresh flesh) in the early-season (September) to ≅ 34% (g dry flesh/100 g fresh flesh) in the late-season (April). The total oil content (determined by chemical extraction - ASE) in the fruit flesh was highly correlated with the dry matter content, which increased from ≅ 13.5% (g oil/100 g fresh flesh) in the early-season to ≅ 23.5% (g oil/100 g fresh flesh) in the late-season (Figure 5.10). These results are in agreement with previous studies of avocado maturity (Hopkirk, 1989; Kikuta & Erickson, 1968; Lawes, 1980; Lee et al., 1983).

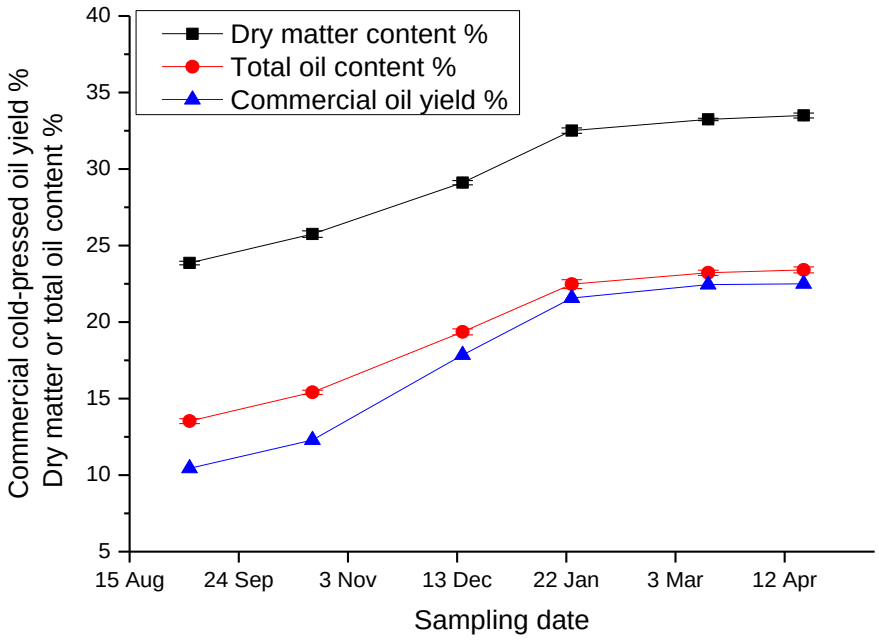

Figure 5.10: Changes in 'Hass' avocado fruit flesh dry matter content % (g dry flesh/100 g fresh flesh), total oil % present in flesh (g oil/100 g fresh flesh; determined by ASE solvent extraction) and commercial cold-pressed extraction oil yield% (g oil/100 g fresh flesh) over the 2016-2017 commercial harvest and oil processing season in New Zealand (mean ± SE, n = 3)

The commercial cold-pressed oil yield at Olivado NZ was obtained based on processing from one malaxer of ≅ 650 kg of avocado. Early in the season, there was ≅ 3% difference between the total oil content in the flesh and the commercial cold-pressed oil yield achieved (Figure 5.10). However, the oil extraction efficiency increased later in the season, the difference between the total oil content and the commercial oil yield decreased to ≅ 1% in March and April 2017 (Figure 5.10). Since commercial oil extractions were carried out on avocado fruits at the same firmness stage (Appendix III), the differences in cold-pressed oil yield were therefore assumed to be not due to any differences in ripeness. These findings agree with the previous study by Woolf et al. (2009) who found the oil was more difficult to be recovered from early maturity 'Hass' avocado by cold-pressed aqueous extraction, although that result was derived from estimated incoming dry matter values and commercial oil yield records, whereas in this experiment these results are derived from measured dry matter and oil yields from a controlled experiment in the factory. The reason for the lower extraction efficiency for cold-pressed oil extraction in early-season fruit rather than for late-season fruit is still unclear. Hence, the hypothesis of this experiment was that there are cell wall changes in the fruit over the season which leads to optimal oil release. This will be explored more in Section 5.3.2.5.

5.3.2.2 Electrical impedance spectroscopy

The electrical resistance of intact avocado fruit flesh measured at six different stages of maturity were found to be not significantly different ($p > 0.05$) when all were compared to each other (Figure 5.11(a)). From this result, it is concluded that the fruit used for the six commercial cold-pressed extractions were carried out with fruit at the same level of ripeness based on results presented in Section 5.3.2.1 (Appendix III).

Avocados harvested at six different maturity stages were subjected to a commercial cold-pressed extraction process, the electrical resistance was monitored in the fruit pulp during the malaxing step. For all maturity stages, the electrical resistance, at 50 Hz, decreased from ≅ 1650 Ω to 400-500 Ω after the grinding step (corresponds to time 0 min malaxing). As shown earlier in Chapter 4, the grinding step resulted in the disruption of the majority of the cells in the avocado flesh. Figures 5.11(b) to 5.11(d) show the resistance measured in the pulp at each sampling point during the malaxing process (0, 60 and 120 min of malaxing). There was a significant decrease ($p < 0.05$) in the electrical resistance from fruit pulp samples collected in September 2016, to October 2016, December 2016 and January 2017 for the frequencies measured at 50 Hz, 10 kHz and 1 MHz. There were no significant changes ($p > 0.05$) in electrical resistance from fruit pulp samples collected in January 2017 to March 2017 and April 2017. The results indicated more cell disruption occurred during extraction of the avocado fruit harvest later in the season. These findings also explained the results in Figure 5.10 that showed that the higher oil extraction efficiency in the late-season was due to the cells in the late maturity fruit being easily disrupted.

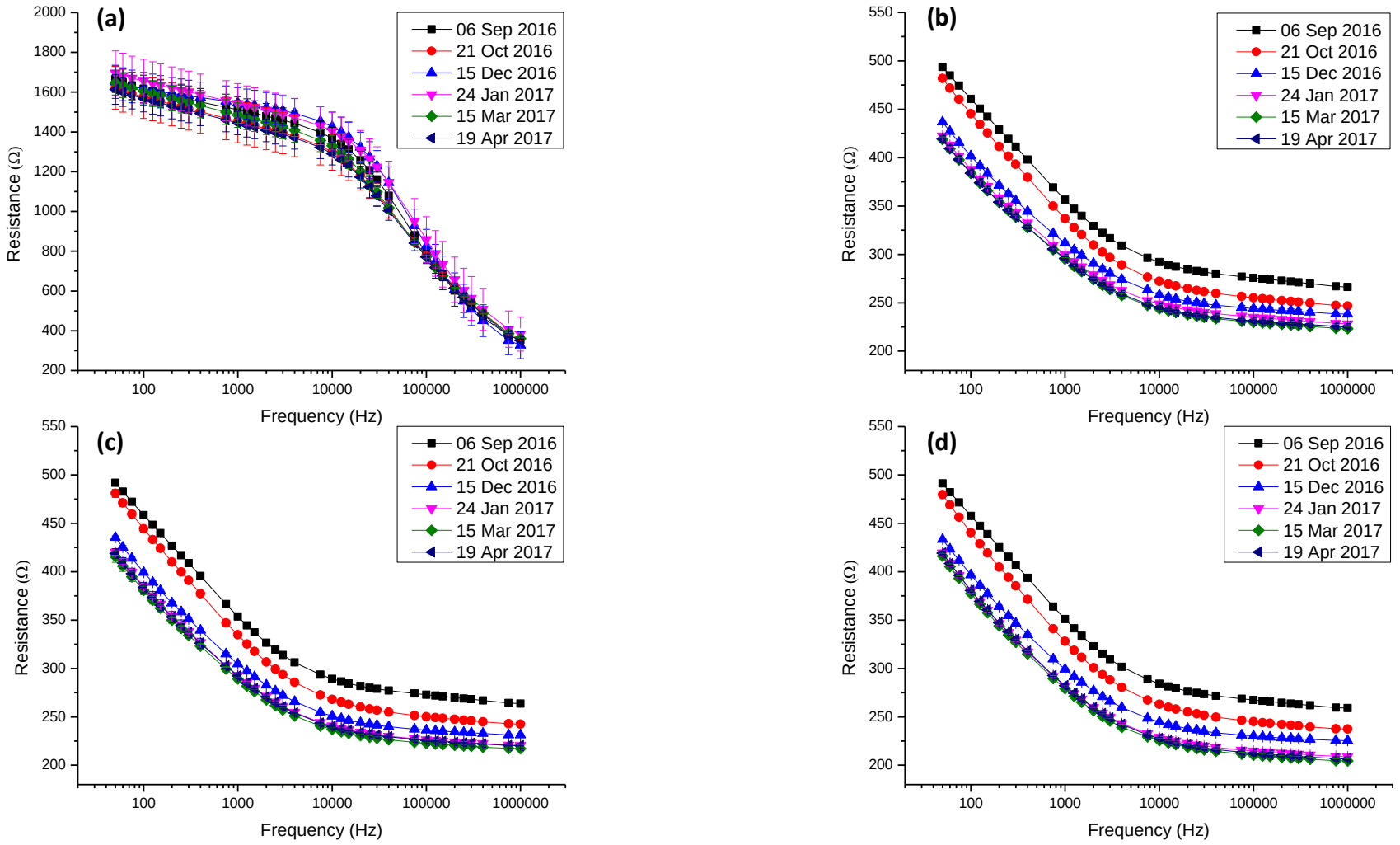

Figure 5.11: Resistance (Ω) of 'Hass' avocado flesh from fruit at six different stages of maturity (harvested between September to April 2016/17 season) (a) Resistance range 200–2000 Ω with intact 'Hass' avocado flesh sample (mean ± SE, n = 10); Resistance range 180–550 Ω with avocado pulp (b) At 0 min malaxing (after grinding); (c) At 60 min malaxing; (d) At 120 min malaxing (mean ± SE, n = 3).

5.3.2.3 Electrical conductivity

For each harvest date no significant difference ($p > 0.05$) was found between the electrical conductivity of intact 'Hass' avocado flesh at six different stages of maturity (Figure 5.12), suggesting there was no significant difference in cell wall and membrane integrity as the fruit matured. After grinding, the electrical conductivity of fruit pulp samples significantly increased and the late-season avocado fruit showed higher conductivity values ($p < 0.05$) at 0, 60 and 120 min of malaxing (Figure 5.12), which indicated greater cellular disruption occurred during the extraction of late maturity avocado fruit and more ions were released into the extracellular fluid.

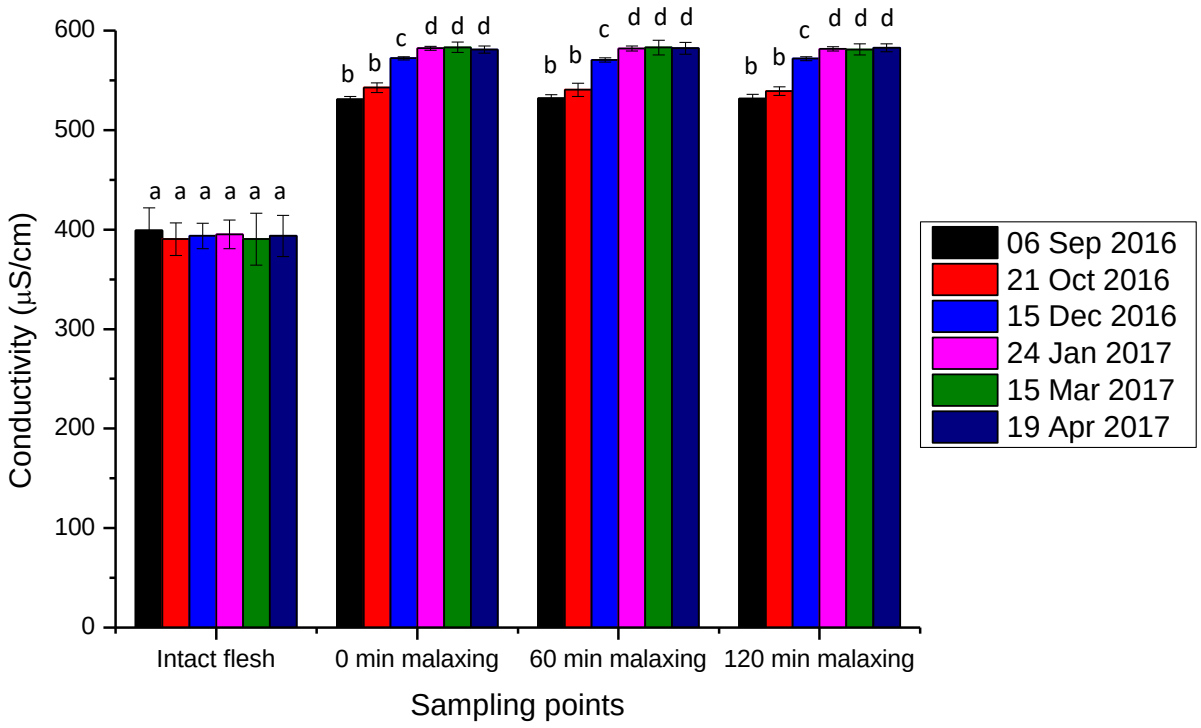

Figure 5.12: Electrical conductivity (µS/cm) of 'Hass' avocado flesh and pulp samples from fruit at six different stages of maturity (mean ± SE, n = 3). Pulp samples collected during commercial cold-pressed oil extraction

[a-d] Different letters denote significantly different conductivity values ($p < 0.05$).

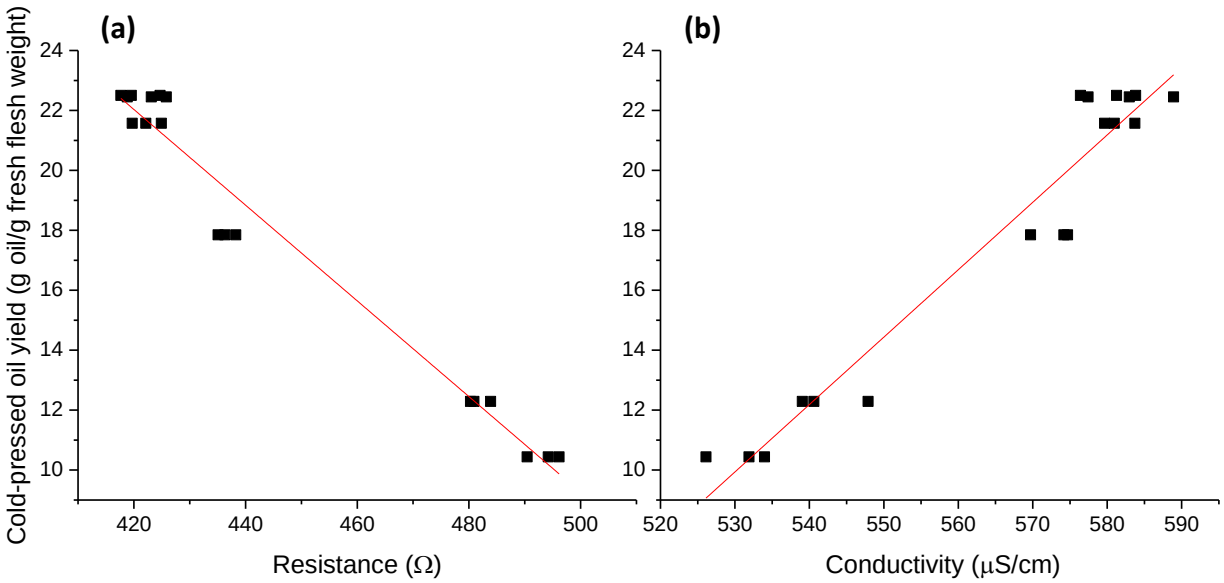

Figure 5.13: Commercial cold-pressed oil yield of malaxed 'Hass' avocado pulp samples at six different stages of maturity as a function of (a) electrical resistance (**Ω**; at 50 Hz) and electrical conductivity (µS/cm) of avocado pulp collected at 0 min malaxing.

Similarly to the previously findings in Section 5.3.1.3, a strong correlation between the commercial cold-pressed oil yield of the pulp (after malaxed at 45 ± 3 °C at 20 rpm for 120 min) and the degree of the cellular disruption in a fruit pulp sample (at 0 min malaxing) and was found in this study (Figure 5.13). The commercial cold-pressed oil yield showed a linear decrease (R^2 0.97) with increasing electrical resistance (at 50 Hz; R) and a linear increase (R^2 0.94) with increasing electrical conductivity (C) (Equations 3 and 4), equations only apply to R and C at 0 min malaxing:

Commercial cold-pressed oil yield = –0.160R + 89.10 (3)

Commercial cold-pressed oil yield = 0.225C – 109.27 (4)

It was expected of the correlation equations for cold-pressed oil yield vs electrical resistance and cold-pressed oil yield vs electrical conductivity for laboratory-based oil extraction (Figure 5.7) and commercial oil extraction (Figure 5.13) to be similar. Equations 1 and 2 have very different slopes to Equations 3 and 4. As the laboratory-

based extractions were carried out with early season fruit it was expected this data would be similar to early season from the commercial oil extraction. However, a lower cold-pressed oil yield and more broken parenchyma cells indicated by lower electrical resistance and higher electrical conductivity values was found in the laboratory-based oil extraction of early season avocado fruit. This difference is firstly due to the different malaxing times, since there was an additional 30 min pre-malaxing in the commercial oil extraction. Secondly, the differences may be due to the different grinders applied in laboratory-based (hammer mill) and commercial oil extraction (attrition mill). Therefore, it is important for the commercial oil industry to use the correlations for commercial oil extraction (Figure 5.13) to estimate the cold-pressed oil yield after 120 min malaxing.

5.3.2.4 Light microscopy

The microstructural changes in avocado fruit at different stages of maturity and during the commercial cold-pressed oil extraction process was also examined with light microscopy. After examining over 100 fields of view, it was concluded that after grinding, fewer unbroken parenchyma cells were found in the pulp of late maturity avocado samples at different stages of malaxing (0 and 120 min) than in the pulp of early maturity fruit samples (Figure 5.14). Also, more unbroken parenchyma cells were found in the pomace sample of early maturity fruit after the decanter (Figure 5.15). The light microscopy results support the findings observed with the EIS and electrical conductivity results (Figure 5.11 and 5.12). As hypothesised, there may be differences in the cell wall composition of the parenchyma cells over the season which lead to differences in the degree of cellular disruption during cold-pressed oil extraction.

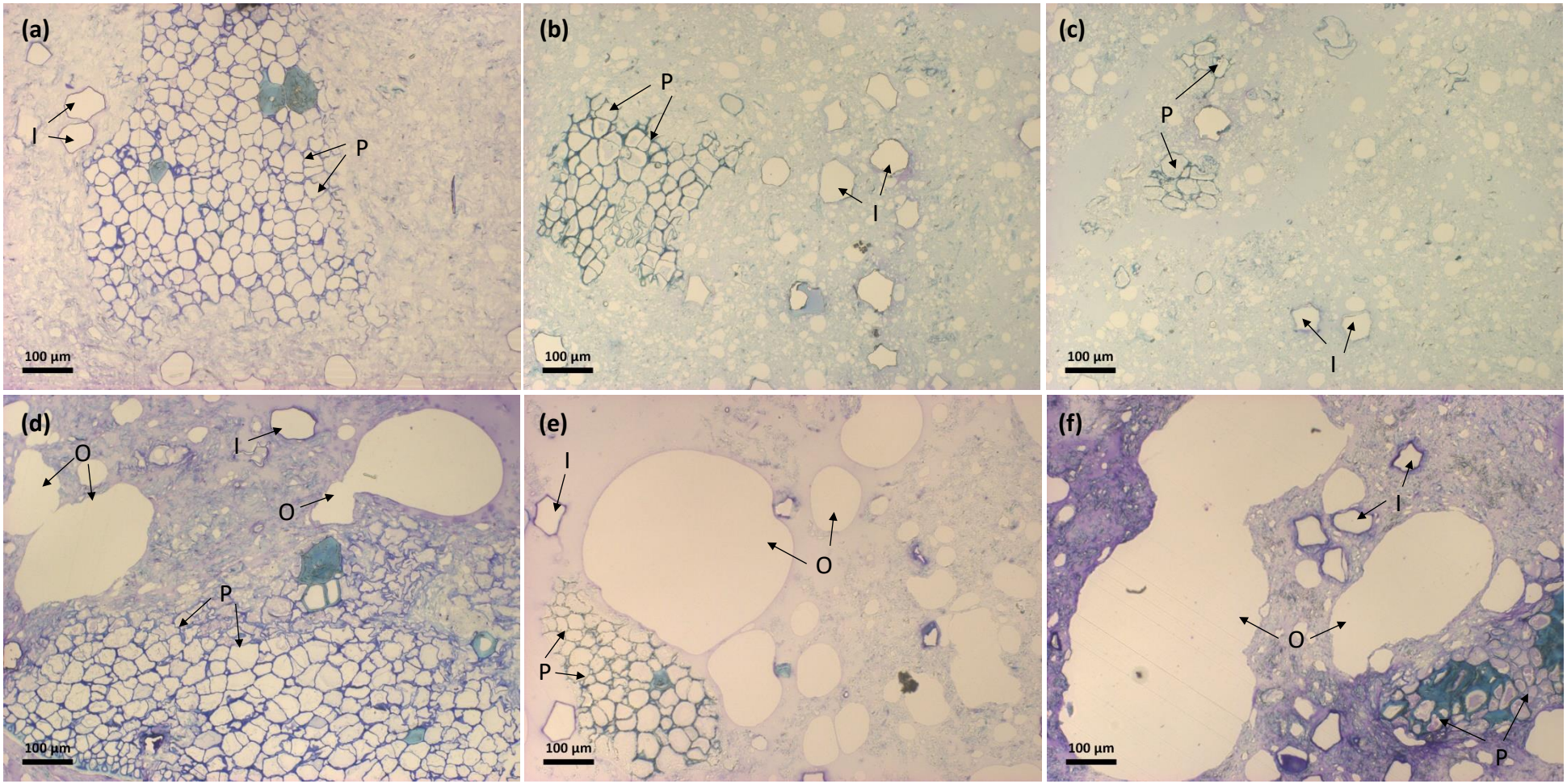

Figure 5.14: Representative light microscopy images of the microstructure of 'Hass' avocado pulped flesh at three different stage of maturity (a) early-season (September), 0 min malaxing; (b) mid-season (December), 0 min malaxing; (c) late-season (March), 0 min malaxing; (d) early-season, 120 min malaxing; (e) mid-season, 120 min malaxing; (c) late-season, 120 min malaxing. Cell walls were stained with toluidine blue staining. **P**: Unbroken parenchyma cells; **I**: Idioblast cell; **O**: Oil droplet from parenchyma cells.

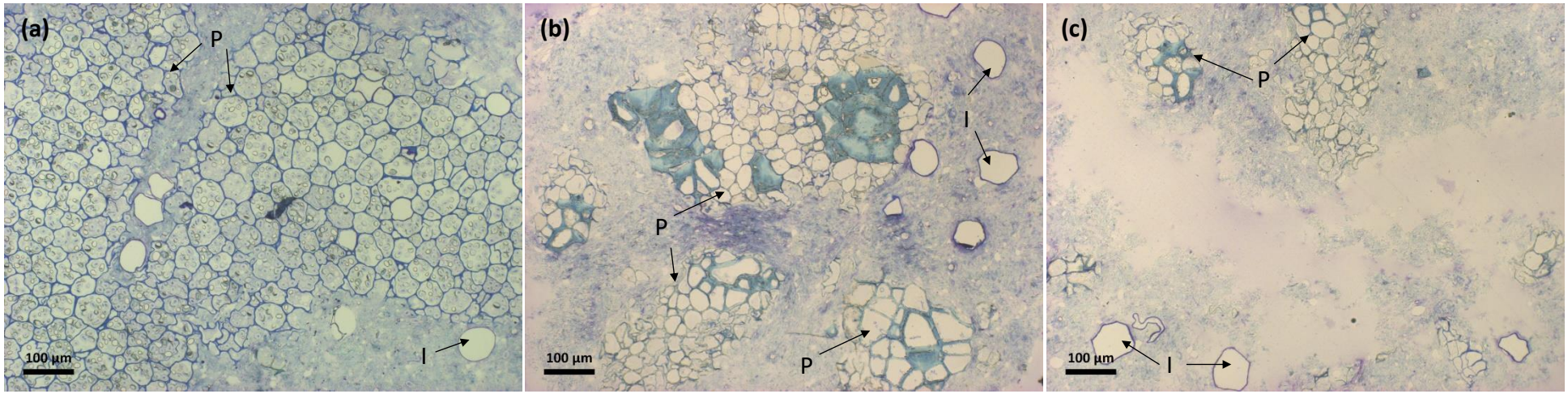

Figure 5.15: Representative light microscopy images of the microstructure of pomace from decanting centrifuge at three different stage of maturity (a) early-season (September), (b) mid-season (December), (c) late-season (March). Cell walls were stained with toluidine blue staining.

P: Unbroken parenchyma cells; **I**: Idioblast cell.

For all maturity stages, larger sizes of the oil droplets were found in the late maturity fruit sample after 120 min of malaxing (Figures 5.14(d) to 5.14(f)). Early in the season, the average diameter of oil droplets was ≅ 90 μm after 120 min of malaxing; however, the average diameter of oil droplets increased to ≅ 190 μm in the mid-season and to ≅ 260 μm in the late-season after 120 min of malaxing. This may firstly be because of the higher total oil content in the late maturity fruit flesh (Figure 5.10). Secondly, this may be due to more cellular disruption in the late maturity fruit samples releasing more oil from the cells which can easily agglomerate during malaxing, or may be due to more breakdown of cell walls therefore the pulp is less viscous and it is easier for the oil to agglomerate.

5.3.2.5 Cell wall composition

As noted previously, it is hypothesised that the composition and structure of the polysaccharides in the cell walls of fruit at different stages of maturity may affect the efficiency of cellular disruption during the cold-pressed avocado oil extraction. However, how the organisation of the polysaccharides and their composition relate to fruit maturity and oil extraction process has not been studied previously.

A cell wall is made up of a network of cellulose microfibrils and cross-linking glycans embedded in a highly cross-linked matrix of pectin polysaccharides (Alberts et al., 2002). Analysis of the cell wall fractions obtained through chemical fractionation allows the determination of the polysaccharide composition of the cell wall, which can give an indication of the binding strength of polysaccharides to cellulose (Brummell, 2006a; Selvendran, Stevens, & O'neill, 1985). Chemical extraction of cell wall fractions is often based on sequential extraction with solvents of increasing strength, from this it is assumed that the higher the solvent concentration needed to solubilise the polysaccharides, the

stronger the bonding of those polysaccharides to cellulose (Redgwell & Selvendran, 1986; Selvendran et al., 1985).

Figure 5.16(a) shows that the yield of the water-soluble polysaccharide fractions from mid-season (December) and late-season (March) avocado fruit pulp was significantly higher ($p < 0.05$) than that from the early-season (September) fruit pulp. Polysaccharides in the water-soluble fraction would be freely soluble in the cell wall and would not be strongly bound in any cell wall network (Brummell, 2006a). An increase in the yield of the water-soluble fraction suggested that polysaccharides originally held in the cell wall by covalent bonds become more weakly attached to the wall and eventually become freely soluble (Brummell, 2006a). Their loss from the cell wall network would contribute to the weakening of cell wall strength. In many fruit such as avocado and kiwifruit, a loosening of the cell wall structure has been positively correlated with pectin solubilisation, characterised by an increase in water-soluble polysaccharides yield (Defilippi, Ejsmentewicz, Covarrubias, Gudenschwager, & Campos-Vargas, 2018; Jeong et al., 2002; Redgwell et al., 1997). Figure 5.16(b) shows that the CDTA-soluble polysaccharide fraction yield decreased ($p < 0.05$) with increasing fruit maturity. CDTA (the chelating agent) is used to solubilise polysaccharides attached by calcium bridges to insoluble cell wall components, which generates a fraction enriched in polysaccharide held in the wall by ionic bonds (Jarvis, 1982; Jarvis, Hall, Threlfall, & Friend, 1981). The result suggests that in late maturity avocado fruit, there are larger amounts of polysaccharides which are freely soluble in the cell wall and less of them are held in the wall by stronger ionic bonds. The result of this is a weakened cell wall. This is likely to be the reason why the parenchyma cells were easier to disrupt during the extraction of late-season fruit. Also, no significant difference ($p > 0.05$) was found for both the water- and CDTA-soluble

polysaccharide fraction yields for fruit pulp collected at 0 min and 120 min of malaxing (Figure 5.16), which indicated that the malaxing did not result in any changes to the composition of the polysaccharides in the cell walls.

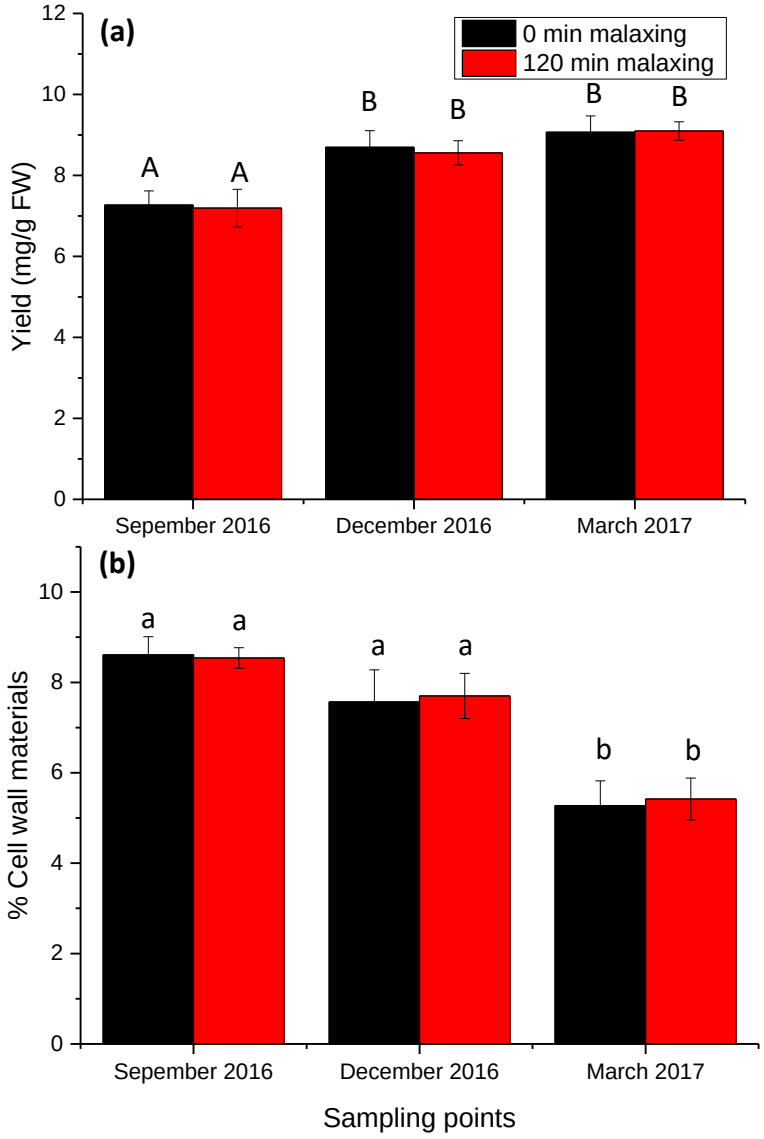

Figure 5.16: Polysaccharide yields of (a) water- and (b) CDTA-soluble fractions of 'Hass' avocado pulp samples at three different stages of maturity (mean ± SE, n = 3). Pulp samples collected during commercial cold-pressed oil extraction

[A,B] Different upper case letters denote significantly different values for water- soluble fractions ($p < 0.05$).

[a,b] Different lower case letters denote significantly different values for CDTA- soluble fractions ($p < 0.05$).

For avocado fruit at different maturity, the commercial cold-pressed oil yield was correlated to the polymer network in parenchyma cell walls and to the degree of cellular disruption, which was examined by light microscopy, EIS, conductivity measurement, and chemical extraction of cell wall fractions. The parenchyma cells in late season fruit have a weaker bonding strength holding the polysaccharides to cellulose in the cell walls, thus were more easily disrupted by grinding which resulting in a lower electrical resistance values and higher conductivity values, and lead to a higher cold pressed oil yields.

5.4 Conclusions

Cold-pressed avocado oil extraction was strongly influenced by fruit ripeness and fruit maturity. Avocado fruit softens during ripening and this corresponds to changes to the cell wall microstructure of the mesocarp, where the cell wall was observed to be more open and diffuse leading to greater cellular disruption. This led to increased conductivity values and resulted in a higher cold-pressed oil yields.

Also, more parenchyma cell disruption occurred during extraction of late maturity avocado fruit which led to decreased electrical resistance values, increased electrical conductivity values and resulted in a higher cold-pressed extraction efficiency. Cells are easier to be disrupted during the oil extraction of late maturity fruit, this is due to the difference in the binding strength of polysaccharides to cell wall.

Chapter 6:

Effect of malaxing conditions and ultrasound treatment on microstructural changes, rheological characterization and cold-pressed oil yield

6.1 Introduction

Malaxing is an important step in oleaginous fruit oil extraction to help the oil droplets aggregate together to form a larger continuous oil phase, which will help to improve the oil yield in the subsequent centrifugation steps (Petrakis, 2006; Wong et al., 2012). Malaxing is achieved in a number of different types of vessels using hot water jackets. The fruit pulp inside the vessel is heated and slowly mixed with stainless steel blades attached to a central rotating shaft (Clodoveo, 2012; Wong et al., 2012). In cold-pressed avocado oil extraction, the avocado pulp is continuously stirred in a malaxer at a low speed (15–25 rpm) for times between 60 to 120 minutes. The malaxer is set to a desired temperature (between 45 to 50 °C) and the aim is to heat the pulp to this temperature to achieve good oil yield without a significant reduction in oil quality, but there is often a delay in heating the pulp to the required temperature (Woolf et al., 2009).

The use of ultrasound waves has been introduced as a novel technology in the food oil industry to improve oil yield. Ultrasound treatment could lead to cellular disruption and oil aggregation to help improve the oil extraction process (Clodoveo, 2012; Juliano et al., 2017). Cellular disruption is due to the cavitation phenomena, the vapour bubbles that are created by ultrasound waves collapse near the biological cells to produce shock waves that can disrupt the cell walls and membranes (Luque Garcìa & Luque de Castro, 2003; Mercer & Armenta, 2011). Oil aggregation is based on the principle of displacing suspended oil droplets exposed to an ultrasonic standing wave field. A primary radial force that is created by ultrasound waves moves the oil droplets towards each other, where the oil droplets then coalesce at these points to form larger oil droplets which are more likely to be effectively separated in the decanter step, thus increasing oil yield (Juliano et al., 2011; Vilkhu et al., 2011).

However, it is not clear how microstructure, rheological properties and oil yield are affected by malaxing conditions and ultrasound treatments during cold-pressed avocado oil extraction. The objective of this study was to investigate the effect of malaxing time and temperature and the potential application of ultrasound treatments using laboratory cold-pressed oil extraction of 'Hass' avocado. Electrical impedance spectroscopy (EIS) and rheological measurements, combined with light microscopy and electrical conductivity measurements were used to monitor the microstructural and rheological properties changes in the flesh of avocados during various stages of the oil extraction process.

6.2 Experimental design

6.2.1 Effect of malaxing temperature on microstructural changes and oil yield during laboratory-based (1L malaxer) cold-pressed extraction

The main steps in the experiment looking at the effect of malaxing conditions on microstructural changes and oil yield during laboratory-based cold-pressed extraction are shown in Figure 6.1.

'Hass' avocado fruit (*Persia americana* Mill.) were harvested in October 2016, December 2016 and March 2017 from Plant and Food Research Ltd orchards in the Bay of Plenty, New Zealand. The fruit were ripened to the target fruit firmness at 80 Fv following the procedures described in Section 3.1.2. Postharvest assessments of avocado fruit, including dry matter determination, firmness measurement, and total oil content determination of fresh fruit were carried out on 20 avocado fruit following the methods described in Sections 3.2.1, 3.2.3 and 3.5.

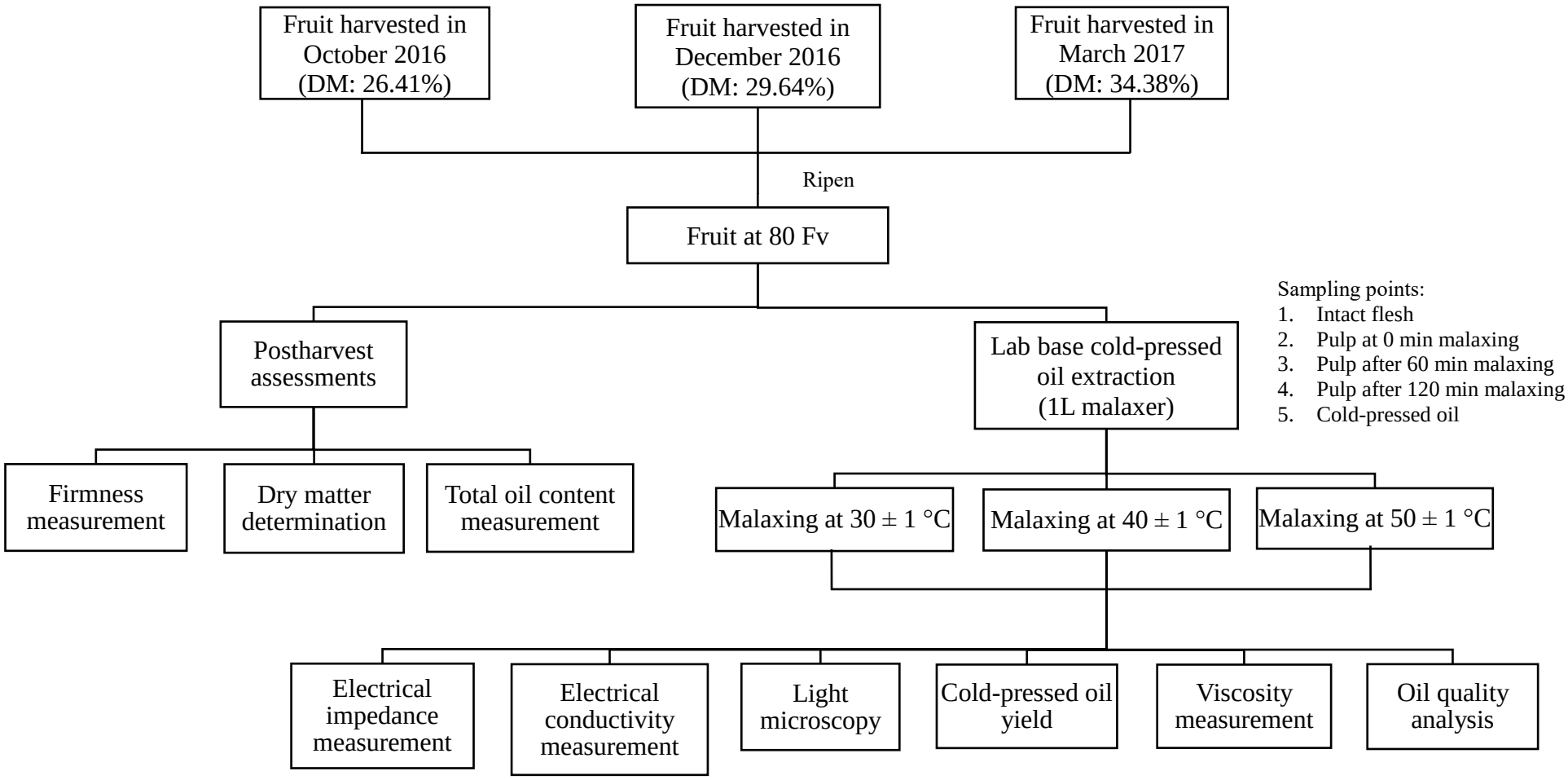

Figure 6.1: Flow diagram for the experimental procedure to investigate the effect of malaxing temperature on microstructural changes and oil yield during laboratory-based cold-pressed extraction. Electrical impedance measurement, electrical conductivity measurement, light microscopy observation and viscosity measurement were carried out at each sampling point during the extraction process.

DM: Dry matter content (g dry flesh/100 g fresh flesh weight).

Laboratory-based cold-pressed oil extraction of avocado fruit was carried out at three different malaxing temperatures, 30 ± 1, 40 ± 1 and 50 ± 1 °C, following the procedures described in Section 3.3.2. For the early-season fruit samples (fruit harvested in October 2016), EIS, electrical conductivity and light microscopy were used to examine avocado flesh structure at defined steps (intact flesh before grinding, fruit pulp at 0 min malaxing, fruit pulp after 60 min malaxing and fruit pulp after 120 min malaxing) during the extraction process following the procedures described in Sections 3.6.2, 3.7.2 and 3.8. The viscosity of fruit pulp samples was measured following the procedures described in Section 3.9.1. Analysis of oils, including the free fatty acid content (FFA%) and the peroxide value (PV) determination, were carried out following the procedures described in Section 3.11.

Statistical analysis was carried out following the methods described in Section 3.12. Postharvest assessments of avocado fruit and the laboratory-based avocado oil extraction experiments were performed in triplicate. Electrical impedance, conductivity, viscosity and cold-pressed oil yield measurements for avocado pulp were carried out in triplicate. FFA% and PV determination for cold-pressed avocado oil were performed in triplicate.

6.2.2 Effect of malaxing temperature on rheological properties and oil yield during malaxing in rheometer (50mL malaxer)

The objective of this experiment was to determine the effect of malaxing temperature on the rheological properties and oil yield during malaxing in a concentric cylinder geometry in a rheometer (Figure 6.2).

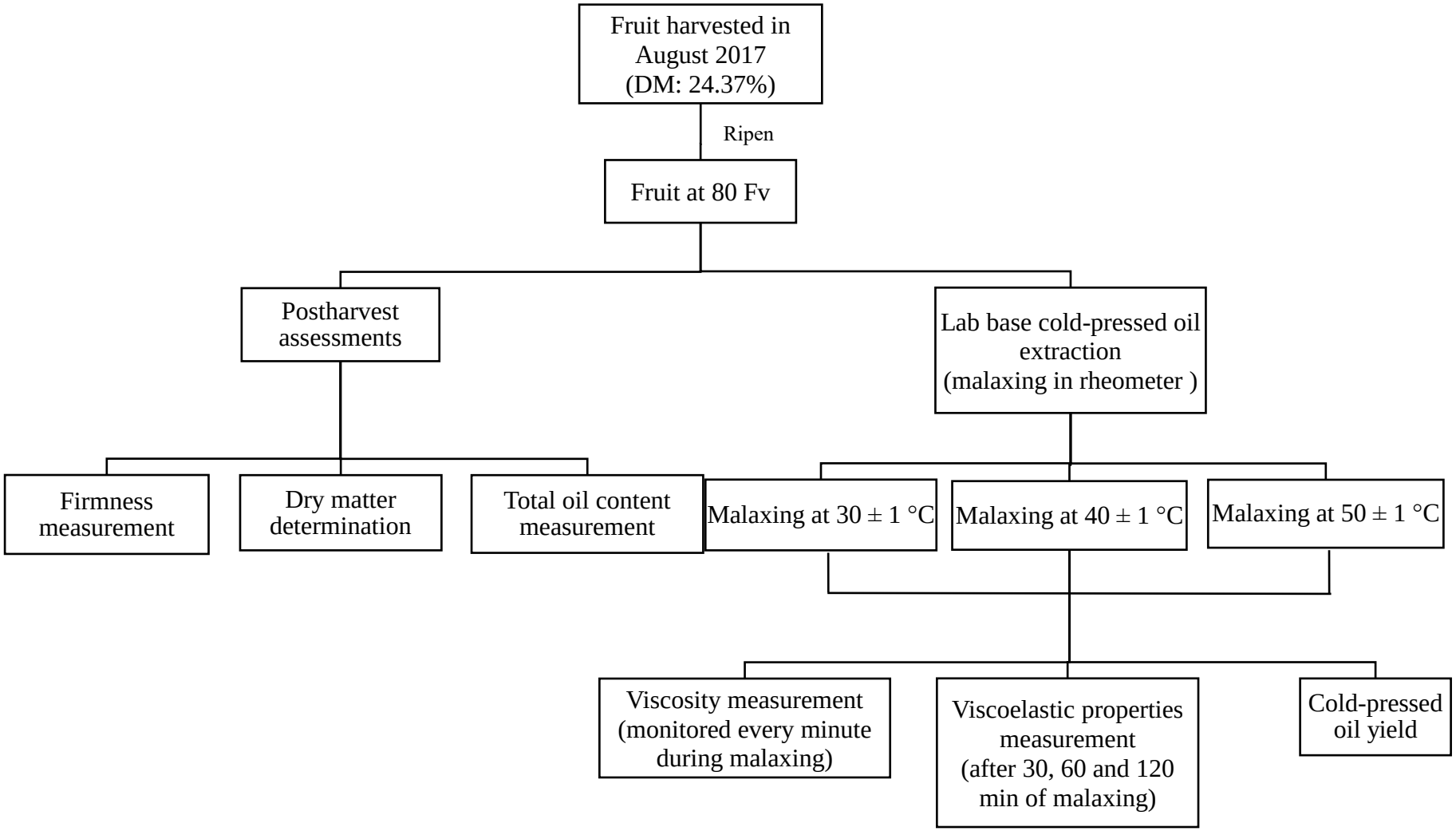

Figure 6.2: Flow diagram for the experimental design to investigate the effect of malaxing conditions on rheological properties and oil yield during malaxing on rheometer.

DM: Dry matter content (g dry flesh/100 g fresh flesh weight).

‘Hass’ avocado fruit were harvested from Plant and Food Research Ltd orchards in the Bay of Plenty, New Zealand, in August 2017 and ripened to the target fruit firmness at 80 Fv following the procedures described in Section 3.1.2. Postharvest assessments of avocado fruit, including dry matter determination, firmness measurement, and total oil content determination of fresh fruit were carried out on 20 avocado fruit following the methods described in Sections 3.2.1, 3.2.3 and 3.5.

The apparent viscosity and the viscoelastic properties of avocado pulp samples were monitored during malaxing using a rheometer (with a concentric cylinder geometry) at three different malaxing temperatures, 30 ± 1, 40 ± 1 and 50 ± 1 °C, respectively then the oil was recovered from fruit pulp sample by the laboratory-based centrifugation following the procedures described in Section 3.9.2.

Statistical analysis was carried out following the methods described in Section 3.12. Postharvest assessments of avocado fruit and the laboratory-based avocado oil extraction experiments were performed in triplicate. The apparent viscosity, viscoelastic properties and cold-pressed oil yield measurements for avocado pulp were carried out in triplicate.

6.2.3 Effect of ultrasound treatments on microstructural changes and oil yield during laboratory-based cold-pressed extraction

The objective of this experiment was to determine the effect of ultrasound treatments on microstructural changes and oil yield during laboratory-based cold-pressed extraction (Figure 6.3).

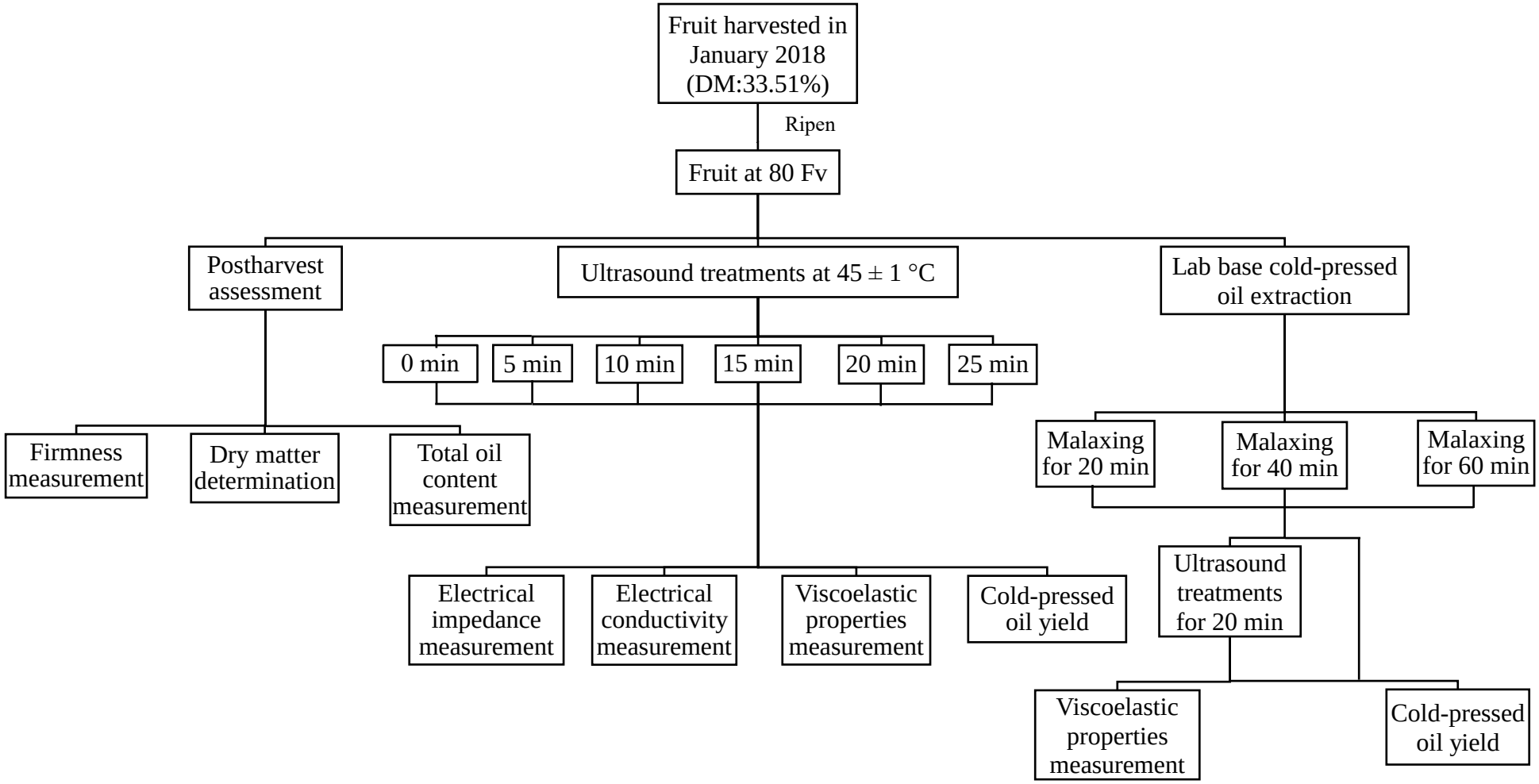

Figure 6.3: Flow diagram for the experimental design to investigate the effect of ultrasound treatments on microstructural changes and oil yield during laboratory-based cold-pressed extraction.

DM: Dry matter content (g dry flesh/100 g fresh flesh weight).

‘Hass’ avocado fruit were harvested from Plant and Food Research Ltd orchards in the Bay of Plenty, New Zealand, in January 2018 and ripened to the target fruit firmness at 80 Fv following the procedures as described in Section 3.1.2. Postharvest assessments of avocado fruit, including dry matter determination and firmness measurement, and total oil content measurement of fruit were carried out 20 avocado fruit following the methods as described in Section 3.2.1, 3.2.3 and 3.5.

The ground avocado pulp samples were sonicated (without malaxing) at 20–25 kHz for 5, 10, 15, 20 and 25 min, respectively, then the oil was recovered from fruit pulp sample by laboratory-based centrifugation following the methods as described in Section 3.4.1. EIS and electrical conductivity were used to examine avocado flesh structure after ultrasound treatment following the procedures as described in Section 3.6.2 and 3.7.2. The viscoelastic properties of fruit pulp samples were measured after ultrasound treatment following the procedures as described in Section 3.9.1.

For a second ultrasound trial, the ground avocado pulp samples were malaxed in the laboratory-based 1 L malaxer at 45 ± 1 °C for 20, 40 and 60 min, respectively prior to the ultrasound treatment at 20–25 kHz for 20 min, then the oil was recovered from fruit pulp sample by laboratory-based centrifugation. This method was following the procedures as described in Section 3.4.2. The viscoelastic properties of fruit pulp samples were measured before and after ultrasound treatment following the procedures as described in Section 3.9.1.

Statistical analysis was carried out following the methods as described in Section 3.12. Postharvest assessments of avocado fruit and the laboratory-based ultrasound trials were

performed in triplicate. Electrical impedance, conductivity, viscoelastic properties and cold-pressed oil yield measurements for avocado pulp were carried out in triplicate.

6.3 Results and discussion

6.3.1 Effect of malaxing temperature on cold-pressed avocado oil extraction

6.3.1.1 Laboratory cold-pressed oil yield and quality

For the laboratory-based cold-pressed oil extraction (carried out in both the 1L malaxer and 50mL malaxer for 120 min malaxing), the cold-pressed oil yield was found to increase significantly ($p < 0.05$) with increasing malaxing temperatures at 30, 40 and 50 °C (Table 6.1). The oil yield increased by 11–21% (g oil/100 g flesh fresh weight) between 30 and 50 °C malaxing temperatures. The increase in oil yield from 30 to 40 °C showed an 8 fold increase, while from 40 to 50 °C the absolute yield increase was only 2–4% (g oil/100 g flesh fresh weight) depending on the total oil content. In addition, at each stage of fruit maturity (early, mid and late season), the cold-pressed oil yield from 30 °C malaxing was much lower than that obtained from malaxing at 40 and 50 °C (Table 6.1). These results are in line with the findings of Di Giovacchino et al. (2002a) on olive oil extraction trials, which reported an increase in cold-pressed oil extraction efficiency from 76.5 to 82.5% (extraction yield/total oil content) can be obtained by increasing the malaxing temperature during extraction, although this was from 18 to 32 °C. The results also showed the difficulty of extracting oil from avocado compared to olive. It should be noted that 30 °C is above the maximum temperature considered ‘cold pressed’ in olive oil (Codex Alimentarius, 2017; International Olive Council, 2006). Woolf et al. (2009) suggested a temperature of 50 °C as the upper limit for avocado oil extraction. The increased yield with higher malaxing temperature is hypothesised to be partly due to the decreased viscosity of avocado pulp and consequently it makes it easier for the oil

droplets to coalescence together to form larger droplets and in turn making it easier to separate the liquid phases from the solid phases during the centrifugation step. This is examined and discussed in more detail in Section 6.3.1.4.

Table 6.1: 'Hass' avocado laboratory-based cold-pressed extraction oil yield at 30, 40 and 50 °C during malaxing, total oil present in flesh (determined by ASE solvent extraction) and fruit flesh dry matter (mean ± SE, n = 3) for fruit harvested at different maturity in the season; early-season (October 2016, August 2017), mid-season (December 2016) and late-season (March 2017)

Fruit harvest date	Dry matter content (g dry flesh/100 g fresh flesh)	Total oil content (g oil/100 g fresh flesh)	Cold-pressed oil yield from different malaxing temperature (g oil/100 g flesh fresh weight)		
			30 °C	40 °C	50 °C
October 2016 *	26.41 ± 0.23% ^{B}	15.99 ± 0.19% ^{e}	1.05 ± 0.07% ^{a}	11.59 ± 0.16% ^{c}	13.43 ± 0.29% ^{d}
December 2016 *	29.64 ± 0.17% ^{C}	19.56 ± 0.20% ^{fg}	1.56 ± 0.07% ^{a}	15.56 ± 0.53% ^{e}	18.02 ± 0.18% ^{f}
March 2017 *	34.38 ± 0.25% ^{D}	24.27 ± 0.21% ^{h}	2.32 ± 0.16% ^{a}	19.90 ± 0.68% ^{g}	23.59 ± 0.76% ^{h}
August 2017 **	24.37 ± 0.20% ^{A}	15.01 ± 0.15% ^{de}	1.01 ± 0.08% ^{a}	8.71 ± 0.12% ^{b}	11.65 ± 0.35% ^{c}

* Laboratory-based cold-pressed extractions were carried out on 1L malaxer for the fruit harvested in October 2016, December 2016 and March 2017.

** Laboratory-based cold-pressed extractions were carried out in a concentric cylinder geometry in a rheometer (50mL malaxer) for the fruit harvested in August 2017.

$^{A-D}$ Different upper case letters denote significantly different dry matter content values ($p < 0.05$).

$^{a-h}$ Different lower case letters denote significantly different total oil content and oil yield values for comparison between rows and columns ($p < 0.05$).

In terms of oil quality, the FFA% and PV were monitored for one harvest time in October 2016. The FFA% and PV did not vary significantly ($p > 0.05$) with malaxing temperature (Figure 6.4). This suggests that increasing malaxing temperature from 30 to 50 °C did not increase the rate of lipid hydrolysis and oxidation. However, these two basic oil quality measurements are not enough to define the overall quality of the oil. They do however provide an initial indication that the extraction process carried out did not lead to poor quality oils. Further research could be carried out to determine the effect of malaxing

temperature on the minor components such as pigments and tocopherols, oxidative stability, smoke point and sensory characteristics of the cold-pressed avocado oil.

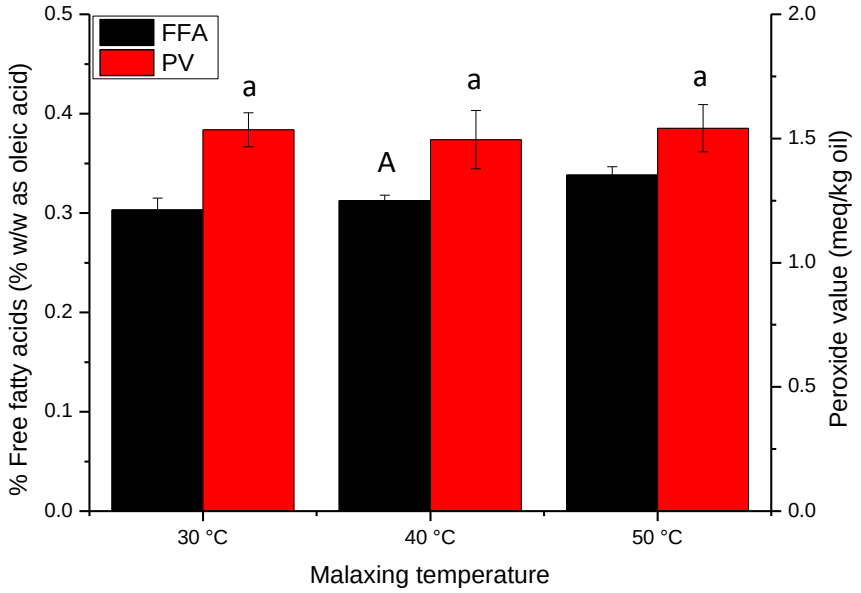

Figure 6.4: Percentage of free fatty acids (FFA%) and peroxide value (PV) for oil extracted from 'Hass' avocado fruit (harvested in October 2016) at 30, 40 and 50 °C malaxing temperature during laboratory-based cold-pressed oil extraction (mean ± SE, n = 3).

[A] Same upper case letters denote no significant difference between free fatty acid content ($p > 0.05$).

[a] Same lower case letters denote no significant difference between peroxide values ($p > 0.05$).

6.3.1.2 Electrical impedance spectroscopy and electrical conductivity

Measurement of EIS of the fruit pulp was used in this study to investigate the effect of malaxing temperatures on microstructural changes during cold-pressed oil extraction. Electrical conductivity measurements were also used to estimate the degree of cellular disruption, to support EIS results.

In fruit and vegetable processing, heating treatments can produce alterations to plant tissue microstructure due to thermal degradation of the middle lamella pectin and other cell wall polysaccharides, which can lead to loss of turgor pressure and purging of occluded air (Gonzalez & Barrett, 2010). For example in kiwifruit, thermal treatment at 100 °C for 5 min was found to lead to the breakdown of cell membranes (Llano, Haedo, Gerschenson, & Rojas, 2003). Fuentes et al. (2014) found potato samples processed at temperatures above 60 °C (heating for 30 min) resulted in ruptured cell walls and membranes which changed the EIS and electrical conductivity of samples, while no significant changes in tissue microstructure and cell wall degradation were found in samples processed below 60 °C.

Significantly, there was no difference ($p > 0.05$) between the electrical resistances (at 50 Hz, 10 kHz and 1 MHz) measured at each stage of malaxing (0, 60 and 120 min) for different malaxing temperatures (Figure 6.5). Figure 6.6 shows the electrical conductivity of avocado fruit pulp tissue did not change significantly ($p > 0.05$) with an increasing malaxing temperature from 30 to 50 °C, for 0, 60 and 120 min malaxing time. These results are in agreement with the EIS results which suggest that over the temperature range between 30 to 50 °C these malaxing temperatures did not influence the breakdown of the cellular structure during cold-pressed avocado oil extraction. This provides additional evidence that EIS is a useful tool to measure cell breakdown, but not the agglomeration of oil vesicles during malaxing. Fuentes et al. (2014) reported that heat treatment below 60 °C did not lead to thermal degradation or loss of turgor pressure in the cells.

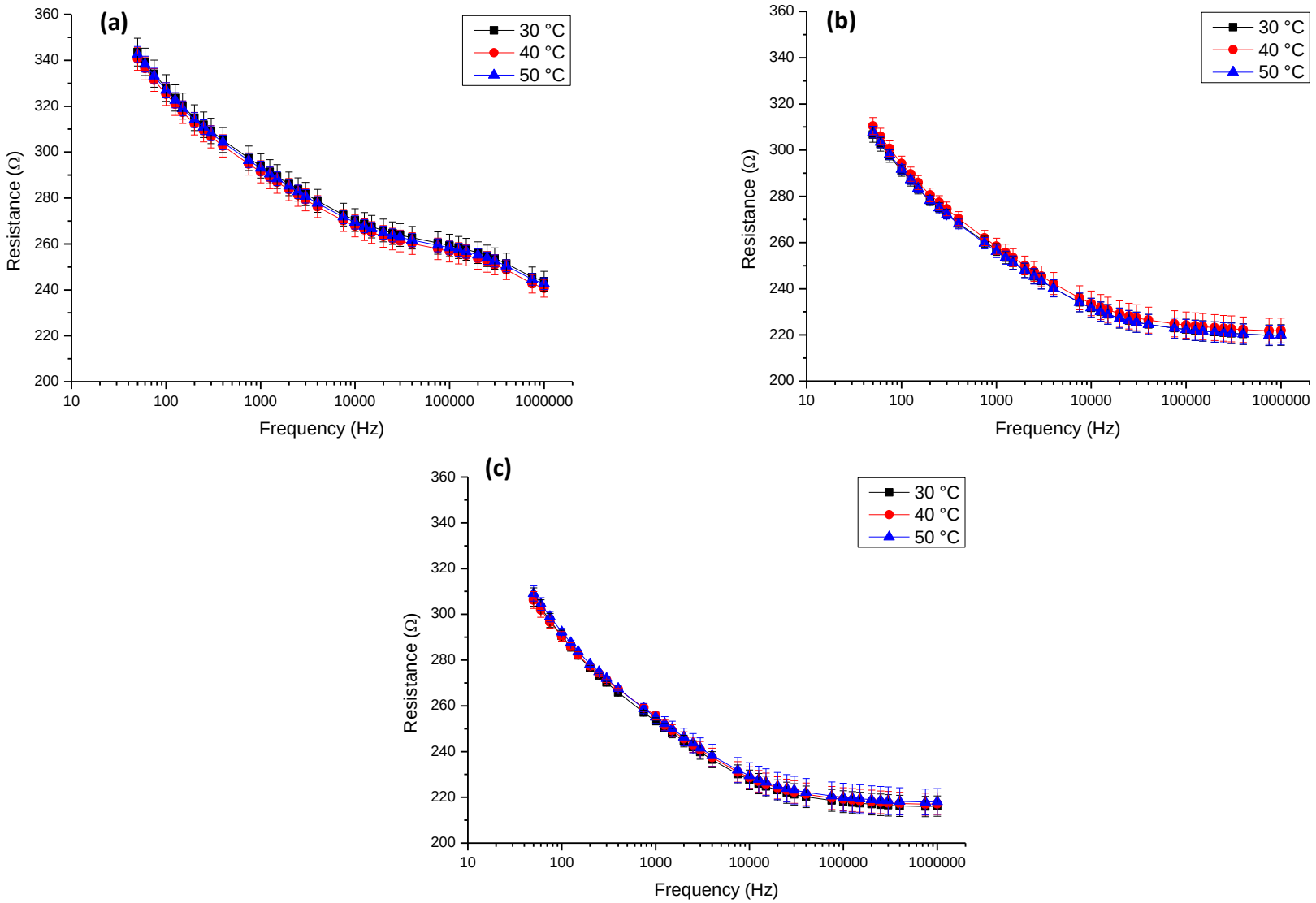

Figure 6.5: Resistance (Ω) of 'Hass' avocado pulp tissue at various stage during malaxing at three different temperatures (30, 40 and 50 °C), (a) At 0 min malaxing (after grinding); (b) At 60 min malaxing; (c) At 120 min malaxing' (mean ± SE, n = 3).

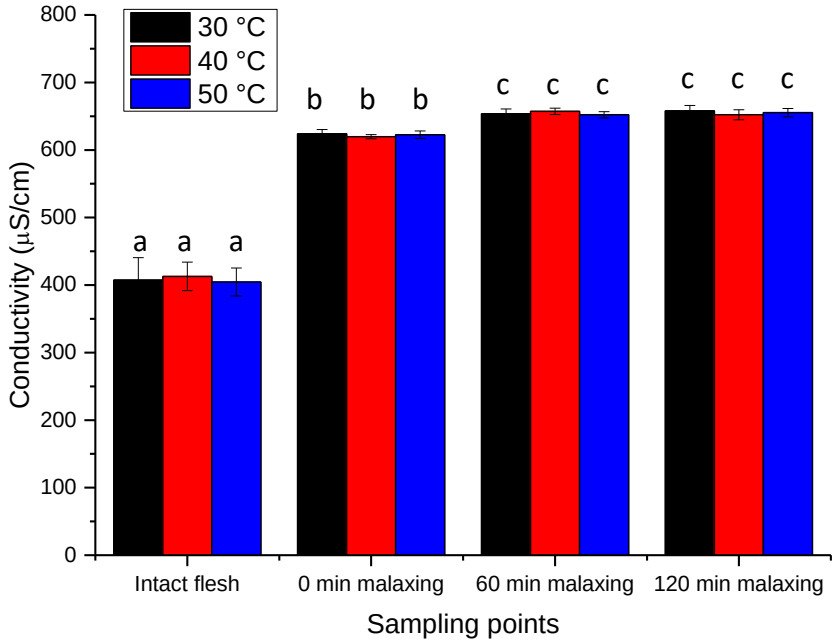

Figure 6.6: Electrical conductivity (µS/cm) of 'Hass' avocado pulp tissue at the various stages during malaxing at three different temperatures (30, 40 and 50 °C) (mean ± SE, n = 3).

[a,b,c] Different letters denote significantly different conductivity values ($p < 0.05$).

The EIS and the electrical conductivity results also suggest the increase in cold-pressed oil yield with increasing malaxing temperature (Table 6.1) was not due to increased cellular disruption that released more oil droplets.

6.3.1.3 Light microscopy

The microstructural changes in avocado pulp tissue during malaxing at different temperatures was also examined with light microscopy. In the stained images, the oil droplets from the parenchyma cells have a grey colour and the cell walls of idioblasts stained a blue colour. The light microscopy images of the avocado pulp at 0 min malaxing (after grinding) is shown in Figure 6.7. The change in the microstructure of the pulp tissue after 60 and 120 min of malaxing at different malaxing temperatures is shown in Figure

6.8.

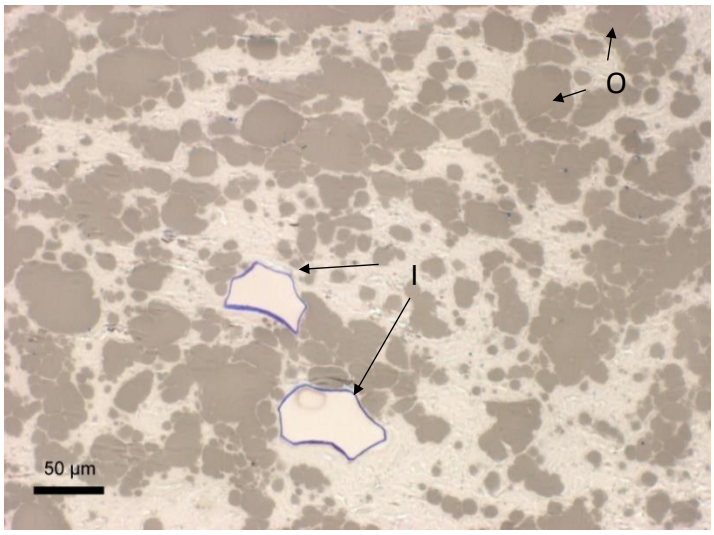

Figure 6.7: Light microscopy images of the microstructure of 'Hass' avocado pulp tissue at 0 min malaxing (after grinding).
O: Oil droplet from parenchyma cells; **I**: Idioblast cell.

After grinding, the free oil droplets from parenchyma cells were scattered in the picture with an average diameter ≅ 15 µm (Figure 6.7). After 60 min malaxing at 30 °C (Figure 6.8a), the size of the oil droplets increased to ≅ 25 µm average diameter, but the oil droplets remained at this size after 120 min of malaxing (Figure 6.8b). During malaxing at 40 °C (Figure 6.8c–6.8d) and 50 °C (Figure 6.8e–6.8f), the average diameter of oil droplets all increased with increasing malaxing time after 60 min (40 °C: ≅ 40 µm; 50 °C: ≅ 70 µm) and 120 min (40 °C: ≅ 65 µm; 50 °C: ≅ 100 µm) of malaxing. These observations are similar to previous studies by Di Giovacchino (1989) and Di Giovacchino (1996) on olive oil extraction and the previous findings in commercial scale cold-pressed avocado oil extraction (in Chapter 4) that the oil droplets aggregate more easily into larger droplets by malaxing to form a continuous oil phase. The increase in malaxing temperature reduces the viscosity of the pulp leading to increased frequency of droplet collisions and more oil aggregation (Jirgensons & Straumanis, 2013).

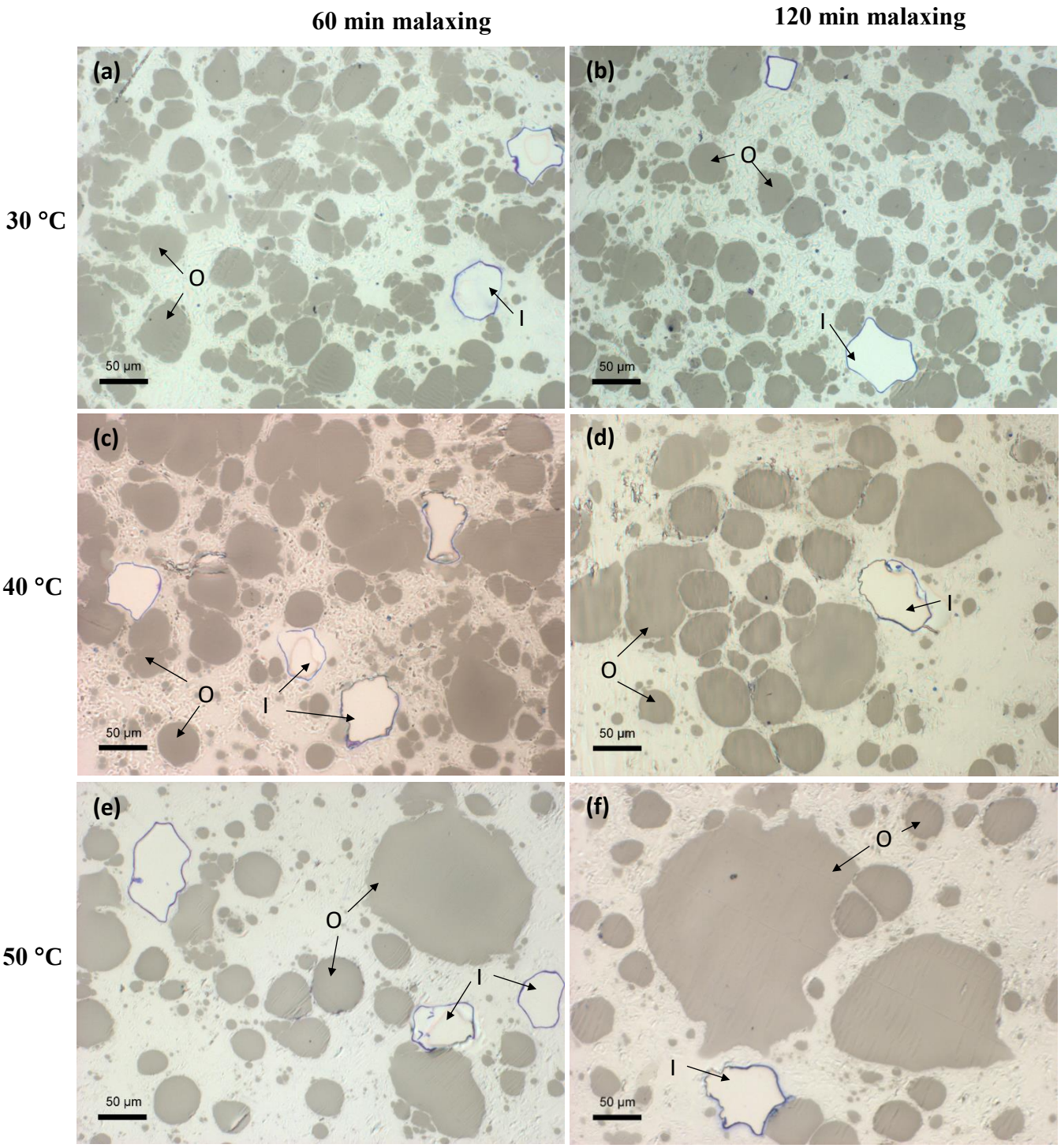

Figure 6.8: Light microscopy images of the microstructure of 'Hass' avocado pulp tissue at three different temperatures (a) 30 °C, 60 min malaxing, (b) 30 °C, 120 min malaxing, (c) 40 °C, 60 min malaxing, (d) 40 °C, 120 min malaxing, (e) 50 °C, 60 min malaxing, (f) 50 °C, 120 min malaxing.

O: Oil droplet from parenchyma cells; **I**: Idioblast cell.

It has been reported that the oil droplets for continuous-process separation (centrifugation, or 'decanting') during olive oil extraction must have a diameter of more than 30 μm to achieve a good oil yield (Di Giovacchino, 1989, 1996). At 30 °C, over 80% of oil droplets still had a diameter less than 30 μm after 120 min malaxing, making the oil difficult to recover by centrifugation and resulting in a much lower cold-pressed oil yield than when the pulp was malaxed at 40 °C and 50 °C (Table 6.1).

6.3.1.4 Apparent viscosity of the avocado pulp during laboratory-based (1L malaxer) cold-pressed extraction

Rheological property measurements are relevant in the food industry as an analytical tool for physical characterization of raw material prior to manufacturing, for intermediate products during processing and for finished food products (Tabilo-Munizaga & Barbosa-Cánovas, 2005).

Viscosity is an important rheological property, which is used to characterize flow behaviour of foods (Tabilo-Munizaga & Barbosa-Cánovas, 2005). The effect of malaxing time and temperature on the viscosity of the avocado pulp were investigated in this study. In Figure 6.9, the apparent viscosity (at a constant shear rate of 40 s^{-1}) of the avocado pulp during laboratory-based (1L malaxer) cold-pressed extraction at 30, 40 and 50 °C is presented. Samples were collected after 60 min and 120 min of malaxing. At 30 °C, there was no significant difference ($p > 0.05$) in the apparent viscosity when the malaxing time increased from 60 to 120 min. During malaxing at both 40 and 50 °C, the apparent viscosity of the avocado pulp decreased significantly ($p < 0.05$) with increasing malaxing time at each temperature and with increasing malaxing temperature at each malaxing time.

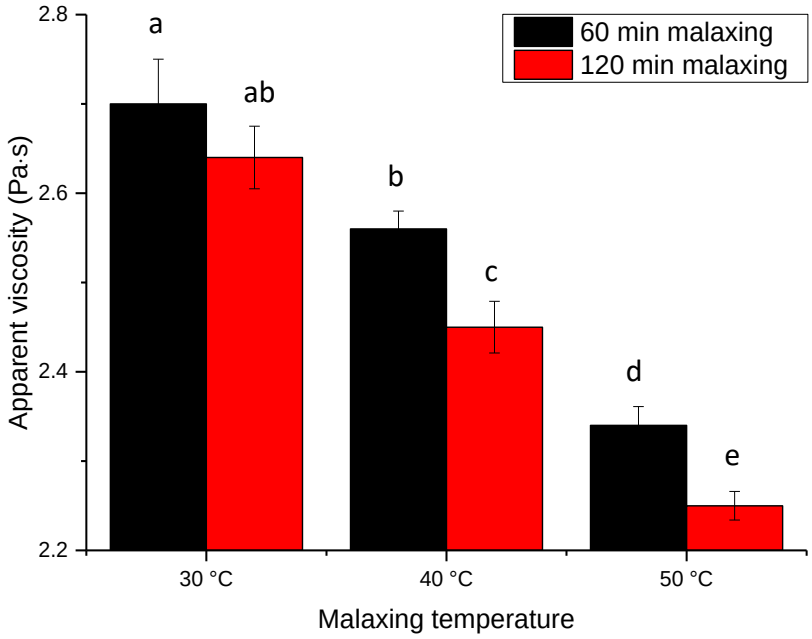

Figure 6.9: Change of apparent viscosity at a shear rate of 40 s^{-1} for 'Hass' avocado pulp during laboratory-based cold-pressed oil extraction at 30, 40 and 50 °C (mean ± SE, n = 3).

[a-e] Different letters denote significantly different apparent viscosity values ($p < 0.05$).

6.3.1.5 Apparent viscosity of the avocado pulp during malaxing in rheometer

The change in the apparent viscosity of the avocado pulp during malaxing in the concentric cylinder geometry in the rheometer (50mL malaxer) at 30, 40 and 50 °C is presented in Figure 6.10. The advantage of malaxing the avocado pulp in the rheometer was that the viscosity of the pulp could be monitored every minute while it was being malaxed, which may provide more information on what is happening during malaxing. The malaxer in the commercial avocado oil production mixed the avocado pulp with a stirrer speed of 20 rpm. To try to simulate this mixing in the Discovery HR-3 hybrid rheometer using a SPC geometry cup, the rheometer was set to a constant shear rate of 0.33 s^{-1}. During malaxing in the commercial malaxers, the shear rate experienced by the pulp would have varied with time as the pulp changed in viscosity. At each malaxing

temperature, the apparent viscosity of the avocado pulp decreased with increasing malaxing time. At 30 °C, the apparent viscosity decreased rapidly in the first 30 min of malaxing and decreased steadily for the next 60 min until it reached a constant apparent viscosity at 90 min. At 50 °C, the apparent viscosity of avocado pulp decreased rapidly between 0 to 90 min of malaxing, then it about remained constant from 90 min.

Malaxing temperature significantly affected the apparent viscosity of avocado pulp, the higher malaxing temperature resulted in a lower ($p < 0.05$) apparent viscosity value with a faster ($p < 0.05$) rate of apparent viscosity decrease. The apparent viscosity of avocado pulp decreased from ≅ 26.0 Pa·s to ≅ 17.0 Pa·s, 14.5 Pa·s and 11.5 Pa·s after 120 min malaxing at 30, 40 and 50 °C, respectively.

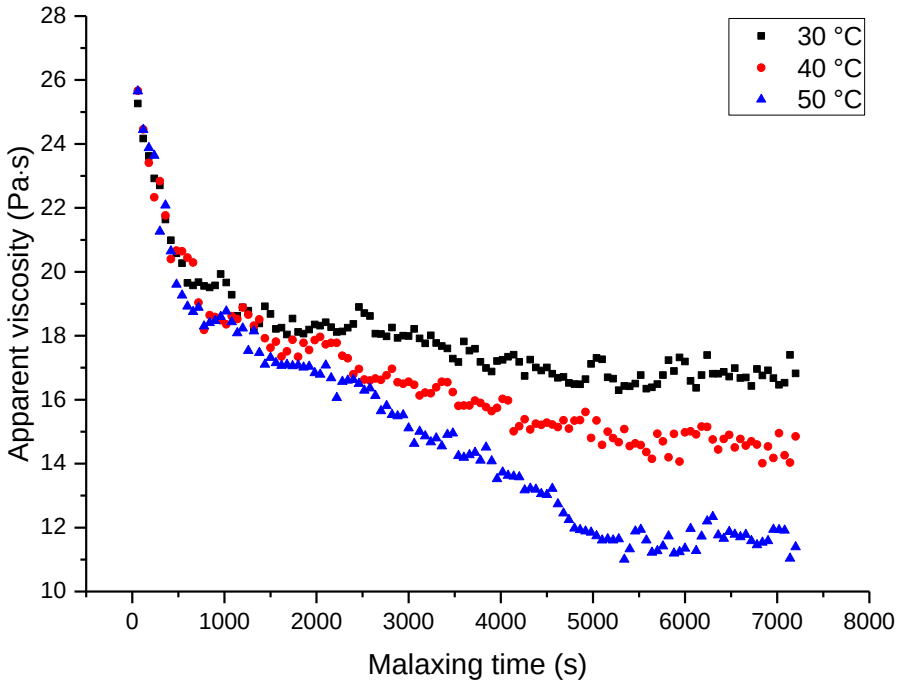

Figure 6.10: Changes of the apparent viscosity (Pa·s) of 'Hass' avocado pulp during malaxing at 20 rpm for 120 min in a rheometer with concentric cylinder geometry at different malaxing temperatures (mean, n = 3).

In liquid or semi-liquid food samples, the increase in oil droplet size is related to a decrease in oil droplet number if all other system variables are kept constant (Hill & Carrington, 2006). Larger oil droplets result in a decrease in the number of droplet-droplet interactions and therefore a decrease in resistance to flow (Hill & Carrington, 2006). Hence, the reduction of the apparent viscosity of avocado pulp tissue with an increasing malaxing time and temperature is likely to be due to the increased oil droplet aggregation. Oil aggregation decreased the number of oil droplets in the pulp thus the number of interactions between oil droplets decreased as well, leading to an overall decrease in apparent viscosity. These results are similar to the findings of Tamborrino, Catalano, and Leone (2014) and Tamborrino et al. (2017) on olive oil extraction, when the apparent viscosity of the olive paste decreased when malaxing time increased during oil extraction. Moreover, these results agree with the previous study from Pal (1996) on the rheological behaviour of oil-in-water emulsions, which indicated the size of oil droplet had a dramatic effect on viscosity of samples. The emulsions which contained larger oil droplets had lower viscosities.

6.3.1.6 Viscoelastic properties of the avocado pulp during malaxing in rheometer

The viscoelastic properties including the elastic and viscous behaviours of the food material can be used to evaluate materials with semi-solid characteristics. In food materials, the storage modulus (*G'*) is a measure of the degree of elastic behaviour; the loss modulus (*G"*) is an indicator of the degree of viscous behaviour (Miri, 2011; Tabilo-Munizaga & Barbosa-Cánovas, 2005). The viscoelastic properties of food materials can be determined from oscillatory testing, when the material is subjected to harmonically varying (usually sinusoidal) small amplitude deformations in a simple shear field (Rao, 2010).

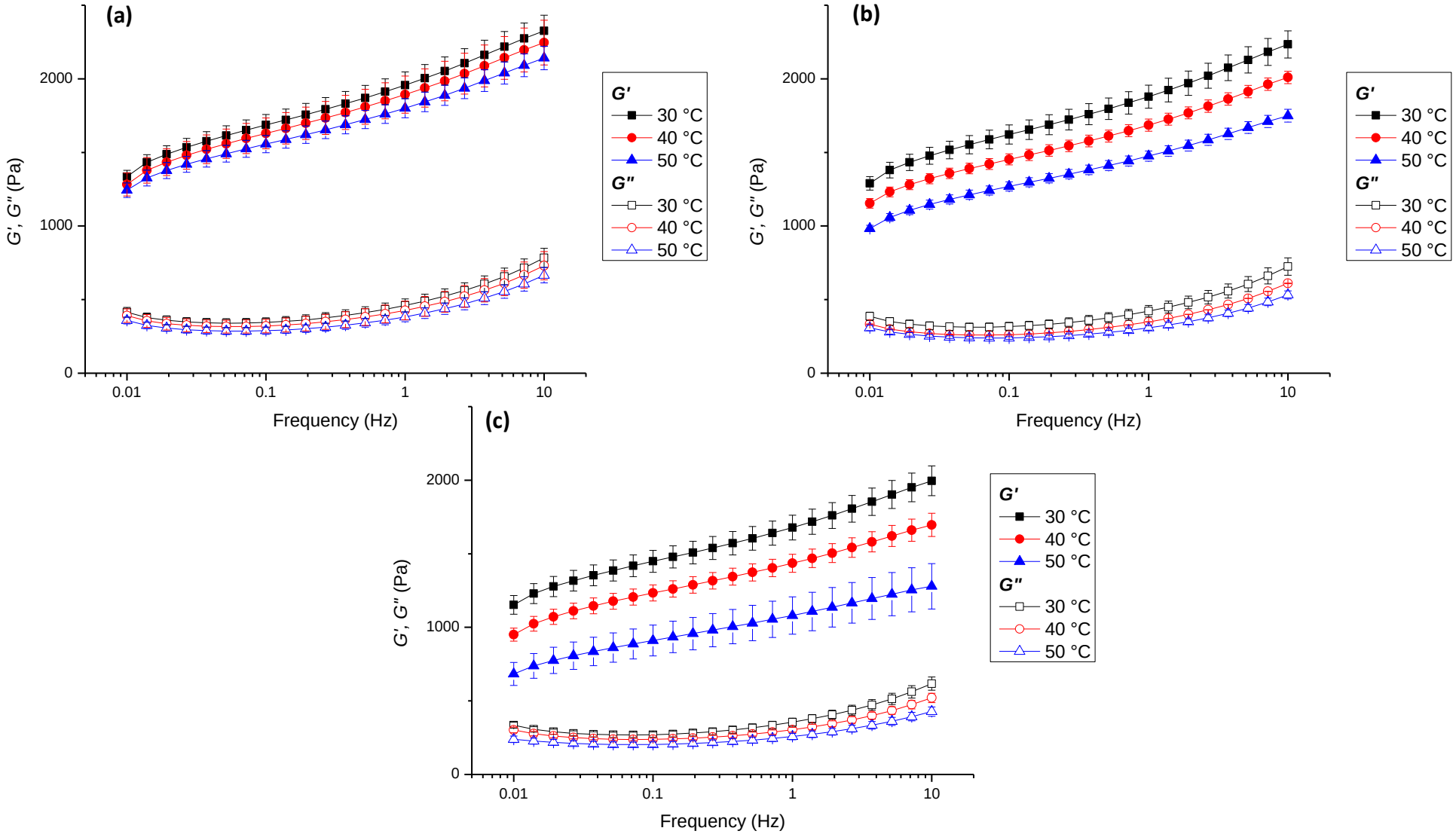

Figure 6.11: Changes of the *G', G"* (Pa) of 'Hass' avocado pulp over a range of frequencies from 0.01 to 10 Hz and at a constant strain of 0.5% after malaxing in rheometer for (a) 30 min; (b) 60 min and (c) 120 min at 30, 40 and 50 °C (mean ± SE, n = 3).

The *G'* and *G"* of avocado pulp collected after 30, 60 and 120 min of malaxing in rheometer (50mL malaxer) at 30, 40 and 50 °C are shown in Figure 6.11. The frequency dependency of the storage modulus, *G'*, and the loss modulus, *G"* were not different for the avocado pulp samples regardless of the malaxing time and temperature. Both *G'* and *G"* increased with frequency for all the avocado pulp samples. Also, Figure 6.11 indicates the predominance of a solid-like behaviour for the avocado pulp as the *G'* was greater than *G"* (Lapasin & Pricl, 1995). Similar rheological behaviours (solid-like behaviour) were also found in the other fruit and vegetable pulp samples including strawberry, blueberry, tomato and potato puree (Ahmed & Ramaswamy, 2006; Bayod, Willers, & Tornberg, 2008; Gao, Yu, Zhang, Xu, & Fu, 2011).

The *G'* values (at 0.01, 0.5 and 10 Hz) of avocado pulp decreased ($p < 0.05$) with an increasing malaxing time from 30 to 120 min (Figure 6.11) at each malaxing temperature (30, 40 and 50 °C). Similarly, Martínez-Padilla et al. (2017) reported that the *G'* of avocado pulp was lower than the initial value after malaxing for 60 min at 45 °C. In addition, the results showed that malaxing at the higher temperature resulted in the lower ($p < 0.05$) *G'* values (at 0.01, 0.5 and 10 Hz) at each sampling point (30, 60 and 120 min) during malaxing. The decreasing *G'* values with increasing malaxing time and temperature may be explained by the increase in the liquid-like behaviour of the avocado pulp corresponding to oil droplets in the avocado pulp coalescing. The *G'* value is a measure of the storage of elastic energy through particle-particle interaction (Larson, 1999). A decrease in *G'* reflects a decrease in particle-particle interaction, which may be due to the increase in oil droplet size in the avocado pulp sample leading to a decrease in the number of "contact" points between the oil droplets (Larson, 1999; Tadros, 2017). These results agree with the findings from Pal (1996) who indicated the larger size of the

droplets gave lower *G'* values for both of the water-in-oil and oil-in-water emulsion. These results also agree with the observations with light microscopy in Section 6.3.4.

6.3.2 Effect of ultrasound treatment on cold-pressed avocado oil extraction

6.3.2.1 Laboratory cold-pressed oil yield during ultrasound treatment

To determine the effect of ultrasound treatments on microstructural changes and oil yield during laboratory-based cold-pressed extraction, avocado fruit were harvested from Plant and Food Research Ltd orchards in the Bay of Plenty, New Zealand, in January 2018. The average dry matter content of fruit flesh was 33.51 ± 0.12% (g dry flesh/100 g fresh flesh) and the total oil content of fruit flesh was 24.08 ± 0.30% (g oil/100 g fresh flesh).

For samples not treated with ultrasound (0 min; control), the extraction yield of these samples at 45 °C was 0.72 ± 0.04% (g oil/100 g fresh flesh). This low yield compared to earlier results (Table 6.1) was due to the less malaxing time, even though the fruit were all at the same firmness/ripeness. When the avocado oil was extracted by ultrasound treatments for 5–25 min at 45 °C (then centrifugation) without malaxing, ultrasound treatment at 20–25 kHz significantly increased ($p < 0.05$) the oil extraction yield between 0 and 20 min of ultrasound treatment at 45 °C, which produced an oil yield of 9.97 ± 0.17% (g oil/100 g fresh flesh) (Figure 6.12). The oil extraction yield did not increase further when the samples were treated with 25 min ultrasound (Figure 6.12). These results agree with a previous study by Juliano et al. (2013a) on laboratory scale trials looking at the effect of ultrasound treatment on cold-pressed olive oil extraction. Juliano et al. (2013a) found the ultrasound treatment for 10 min at 35 kHz significantly increased the olive oil extraction yield from 1.0% to 5.4% (g oil/100 g fresh flesh) without the malaxing step. In comparison to the laboratory-based cold-pressed oil extraction for late season avocado

with the similar total oil content at 24.27 ± 0.21 (g of oil/100 g of fresh flesh), the ultrasound treatment at 20–25 kHz gave a significantly higher ($p < 0.05$) oil yield than that from 120 min malaxing at 30 °C (2.32 ± 0.16%, g oil/100 g fresh flesh), but a significant lower ($p < 0.05$) oil yield than that from 120 min malaxing at 40 °C (19.90 ± 0.68%, g oil/100 g fresh flesh) and 50 °C (23.59 ± 0.76%, g oil/100 g fresh flesh).

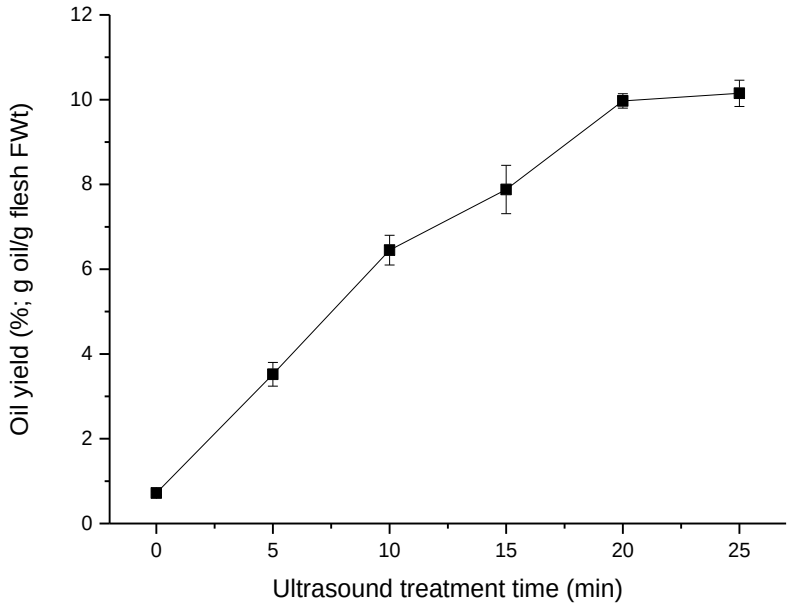

Figure 6.12: 'Hass' avocado extraction oil yield after ultrasound treatment at 20–25 kHz for 0 to 25 min at 45 °C, without a malaxing step (mean ± SE, n = 3).

6.3.2.2 Change in electrical impedance and conductivity during ultrasound treatment

Ultrasound treatment has been introduced as a novel technology in fruit and vegetable processing to disrupt the cell walls and membranes, by which vapour bubbles very rapidly form, grow and undergo implosive collapse near the cells, known as 'cavitation' (Luque Garcìa & Luque de Castro, 2003; Mercer & Armenta, 2011). In the previous study, Fava, Alzamora, and Castro (2006) found ultrasound treatment on blueberry flesh samples at 20 kHz for 5 min resulted in cell wall shrinkage and rupture. However, in other fruits such as melon and pineapple, ultrasound treatments at 25 kHz for 10–30 min did not induce

breakdown of the cells in fruit flesh tissue (Fernandes, Gallão, & Rodrigues, 2008, 2009).

There was no significant difference ($p > 0.05$) between the electrical resistances (at 50 Hz, 10 kHz and 1 MHz) of avocado pulp samples after ultrasound treatment at 20–25 kHz for 0, 5, 10, 15, 20 and 25 min (Figure 6.13). The ultrasound treatments at 20–25 kHz for 0–25 min did not significantly ($p > 0.05$) affect the electrical conductivity of avocado fruit pulp tissue (Figure 6.14), which was in agreement with the EIS results. These results indicated that the ultrasound treatments did not assist in cellular disruption in the ground avocado pulp. Compared to the study by Fernandes et al. (2008) and Fernandes et al. (2009), who found ultrasound treatment at 20–25 kHz on melons and pineapples resulted in cellular disruptions in fruit tissue, this may be due to the different fruit tissue microstructure and the composition and structure of the polysaccharides in the cell walls.

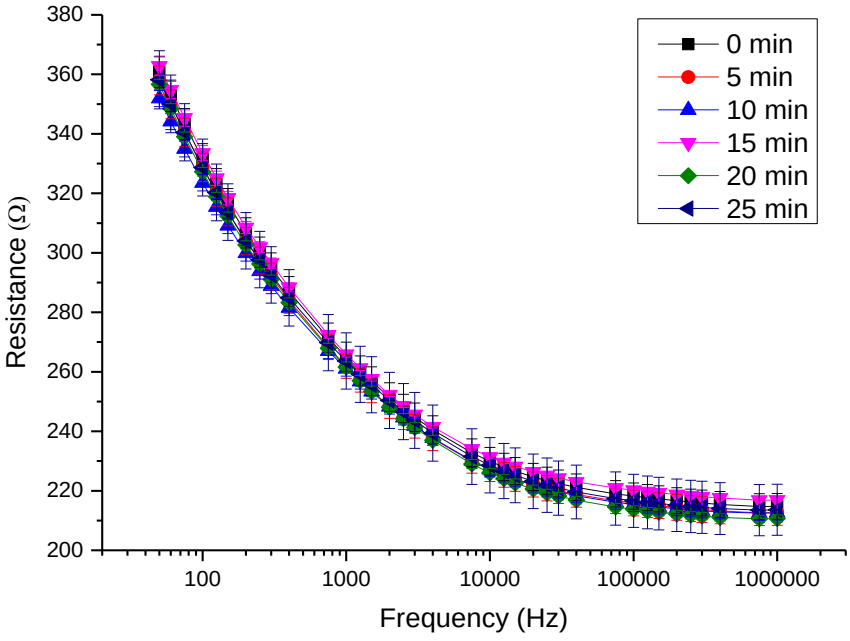

Figure 6.13: Resistance (Ω) of 'Hass' avocado pulp before and after ultrasound treatment at 20–25 kHz for 5 to 25 min without malaxing step (mean ± SE, n = 3).

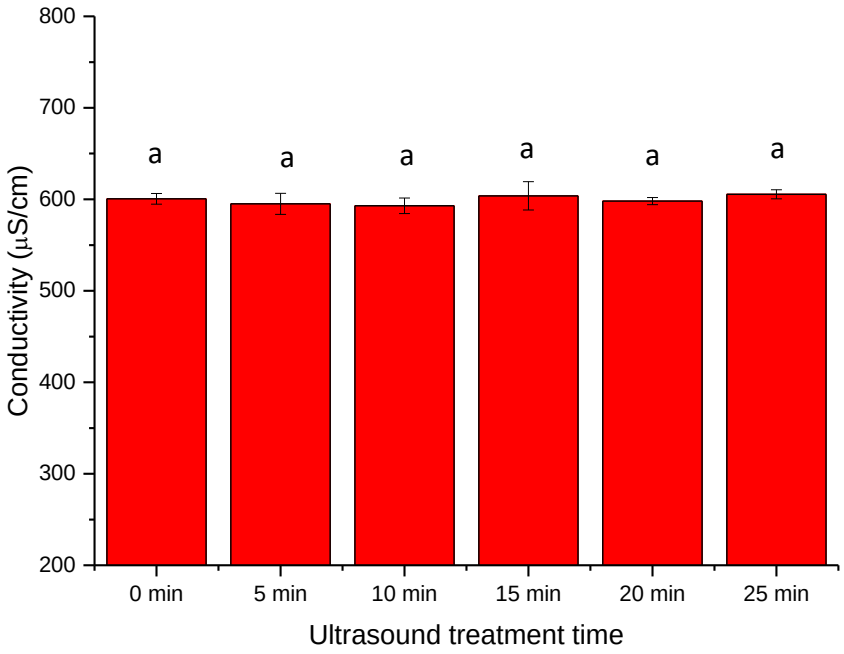

Figure 6.14: Electrical conductivity (µS/cm) of 'Hass' avocado pulp tissue before and after ultrasound treatment at 20–25 kHz for 5 to 25 min without malaxing step (mean ± SE, n = 3).

[a] Same letters denotes no significant difference between conductivity values ($p > 0.05$).

6.3.2.3 Change in rheological properties during ultrasound treatment

Figure 6.15 shows the effects of ultrasound treatment (without malaxing) on the viscoelastic properties of avocado pulp. The results showed decreasing *G'* values ($p < 0.05$) at 0.01, 0.5 and 10 Hz with an increasing ultrasound treatment time from 5–20 min, with no further change in *G'* observed at 20 min ultrasound treatment. These results are correlated with the oil extraction yields in Figure 6.12, in that the yields significantly increased with ultrasound treatment for 5–20 min at 20–25 kHz, and did not increase further with 25 min of ultrasound treatment. The decreased *G'* values are related to the oil globules coalescing in the avocado pulp. The ultrasonic waves alter the interaction between oil globules through acoustic pressure; other studies have shown oil droplets move towards each other to allow aggregation, forming larger oil droplets (Juliano et al.,

2011; Vilkhu et al., 2011). Larger oil droplets resulted in a decrease in the number of particle-particle interactions in avocado pulp, which gave lower *G'* values and improved the extraction oil yield.

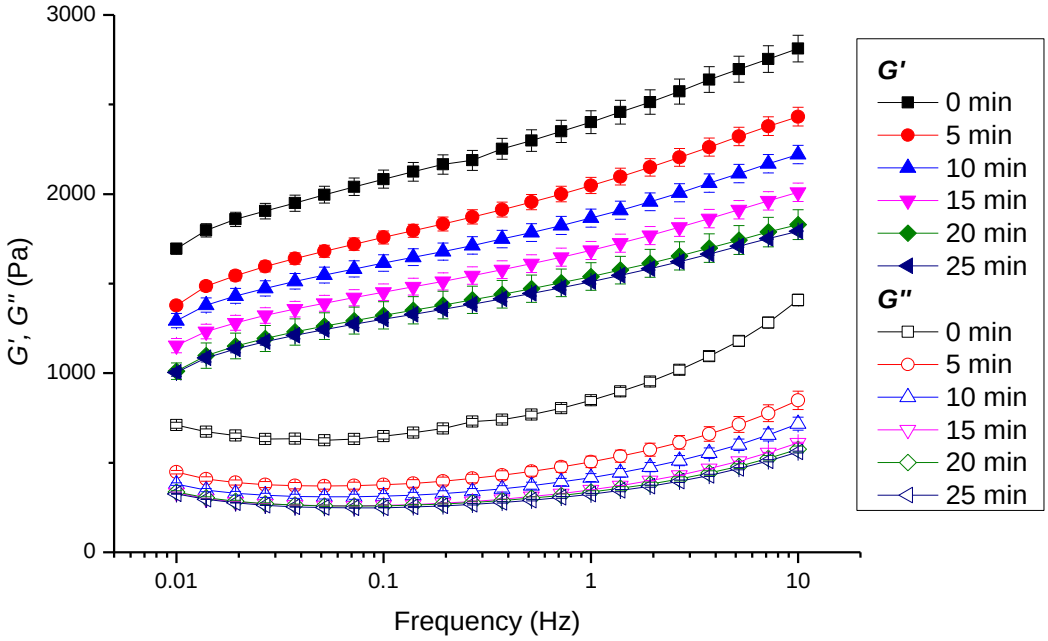

Figure 6.15: Changes of the *G'*, *G''* (Pa) of 'Hass' avocado pulp after ultrasound treatment at 20–25 kHz for 5 to 25 min without malaxing step (mean ± SE, n = 3).

6.3.2.4 Laboratory cold-pressed oil yield during malaxing with ultrasound treatment

Figure 6.16 shows the effect of ultrasound treatments on oil extraction yield with and without ultrasound treatment applied to the malaxed avocado pulp samples. The results show that increasing malaxing time with no ultrasound treatment increased the cold-pressed oil yield due to the aggregation of oil droplets to form a continuous oil phase, which made it easier to recover the oil by the centrifugation step. After 20 and 40 min of malaxing, the addition of 20 min ultrasound treatment at 20–25 kHz on avocado pulp samples significantly increased ($p < 0.05$) the oil extraction yield by 6.83 ± 0.63% and 2.07 ± 0.17%, respectively. However, the ultrasound treatment did not significantly change ($p > 0.05$) the oil extraction yield after the avocado pulp had been malaxed for 60

min when compared to samples which had not been treated with ultrasound. Also, 20 min malaxing followed by 20 min ultrasound treatment of avocado pulp samples gave a significantly lower ($p < 0.05$) oil extraction yield than that of 40 min malaxing only samples. There was no significant difference ($p > 0.05$) between the oil extraction yield from 40 min malaxing samples followed by 20 min ultrasound treatment and 60 min malaxing only samples.

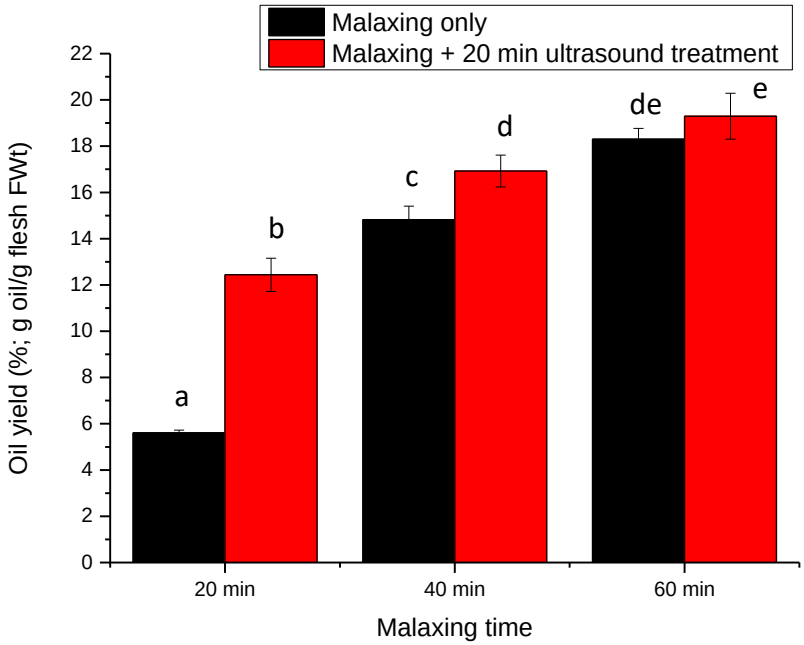

Figure 6.16: 'Hass' avocado extraction oil yield effect without and with (20–25 kHz) ultrasound treatment (20 min) at various malaxing times for 20, 40 and 60 min (mean ± SE, n = 3).

[a-e] Different letters denote significantly different oil yield values ($p < 0.05$).

The results in Figure 6.12 and 6.16 for oil yield show that ultrasound treatment at 20–25 kHz for 20 min alone cannot achieve the desired oil yields but could help to reduce the malaxing time if it can be applied at the same time as malaxing. Further research could be carried out to determine the effect of ultrasound treatment on cold-pressed oil yield when it is applied simultaneously with malaxing.

6.3.2.5 Change in rheological properties during malaxing with ultrasound treatment

The impact of ultrasound treatment on viscoelastic properties of avocado pulp when the malaxed fruit pulp samples were treated is shown in Figure 6.17. Firstly, the *G'* values (at 0.01, 0.5 and 1 Hz) of avocado pulp decreased ($p < 0.05$) with an increasing malaxing time from 20, 40 to 60 min, which are similar to the findings in Figure 6.11.

After the avocado pulp was malaxed for 20 and 40 min at 45 °C, the addition of 20 min ultrasound treatment to the samples significantly decreased ($p < 0.05$) the *G'* values (at 0.01, 0.5 and 1 Hz) for avocado pulp, which indicated that the oil droplets aggregated in the pulp. When the pulp was malaxed for 60 min and then subjected to ultrasound treatment, the *G'* values (at 0.01, 0.5 and 1 Hz) for avocado pulp did not change significantly ($p > 0.05$) after the ultrasound treatment. These results agree with the cold-pressed oil yield results in Figure 6.16. After 20 and 40 min of malaxing, the addition of 20 min ultrasound treatment at 20–25 kHz on avocado pulp samples helped the oil droplets to aggregate, hence lowering the *G'* values.

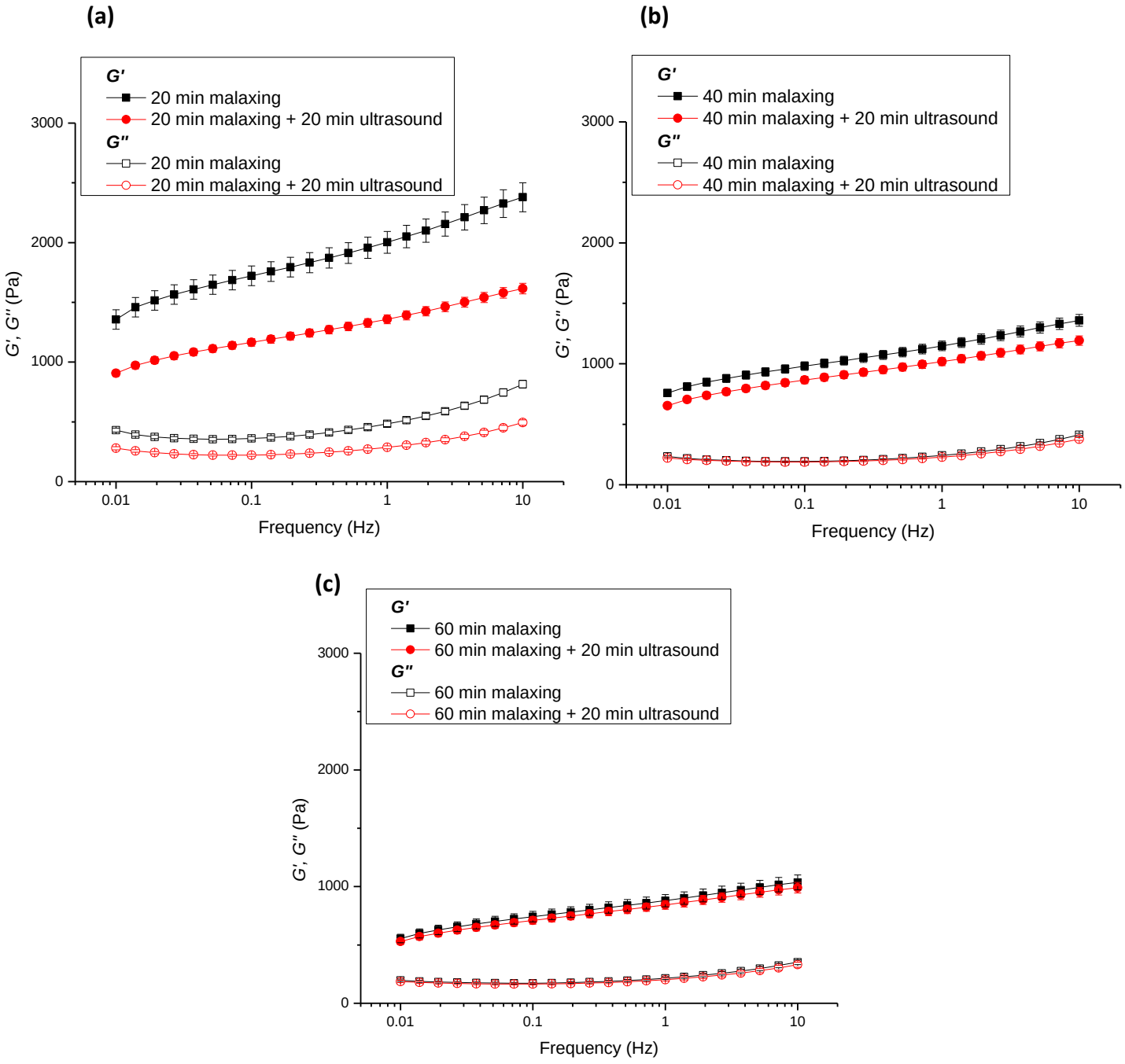

Figure 6.17: Changes of the *G'*, *G''* (Pa) of 'Hass' avocado pulp after malaxing for a) 20 min; b) 40 min and c) 60 min at 45 °C, with and without 20 min ultrasound treatment at 20–25 kHz (mean ± SE, n = 3).

6.4 Conclusions

It can be concluded that the malaxing conditions, including time and temperature, are key variables in the oil aggregation process during the cold-pressed avocado oil extraction. Increasing the malaxing time assisted with oil aggregation and higher malaxing temperatures also led to oil droplets aggregating more easily, which resulted in a higher cold-pressed oil yield. The information about the oil aggregation in the avocado pulp can be obtained by measuring the rheological properties of fruit pulp tissues. Raising the malaxing time and temperature decreased the viscosity and reduced the solid-like behaviour of the avocado pulp. This is because of the increased malaxing time and increased temperature, which promotes aggregation of oil droplets thus decreasing the number of interactions between oil droplets.

Ultrasound treatment at 20–25 kHz resulted in a reduction in the solid-like behaviour of the avocado pulp and therefore this had a positive effect on avocado oil extraction yield if the samples had been pre-malaxed or not. However, the higher malaxing temperature and ultrasound treatments at 20–25 kHz did not appear to assist in cellular disruption during cold-pressed avocado oil extraction.

The FFA% and PV of the cold-pressed avocado oil did not increase significantly with malaxing temperature between 30 to 50 °C.

Chapter 7:

Cellular changes in ‘J5’ olive mesocarp during commercial cold-pressed oil extraction

7.1 Introduction

Since the process for commercial cold-pressed extraction of avocado oil has been developed based on that for virgin olive oil extraction, the cellular changes in 'J5' olive mesocarp were studied in this project to compare with the results obtained on 'Hass' avocado cold-pressed oil extraction. In addition, we have used techniques that have not generally been used to study olive oil extraction, and this provides an additional comparison of both the techniques and the systems.

In olive flesh, oil droplets are stored in the oil-bearing parenchyma cells in the mesocarp (Marsilio, Lanza, & Angelis, 1996; Rapoport et al., 2016). During virgin olive oil extraction, olive fruit are firstly washed then ground (including the stone) to disrupt the parenchyma cells and release the oil droplets (Petrakis, 2006; Wong et al., 2012). After grinding, a malaxing process is applied to coalesce the oil droplets then centrifugation is used to separate the oil phase from the pomace and wastewater, which is what the process for cold-pressed avocado oil extraction is based on (Petrakis, 2006; Wong et al., 2012).

One main difference between the cold-pressed oil extraction of olive and avocado are the malaxing temperature and time. The virgin olive oil extraction must be carried out at no higher than 27 °C and the malaxing time is normally less than 90 min, thus the composition or organoleptic characteristics of the oil are not changed (Codex Alimentarius, 2017; European Commission, 2002; International Olive Council, 2006; Petrakis, 2006; Wong et al., 2012). The low temperature recommended also helps to reduce lipase activity in olive fruit (Wong et al., 2012). Furthermore, the destoning step is generally not applied in the virgin olive oil extraction due to the smaller size of fruit stone and the higher flesh: stone ratio (ranging from 5:1 to 12:1 depending on the cultivar)

in olive fruit (Petrakis, 2006; Therios, 2009). Also, the olive fruit stone was originally left in to aid with the grinding step which can increase the cold-pressed oil yield by up to 1.5% compared to processing with de-stoned olive fruit (Petrakis, 2006).

The use of electrical and rheological properties in the analysis of cell structure changes in olive mesocarp during oil extraction has not been investigated. The objective of this study was to use light microscopy, electrical impedance spectroscopy (EIS), electrical conductivity and rheological measurements for determining whether different physical assessment methods could be combined to monitor key steps in olive oil extraction and guide improvements for extraction efficiency. This chapter will present results from samples collected from a commercial factory trial to investigate the cellular changes in 'J5' olive mesocarp during cold-pressed oil extraction, and from a laboratory trial looking at the effect of olive pulp storage time on EIS, conductivity and rheological measurements. The results in this chapter have been published in Yang, Hallett, Oh, Woolf, and Wong (2019).

7.2 Experimental design

7.2.1 Effect of sample storage time on electrical impedance, conductivity and rheology measurements from laboratory-based experiments

Laboratory-based experiments were carried out to determine if the electrical impedance, conductivity and rheological properties of olive pulp samples changed within the 4 h required to transport samples back to from Olivado Ltd NZ's Kerikeri plant to the laboratory at the Mt. Albert Research Centre of Plant and Food Research Ltd, Auckland.

The main steps in the experiment looking at the effect of sample storage time on electrical

impedance, conductivity and rheological measurements for cold-pressed olive oil extraction are shown in Figure 7.1.

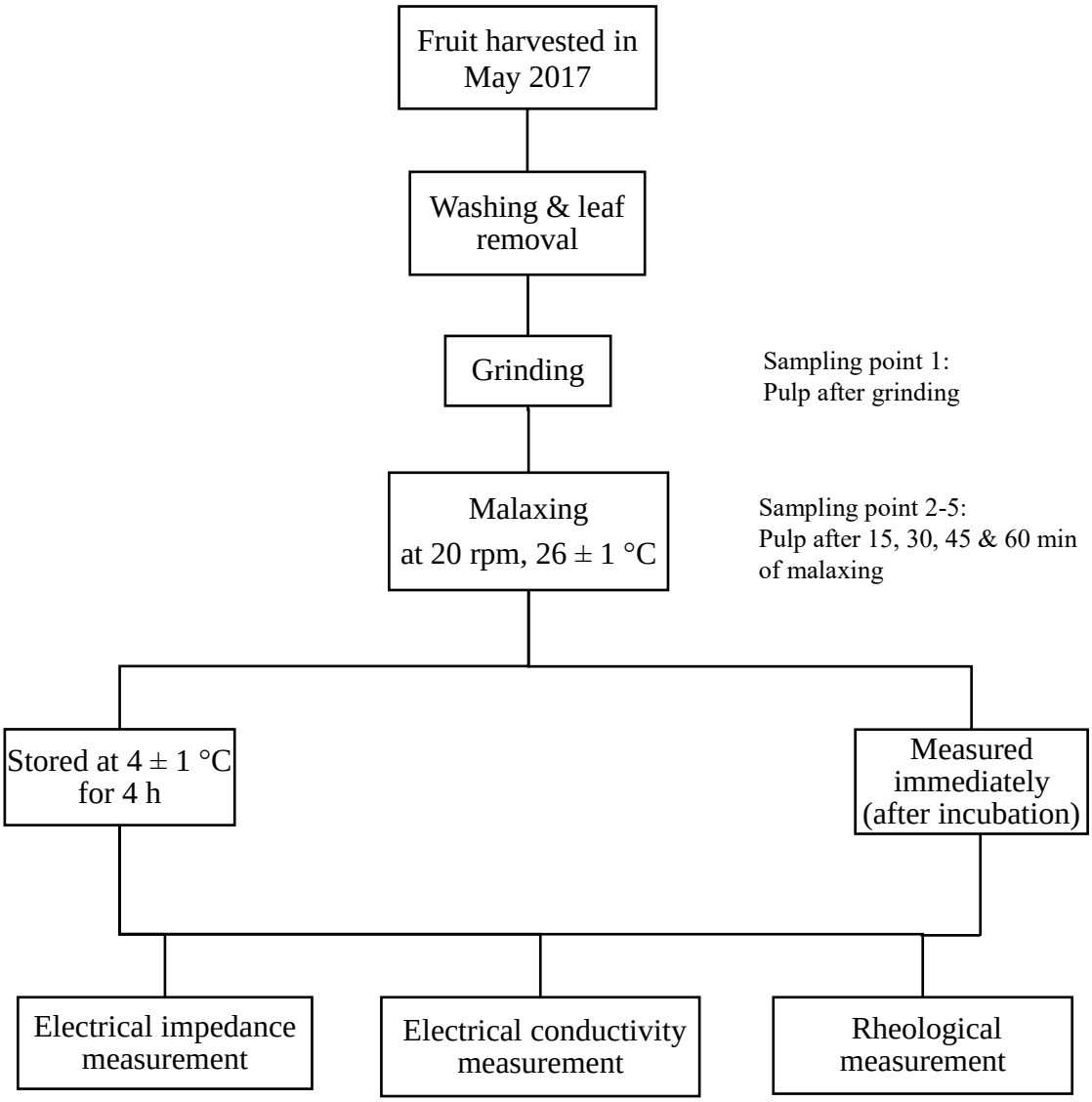

Figure 7.1: Flow diagram for the experimental procedure to investigate the effect of sample storage time on electrical impedance, conductivity and rheological measurements for virgin olive oil extraction. Electrical impedance measurement, electrical conductivity measurement and rheological measurement were carried out at each sampling point during the extraction process.

'J5' olive fruit (*Olea europaea* L, ≅ 10 kg) were harvested in May 2017, held at 15 ± 2 °C and were extracted within 12 h of harvesting. Effect of sample storage time (i.e. during transport to Auckland) on electrical impedance, conductivity and rheological measurements were studied following the methods described in Sections 3.6.3, 3.7.3 and 3.9.4. Statistical analysis was carried out following the methods as described in Section 3.12. The laboratory-based olive oil extraction experiments were performed in triplicate. Electrical impedance, conductivity and rheological properties measurements were carried out in triplicate.

7.2.2 Cellular changes in 'J5' olive mesocarp during commercial cold-pressed oil extraction

The main steps in the experiment looking at cellular changes during commercial based cold-pressed oil extraction for 'J5' olive are shown in Figure 7.2.

'J5' olive fruit (≅ 650 kg) were harvested and processed at Olivado Ltd, Kerikeri, New Zealand in May 2017 following the procedures described in Sections 3.1.3 and 3.3.3. Postharvest assessments of olive fruit, including dry matter determination, firmness measurement, and total oil content determination of fresh fruit were carried out following the methods described in Sections 3.2.2, 3.2.4 and 3.5. Firmness measurement of fresh fruit were performed on 50 olive fruit.

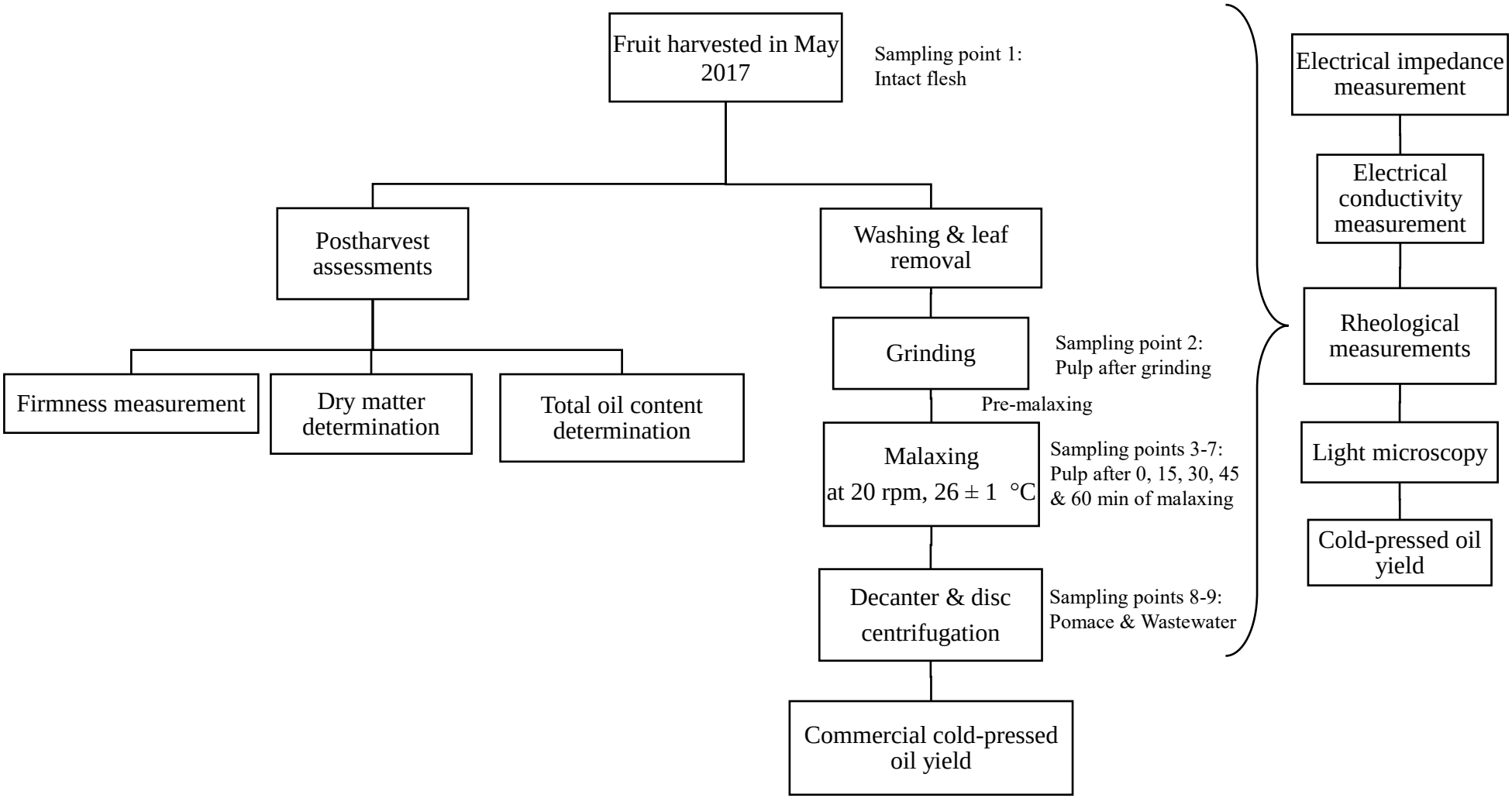

Figure 7.2: Flow diagram for the experimental procedure to investigate cellular changes during commercial cold-pressed oil extraction for 'J5' olive fruit. Electrical impedance measurements, electrical conductivity measurements, light microscopy observations, cold-pressed oil yield determination and rheological measurements were carried out at each sampling point during the extraction process.

Sampling point 2 was the pulp sample existing the grinder; the pre-malaxer took 30 min to fill and then the pulp was transferred to the main malaxer, Sampling point 3 was when the main malaxer was full (0 min malaxing); Sampling point 4-7 were 15, 30, 45 and 60 min after the malaxer was full.

EIS, electrical conductivity, light microscopy and rheological measurements were used to examine olive flesh structure at defined steps during the extraction process (grinding, malaxing and decanting) following the procedures described in Sections 3.6.1, 3.7.1, 3.8 and 3.9.3. The cold-pressed oil yield at each stage of malaxing in the commercial trial was determined following the method described in Section 3.3.4.

Statistical analysis was carried out following the methods as described in Section 3.12. A single commercial-based olive oil extraction trial and firmness measurement were performed. Dry matter determination and total oil content determination for olive pulp were carried out in triplicate. Electrical impedance measurement for intact olive fruit was carried out on ten replicates. Electrical impedance, conductivity, rheological properties and cold-pressed oil yield measurements for olive pulp were carried out in triplicate.

7.3 Results and discussion

7.3.1 Effect of sample storage time on electrical impedance, conductivity and rheological measurements

Similarly to the factory extraction trials for cold-pressed avocado oil, the olive pulp samples collected at Olivado Ltd NZ's Kerikeri plant were rapidly cooled at the factory with ice and stored in a chilly bin with ice to keep the samples at 4 ± 1 °C. Olive fruit pulp samples were required to be held for 4 h for transport before electrical impedance, conductivity and rheological measurements were carried out at the Mt. Albert Research Centre of Plant and Food Research Ltd, Auckland. An experiment was carried out to investigate if the electrical impedance, conductivity and rheological properties of olive pulp samples changed after the 4 h storage at 4 ± 1 °C.

'J5' olive fruit was ground and malaxed using the laboratory-based cold-pressed extraction process and samples were collected at 0 (after grinding), 15, 30, 45 and 60 min during malaxing. Samples were divided into two groups: one group of samples were measured for electrical impedance, conductivity and rheological properties immediately after collection, another group of samples were stored at 4 ± 1 °C for 4 h then the electrical impedance, conductivity and rheological properties were measured.

Figure 7.3 shows in comparison of olive pulp samples before and after 4 h storage at 4 ± 1 °C, there were no significant changes ($p \leq 0.05$) on the electrical resistance in the low frequency (50 Hz), medium frequency (10 kHz) and high frequency domains (1 MHz) for olive pulp tissue collected at various stages during malaxing. Moreover, the electrical conductivity and the viscoelastic properties (*G'* and *G"* at 0.1, 1 and 10 Hz) of the olive pulp tissue were not significantly affected ($p \leq 0.05$) by the 4 h storage at 4 ± 1 °C (Figures 7.4 & 7.5). Therefore, storing and transporting the olive pulp samples for 4 h at 4 ± 1 °C from Olivado Ltd NZ's Kerikeri plant to the Mt. Albert Research Centre of Plant and Food Research Ltd, Auckland did not significantly influence the electrical impedance, conductivity and rheological properties results in this project.

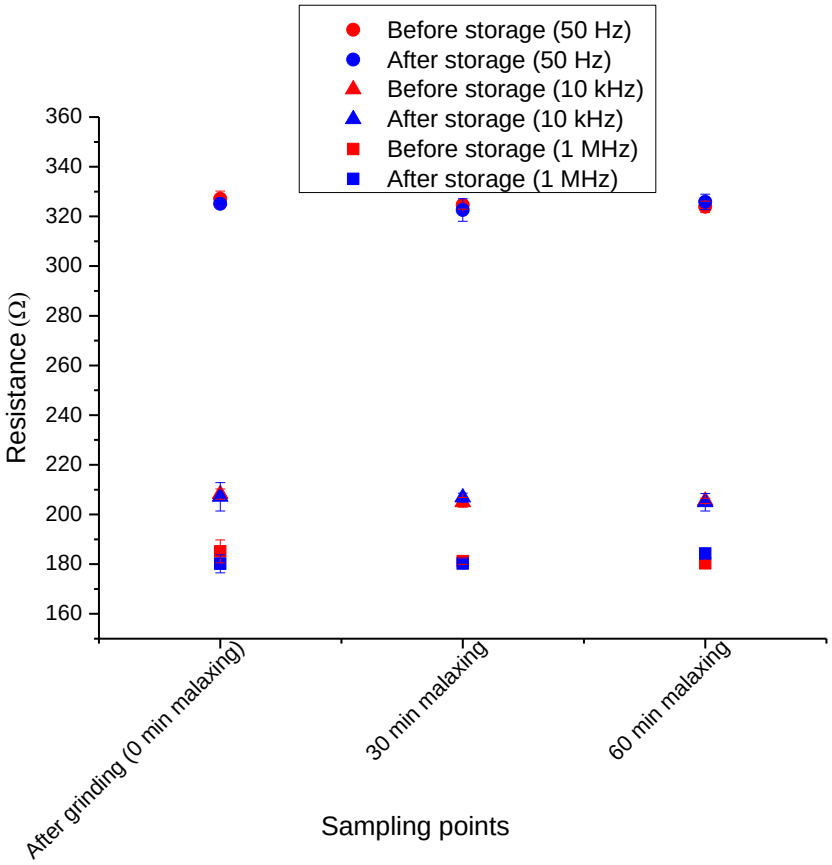

Figure 7.2: Comparison of resistance of 'J5' olive pulp tissue at 50 Hz, 10 kHz and 1 MHz before and after 4 h storage at 4 ± 1 °C (mean ± SE, n = 3).

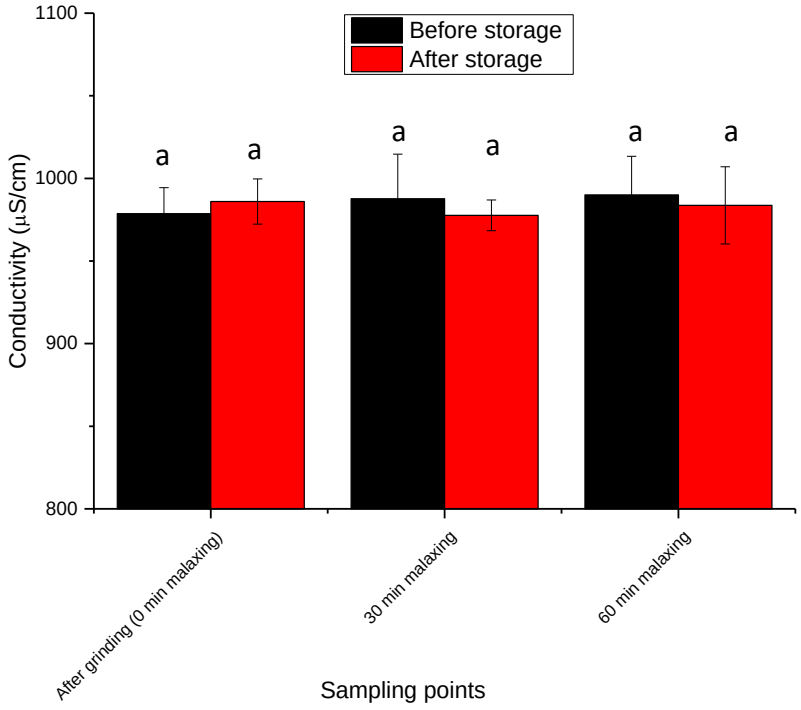

Figure 7.3: Comparison of electrical conductivity of 'J5' olive pulp tissue before and after 4 h storage at 4 ± 1 °C (mean ± SE, n = 3).

[a] Same letters denote no significant difference between conductivity values ($p > 0.05$).

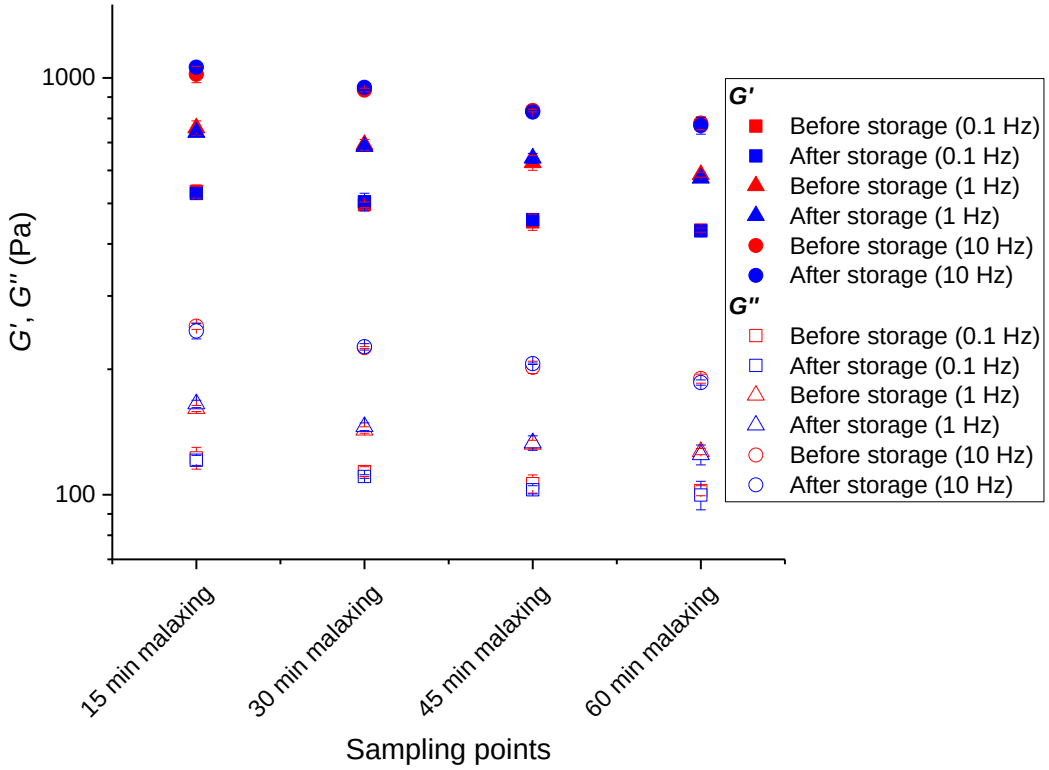

Figure 7.4: Comparison of viscoelastic properties (*G', G"*) of 'J5' olive pulp tissue at 0.1 Hz, 1 Hz and 10 Hz before and after 4 h storage at 4 ± 1 °C (mean ± SE, n = 3).

7.3.2 Cellular changes in 'J5' olive mesocarp during commercial cold-pressed oil extraction

7.3.2.1 Olive fruit for commercial oil extraction trial

Unlike avocado fruit which does not ripen (soften) while attached to the tree, olive fruit ripens during fruit development but their natural ripening does not continue once the fruit has been harvested (Kailis & Harris, 2007; Schaffer et al., 2013). The dry matter and total oil content in olive fruit flesh are highly correlated, and largely increase during the ripening period of fruit. Furthermore, an inverse relationship has been found between total oil content and fruit firmness that the softer fruit give a higher total oil content (Beltrán et al., 2004; Requejo-Jackman et al., 2010; Salvador et al., 2001).

For virgin olive oil extraction, the optimal fruit harvesting time is when oil content is high in the fruit (Petrakis, 2006). According to the previous study of Requejo-Jackman et al. (2010) on New Zealand 'Frantoio' olives, which is the cultivar similar to New Zealand 'J5' cultivar used in the current research, the firmness of the fruit at 500–700 g/mm is most suitable for oil extraction. The olive fruit selected for oil production in May 2017 were found to have an average firmness of 638.5 ± 15.1 g/mm, which is in the target firmness range. The average dry matter content (determined for pulp obtained from the malaxer during extraction) of the fruit flesh extracted in the commercial trial in May 2017 was 39.59 ± 0.18% (g of dry flesh/100 g of fresh flesh).

7.3.2.2 Total oil content and commercial olive oil yield

The total oil content (determined by ASE for pulp obtained from the malaxer during extraction) of the olive fruit flesh extracted in the commercial trial in May 2017 was 17.1 ± 0.4% (g of oil/100 g of fresh flesh), and the commercial oil yield obtained was 14.1% (g of oil/100 g of fresh flesh) (Table 7.1). Similarly to the factorial trial for cold-pressed avocado oil extraction (Sections 4.3.2 and 5.3.1), it was found that all the oil present was not able to be extracted from the fruit via the commercial extraction process for virgin olive oil extraction. The causes of this inefficiency will be further discussed in the microscopy study below.

For determining the cold-pressed oil yield at each stage of malaxing in the commercial trial (Table 7.1), olive pulp samples were collected at the factory at 15, 30, 45 and 60 min malaxing and centrifuged by using a laboratory centrifuge to mimic the commercial centrifugation system as the commercial system cannot be applied in the middle of malaxing process due to technical and economic reasons. The cold-pressed oil yield

increased with an increasing malaxing time from 15 to 60 min, which corresponded to the previous studies from Amirante, Cini, Montel, and Pasqualone (2001) and Di Giovacchino et al. (2002a) on olive oil extraction as well as the findings in Section 4.3.2 for cold-pressed avocado oil extraction. In comparison to the factory trial of cold-pressed 'Hass' avocado oil extraction, olive pulp gave higher oil extraction efficiencies (extraction yield/total oil content) in that 73.0% and 84.9% of the oil was recovered after 30 and 60 min of malaxing, respectively. For avocado with the similar total oil content at 15.4 ± 0.3 (g of oil/100 g of fresh flesh), the oil extraction efficiencies were only 5.2% and 37.0% after 30 and 60 min of malaxing, respectively, in the factory malaxers (Section 4.3.2.1). The different oil extraction efficiencies may be due to the different structure and texture of fruit, which results in a faster oil droplets aggregation in olive fruit pulp than that of avocado fruit pulp during malaxing.

Table 7.1: Total available oil and extraction yield from commercial cold-pressed 'J5' olive extraction and from samples collected during the extraction process (mean ± SE, n = 3).

	Malaxing time (min)				
	0	15	30	45	60
Total oil content measured by ASE (g of oil/100 g of fresh flesh)	15.2 ± 0.4^{d}				
Extraction yield at different malaxing times (g of oil/100 g of fresh flesh)	-	9.8 ± 0.2^{a}	11.1 ± 0.2^{b}	12.2 ± 0.4^{bc}	12.9 ± 0.4^{c}
Commercial cold-pressed oil yield (g of oil/100 g of fresh flesh)	-	-	-	-	12.6

[a-d] Different letters denote significantly different oil yield values across rows and columns ($p < 0.05$).

7.3.2.3 Change in electrical impedance during commercial olive oil extraction

The degree of cell integrity in the olive flesh during the extraction process was investigated using EIS. In the plot of EIS (Figure 7.6), a significant difference ($p < 0.05$)

in electrical resistance at 50 Hz was found between the intact olive flesh (7373.6 ± 283.3 Ω) and ground flesh pulp samples (361.2 ± 1.1 Ω) after grinding. The loss of cellular structure due to the grinding step led to a reduction in resistance at low frequency (Hayden et al., 1969). The electrical impedance results did not change significantly ($p > 0.05$) after grinding up to 60 min malaxing, indicating that grinding is the key step involved in cell wall and membrane breakdown.

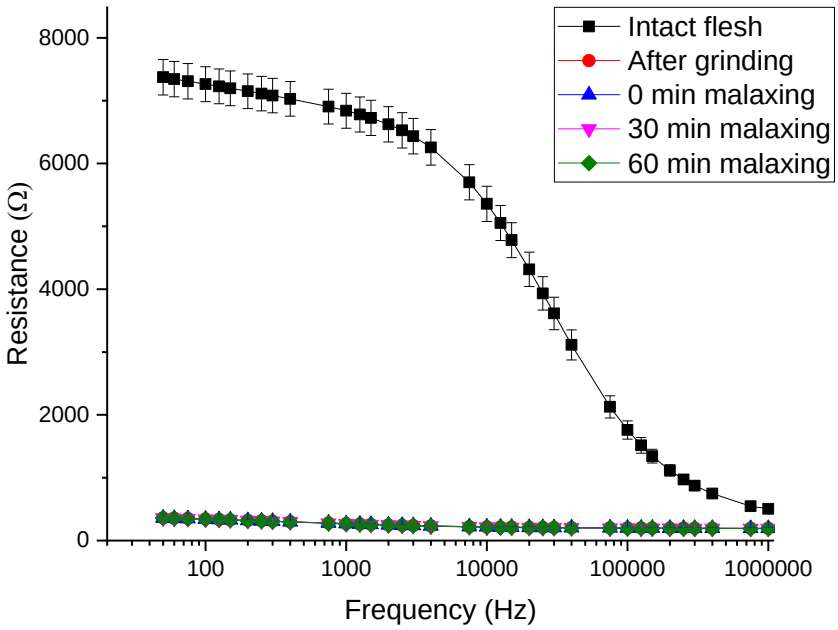

Figure 7.5: Resistance (Ω) determined by electrical impedance spectroscopy of 'J5' olive flesh (mean ± SE, n = 10) and pulp (mean ± SE, n = 3) before grinding and at various times during the oil extraction process.

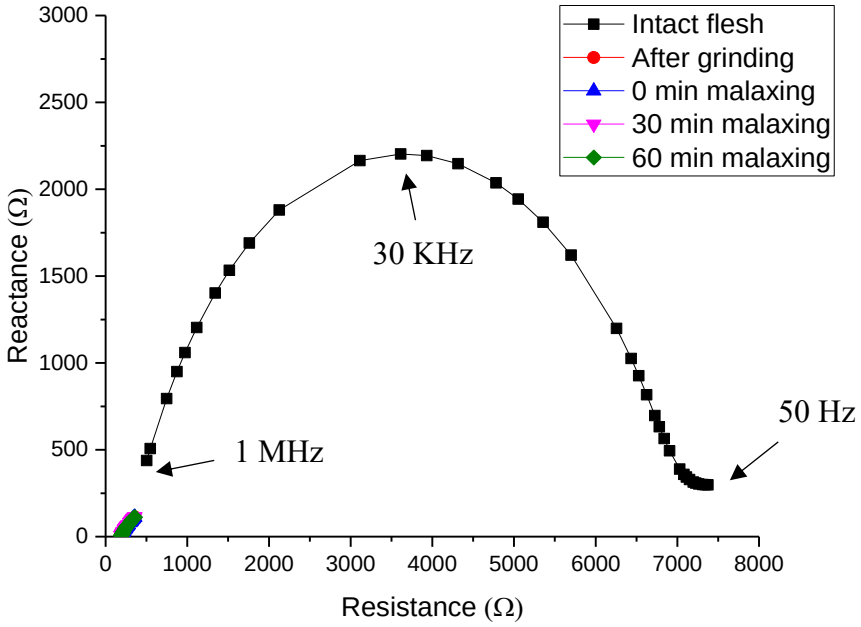

Figure 7.6: Nyquist plot of 'J5' olive flesh and pulp during cold-pressed oil extraction at various stages of the oil extraction process (mean ± SE, n = 3).

The loss of cellular structure due to the grinding step is further confirmed in the Nyquist plot of olive flesh and pulp during cold-pressed oil extraction at various stages of the oil extraction process (Figure 7.7). The Nyquist plot for the 'intact flesh' olive sample showed a typical characteristic arc corresponding to an intact cellular structure. However, such an arc was not seen for the Nyquist plot associated with olive pulp samples collected after grinding during malaxing, indicating the cell walls and membranes had been disrupted.

7.3.2.4 Change in electrical conductivity during commercial olive oil extraction

Measurement of the electrical conductivity of plant tissue was used to estimate the degree of the cell wall and membrane intactness during processing (Figure 7.8). During fruit processing, any damage to cell walls and membranes leads to diffusion of ions out of the cell into the extracellular fluid, resulting in an increase in solution electrical conductivity

(Palta et al., 1977). In this study, the electrical conductivity of '0 min malaxing' olive paste sample was found to be significantly higher ($p < 0.05$) than that of the 'intact flesh' sample (Figure 7.8), suggesting a loss of cell integrity in the olive mesocarp after grinding. However, no significant difference ($p > 0.05$) was found between the electrical conductivity of olive paste collected at 0 and 60 min malaxing, indicating the cellular structure in the olive paste was not further ruptured during malaxing, as found in avocados. The conductivity measurement confirms the results with EIS.

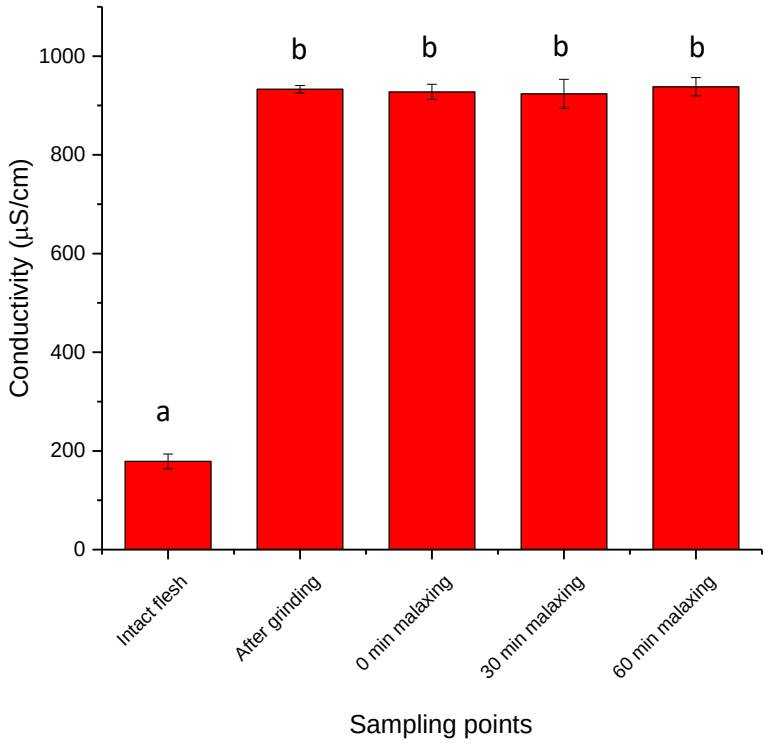

Figure 7.7: Electrical conductivity (µS/cm) of 'J5' olive flesh during cold-pressed oil extraction at various stages of oil extraction process (mean ± SE, n = 3).
[a,b] Different letters denote significantly different conductivity values ($p < 0.05$).

7.3.2.5 Changes in olive cellular microstructure during commercial oil extraction monitored with light microscopy

In the intact olive fruit, well-structured parenchyma cells with a diameter of approximately 80 µm were found in the mesocarp (Figure 7.9a); this is slightly larger than that from the avocado flesh (≅ 50 µm diameter). The oil droplets were trapped inside the cell walls and membranes (Figure 7.9b), as has been reported in previous studies (Marsilio et al., 1996; Rapoport et al., 2016). No idioblast cells were found in the olive flesh.

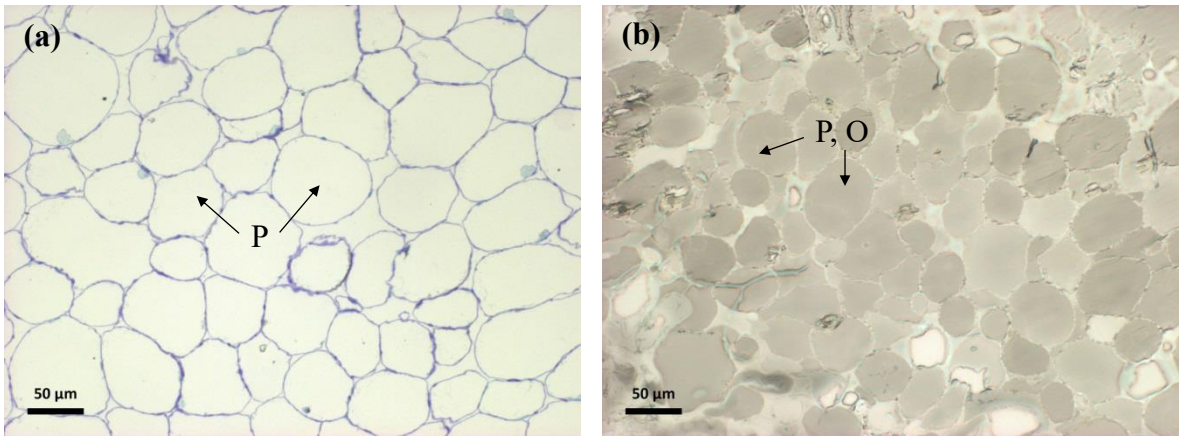

Figure 7.8: Microstructure of intact 'J5' olive flesh under light microscopy. (a) Image from samples embedded in LR white resin, cell walls stain blue by toluidine blue staining in the LR White embedded tissue. (b) Image from samples embedded in Spurr's resin, oil from parenchyma cells shows a grey colouration by osmium tetroxide fixation/staining of the Spurr's embedded material.
P: Parenchyma cells; **O**: Oil droplet(s).

A series of cellular changes in olive tissue were found throughout the extraction process. After grinding, most of the parenchyma cells were ruptured and oil droplets were released (Figures 7.10a & 7.10b), which was in agreement with the EIS and electrical conductivity results (Figures 7.6, 7.7 & 7.8). The changes in olive pulp during malaxing indicated that this step promotes aggregation of the oil droplets (Figures 7.10b, 7.10d & 7.10f). Before

malaxing starts (0 min malaxing), the free oil droplets were scattered in the image with an average diameter of ≅ 10 μm (Figure 7.10b); however, the average diameter of oil droplets increased to ≅ 60 μm after 30 min malaxing (Figure 7.10d) and ≅ 110 μm after 60 min malaxing (Figure 7.10f). These results confirm the findings of Di Giovacchino (1989) and Di Giovacchino (1996) on the study of virgin olive oil extraction, as well as the previous study in Chapter 4 on the study of cold-pressed avocado oil extraction, that the oil droplets aggregate into larger oil droplets with an increasing malaxing time. Therefore, the function of the malaxing step during olive oil extraction process was not to disrupt the parenchyma cells in the mesocarp, but to promote the aggregation of oil droplets to form a liquid oil phase for easier recovery of the oil in the next centrifugation step.

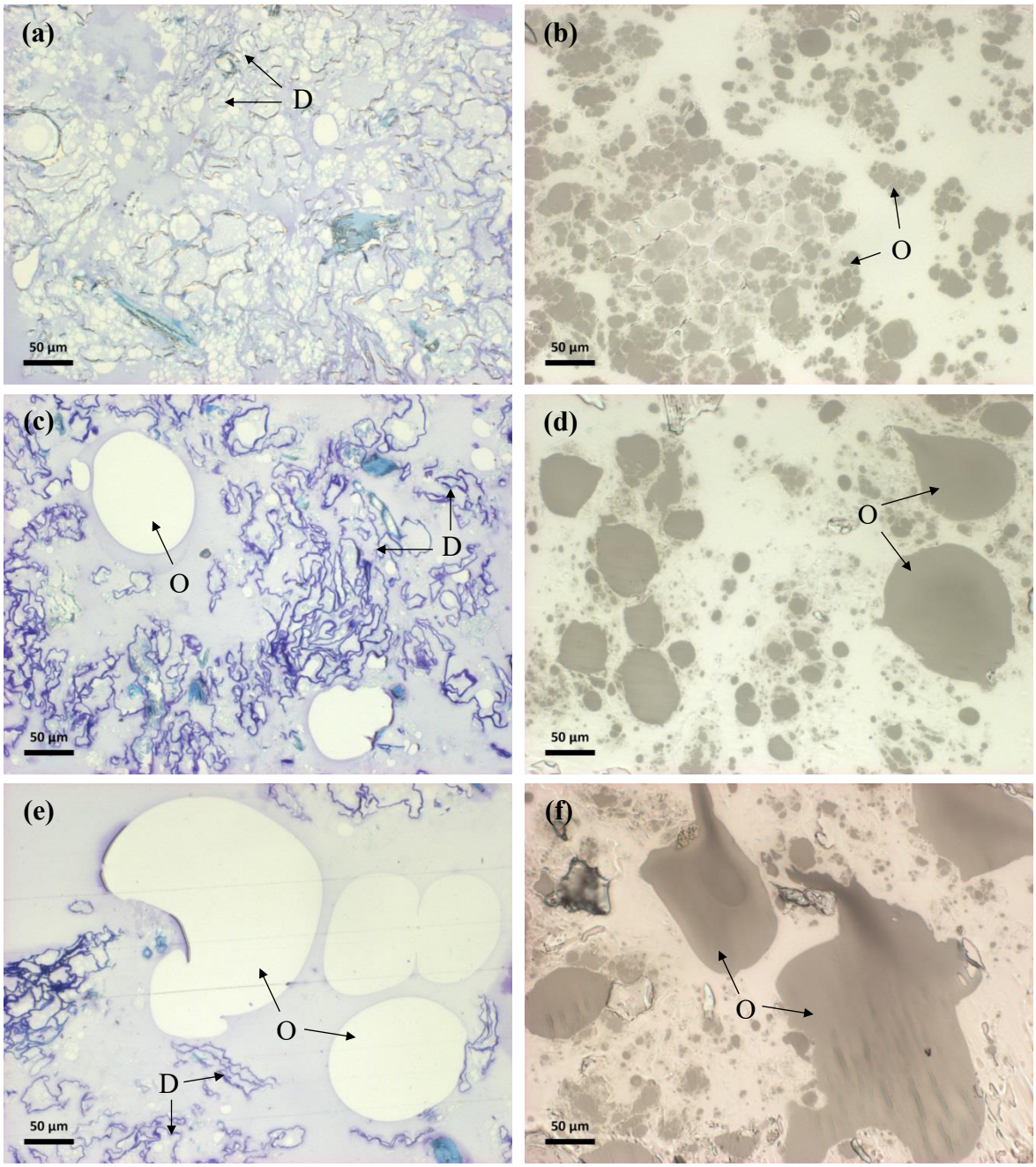

Figure 7.9: Microstructure of 'J5' olive paste (a) at 0 min malaxing, embedded in LR White resin, (b) at 0 min malaxing, embedded in Spurr's resin, (c) after 30 min malaxing, embedded in LR White resin, (d) after 30 min malaxing, embedded in Spurr's resin, (e) after 60 min malaxing, embedded in LR White resin, (f) after 60 min malaxing, embedded in Spurr's resin.

D: Parenchyma cells debris; **O**: Oil droplet(s).

In comparison to the microstructure of 'Hass' avocado pulp (with the same total oil content) during factory based cold-pressed oil extraction (Figure 7.11), much larger oil droplets (≅ 110 µm average diameter) were found in the olive fruit pulp after 60 min malaxing than in the avocado fruit pulp (≅ 40 µm average diameter) although a lower malaxing temperature was applied. It was concluded that the oil droplets aggregate faster during virgin olive oil extraction, which agrees with the cold-pressed oil yield results in Section 7.3.2.2 that the olive pulp gave higher oil extraction efficiencies after 30 and 60 min of malaxing.

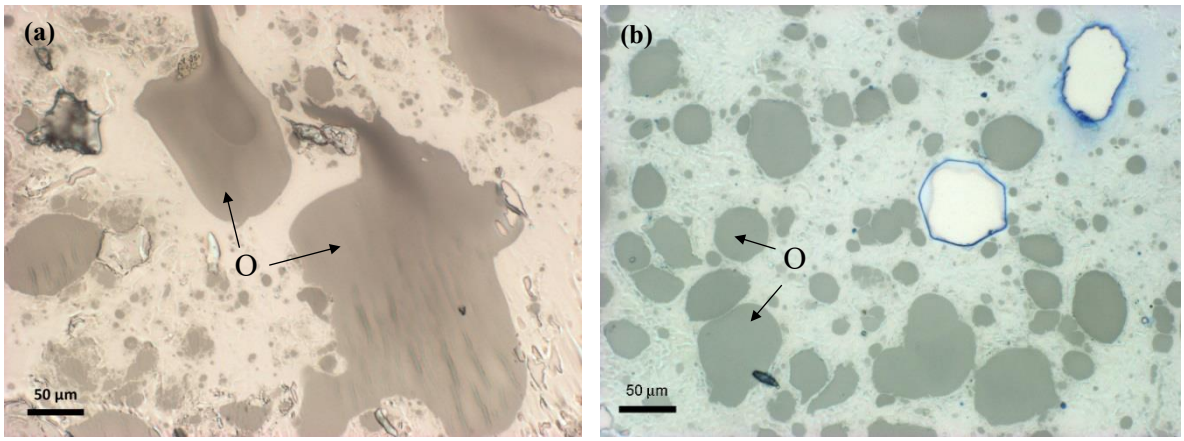

Figure 7.10: Microstructure of 'J5' olive pulp after 60 min malaxing at 26 °C (a) and 'Hass' avocado pulp after 60 min malaxing at 45 °C (b) under light microscopy. Images were from samples embedded in Spurr's resin.
O: Oil droplet(s).

Similarly to the factory trials for cold-pressed avocado oil extraction, some unbroken parenchyma cells were found in the olive pomace sample collected from the decanter (Figures 7.12a & 7.12b). Figure 7.12b shows that the unbroken parenchyma cells contain oil droplets still trapped in the cytoplasm of the cells. This indicates that not all the cells in the olive mesocarp were disrupted by the grinding process and that these are not broken down during the malaxing step, thus resulting in oil loss and less oil recovery. Also, some

free oil droplets were found in both the pomace and wastewater exiting the decanter (Figures 7.12c & 7.12d), which suggested that not all of the oil was recovered from the olive paste during the decanting step.

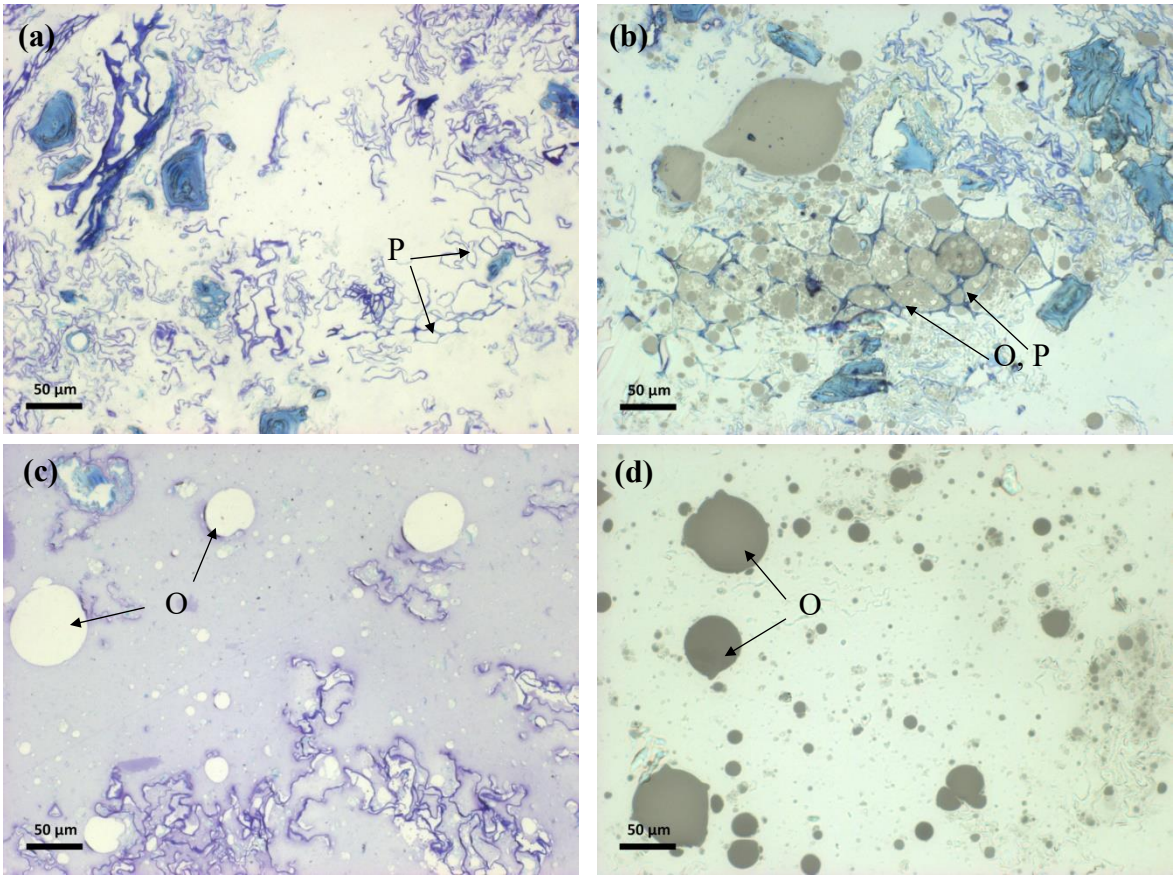

Figure 7.11: Microstructure of pomace and wastewater under light microscopy, (a) pomace, embedded in LR White resin, (b) pomace, embedded in Spurr's resin, (c) wastewater, embedded in LR White resin, (d) wastewater, embedded in Spurr's resin.
P: Parenchyma cells; **O**: Oil droplet(s).

7.3.2.5 Change in rheological properties during commercial olive oil extraction

The changes in the elastic modulus, *G'*, and the viscous modulus, *G"* of the olive pulp during malaxing in the factory extraction trials is presented in Figure 7.13. The frequency dependency of *G'* and *G"* were not affected by malaxing time. For all the olive pulp samples, both *G'* and *G"* increased with frequency (Figure 7.13). The plots of *G'* and *G"* were all straight lines with a slopes of 0.12–0.13 on a log scale, *G'* was greater than *G"* but by less than one log, indicating that the olive pulp had a solid-like behaviour (Lapasin

& Pricl, 1995). Similar rheological behaviours (solid-like behaviour) have been found in other fruit and vegetable paste samples including avocado paste, tomato paste and potato puree (Ahmed & Ramaswamy, 2006; Bayod et al., 2008; Martínez-Padilla et al., 2017).

The *G'* and *G''* values of olive pulp decreased with increasing malaxing time from 15 to 60 min indicating an decrease in the solid-like behaviour of the olive pulp (Figure 7.13). A decrease in *G'* value may be explained by a decrease in particle-particle interaction in the olive pulp due to the oil droplets aggregation in the pulp by malaxing (Larson, 1999; Petrakis, 2006; Tadros, 2017; Tamborrino et al., 2017). These results agree with the findings of Martínez-Padilla et al. (2017) on the research of avocado paste during malaxing, the elastic modulus decreased after the malaxing treatment was applied for 1 h at 45 °C due to the increased availability of the liquid fraction as a result of oil aggregation in the avocado paste sample after malaxing. These results also agree with the observations of light microscopy in Section 7.3.2.5 that the oil droplets in olive paste aggregated into larger droplets during malaxing.

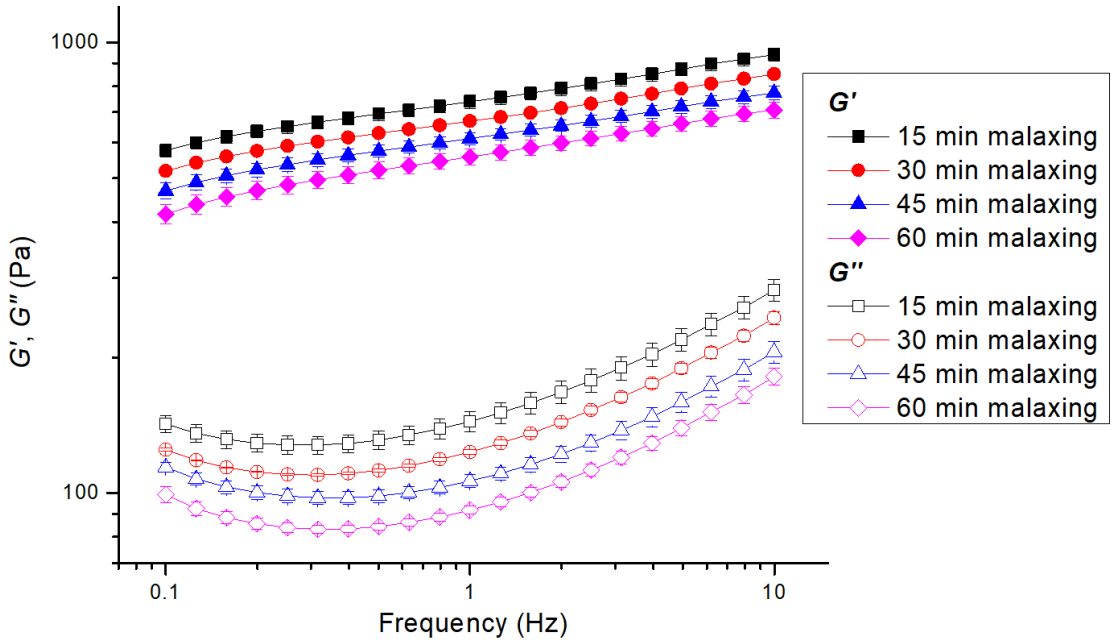

Figure 7.12: Rheological properties (*G', G''*) of 'J5' olive pulp during factory based malaxing (mean ± SE, n = 3).

The variation of the elastic and viscous modulus of malaxed olive paste with average oil droplet size at 1 Hz, 20 °C are shown in Figure 7.14. Various average oil droplet sizes in olive paste were obtained during malaxing at 26 °C from 15 min to 60 min. Both of the *G'* and *G"* values show an exponential decrease (R^2 0.99 for both *G'* and *G"*) with increasing average oil droplet size (D) in the malaxed olive paste (Equations 1 and 2). The following models (Equations 1 and 2) are proposed after correlating the measured *G'* and *G"* value to oil droplet size (D) during malaxing of the olive paste sample.

$$G' = 782.66\ e^{(-0.003D)} \quad (1)$$

$$G'' = 158.67\ e^{(-0.005D)} \quad (2)$$

Therefore, the measurement of the viscoelastic properties of the olive paste can be applied in the oil industry to monitor the changes in the degree of oil aggregation during malaxing to assist with improved extraction efficiency and extraction yields.

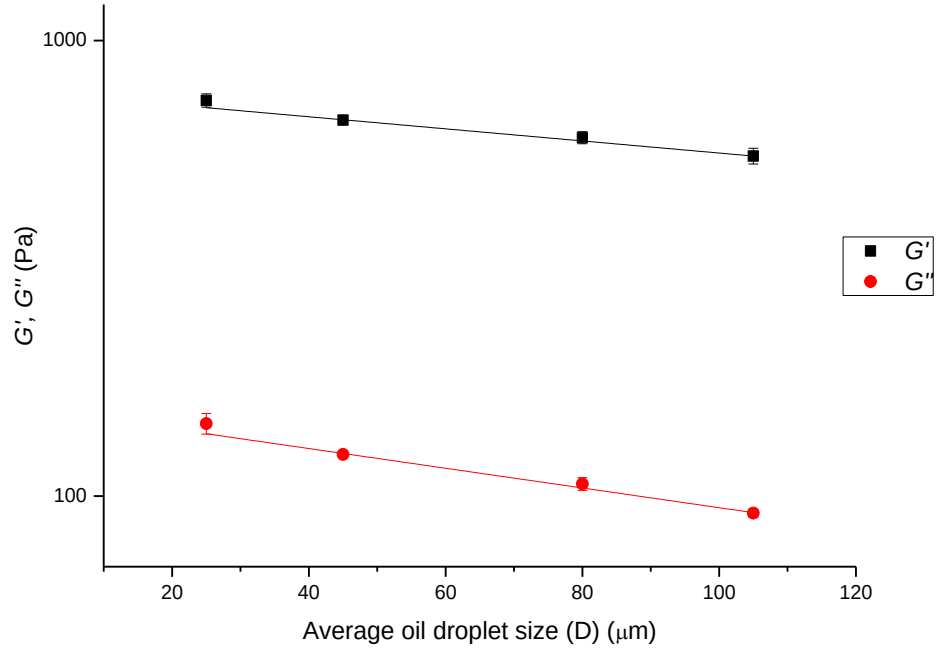

Figure 7.13: Viscoelastic properties of 'J5' olive paste during commercial oil extraction evaluated at a constant frequency (1 Hz) as a function of average oil droplet size (D) in malaxed olive paste samples (mean ± SE, n = 3).

The viscoelastic properties (*G'*, *G"*) of 'Hass' avocado pulp was also determined during factory based cold-pressed oil extraction in October 2016. The total oil content of the avocado fruit selected for oil production was 15.4 ± 0.1 (g of oil/100 g of fresh flesh), which was not significantly different ($p > 0.05$) to the total oil content in the olive fruit (15.4 ± 0.1, g of oil/100 g of fresh flesh) selected for oil production in the current research. After 30 and 60 min malaxing, the *G'* and *G"* values of avocado pulp were significantly higher ($p < 0.05$) than that of olive pulp, indicating a less solid-like behaviour for the olive pulp sample (Figure 7.14; Appendix IV). Since the water content of the olive pulp (60.4 ± 0.2%) was lower ($p < 0.05$) than that of avocado pulp (74.3 ± 0.2%), the lower solid-like behaviour of the olive pulp is likely to be explained by the higher level of oil aggregation in the pulp, which corresponded to the observations from light microscopy in Section 7.3.2.5.

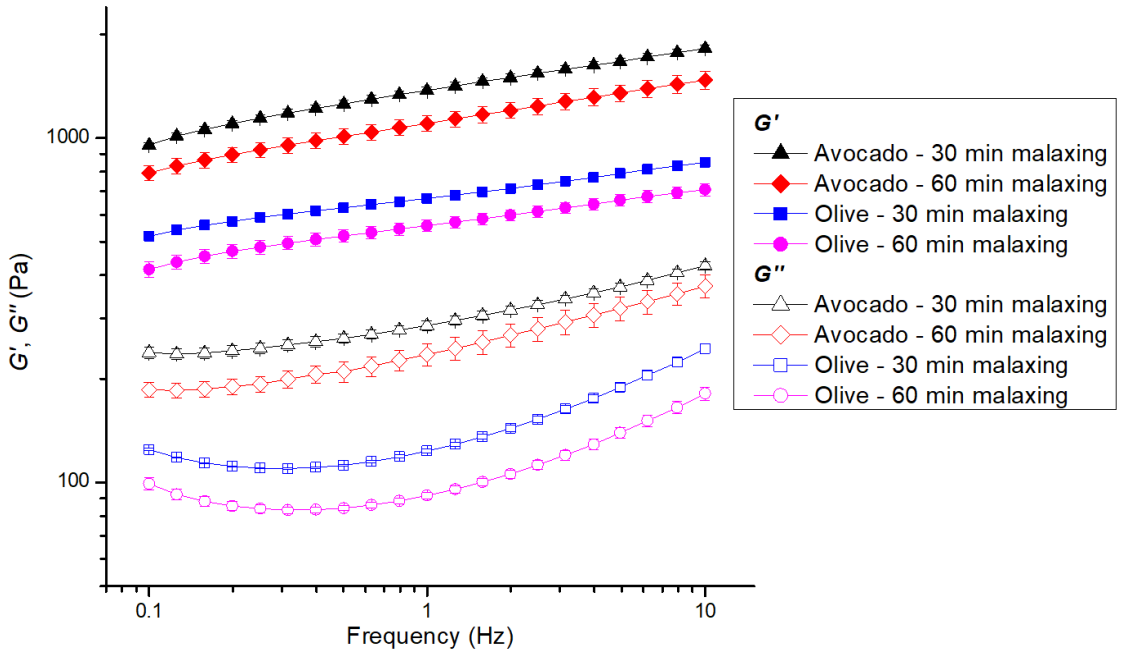

Figure 7.14: Comparison of viscoelastic properties (*G', G"*) of 'J5' olive pulp tissue and 'Hass' avocado pulp tissue during malaxing (mean ± SE, n = 3) in commercial extraction.

7.4 Conclusions

Based on the results, it can be concluded that during the ‘J5’ olive oil extraction process, the parenchyma cells in olive mesocarp were ruptured only at the grinding step. The malaxing step promoted aggregation of the oil droplets, which helped to improve the oil recovery. Similarly to the previous study for avocado oil extraction, the measures of electrical impedance, conductivity and rheological properties of the olive pulp tissue showed a correlation with microscopic cellular structure. The changes in olive pulp microstructure can be detected using the relatively fast and simple EIS technique. Also, rheological properties of the olive pulp can give an indication of the extent of oil droplet aggregation during malaxing. In comparison to the cold-pressed oil extraction of ‘Hass’ avocado, olive oil is much easier to recover from ‘J5’ olive during cold-pressed extraction (e.g. lower temperatures and shorter times) as the olive paste is less solid-like allowing the oil droplets to aggregate more easily.

Chapter 8:

Overall discussion

8.1 Factors affecting 'Hass' avocado cold-pressed oil yield and quality

Optimizing cold-pressed oil extraction yields from avocado flesh is important for the high-value avocado oil industry. The overall objective of this research project was to understand cellular changes during cold-pressed 'Hass' avocado oil extraction with respect to improving oil yield. In this study, postharvest factors including fruit maturity and fruit ripeness (Chapter 5), and the processing conditions including malaxing time (Chapter 4), malaxing temperature and ultrasound treatments (Chapter 6) were found to be important factors that affect either the cellular structure in avocado flesh or oil aggregation in the malaxed pulp before and during cold-pressed avocado oil extraction and thus affected the cold-pressed oil yield.

Horticultural maturity, or the time of year within the harvest season, has been found to have an impact on the oil yield for cold-pressed avocado oil manufacturers by Woolf et al. (2009), however the reasons for the differences in the in oil yield between early and late season is still unclear. One of the key objectives for this project was to understand the microstructural changes during fruit maturation before extraction, and how the fruit maturity influenced the cellular structure changes in avocado flesh during malaxing. In this project, the total oil content of the 'Hass' avocado in 2016/17 season was found to increase from ≅ 13.5% (g oil/100 g fresh flesh) in September, early-season, to ≅ 23.5% (g oil/100 g fresh flesh) in April, end of the season (Chapter 5). It was observed in late-season avocado fruit, more parenchyma cells in the avocado mesocarp were ruptured during grinding, which resulted in a higher cold-pressed oil extraction yield. When the cellular structure of the avocado pulp was investigated with a chemical fractionation technique, a larger amount of water- and CDTA-soluble polysaccharide fractions were found in cell walls extracted from early-season 'Hass' avocado fruit, which indicates a

stronger binding strength of polysaccharides to the cellulose compared to late-season fruit. The stronger cell wall structure of early-season fruit is the likely reason for the cells being more difficult to rupture during grinding. These results help to explain the question raised by the previous study by Woolf et al. (2009). This research did not dig very deep into cell wall structure, hence some future research could be carried out to treat the fruit cell walls by using dilute alkali (0.05 M Na_2CO_3, 1 M KOH and 4 M KOH) successively following the extraction by chelating agents (CDTA), to obtain more information about the cellular structure changes that take place during avocado fruit maturation. Pectin with galactan and arabinan side chains are usually extracted by alkaline solvents and are thought to be very tightly bound to cellulose via hydrogen bonds (Redgwell, Melton, & Brasch, 1988; Renard, Voragen, Thibault, & Pilnik, 1991).

During avocado fruit ripening, a loosening of the polymer networks of the parenchyma cell wall gradually occurs due to the action of the cell wall-degrading enzymes in the avocado flesh (Brummell, 2006b; Jeong et al., 2002). A more open and diffuse cell wall structure was found in a softer and riper fruit, which resulted in more parenchyma cell disruption by grinding (Chapter 5). A higher conductivity and a lower electrical resistance value, which indicated a higher degree of cellular disruption, was found in the pulp of softer and riper avocados at different stages of malaxing (0, 60 and 120 min). Hence more oil was released and recovered from the pulp after malaxing of softer and riper avocado fruit, and the cold-pressed oil yield increased with increased fruit ripening. In terms of the recovered oils' quality, the free fatty acids levels (FFA%) and peroxide values (PV) in the cold-pressed avocado oil significantly increased ($p < 0.05$) with fruit ripeness from 0.24 to 0.37% (as oleic acid) and 1.18 to 2.23 (meq/kg oil), respectively. The increases in FFA% and PV were likely due to the lipid hydrolysis reactions and oxidation of oil after

oil is released from the cells. For optimizing the cold-pressed oil extraction yields, firstly, avocado fruit needs to be fully ripened before processing for oil production since the oil in riper avocado fruit is more easily released by grinding. In terms of oil quality, the cold-pressed avocado oil extracted from over ripe fruit at 105 Fv had FFA% at 0.37% (as oleic acid) and PV at 2.23 meq/kg oil. This result showed that the oil could still be considered as 'extra virgin' quality according to the Proposed International Quality Standards for Avocado Oil as the FFA% was less than 0.5% and the PV was less than 4.0 meq/kg oil (Woolf et al., 2009). However, except for FFA% and PV, the oil was also required to meet the other recommended quality measures, such as total vitamin E content, stability, smoke point and sensory characteristics, to be considered as 'extra virgin' oil (Woolf et al., 2009). Therefore, more detailed oil quality analysis and sensory tests are required for the oil extracted from the over ripe avocado fruit (with different rot levels) before they are used for oil production. The fruit firmness prior to cold-pressed avocado oil extraction is a critical factor in oil extraction and a balance is required to maximise yield while maintaining oil quality.

During cold-pressed avocado oil extraction, the malaxing time and temperature can also significantly affect the cold-pressed oil yield (Chapter 4 and 6). Increased malaxing time allowed for more time for the oil droplets to come in contact with each other and aggregate to form larger droplets which were easier to separate from the pulp and water by centrifugation (Chapter 4). Oil droplets for continuous-process centrifugation during oil extraction must have a diameter of more than 30 μm to achieve a good oil yield (Di Giovacchino, 1989, 1996). The increased temperature of malaxing reduces the viscosity of the pulp and oil and increases the mobility of oil droplets so they collide and coalesce to form larger droplets, and the larger droplets are easier to recover by centrifugation

(Chapter 6). Malaxing at 50 °C for 120 min resulted in the more oil droplets coalescing and an increased oil yield result. After 120 min of malaxing, the average diameter of oil droplets increased from ≅ 25 µm to ≅ 100 µm with increasing temperature from 30 to 50 °C. The avocado pulp became more liquid-like (decreased *G'* values) with the increasing malaxing time and temperature corresponding to oil droplets coalescing in the avocado pulp. The increased malaxing time and temperature did not assist in cellular disruption during cold-pressed avocado oil extraction. The FFA% and PV in the cold-pressed avocado oil were not significantly influenced ($p > 0.05$) by the increased malaxing temperature from 30 to 50 °C. These two basic oil quality measurements are not enough to define the overall quality of the oil, but provide an indication that the extraction process carried out did not lead to a reduction in oil quality. Further research could be carried out to determine the effect of malaxing temperature on the minor components such as pigments and tocopherols, oxidative stability, smoke point and sensory characteristics of the cold-pressed avocado oil.

In this project, laboratory-based ultrasound treatment at 20–25 kHz, 45 ± 1 °C was shown to have a positive impact on oil aggregation in both non-malaxed and malaxed avocado pulp samples to improve the cold-pressed oil yield (Chapter 6). A higher degree of oil aggregation in the pulp was due to the ultrasonic waves altering the interaction between oil droplets through acoustic pressure and moving the oil droplets towards each other to improve aggregation and form larger oil droplets (Juliano et al., 2011; Vilkhu et al., 2011). The ultrasound treatment at 20–25 kHz may not be applied to replace the malaxing step in cold-pressed avocado oil extraction, as the ultrasound treatment used was not found to give a higher oil extraction yield than that from malaxing only at 45 ± 1 °C for the same length of time. However, the results from Chapter 6 provided an indication that ultrasound

treatment at 20–25 kHz may assist in shortening the malaxing time if it is applied simultaneously with malaxing. Further research is recommended to investigate the effect of ultrasound treatment on cold-pressed oil yield when it is applied simultaneously with malaxing at 45 ± 1 °C. Oil composition analysis, oil quality analysis and sensory tests are also required for the avocado oil extracted by ultrasound treatment.

After 30 and 60 min of commercial based malaxing, 'Hass' avocado pulp gave a significantly lower ($p < 0.05$) oil extraction efficiency (extracted oil/total oil content) in comparison to 'J5' olive fruit pulp with the similar total oil content (Chapter 4 and 7). Also, smaller oil droplets and higher *G'* values were found in avocado pulp than that found in the olive pulp after 30 and 60 min of malaxing. Therefore, the oil was more difficult to be recovered from avocado during the extraction process as the avocado pulp was more solid-like, which resulted in less coalescence of oil globules in the pulp, with less chances for collisions between oil droplets.

In terms of the cells present in the fruit mesocarp, idioblast cells (≅ 2%) were found in avocado mesocarp but were not observed in olive flesh. The idioblast cells appeared to remain unruptured and intact during the extraction process, and were removed into the waste streams after centrifugation. This may be because the idioblast cell wall contains a specialized suberin layer rather than the single cellulosic wall of parenchyma cells, which makes the cell wall stronger and more resistant to grinding and enzymatic disruption (Platt-Aloia et al., 1983; Platt-Aloia et al., 1980). In previous studies, the oil in idioblast cells were extracted by chemical solvents and determined by thin layer chromatography and high performance liquid chromatography (Platt-Aloia et al., 1992; Domergue et al., 2000). Idioblast cells were isolated from soft, ripe avocado fruit by homogenization

and/or enzyme treatment to disrupt parenchyma cells, following by filtration through a 200-µm nylon mesh and 48-µm mesh to remove the TAG (released from parenchyma cells) and parenchyma cell debris (Platt-Aloia et al., 1992; Domergue et al., 2000). The oil in idioblast cells were obtained by chloroform: methanol 2:1 (v/v) extraction, and found to contain alkaloids and sesquiterpene hydroperoxides which inhibit the in vitro vegetative growth of the avocado fungal pathogen *Colletotrichum gloeosporioides* (Platt-Aloia et al., 1992; Domergue et al., 2000). Future idioblast oil research could involve evaluation of the contents of the idioblast cell for any functional ingredients or as antimicrobial agents.

8.2 Techniques for monitoring microstructural changes and oil aggregation

Rapid techniques for monitoring the extent of cellular disruption and oil aggregation will assist processors to maximize extraction yields and reduce processing times, to achieve greater throughputs with reduced costs. The light microscopy technique was used in this project to examine the microstructure changes in fruit mesocarp and pulp during the cold-pressed oil extraction of 'Hass' avocado and 'J5' olive fruit. Other techniques, including electrical impedance spectroscopy (EIS), electrical conductivity and rheological measurements were also applied in this study to obtain information about cellular disruption and oil aggregation in fruit pulp. For each extraction trial carried out in this project, the results from the various techniques showed a strong correlation to each other. For example, a reduction in electrical impedance was concurrent with an increase in conductivity of fruit tissue which occurred when cellular disruption was observed by light microscopy. These findings provided strong evidence of the usefulness of these techniques for monitoring and understanding cell disruption in cold-pressed oil extraction

systems.

For the light microscopy method, the microstructure of the fruit cell walls and the oil droplets at each step during the extraction process can be clearly observed. However, the most noticeable disadvantages of the light microscopy method is that it is expensive and time-consuming; the embedding and sectioning process for each batch of fruit flesh/pulp samples took 20–25 days to complete. Also, it is more difficult to obtain quantitative data from light microscopy images compared to other techniques used in this project. Nevertheless, microscopy images provided important information from the visual observation and appearance of the different cells and their cell wall structures in the fruit flesh/pulp, pomace and wastewater. The appearance of cells and their cell wall structures (i.e. cell wall swelling and cell wall intactness) could not be found using the other techniques employed in this project. The light microscopy method is a valuable tool for those who are carrying out research in this area.

EIS and electrical conductivity measurements were found to be useful tools to estimate the degree of cell intactness in avocado and olive fruit mesocarp during the cold-pressed oil extraction process. For example in Chapter 5, the results from EIS and electrical conductivity measurements showed a strong correlation with the light microscopy and cold-pressed oil yield results; results showed more cellular disruption occurred in the softer and late maturity avocado fruit. The EIS technique applies an electrical current to a fruit tissue sample and any cell wall and membrane disruption allows a low-frequency current to flow through the entire cross-section of the cell, this then results in a reduction in electrical resistance measured and semicircular arcs of the Nyquist plots of the samples disappear (Ando et al., 2014; Ohnishi et al., 2004). When a cell wall and membrane is

damaged during processing, the ions in cells diffuse through into the extracellular liquid which results in an increase in electrical conductivity of the fruit tissue sample (Pesis et al., 2003). Both of the EIS and electrical conductivity techniques are simple to use. In addition, the EIS technique only takes 10 seconds to measure the resistance and reactance values of electrical impedance at 500 mV over the frequency range from 50 Hz and 1 MHz by simply placing the two Ag/AgCl electrodes into the fruit flesh sample. The electrical conductivity measurement is relatively slow compared to the EIS technique, which requires the samples to be incubated in mannitol solution for 80 min before measuring the conductivity, but is much less work than microscopy.

The results in Chapter 6 and 7 show the viscosity and viscoelastic properties of fruit pulp are strongly correlated with the light microscopy and cold-pressed oil yield results. When oil droplets were observed to aggregate in fruit pulp, a decreased viscosity and *G'* value were detected by rheological properties measurements, and a higher cold-pressed oil yield was obtained. These findings indicated the measurement of the rheological properties of fruit pulp can provide information about the oil aggregation in the avocado and olive pulp during malaxing. The number of oil droplets in fruit pulp decreased when oil droplets aggregate into larger drops to form a continuous oil phase, which resulted in a decrease in the number of 'particle-particle' interactions between oil droplets and therefore a decrease in resistance to flow (viscosity) and solid-like behaviour (*G'*) of the pulp sample. It is reasonably fast to determine the viscosity or solid-like behaviour of fruit pulp sample by using a rheometer, which only takes 10–15 min.

During commercial cold-pressed oil extraction, the changes in the degree of cellular disruption and oil aggregation in fruit tissue are only monitored based on the experience

of the operation staff in the oil factory, by observing the surface of the tissue in the malaxer. The changes occurring in fruit tissue during the oil extraction process can be described, such as 'fruit pulp colour change from green to yellowish brown' and 'a very thin layer of oil phase is observed on top of the pulp in malaxer', but individuals may interpret these descriptions differently. However, there are some difficulties with this method since trained and experienced staff are required, training takes time, and the assessment is relatively subjective. It is also not easy to make the assessment quantitative. Therefore, rapid and quantitative techniques for monitoring cellular disruption and oil aggregation during avocado and olive oil extraction process could be important for the industry to assist in optimizing cold-pressed oil extraction yields and reduce processing time.

The EIS technique could be used commercially in the oil industry. It may not be necessary to measure the EIS over the whole frequency range from 50 Hz to 1 MHz in the oil factory, as the electrical resistance at 50 Hz was found to be enough to give a simple indication of the degree of cellular disruption in fruit tissue. An example of a potential solution is the Torrymeter, a small hand held impedance meter (Distell, Scotland, UK) designed for measuring the electrical resistance of skin and muscle flesh of fish at 50–60 Hz to determine the freshness of fish (Distell, 2019). However, a Torrymeter tested during this project did not give reproducible results for avocado pulp samples in the preliminary experiment. This may have been due to the different shape and/or type of electrodes, the different distance between electrodes, or a different generator voltage between Torrymeter and Hewlett-Packard Precision LCR Meter used in this research. A similar instrument as a Torrymeter could be designed with Ag/AgCl electrodes (2 mm diameter × 4 mm length, 10 mm apart) and a generator voltage of 500 mV to measure the cellular structure of fruit tissue at 50 Hz during commercial cold-pressed oil extraction.

The impedance will give a measure of cellular disruption but the key to obtaining an optimum oil yield during processing is to ensure all the oil has aggregated to larger droplets during malaxing. A rheological technique can be used commercially in oil industry to rapidly measure the degree of oil aggregation in fruit pulp tissue by simply comparing the viscosities of fruit pulp at a constant shear rate (e.g. 40 s^{-1}) or monitoring solid-like behaviour at a certain frequency using an oscillation technique (e.g. 0.5 Hz). Although rheometers can measure both the viscosity and the solid-like behaviour of fruit pulp tissue under various conditions and parameters, they can cost from US$40,000 for an entry-level system to upwards of US$200,000 for a full-featured and fully configurable research-level system (Labcompare, 2019). A viscometer is a simple instrument can only be used to measure the viscosity of sample at a limited range of shear rates and temperatures. However, viscometers are much cheaper than rheometers, which range from a few hundred dollars up to US $20,000 (Labcompare, 2019). Viscometers may be more suitable and economic for the commercial oil industry and simple versions should be explored.

As the majority of the research presented in this thesis is focused on 'Hass' avocados, then the application of the recommended impedance or rheology values as control measures to aim for could be different for different cultivars or fruit grown in different regions or climates. The avocado fruit cultivar, growing region and climate may have significant impacts on cell wall composition and oil composition in the fruit flesh, hence this research may need to be expanded to other cultivars e.g 'Fuerte' or fruit from other regions.

8.3 Improvements of cold-pressed avocado oil extraction process for the factory

The inefficient disruption of parenchyma cells in 'Hass' avocado mesocarp during grinding and the inability of the oil droplets to aggregate in avocado pulp during malaxing, leaving small oil droplets in the paste were found to be the two main reasons that lead to the loss of oil during cold-pressed 'Hass' avocado oil extraction.

Fully ripened avocado fruit (80 Fv) are recommended to be used for cold-pressed oil extraction in commercial factories to maximise oil yield while maintaining oil quality. In Olivado Ltd NZ's, Kerikeri plant, avocado fruit for oil production are ripened naturally without ethylene treatment. This has many disadvantages which may lead to the presence of unevenly ripened fruit and the requirements for regular sorting to separate ripe and unripe fruit and remove fruit with unacceptable levels of rots. It is suggested to design and build fruit ripening rooms at the factory to use ethylene treatment as a means of accelerating and synchronizing avocado fruit ripening (Hofman et al., 2002). Also, instruments for measuring fruit firmness, such as a Firmometer, are recommended to be used together with the traditional hand rating method which is currently used in the factory, to achieve a more accurate fruit firmness measurements (White et al., 2005). Ensuring staff are well trained in rapid assessment of ripeness and detecting rotten fruit is recommended.

Late maturity avocado fruit (fruit flesh dry matter content > 30%, g dry flesh/100 g fresh flesh) is more suitable to be used in oil production due to its higher total oil content in the fruit mesocarp and the loose polymer networks of the parenchyma cell which are easier to rupture. However, the fruit quality and maturity are sometimes difficult to control by

the oil manufacturers as the fruit for oil production is generally the "reject grade" fruit from commercial packhouses, which have not met export or local-market quality standards (Woolf et al., 2009). Therefore, an improved grinding system may also be required during the oil extraction from early maturity 'Hass' avocado. An attrition mill (Alfa Laval, Lund, Sweden) with rotational speed of 1,400 rpm is currently used in Olivado Ltd NZ's, Kerikeri plant for grinding of avocado and olive fruit. A hammer mill (Siemens, Munich, Germany) with aperture size of 4 mm and rotational speed of 2,855 rpm was used in the laboratory-based oil extraction in this project. The hammer mill may achieve more cellular disruption in avocado flesh than the attrition mill, as the EIS electrical resistance value at 50 Hz for the ground flesh from the hammer mill was significantly lower ($p < 0.05$) than that obtained from the attrition mill (Chapter 5 and 6; fruit are at a same firmness level of 80 Fv). A similar result was found by Amirante, Dugo, and Gomez (2002) and Caponio, Gomes, Summo, and Pasqualone (2003) on cold-pressed olive oil extraction, that the hammer mill resulted in a smaller stone fragment size than the attrition mill, which may have indicated a higher grinding efficiency. However, the hammer mill increased the olives temperature by 6 °C during grinding, whereas the olives temperature was raised by 4 °C when the fruit were ground by the attrition mill. The more substantial increase in olive pulp temperature given by the hammer mill had a major impact on the quality and shelf life of the resulting olive oil (Caponio & Catalano, 2001; Caponio et al., 2003). In cold-pressed avocado oil extraction, the oil quality and shelf life is likely to be not affected by the hammer mill due to the lower internal lipase level in avocado fruit which allows a higher processing temperature limit (50 °C) than that of virgin olive oil extraction (27 °C) (Wong et al., 2012). The laboratory-based cold-pressed oil extraction using a hammer mill and ripe avocado fruit at 80 Fv gave good quality avocado oils (Chapter 5 and 6). Therefore, a hammer mill grinder or a double grinding

system using an attrition mill following a hammer mill is recommended for commercial cold-pressed avocado oil extraction.

A malaxing process with 120 min to allow oil aggregation and at least 45 °C temperature is recommended, as it was found the longer malaxing time and higher malaxing temperature can decrease the viscosity of the avocado pulp and improve oil droplet aggregation, thus increasing cold-pressed oil yield. A more efficient heating system is also recommended to be used in cold-pressed avocado oil production. Warm water at 45–50 °C can be added during malaxing to help reduce pulp viscosity, hence allowing malaxing at higher shear rates and subsequently it makes it easier for the oil droplets to aggregate to form larger droplets (Petrakis, 2006; Wong et al., 2012). However, this process can increase the amounts of wastewater due to increased water utilization (Petrakis, 2006). Also, the addition of water may lead to emulsion problems in the extraction process (Wong et al., 2012). The relationship among the required malaxing time, the amount of additional water, and the cold-pressed oil yield are required to be investigated in future study.

Ultrasonication at 20–25 kHz also has the potential to be applied in the factory to improve the cold-pressed avocado oil yield by assisting in oil aggregation in the fruit pulp tissue. During malaxing, the avocado pulp is continuously stirred by the stainless steel blades which make it difficult to place an extra ultrasound probe in the centre of the malaxer. A specially designed malaxer with an ultrasound probe in the central axis could be used to apply ultrasound treatment in commercial oil factories. However, the ultrasound treatment for cold-pressed avocado oil extraction was only carried out in a small-scale (50 mL) laboratory experiment in current research, the results may still not be enough to

determine the benefits of ultrasound technique in the commercial factories. A pilot plant experiment is recommended before the ultrasound technique is applied in commercial cold-pressed oil extraction. In addition, ultrasonic noise may cause headache, dizziness, tinnitus, balance disturbances and nausea for workers exposed to ultrasounds of low frequencies at 10–40 kHz (Smagowska & Pawlaczyk-Łuszczyńska, 2013). Therefore, soundproofing systems would be needed around the malaxers to reduce noise.

During commercial cold-pressed oil extraction on early-season avocado fruit, around 3% (g of oil/100 g of fresh flesh) of oil was lost in both the solid and liquid waste streams (Chapter 4 and 6). This is because some oil droplets were trapped in the unbroken parenchyma cells and left in the pomace after decanting centrifugation. Also, a small number of free oil droplets did not aggregate into large enough droplets during malaxing, which cannot be recovered by centrifugation. A commercial chemical extraction system could be applied on the wastewater and the ground pomace to recover the oil from the waste streams by using hexane.

Chapter 9:

Overall conclusions and recommendations for future work

9.1 Overall conclusions

Based on the results of this project, it can be concluded that during both of the cold-pressed 'Hass' avocado and 'J5' olive oil extraction, oil was only recovered from the parenchyma cells in the flesh. The idioblast cells in the avocado flesh remained intact during the whole oil extraction process, and were removed into the waste streams. Adequate grinding of the fruit flesh played an important role to release the oil as it disrupted the cellular structure in the flesh.

'Hass' avocado fruit ripeness and fruit maturity can heavily affect the cold-pressed oil extraction. More parenchyma cell disruption occurred during extraction of softer and late maturity avocado fruit, which resulted in a higher cold-pressed extraction yield. Microstructural changes in the parenchyma cell walls during fruit ripening and maturation contribute to softer cell walls which are easily broken. The quality of the cold-pressed avocado oil decreased with fruit ripeness.

The malaxing step is a critical factor in oil extraction. Increasing the malaxing time and temperature promotes coalescence of oil droplets thus decreasing the number of interactions between oil droplets, which decreased the viscosity and reduced the solid-like behaviour of the avocado pulp and eventually resulted in a higher cold-pressed oil yield. The free fatty acids levels (FFA%) and peroxide values (PV) in the cold-pressed avocado oil did not increase significantly with malaxing temperature between 30 to 50 °C.

Ultrasound treatment at 20–25 kHz, when applied on both of the pre-malaxed and non-pre-malaxed avocado pulp, assisted oil aggregation in the pulp. Ultrasound treatment reduced the solid-like behaviour of the avocado pulp and increased the cold-pressed oil

yield.

In comparison to ‘Hass’ avocado, ‘J5’ olive pulp is less solid-like allowing the oil droplets to coalesce more easily in the fruit pulp during malaxing.

9.2 Recommendations for future work

Based on the findings of the present study and literature, suggestions for future work are as follows:

- Determine the amount of pectin with galactan and arabinan side chains in the cell wall of ‘Hass’ avocado fruit at various maturation stage, by using 0.05 M Na_2CO_3, 1 M KOH and 4 M KOH successively to treat the cell walls following the extraction by CDTA. This future research will provide more fundamental knowledge of cellular changes in avocado cell walls during maturation which has not been published before. This could also lead to providing recommendations for the application of commercial exogenous enzymes in the extraction process to assist disruption of cell walls in early maturity fruit.
- Investigate the effect of avocado fruit ripeness, malaxing temperature and ultrasound treatment on fatty acid composition, total vitamin E content, stability, smoke point and sensory characteristics during cold-pressed oil extraction of ‘Hass’ avocado. As the research presented in this thesis did not investigate the chemical, quality and sensory changes in the resulting avocado oil dependent on maturity, ripeness or processing conditions, these aspects will be important to further help commercial oil factories to maximise oil yield while maintaining oil quality and will determine if any of these processes are detrimental to avocado oil composition and quality.

- Study on the effect of laboratory-based ultrasound treatment at 20–25 kHz on cold-pressed avocado oil yield when it is applied simultaneously with malaxing at 45 ± 1 °C, by malaxing the avocado pulp in a specially designed 1 L ultrasonic bath or using a specially designed laboratory-based malaxer with placing the ultrasound probe into the rotation axis in the malaxer. The application of ultrasound will need to be evaluated at different conditions and at a pilot scale process as all results presented in this thesis are with a laboratory ultrasound probe. Results obtained may vary considerably, hence these will need to be carried out before recommendations are made for the application of ultrasound in a commercial cold-pressed oil extraction plant.
- Determine the influence of a double grinding system (using a attrition mill following a hammer mill for grinding) on cold-pressed avocado oil yield, fatty acid composition, total vitamin E content, stability, smoke point and sensory characteristics of the resulting avocado oil during cold-pressed oil extraction of 'Hass' avocado. This future research could explore a more efficient grinding systems which would lead to greater disruption of the avocado fruit cell walls ultimately releasing more oil during malaxing for application in commercial oil factories and increase the cold-pressed extraction oil yield. As grinding can generate considerable heat, its impact on oil composition and quality will be important.

References

Aguilera, J. M. (2005). Why food microstructure? *Journal of Food Engineering, 67*(1), 3-11.

Ahmed, D. M., Yousef, A. R., & Hassan, H. (2010). Relationship between electrical conductivity, softening and color of Fuerte avocado fruits during ripening. *Agriculture and Biology Journal of North America, 1*(5), 878-885.

Ahmed, J., & Ramaswamy, H. S. (2006). Viscoelastic properties of sweet potato puree infant food. *Journal of Food Engineering, 74*(3), 376-382.

Alberts, B., Johnson, A., Lewis, J., Raff, M., Roberts, K., & Walter, P. (2002). Molecular biology of the cell. New York: Garland Science.

Amirante, P., Dugo, G., & Gomez, T. (2002). Influence of technological innovation in improving the quality of extra virgin olive oil. *Olivae, 93*(34–42).

Amirante, R., Cini, E., Montel, G., & Pasqualone, A. (2001). Influence of mixing and extraction parameters on virgin olive oil quality. *Grasas y Aceites, 52*(3-4), 198-201.

Ando, Y., Mizutani, K., & Wakatsuki, N. (2014). Electrical impedance analysis of potato tissues during drying. *Journal of Food Engineering, 121*, 24-31.

AOCS. (2009). Official methods and recommended practices of the American Oil Chemists' Society. Champaign: American Oil Chemists'Society.

Ashton, O. B. O., Wong, M., McGhie, T. K., Vather, R., Wang, Y., Requejo-Jackman, C., Ramankutty, P., & Woolf, A. B. (2006). Pigments in avocado tissue and oil. *Journal of Agricultural and Food Chemistry, 54*(26), 10151-10158.

Avocadosource. (2006). Retrieved 10/11/2018 from http://www.avocadosource.com/world.asp

Awad, M., & Young, R. E. (1979). Postharvest variation in cellulase, polygalacturonase, and pectinmethylesterase in avocado (Persea americana Mill, cv. Fuerte) fruits in relation to respiration and ethylene production. *Plant Physiology, 64*(2), 306-308.

Barbosa-Cánovas, G. V., Kokini, J. L., Ma, L., & Ibarz, A. (1996). The rheology of semiliquid foods. In *Advances in food and nutrition research* (Vol. 39, pp. 1-69). Burlington, Massachusetts: Elsevier.

Barmore, C. R. (1977). Avocado fruit maturity. In J. W. Sauls, R. L. Phillips, & L. K. Jackson (Eds.), *Proceedings of the first international tropical fruit short course: the avocado* (pp. 103-109). Gainesville, Florida: Fruit Crops Department, Florida

Cooperative Extension Service, Institute of Food and Agricultural Sciences, University of Florida.

Barnes, H. A. (1999). The yield stress—a review or ‘παντα ρει’—everything flows? *Journal of Non-Newtonian Fluid Mechanics, 81*(1-2), 133-178.

Batchelor, G. K. (2000). An introduction to fluid dynamics. Cambridge, England: Cambridge University Press.

Bauchot, A. D., Harker, F. R., & Arnold, W. M. (2000). The use of electrical impedance spectroscopy to assess the physiological condition of kiwifruit. *Postharvest Biology and Technology, 18*(1), 9-18.

Bayod, E., Willers, E. P., & Tornberg, E. (2008). Rheological and structural characterization of tomato paste and its influence on the quality of ketchup. *LWT-Food Science and Technology, 41*(7), 1289-1300.

Bejaoui, M. A., Beltran, G., Aguilera, M. P., & Jimenez, A. (2016). Continuous conditioning of olive paste by high power ultrasounds: Response surface methodology to predict temperature and its effect on oil yield and virgin olive oil characteristics. *LWT-Food Science and Technology, 69*, 175-184.

Beltrán, G., del Río, C., Sánchez, S., & Martínez, L. (2004). Seasonal changes in olive fruit characteristics and oil accumulation during ripening process. *Journal of the Science of Food and Agriculture, 84*(13), 1783-1790.

Bermúdez-Aguirre, D., Mobbs, T., & Barbosa-Cánovas, G. V. (2011). Ultrasound applications in food processing. In H. Feng, G. V. Barbosa-Cánovas, & J. Weiss (Eds.), *Ultrasound technologies for food and bioprocessing* (pp. 65-105). New York: Springer.

Bettelheim, F., Brown, W., Campbell, M., Farrell, S., & Torres, O. (2010). Enzymes. In *Introduction to general, organic and biochemistry* (pp. 614-628). Belmont, California: Nelson Education.

Bizimana, V., Breene, W. M., & Csallany, A. S. (1993). Avocado oil extraction with appropriate technology for developing countries. *Journal of the American Oil Chemists' Society, 70*(8), 821-822.

Boskou, D. (2006). *Olive oil: chemistry and technology*. Champaign, Illinois: AOCS Press.

Bost, J. B., Smith, N. J. H., & Crane, J. H. (2013). History, distribution and uses. In B. Schaffer, B. N. Wolstenholme, & A. W. Whiley (Eds.), *The avocado: botany,*

production and uses (2 ed., pp. 10-31). Wallingford, Oxon: CAB International Press.

Bower, J. P. (1988). Pre-and postharvest measures for long-term storage of avocados. *South African Avocado Growers' Association Yearbook, 11*, 68-72.

Brown, A. C. (2007). Understanding food: principles and preparation. Stamford, Connecticut: Cengage Learning.

Brown, B. I. (1984). Market maturity indices and sensory properties of avocados grown in Queensland. *Food Technology in Australia, 37*, 474-476.

Brummell, D. A. (2006a). Cell wall disassembly in ripening fruit. *Functional Plant Biology, 33*(2), 103-119.

Brummell, D. A. (2006b). Primary cell wall metabolism during fruit ripening. *New Zealand Journal of Forestry Science, 36*(1), 99.

Buenrostro, M., & López-Munguia, A. C. (1986). Enzymatic extraction of avocado oil. *Biotechnology Letters, 8*(7), 505-506.

Burgess, J., Marten, M., & Taylor, R. (1990). Under the microscope: a hidden world revealed. Cambridge, England: Cambridge University Press.

Burke, M. J., Gusta, L. V., Quamme, H. A., Weiser, C. J., & Li, P. H. (1976). Freezing and injury in plants. *Annual Review of Plant Physiology, 27*(1), 507-528.

Campbell, K. A., & Glatz, C. E. (2009). Mechanisms of aqueous extraction of soybean oil. *Journal of Agricultural and Food Chemistry, 57*(22), 10904-10912.

Caponio, F., & Catalano, P. (2001). Hammer crushers vs disk crushers: the influence of working temperature on the quality and preservation of virgin olive oil. *European Food Research and Technology, 213*(3), 219-224.

Caponio, F., Gomes, T., Summo, C., & Pasqualone, A. (2003). Influence of the type of olive‐crusher used on the quality of extra virgin olive oils. *European Journal of Lipid Science and Technology, 105*(5), 201-206.

Clodoveo, M. L. (2012). Malaxation: Influence on virgin olive oil quality. Past, present and future–An overview. *Trends in Food Science & Technology, 25*(1), 13-23.

Clodoveo, M. L., Durante, V., La Notte, D., Punzi, R., & Gambacorta, G. (2013). Ultrasound‐assisted extraction of virgin olive oil to improve the process efficiency. *European Journal of Lipid Science and Technology, 115*(9), 1062-1069.

Clodoveo, M. L., & Hbaieb, R. H. (2013). Beyond the traditional virgin olive oil extraction systems: Searching innovative and sustainable plant engineering solutions. *Food Research International, 54*(2), 1926-1933.

Codex Alimentarius. (2017). Proposed draft revision to the Standard for Olive Oils and Olive Pomace Oils (CODEX STAN 33-1981): Revision of the Limit for Campesterol. Retrieved 06/09/2017 from http://www.fao.org/fao-who-codexalimentarius/en/

Coppen, P. P. (1994). Use of antioxidants. In J. C. Allen & R. J. Hamilton (Eds.), *Rancidity in foods* (pp. 84-103). London, England: Blackie Academic & Professional.

Costagli, G., & Betti, M. (2015). Avocado oil extraction processes: method for cold-pressed high-quality edible oil production versus traditional production. *Journal of Agricultural Engineering, 46*(3), 115-122.

Cox, K. A., McGhie, T. K., White, A., & Woolf, A. B. (2004). Skin colour and pigment changes during ripening of 'Hass' avocado fruit. *Postharvest Biology and Technology, 31*(3), 287-294.

Crane, J. H., Douhan, G., Faber, B. A., Arpaia, M. L., Bender, G. S., Balerdi, C. F., & Barrientos-Priego, A. F. (2013). Cultivars and rootstocks. In B. Schaffer, B. N. Wolstenholme, & A. W. Whiley (Eds.), *The avocado: botany, production and uses* (pp. 200-234). Wallingford, Oxon: CAB International Press.

Criado, M., Motilva, M., Goñi, M., & Romero, M. (2007). Comparative study of the effect of the maturation process of the olive fruit on the chlorophyll and carotenoid fractions of drupes and virgin oils from Arbequina and Farga cultivars. *Food Chemistry, 100*(2), 748-755.

Crookes, P. R., & Grierson, D. (1983). Ultrasturcture of tomato fruit ripening and role of polygalacturonase isoenzymes. *Plant Physiology, 72*(4), 1088-1093.

Cummings, K., & Schroeder, C. A. (1942). Anatomy of the avocado fruit. *California Avocado Society Yearbook, 27*, 56-64.

Cutting, J. G., & Wolstenholme, B. N. (1992). Maturity effects on avocado postharvest physiology in fruit produced under cool environmental conditions. Paper presented at the Proceedings of the Second World Avocado Congress.

De Greyt, W., & Kellens, M. (2000). Refining practice. In W. Hamm & R. J. Hamilton (Eds.), *Edible oil processing* (pp. 79-127). Sheffield, England: Sheffield Academic Press.

Dean, J. R. (2010). Classical approaches for solid-liquid extraction. In *Extraction techniques in analytical sciences* (Vol. 34, pp. 127-139). Chichester, West sussex: John Wiley & Sons.

Defilippi, B. G., Ejsmentewicz, T., Covarrubias, M. P., Gudenschwager, O., & Campos-Vargas, R. (2018). Changes in cell wall pectins and their relation to postharvest mesocarp softening of "Hass" avocados (Persea americana Mill.). *Plant Physiology and Biochemistry, 128*, 142-151.

Dejmek, P., & Miyawaki, O. (2002). Relationship between the electrical and rheological properties of potato tuber tissue after various forms of processing. *Bioscience, Biotechnology, and Biochemistry, 66*(6), 1218-1223.

Di Giovacchino, L. (1989). Olive processing systems. Separation of the oil from the must. *Olivae, 26*, 21-29.

Di Giovacchino, L. (1996). Influence of extraction systems on olive oil quality. *Olivae, 63*, 52-63.

Di Giovacchino, L., Costantini, N., Ferrante, M., & Serraiocco, A. (2002a). Influence of malaxation time of olive paste on oil extraction yields and chemical and organoleptic characteristics of virgin olive oil obtained by a centrifugal decanter at water saving. *Grasas y Aceites, 53*(2), 179-186.

Di Giovacchino, L., Sestili, S., & Di Vincenzo, D. (2002b). Influence of olive processing on virgin olive oil quality. *European Journal of Lipid Science and Technology, 104*, 587-601.

Distell. (2019). Retrieved 15/02/2019 from https://www.distell.com/

Dixon, J., Lamond, C. B., Smith, D. B., & Elmlsy, T. A. (2006). Patterns of fruit growth and fruit drop of 'Hass' avocado trees in the Western Bay of Plenty, New Zealand. *New Zealand Avocado Grower's Association Annual Research Report, 6*, 47-54.

Domergue, F., Helms, G. L., Prusky, D., & Browse, J. (2000). Antifungal compounds from idioblast cells isolated from avocado fruits. *Phytochemistry, 54*(2), 183-189.

Dorantes-Alvarez, L., Ortiz-Moreno, A., & Garcia-Ochoa, F. (2012). Avocado. In M. Siddiq, J. Ahmed, M. G. Lobo, & F. Ozadali (Eds.), *Tropical and subtropical fruits: postharvest physiology, processing and packaging* (pp. 437-454). Ames, Iowa: John Wiley & Sons.

Duester, K. C. (2001). Avocado fruit is a rich source of beta-sitosterol. *Journal of the American Dietetic Association, 101*, 404-405.

Eaks, I. L. (1990). Change in the fatty acid composition of avocado fruit during ontogeny, cold storage and ripening. *Acta Horticulturae, 269*, 141-151.

Edwards, M. (2007). The development of the New Zealand extra virgin olive oil industry. In *Handbook of Australasian edible oils* (pp. 38-81). Auckland, New Zealand: Oils and Fats Specialist Group of the New Zealand Institute of Chemistry.

Ellis, E. A. (2006). Corrected formulation for Spurr low viscosity embedding medium using the replacement epoxide ERL 4221. *Microscopy and Microanalysis, 12*(S02), 288-289.

Ersus, S., & Barrett, D. M. (2010). Determination of membrane integrity in onion tissues treated by pulsed electric fields: use of microscopic images and ion leakage measurements. *Innovative Food Science & Emerging Technologies, 11*(4), 598-603.

European Commission. (2002). No 796/2002 of 6 May 2002 amending Regulation (EEC) No 2568/91 on the characteristics of olive oil and olive pomace oil and on the relevant methods of analysis and the additional notes in the Annex to Council Regulation (EEC) No 2658/87 on the tariff and statistical nomenclature and on the Common Customs Tariff. Retrieved 06/09/2017 from http://eur-lex.europa.eu/legal-content/EN/TXT/?uri=LEGISSUM:l11054

Eyres, L., Sherpa, N., & Hendriks, G. (2001). Avocado oil: a new edible oil from Australasia. *Lipid Technology, 13*(4), 84-88.

FAOSTAT. (2018). Food and Agriculture Organisation of United Nations. Retrieved 08/05/2018 from http://faostat3.fao.org/

Fasmin, F., & Srinivasan, R. (2017). Nonlinear electrochemical impedance spectroscopy. *Journal of The Electrochemical Society, 164*(7), H443-H455.

Fava, J., Alzamora, S. M., & Castro, M. A. (2006). Structure and nanostructure of the outer tangential epidermal cell wall in vaccinium corymbosum L.(Blueberry) fruits by blanching, freezing-thawing and ultrasound. *Food Science and Technology International, 12*(3), 241-251.

Fernandes, F. A. N., Gallão, M. I., & Rodrigues, S. (2008). Effect of osmotic dehydration and ultrasound pre-treatment on cell structure: melon dehydration. *LWT-Food Science and Technology, 41*(4), 604-610.

Fernandes, F. A. N., Gallão, M. I., & Rodrigues, S. (2009). Effect of osmosis and ultrasound on pineapple cell tissue structure during dehydration. *Journal of Food Engineering, 90*(2), 186-190.

Frankel, E. N. (2014). Lipid oxidation (2 ed.). Cambridge, England: Woodhead Publishing Ltd.

Fuentes, A., Vázquez-Gutiérrez, J. L., Pérez-Gago, M. B., Vonasek, E., Nitin, N., & Barrett, D. M. (2014). Application of nondestructive impedance spectroscopy to determination of the effect of temperature on potato microstructure and texture. *Journal of Food Engineering, 133*, 16-22.

Gallegos, C., & Franco, J. M. (1999). Rheology of food, cosmetics and pharmaceuticals. *Current Opinion in Colloid & Interface Science, 4*(4), 288-293.

Gao, X., Yu, T., Zhang, Z. H., Xu, J. C., & Fu, X. T. (2011). Rheological and sensory properties of four kinds of jams. *Journal of Stored Products and Postharvest Research, 2*(11), 227-234.

García, J. M., Gutiérrez, F., Castellano, J. M., Perdiguero, S., Morilla, A., & Albi, M. A. (1996). Influence of storage temperature on fruit ripening and olive oil quality. *Journal of Agricultural and Food Chemistry, 44*(1), 264-267.

Gavahian, M., Farhoosh, R., Farahnaky, A., Javidnia, K., & Shahidi, F. (2015). Comparison of extraction parameters and extracted essential oils from Mentha piperita L. using hydrodistillation and steamdistillation. *International Food Research Journal, 22*(1), 283-288.

Gonzalez, M. E., & Barrett, D. M. (2010). Thermal, high pressure, and electric field processing effects on plant cell membrane integrity and relevance to fruit and vegetable quality. *Journal of Food Science, 75*(7).

Gonzalez, M. E., Jernstedt, J. A., Slaughter, D. C., & Barrett, D. M. (2010). Microscopic quantification of cell integrity in raw and processed onion parenchyma cells. *Journal of Food Science, 75*(7), 402-408.

Grove. (2018). Retrieved 28/05/2018 from https://avocado-oil.co.nz/product-range/

Guldhe, A., Singh, B., Ansari, F. A., Sharma, Y., & Bux, F. (2016). Extraction and conversion of microalgal lipids. In F. Bux & Y. Chisti (Eds.), *Algae biotechnology: products and processes* (pp. 91-110). Cham, Switzerland: Springer.

Gupta, P. K. (2007). Plant tissue and tissue system. In *Genetics classical to modern* (pp. 247-272). New Delhi, India: Rastogi Publications.

Halder, A., Datta, A. K., & Spanswick, R. M. (2011). Water transport in cellular tissues during thermal processing. *AIChE Journal, 57*(9), 2574-2588.

Harker, F. R., & Dunlop, J. (1994). Electrical impedance studies of nectarines during coolstorage and fruit ripening. *Postharvest Biology and Technology, 4*(1), 125-134.

Harker, F. R., & Forbes, S. K. (1997). Ripening and development of chilling injury in persimmon fruit: an electrical impedance study. *New Zealand Journal of Crop and Horticultural Science, 25*(2), 149-157.

Harker, F. R., & Maindonald, J. H. (1994). Ripening of nectarine fruit: changes in the cell wall, vacuole, and membranes detected using electrical impedance measurements. *Plant Physiology, 106*(1), 165-171.

Harker, F. R., White, A., Freeth, B., Gunson, F. A., & Triggs, C. M. (2003). Simultaneous instrumental measurement of firmness and juiciness of apple tissue discs. *Journal of Texture Studies, 34*(3), 271-285.

Hatfield, R., & Nevins, D. J. (1986). Characterization of the hydrolytic activity of avocado cellulase. *Plant and Cell Physiology, 27*(3), 541-552.

Hayden, R. I., Moyse, C. A., Calder, F. W., Crawford, D. P., & Fensom, D. S. (1969). Electrical impedance studies on potato and alfalfa tissue. *Journal of Experimental Botany, 20*(2), 177-200.

Hershkovitz, V., Saguy, S. I., & Pesis, E. (2005). Postharvest application of 1-MCP to improve the quality of various avocado cultivars. *Postharvest Biology and Technology, 37*(3), 252-264.

Hill, A., & Carrington, S. (2006). Understanding the links between rheology and particle parameters. *American Laboratory, 38*(21), 22.

Hofman, P. J., Fuchs, Y., Milne, D. L., Whiley, A. W., Schaffer, B., & Wolstenholme, B. N. (2002). Harvesting, packing, postharvest technology, transport and processing. In A. W. Whiley, B. Schaffer, & B. N. Wolstenholme (Eds.), *The avocado: botany, production and uses* (1 ed., pp. 363-401). Wallingford, Oxon: CAB International Press.

Hopkirk, G. (1989). Avocado Maturity Assessment. *Division of Horticulture and Processing. DSIR*.

Hopkirk, G., White, A., Beever, D., & Forbes, S. (1994). Influence of postharvest temperatures and the rate of fruit ripening on internal postharvest rots and disorders of New Zealand 'Hass' avocado fruit. *New Zealand Journal of Crop and Horticultural Science, 22*(3), 305-311.

Huber, D. J., & O'Donoghue, E. M. (1993). Polyuronides in avocado (Persea americana) and tomato (Lycopersicon esculentum) fruits exhibit markedly different patterns of molecular weight downshifts during ripening. *Plant Physiology, 102*(2), 473-480.

Human, T. P. (1987). Oil as a byproduct of the avocado. *South African Avocado Grower's Assoc. Yearbook, 10*, 159-162.

Inoue, H., & Tateishi, A. (1995). Ripening and fatty acid composition of avocado fruit in Japan. Paper presented at the Proceedings of The World Avocado Congress III.

International Olive Council. (2006). Trade standard applying to olive oils and oilve-pomace oils. Retrieved 01/09/2017 from http://www.internationaloliveoil.org

Ishikawa, E., Seoung-Kwon, B., Miyawaki, O., Nakamura, K., Shiinoki, Y., & Ito, K. (1997). Freezing injury of cultured rice cells analyzed by dielectric measurement. *Journal of Fermentation and Bioengineering, 83*(3), 222-226.

Jackson, P. J., & Harker, F. R. (2000). Apple bruise detection by electrical impedance measurement. *HortScience, 35*(1), 104-107.

Jacobsen, C., Let, M. B., Nielsen, N. S., & Meyer, A. S. (2008). Antioxidant strategies for preventing oxidative flavour deterioration of foods enriched with n-3 polyunsaturated lipids: a comparative evaluation. *Trends in Food Science & Technology, 19*(2), 76-93.

Jarvis, M. C. (1982). The proportion of calcium-bound pectin in plant cell walls. *Planta, 154*(4), 344-346.

Jarvis, M. C., Hall, M. A., Threlfall, D. R., & Friend, J. (1981). The polysaccharide structure of potato cell walls: chemical fractionation. *Planta, 152*(2), 93-100.

Jeong, J., Huber, D. J., & Sargent, S. A. (2002). Influence of 1-methylcyclopropene (1-MCP) on ripening and cell-wall matrix polysaccharides of avocado (Persea americana) fruit. *Postharvest Biology and Technology, 25*(3), 241-256.

Jiménez, A., Beltrán, G., & Uceda, M. (2007). High-power ultrasound in olive paste pretreatment. Effect on process yield and virgin olive oil characteristics. *Ultrasonics Sonochemistry, 14*(6), 725-731.

Jirgensons, B., & Straumanis, M. E. (2013). The kinetic properties of disperse systems. In *A short textbook of colloid chemistry* (pp. 33-43). Oxford, England: Pergamon Press.

Johnson, L. A. (1997). Theoretical, comparative, and historical analyses of alternative technologies for oilseeds extraction. In P. J. Wan & P. J. Wakelyn (Eds.),

Technology and solvents for extracting oilseeds and nonpetroleum oils (pp. 16-18). Champaign, Illinois: AOCS Press.

Juliano, P., Augustin, M. A., Xu, X.-Q., Mawson, R., & Knoerzer, K. (2017). Advances in high frequency ultrasound separation of particulates from biomass. *Ultrasonics Sonochemistry, 35*, 577-590.

Juliano, P., Kutter, A., Cheng, L. J., Swiergon, P., Mawson, R., & Augustin, M. (2011). Enhanced creaming of milk fat globules in milk emulsions by the application of ultrasound and detection by means of optical methods. *Ultrasonics Sonochemistry, 18*(5), 963-973.

Juliano, P., Swiergon, P., Lee, K., Gee, P., Clarke, P., & Augustin, M. (2013a). Effects of pilot plant-scale ultrasound on palm oil separation and oil quality. *Journal of the American Oil Chemists' Society, 90*(8), 1253-1260.

Juliano, P., Swiergon, P., Mawson, R., Knoerzer, K., & Augustin, M. (2013b). Application of ultrasound for oil separation and recovery of palm oil. *Journal of the American Oil Chemists' Society, 90*(4), 579-588.

Kailis, S., & Harris, D. J. (2007). Producing table olives. Collingwood, Australia: Landlinks Press.

Kaiser, C. (1993). Vascular and associated tissue of 'Hass' avocado (Persea americana Mill.) Fruit. *South Africa Avocado Growers' Association Yearbook, 16*, 22-27.

Kaiser, C., Smith, M. T., & Wolstenholme, B. N. (1992). Overview of lipids in the avocado fruit, with particular reference to the Natal Midlands. *South African Avocado Growers' Association Yearbook, 15*, 78-82.

Kidmose, U., Edelenbos, M., Nørbæk, R., Christensen, L., & MacDougall, D. (2002). Colour stability in vegetables. In D. B. MacDougall (Ed.), *Colour in food: Improving quality* (pp. 179-232). Cambridge, England: CRC Press.

Kikuta, Y., & Erickson, L. C. (1968). Seasonal changes of avocado lipids during fruit development and storage. *California Avocado Society Yearbook, 52*, 102-108.

Kiritsakis, A., Nanos, G., Polymenopulos, Z., Thomai, T., & Sfakiotakis, E. (1998). Effect of fruit storage conditions on olive oil quality. *Journal of the American Oil Chemists' Society, 75*(6), 721-724.

Kou, D., & Mitra, S. (2004). Extraction of semivolatile organic compounds from solid matrices. In S. Mitra (Ed.), *Sample preparation techniques in analytical chemistry* (Vol. 237, pp. 139-182). Hoboken, New Jersey: John Wiley & Sons.

Kris-Etherton, P. M. (1999). Monounsaturated fatty acids and risk of cardiovascular disease. *Circulation, 100*(11), 1253-1258.

Labcompare. (2019). Rheometry Buyers' Guide. Retrieved 15/02/2019 from https://www.labcompare.com

Lapasin, R., & Pricl, S. (1995). Rheology of polysaccharide systems. In *Rheology of industrial polysaccharides: Theory and applications* (pp. 250-494). Glasgow, Scotland: Blackie Academic and Professional.

Larson, R. G. (1999). The structure and rheology of complex fluids (Vol. 150). New York: Oxford University Press.

Lasia, A. (2014). Electrochemical impedance spectroscopy and its applications. New York: Springer.

Lawes, G. S. (1980). Maturity and quality in avocados. *Orchardist of New Zealand, 53*(2), 63-64.

Lee, S. K., & Young, R. E. (1983). Growth measurement as an indication of avocado maturity. *Journal of the American Society for Horticultural Science, 108*(3), 395-397.

Lee, S. K., Young, R. E., Schiffman, P. M., & Coggins, C. W. (1983). Maturity studies of avocado fruit based on picking dates and dry weight. *Journal of the American Society for Horticultural Science, 108*(3), 390-394.

Lewis, C. E. (1978). The maturity of avocados— a general review. *Journal of the Science of Food and Agriculture, 29*(10), 857-866.

Llano, K. M., Haedo, A. S., Gerschenson, L. N., & Rojas, A. M. (2003). Mechanical and biochemical response of kiwifruit tissue to steam blanching. *Food Research International, 36*(8), 767-775.

Lu, Q.-Y., Arteaga, J. R., Zhang, Q., Huerta, S., Go, V. L. W., & Heber, D. (2005). Inhibition of prostate cancer cell growth by an avocado extract: role of lipid-soluble bioactive substances. *The Journal of Nutritional Biochemistry, 16*(1), 23-30.

Luque Garcìa, J. L., & Luque de Castro, M. D. (2003). Ultrasound: a powerful tool for leaching. *TrAC Trends in Analytical Chemistry, 22*(1), 41-47.

Lvovich, V. F. (2012). Impedance spectroscopy: applications to electrochemical and dielectric phenomena. Hoboken, New Jersey: John Wiley & Sons.

Macdonald, J. R., & Johnson, W. B. (2005). Fundamentals of impedance spectroscopy. In E. Barsoukov & J. R. Macdonald (Eds.), *Impedance spectroscopy: theory,*

experiment, and applications (second ed., pp. 1-20). Hoboken, New Jersey: John Wiley & Sons.

Marsilio, V., Lanza, B., & Angelis, M. D. (1996). Olive cell wall components: physical and biochemical changes during processing. *Journal of the Science of Food and Agriculture, 70*(1), 35-43.

Martínez-Padilla, L. P., Franke, L., & Juliano, P. (2017). Characterisation of the viscoelastic properties of avocado puree for process design applications. *Biosystems Engineering, 161*, 62-69.

Masot, R., Alcañiz, M., Fuentes, A., Schmidt, F. C., Barat, J. M., Gil, L., Baigts, D., Martínez-Máñez, R., & Soto, J. (2010). Design of a low-cost non-destructive system for punctual measurements of salt levels in food products using impedance spectroscopy. *Sensors and Actuators A: Physical, 158*(2), 217-223.

Mercer, P., & Armenta, R. E. (2011). Developments in oil extraction from microalgae. *European Journal of Lipid Science and Technology, 113*(5), 539-547.

Mínguez-Mosquera, M. I., Gandul-Rojas, B., Gallardo-Guerrero, L., Roca, M., & Jarén-Galán, M. (2008). Chlorophylls. In W. J. Hurst (Ed.), *Methods of analysis for functional foods and nutraceuticals* (pp. 337–400). Boca Raton, Florida: CRC Press.

Miri, T. (2011). Viscosity and oscillatory rheology. In I. T. Norton, F. Spyropoulos, & P. Cox (Eds.), *Practical food rheology: an interpretive approach* (pp. 7-28). Chichester, West Sussex: Blackwell Publishing Ltd.

Montoro, P., Masullo, M., Piacente, S., & Pizza, C. (2015). Extraction, sample preparation, and analytical methods for quality issues of essential oils. In G. Bagetta, M. Cosentino, & T. Sakurada (Eds.), *Aromatherapy: basic mechanisms and evidence based clinical use* (pp. 110). Boca Raton, Florida: CRC Press.

Montoya, M., De La Plaza, J., & Lopez-Rodriguez, V. (1994). Electrical conductivity of avocado fruits during cold storage and ripening. *LWT-Food Science and Technology, 27*(1), 34-38.

Moore-Gordon, C., Cutting, J. G. M., & Wolstenholme, B. N. (1994). Progress report: a preliminary report on the effect of mulching on 'Hass' avocado fruit growth. *South African Avocado Growers' Association Yearbook, 17*, 83-87.

Morris, R., & O'Brien, K. (1980). Testing avocados for maturity. *California Avocado Society Yearbook, 64*, 67-70.

Mostert, M. E., Botha, B. M., Du Plessis, L. M., & Duodu, K. G. (2007). Effect of fruit ripeness and method of fruit drying on the extractability of avocado oil with hexane and supercritical carbon dioxide. *Journal of the Science of Food and Agriculture, 87*(15), 2880-2885.

MRC Ltd. (2018). Retrieved 06/19/2018 from https://www.mrclab.com

New Zealand Avocado. (2019). Retrieved 03/10/2019 from https://www.nzavocado.co.nz/

Ohnishi, S., Fujii, T., & Miyawaki, O. (2002). Electrical and rheological analysis of freezing injury of agricultural products. *International Journal of Food Properties, 5*(2), 317-332.

Ohnishi, S., Shimiya, Y., Kumagai, H., & Miyawaki, O. (2004). Effect of freezing on electrical and rheological properties of food materials. *Food Science and Technology Research, 10*(4), 453-459.

Olivado. (2018). Retrieved 28/05/2018 from https://www.olivado.com/shop/nz

Ortiz, M. A., Dorantes, A. L., Gallndez, M. J., & Cardenas, S. E. (2004). Effect of a novel oil extraction method on avocado (Persea americana Mill) pulp microstructure. *Plant Foods for Human Nutrition, 59*(1), 11-14.

Owusu-Ansah, Y. J. (1997). Enzyme-assisted extractions. In P. J. Wan & P. J. Wakelyn (Eds.), *Technology and solvents for extracting oilseeds and nonpetroleum oils* (pp. 323 – 332). Champaign, Illinois: AOCS Press.

Pak, H. A., Dixon, J., & Cutting, J. G. M. (2003). Influence of Early Season Maturity on Fruit Quality in New Zealand 'Hass' Avocados. Paper presented at the Proceedings of the fifth world avocado congress.

Pal, R. (1996). Effect of droplet size on the rheology of emulsions. *AIChE Journal, 42*(11), 3181-3190.

Palta, J. P., Levitt, J., & Stadelmann, E. J. (1977). Freezing injury in onion bulb cells I. Evaluation of the conductivity method and analysis of ion and sugar efflux from injured cells. *Plant Physiology, 60*(3), 393-397.

Paz-Vega, R. (2015). Avocado production, marketing and consumption: a global perspective. Paper presented at the Proceedings of the VIII World Avocado Congress, Lima, Peru.

Pearson, D. (1975). Seasonal English market variations in the composition of South African and Israeli avocados. *Journal of the Science of Food and Agriculture, 26*(2), 207-213.

Pesis, E., Krilo, V., Feygenberg, O., Ackerman, M., Arie, R. B., & Prusky, D. (2003). Postharvest effect of 1-MCP on ripening of avocado CV. ettinger. In M. Vendrell (Ed.), *Biology and biotechnology of the plant hormone ethylene III* (Vol. 349, pp. 397-407). Amsterdam, Netherlands: IOS Press.

Petrakis, C. (2006). Olive oil extraction. In D. Boskou (Ed.), *Olive oil: chemistry and technology* (2nd ed., pp. 191-224). Urbana, Illinois: AOCS Press.

Petrovic, M., Eljarrat, E., De Alda, M. L., & Barceló, D. (2004). Endocrine disrupting compounds and other emerging contaminants in the environment: a survey on new monitoring strategies and occurrence data. *Analytical and Bioanalytical Chemistry, 378*(3), 549-562.

Phillips, K. M., Ruggio, D. M., Toivo, J. I., Swank, M. A., & Simpkins, A. H. (2002). Free and esterified sterol composition of edible oils and fats. *Journal of Food Composition and Analysis, 15*(2), 123-142.

Piironen, V., Lindsay, D. G., Miettinen, T. A., Toivo, J., & Lampi, A. M. (2000). Plant sterols: biosynthesis, biological function and their importance to human nutrition. *Journal of the Science of Food and Agriculture, 80*(7), 939-966.

Plant & Food Research Ltd. (2015). Fresh Facts: New Zealand horticulture. Retrieved 05/12/2016 from http://www.freshfacts.co.nz/files/freshfacts-2015.pdf

Platt-Aloia, K. A., Oross, J. W., & Thomson, W. W. (1983). Ultrastructural study of the development of oil cells in the mesocarp of avocado fruit. *Botanical Gazette, 144*(1), 49-55.

Platt-Aloia, K. A., & Thomson, W. W. (1981). Ultrastructure of the mesocarp of mature avocado fruit and changes associated with ripening. *Annals of Botany, 48*(4), 451-466.

Platt-Aloia, K. A., & Thomson, W. W. (1989). Advantages of the use of intact plant tissues in freeze‐fracture electron microscopy. *Journal of Electron Microscopy Technique, 13*(4), 288-299.

Platt-Aloia, K. A., & Thomson, W. W. (1992). Idioblast oil cells of avocado: distribution, isolation, ultrastructure, histochemistry, and biochemistry. *International Journal of Plant Sciences, 153*(3), 301-310.

Platt-Aloia, K. A., Thomson, W. W., & Young, R. E. (1980). Ultrastructural changes in the walls of ripening avocados: transmission, scanning, and freeze fracture microscopy. *Botanical Gazette, 141*(4), 366-373.

Poucher, W. A. (1974). The materials of perfumery. In *Perfumes Cosmetics and Soaps* (pp. 44-47). London, England: Chapman and Hall.

Pryor, W. A. (2000). Vitamin E and heart disease:: Basic science to clinical intervention trials. *Free Radical Biology and Medicine, 28*(1), 141-164.

Rangel, B., Platt, K. A., & Thomson, W. W. (1997). Ultrastructural aspects of the cytoplasmic origin and accumulation of oil in olive fruit (Olea europaea). *Physiologia Plantarum, 101*(1), 109-114.

Ranney, C. A., Gillette, G., Brydon, A., McIntyre, S., Rivers, O., Vasquez, C. A., & Wilson, E. (1992). Physiological maturity and percent dry matter of California avocado. Paper presented at the Proceedings of the Second World Avocado Congress.

Rao, M. A. (2010). *Rheology of fluid and semisolid foods: principles and applications* (second ed.). New York: Springer Science & Business Media.

Rapoport, H. F., Fabbri, A., & Sebastiani, L. (2016). Olive Biology. In E. Rugini, L. Baldoni, R. Muleo, & L. Sebastiani (Eds.), *The olive tree genome* (pp. 13-25). Cham, Switzerland: Springer.

Ratovohery, J. V., Lozano, Y. F., & Gaydou, E. M. (1988). Fruit development effect on fatty acid composition of Persea americana fruit mesocarp. *Journal of Agricultural and Food Chemistry, 36*(2), 287-293.

Redgwell, R. J., MacRae, E., Hallett, I., Fischer, M., Perry, J., & Harker, R. (1997). In vivo and in vitro swelling of cell walls during fruit ripening. *Planta, 203*(2), 162-173.

Redgwell, R. J., Melton, L. D., & Brasch, D. J. (1988). Cell-wall polysaccharides of kiwifruit (Actinidia deliciosa): chemical features in different tissue zones of the fruit at harvest. *Carbohydrate Research, 182*(2), 241-258.

Redgwell, R. J., & Selvendran, R. R. (1986). Structural features of cell-wall polysaccharides of onion Allium cepa. *Carbohydrate Research, 157*, 183-199.

Reilly, J. P. (2012). Stimulation via electric and magnetic fields. In J. P. Reilly (Ed.), *Applied bioelectricity: from electrical stimulation to electropathology* (pp. 321-412). Silver Spring, Maryland: Springer Science & Business Media.

Renard, C. M., Voragen, A., Thibault, J., & Pilnik, W. (1991). Comparison between enzymatically and chemically extracted pectins from apple cell walls. *Animal Feed Science and Technology, 32*(1-3), 69-75.

Repo, T., Zhang, M. I. N., Ryyppö, A., Vapaavuori, E., & Sutinen, S. (1994). Effects of freeze-thaw injury on parameters of distributed electrical circuits of stems and needles of Scots pine seedlings at different stages of acclimation. *Journal of Experimental Botany, 45*(6), 823-833.

Requejo-Jackman, C., Farrell, M., Ogwaro, J., Olsson, S., M, B., Harker, R., McGhie, T., Wang, Y., Wong, M., & Woolf, A. (2010). Effects of harvest maturity on extra virgin olive oil year 2. The New Zealand Institute for Plant & Food Research Limited.

Requejo-Jackman, C., Wong, M., Wang, Y., McGhie, T., Petley, M., & Woolf, A. (2005). The good oil on avocado cultivars - a preliminary evaluation. *The Orchardist, 78*(10), 54-58.

Requejo-Tapia, L. C. (1999). International trends in fresh avocado and avocado oil production and seasonal variation of fatty acids in New Zealand-grown cv. Hass. (Master), Massey University, Palmerston North, New Zealand.

Richter, B. E., Jones, B. A., Ezzell, J. L., Porter, N. L., Avdalovic, N., & Pohl, C. (1996). Accelerated solvent extraction: a technique for sample preparation. *Analytical Chemistry, 68*(6), 1033-1039.

Romaniello, R., Leone, A., & Tamborrino, A. (2017). Specification of a new de‐stoner machine: evaluation of machining effects on olive paste's rheology and olive oil yield and quality. *Journal of the Science of Food and Agriculture, 97*(1), 115-121.

Russ, J. C. (2015). The image processing handbook. In. Boca Raton, Florida: CRC press.

Saini, B. L. (2010). Enzymes. In *Introduction to biotechnology* (pp. 40-49). New Delhi, India: Laxmi Publications.

Salvador, M., Aranda, F., & Fregapane, G. (2001). Influence of fruit ripening on ‘Cornicabra’virgin olive oil quality A study of four successive crop seasons. *Food Chemistry, 73*(1), 45-53.

Sarang, S., Sastry, S. K., & Knipe, L. (2008). Electrical conductivity of fruits and meats during ohmic heating. *Journal of Food Engineering, 87*(3), 351-356.

Schaffer, B., Wolstenholme, B. N., & Whiley, A. W. (2013). The avocado: botany, production and uses (2 ed.). Wallingford, Oxon: CAB International Press.

Schroeder, C. A. (1953). Growth and development of the Fuerte avocado fruit. *American Society for Horticultural Science, 61*, 103-109.

Scoular, J. (2019). Spotlight on quality avocado. *The New Zealand Herald*.

Selvendran, R. R., Stevens, B. J. H., & O'neill, M. A. (1985). Developments in the isolation and analysis of cell walls from edible plants. In C. T. Brett & J. R. Hillman (Eds.), *Biochemistry of plant cell walls* (pp. 39-78). Cambridge, England: Cambridge University Press.

Seymour, G. B., & Tucker, G. A. (2012). Avocado. In G. B. Seymour, J. E. Taylor, & G. A. Tucker (Eds.), *Biochemistry of fruit ripening* (pp. 53-76). Chichester, West sussex: Springer

Sherpa, N. (2002). The oxidation stability of extra virgin avocado oil. (Master), Massey University.

Shoemaker, C. F., & Borwankar, R. P. (1992). Rheology of foods. New York: Elsevier.

Sinha, N., Hui, Y. H., Evranuz, E. O., Siddiq, M., & Ahmed, J. (2011). Handbook of vegetables and vegetable processing. Ames, Iowa: Blackwell Publishing Ltd.

Singh, H., Batish, D. R., & Kohli, R. (1999). Autotoxicity: concept, organisms, and ecological significance. *Critical Reviews in Plant Sciences, 18*, 757-772.

Sivanathan, S., & Adikaram, N. K. B. (1989). Biological activity of four antifungal compounds in immature avocado. *Journal of Phytopathology, 125*(2), 97-109.

Skalicka-Wozniak, K., Widelski, J., & Glowniak, K. (2008). Plant materials in modern pharmacy ad methods of their investigations. In M. Waksmundzka-Hajnos, J. Sherma, & T. Kowalska (Eds.), *Thin layer chromatography in phytochemistry* (pp. 22-27). Boca raton, Florida: CRC Press.

Smagowska, B., & Pawlaczyk-Łuszczyńska, M. (2013). Effects of ultrasonic noise on the human body—a bibliographic review. *International Journal of Occupational Safety and Ergonomics, 19*(2), 195-202.

Spurr, A. R. (1969). A low-viscosity epoxy resin embedding medium for electron microscopy. *Journal of Ultrastructure Research, 26*(1-2), 31-43.

Steponkus, P. L. (1984). Role of the plasma membrane in freezing injury and cold acclimation. *Annual Review of Plant Physiology, 35*(1), 543-584.

Sugiyama, J. (1988). Electrical properties of foods for quality evaluation, 1. *Journal of the Japanese Society for Food Science and Technology (Japan), 35*, 647-653.

Swisher, H. E. (1988). Avocado oil. *Journal of the American Oil Chemists' Society, 65*, 1704-1706.

Tabilo-Munizaga, G., & Barbosa-Cánovas, G. V. (2005). Rheology for the food industry. *Journal of Food Engineering, 67*(1-2), 147-156.

Tadros, T. F. (2017). Handbook of colloid and interface science: industrial applications-agrochemicals, paints, coatings and food systems. Berlin, Germany: Walter de Gruyter GmbH.

TA Instruments. (2018). Retrieved 19/06/2018 from http://www.tainstruments.com/

Tamborrino, A., Catalano, P., & Leone, A. (2014). Using an in-line rotating torque transducer to study the rheological aspects of malaxed olive paste. *Journal of Food Engineering, 126*, 65-71.

Tamborrino, A., Squeo, G., Leone, A., Paradiso, V. M., Romaniello, R., Summo, C., Pasqualone, A., Catalano, P., Bianchi, B., & Caponio, F. (2017). Industrial trials on coadjuvants in olive oil extraction process: Effect on rheological properties, energy consumption, oil yield and olive oil characteristics. *Journal of Food Engineering, 205*, 34-46.

Therios, L. N. (2009). Olives (Vol. 18). Oxford, England: CABI.

ThermoScientific. (2012). Automated sample preparation: Accelerated solvent extraction. Retrieved 10/08/2015 from https://www.thermoscientific.com/dionex

ThermoScientific. (2013). Methods optimization in accelerated solvent extraction. Retrieved 16/08/2015 from https://www.thermoscientific.com/samplepreparation

ThermoScientific. (2018). Retrieved 06/19/2018 from https://www.thermoscientific.com/

Tiwari, B. K., Brunton, N. P., & Brennan, C. (2013). Handbook of plant food phytochemicals: sources, stability and extraction. Hoboken, New Jersey: John Wiley & Sons.

Trent, N. (2019). Extra virgin avocado oil market 2019: global key players analysis, sales, supply, demand and forecast to 2025. Wise Guy Consultants Pvt. Ltd.

Van Rooyen, Z., & Bower, J. P. (2006). Effects of storage temperature, harvest date and fruit origin on post-harvest physiology and the severity of mesocarp discolouration in 'Pinkerton'avocado (Persea americana Mill.). *The Journal of Horticultural Science and Biotechnology, 81*(1), 89-98.

Van Vliet, T., Van Aken, G. A., De Jongh, H. H. J., & Hamer, R. J. (2009). Colloidal aspects of texture perception. *Advances in Colloid and Interface Science, 150*(1), 27-40.

Varlan, A. R., & Sansen, W. (1996). Nondestructive electrical impedance analysis in fruit: normal ripening and injuries characterization. *Electro-and Magnetobiology, 15*(3), 213-227.

Verleyen, T., Forcades, M., Verhé, R., Dewettinck, K., Huyghebaert, A., & De Greyt, W. (2002). Analysis of free and esterified sterols in vegetable oils. *Journal of the American Oil Chemists' Society, 79*(2), 117-122.

Vilkhu, K., Manasseh, R., Mawson, R., & Ashokkumar, M. (2011). Ultrasonic recovery and modification of food ingredients. In H. Feng, B.-C. G, & J. Weiss (Eds.), *Ultrasound technologies for food and bioprocessing* (pp. 345-368). New York: Springer.

Watada, A. E., Herner, R. C., Kader, A. A., Romani, R. J., & Staby, G. L. (1984). Terminology for the description of developmental stages of horticultural crops. *HortScience, 19*(1), 21-21.

Webb, M. S., Uemura, M., & Steponkus, P. L. (1994). A comparison of freezing injury in oat and rye: two cereals at the extremes of freezing tolerance. *Plant Physiology, 104*(2), 467-478.

Werman, M. J., & Neeman, I. (1987). Avocado oil production and chemical characteristics. *Journal of the American Oil Chemists' Society, 64*(2), 229-232.

Weststrate, J., & Meijer, G. (1998). Plant sterol-enriched margarines and reduction of plasma total-and LDL-cholesterol concentrations in normocholesterolaemic and mildly hypercholesterolaemic subjects. *European Journal of Clinical Nutrition, 52*(5), 334-343.

Whiley, A. W., Schaffer, B. A., & Wolstenholme, B. N. (2002). The avocado: botany, production and uses. Wallingford, Oxon: CAB International Press.

White, A., Woolf, A. B., Hofman, P. J., & Arpaia, M. L. (2005). The International Avocado Quality Manual. Auckland, New Zealand: HortResearch.

Williams, L. O. (1977). The avocados, a synopsis of the genus Persea, subg. Persea. *Economic Botany, 31*(3), 315-320.

Wills, R. B. H., Lee, T. H., Graham, D., McGlasson, W. B., & Hall, E. G. (1981). Postharvest: An introduction to the physiology and handling of fruit and vegetables. New South Wales, Australia: New South Wales University Press.

Wilson, K., & Walker, J. (2000). Principles and techniques of practical biochemistry (5 ed.). Cambridge, England: Cambridge University Press.

Wong, M., Ashton, O. B. O., McGhie, T. K., Requejo-Jackman, C., Wang, Y., & Woolf, A. B. (2011). Influence of proportion of skin present during malaxing on pigment composition of cold pressed avocado oil. *Journal of the American Oil Chemists' Society, 88*(9), 1373-1378.

Wong, M., Ashton, O. B. O., Requejo-Jackman, C., McGhie, T., White, A., Eyres, L., Sherpa, N., & Woolf, A. B. (2008). Avocado oil—the colour of quality. In C. A. Culver & R. E. Wrolstad (Eds.), *Color quality of fresh and processed foods* (pp. 328-349). Washington, DC: American Chemical Society.

Wong, M., Eyres, L., & Ravetti, L. (2012). Modern aqueous oil extraction—centrifugation systems for olive and avocado oils. In W. E. Farr & A. Proctor (Eds.), *Green vegetable oil processing* (pp. 19-51). Urbana, Illonoi: AOCS Press.

Wong, M., Requejo-Jackman, C., & Woolf, A. B. (2010). What is unrefined, extra virgin cold-pressed avocado oil? *Inform, 21*(4), 198-201.

Woolf, A. (1997). Reduction of chilling injury in stored 'Hass' avocado fruit by 38 °C water treatments. *HortScience, 32*(7), 1247-1251.

Woolf, A., Requejo-Jackman, C., Lund, C., McGhie, T., Olsson, S., Eyres, L., Wang, Y., Bulley, C., & Wong, M. (2007). Avocado oil and other niche culinary oils in New Zealand. In C. J. O'Connor (Ed.), *Handbook of Australasian edible oils* (pp. 12-34). Auckland: Oils and Fats Specialist Group of NZIC.

Woolf, A., Wong, M., Eyres, L., McGhie, T., Lund, C., Olsson, S., Wang, Y., Bulley, C., Wang, Y., Friel, E., & Requejo-Jackman, C. (2009). Avocado oil. In R. A. Moreau & A. Kamel-Eldin (Eds.), *Gourmet and health-promoting specialty Oils* (pp. 73-125). Urbana, Illinois: AOCS Press.

Wu, L., Ogawa, Y., & Tagawa, A. (2008). Electrical impedance spectroscopy analysis of eggplant pulp and effects of drying and freezing–thawing treatments on its impedance characteristics. *Journal of Food Engineering, 87*(2), 274-280.

Yahia, E. M., & Woolf, A. B. (2011). Avocado (Persea americana Mill.). In E. M. Yahia (Ed.), *Postharvest biology and technology of tropical and subtropical fruits: açai to citrus* (Vol. 2, pp. 125-185). Cambridge, England: Woodhead Publishing Limited.

Yang, S., Hallett, I., Oh, H. E., Woolf, A. B., & Wong, M. (2019). Application of electrical impedance spectroscopy and rheology to monitor changes in olive (Olea europaea L.) pulp during cold-pressed oil extraction. *Journal of Food Engineering, 245*, 96-103.

Yang, S., Hallett, I., Rebstock, R., Oh, H. E., Woolf, A. B., & Wong, M. (2018). Cellular changes in “Hass” avocado mesocarp during cold‐pressed oil extraction. *Journal of the American Oil Chemists' Society, 95*(2), 229-238.

Yu, T. H., Liu, J., & Zhou, Y. X. (2004). Using electrical impedance detection to evaluate the viability of biomaterials subject to freezing or thermal injury. *Analytical and Bioanalytical Chemistry, 378*(7), 1793-1800.

Zhang, L., Shen, H., & Luo, Y. (2010). Study on the electric conduction properties of fresh and frozen–thawed grass carp (Ctenopharyngodon idellus) and tilapia (Oreochromis niloticus). *International Journal of Food Science & Technology, 45*(12), 2560-2564.

Zhang, M., & Willison, J. (1992a). Electrical impedance analysis in plant tissues: in vivo detection of freezing injury. *Canadian Journal of Botany, 70*(11), 2254-2258.

Zhang, M. I. N., & Willison, J. H. M. (1991). Electrical impedance analysis in plant tissues: a double shell model. *Journal of Experimental Botany, 42*(11), 1465-1475.

Zhang, M. I. N., & Willison, J. H. M. (1992b). Electrical impedance analysis in plant tissues: in vivo detection of freezing injury. *Canadian Journal of Botany, 70*(11), 2254-2258.

Zhang, M. I. N., Willison, J. H. M., Cox, M. A., & Hall, S. A. (1993). Measurement of heat injury in plant tissue by using electrical impedance analysis. *Canadian Journal of Botany, 71*(12), 1605-1611.

Zinoviadou, K. G., Galanakis, C. M., Brnčić, M., Grimi, N., Boussetta, N., Mota, M. J., Saraiva, J. A., Patras, A., Tiwari, B., & Barba, F. J. (2015). Fruit juice sonication: Implications on food safety and physicochemical and nutritional properties. *Food Research International, 77*, 743-752.

Appendices

Appendix I: Preliminary experiment investigating the effect of measurement temperature on electrical resistance of 'Hass' avocado pulp

(a) Resistance (Ω) of 'Hass' avocado pulp as a function of frequency at different temperature from 5 °C to 35 °C; (b) Resistance (Ω) of 'Hass' avocado pulp evaluated at a constant frequency (50 Hz, 7500 Hz and 1 MHz) as a function of temperature in ground avocado pulp samples (mean ± SE, n = 3).

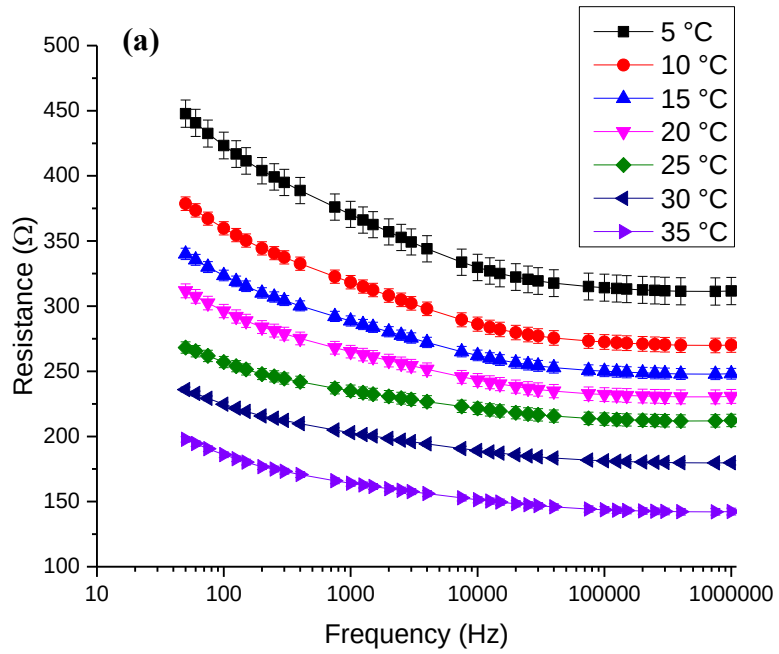

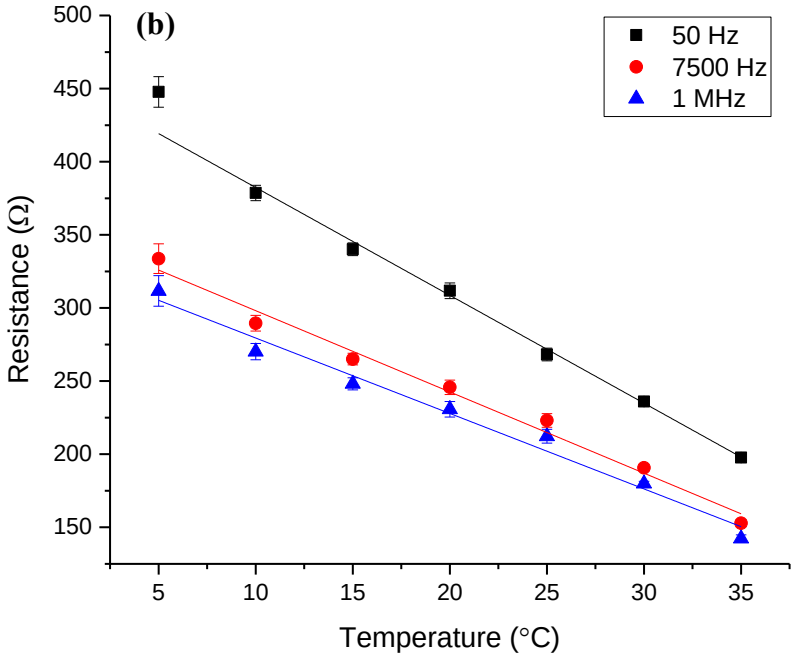

Appendix II: Preliminary experiment investigating the effect of shaking time on electrical conductivity of 'Hass' avocado pulp and 'J5' olive pulp

Electrical conductivity (µS/cm) of (a) 'Hass' avocado pulp and (b) 'J5' olive pulp after shaking at 150 rpm, 30 °C in an orbital shaker from 20 to 120 min (mean ± SE, n = 3). [a-d] Different letters denote significantly different conductivity values ($p < 0.05$).

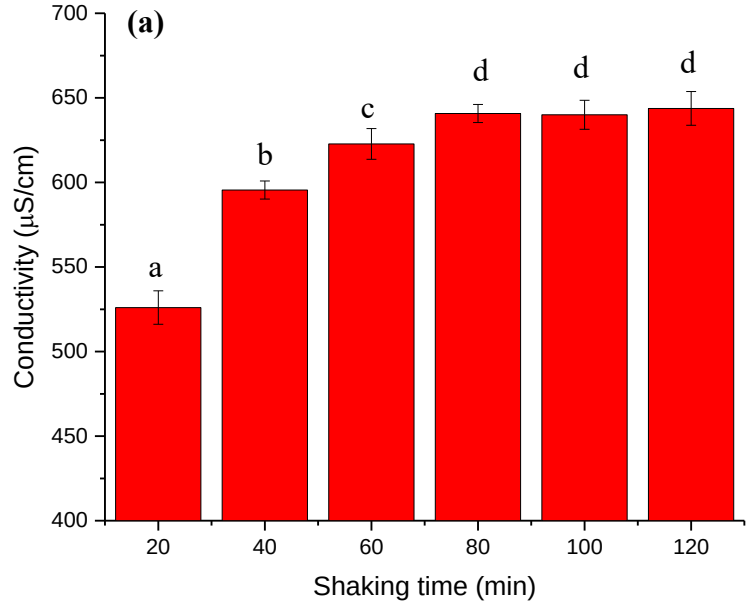

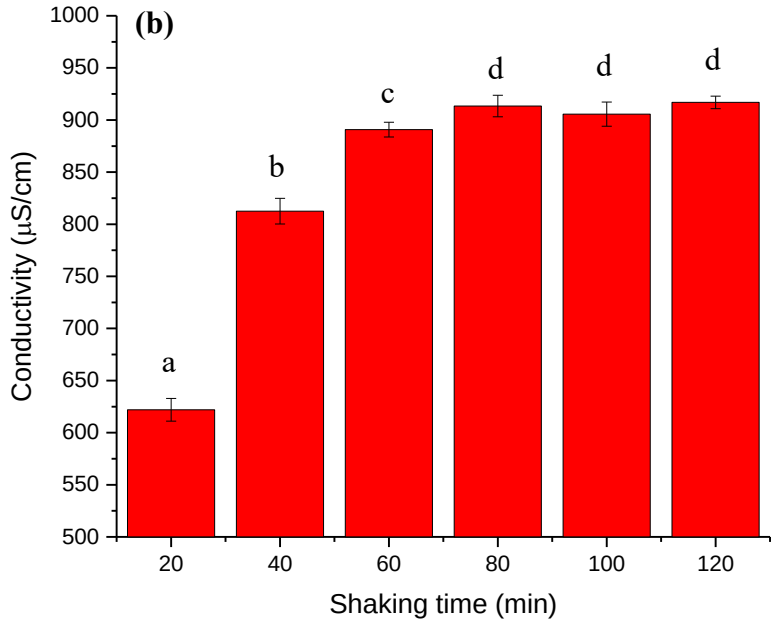

Appendix III: Firmness of 'Hass' avocado fruit for commercial cold-pressed extraction over the 2016-2017 commercial harvest and oil processing season in New Zealand (mean ± SE, n = 30).

[a] Same letters denote no significant difference between fruit firmness ($p > 0.05$).

Harvest date	Firmness (Fv)
September 2016	81.1 ± 1.5 [a]
October 2016	80.6 ± 1.6 [a]
December 2016	80.9 ± 0.9 [a]
January 2017	79.5 ± 1.6 [a]
March 2017	79.8 ± 1.4 [a]
April 2017	80.7 ± 1.9 [a]

Appendix IV: Preliminary experiment investigating the viscoelastic properties of 'Hass' avocado pulp during commercial cold-pressed oil extraction

Changes of the *G', G''* (Pa) of 'Hass' avocado pulp from fruit at four different stage of maturity (harvested between December to April 2016/17 season) during commercial malaxing from 30 to 120 min at 45 °C (a) Fruit harvested in December 2016; (b) Fruit harvested in January 2017; (c) Fruit harvested in March 2017; (d) Fruit harvested in April 2017 (mean ± SE, n = 3).